

University of KwaZulu-Natal

**Synthesis, characterization and bioactivity of
quinoxaline and benzimidazole derivatives**

2016

Suhas Ashok Shintre

Synthesis, characterization and bioactivity of quinoxaline and benzimidazole derivatives

A Thesis

submitted in fulfillment for the requirements

for the award of the degree of

Doctor of Philosophy

in the

School of Chemistry and Physics

College of Agriculture, Engineering & Science,

By

Suhas Ashok Shintre

2016

Supervisor: Prof. N.A. Koorbanally

Co-supervisor: Prof. D. Ramjugernath

Synthesis, characterization and bioactivity of quinoxaline and benzimidazole derivatives

by

Suhas Ashok Shintre

2016

A thesis submitted to the School of Chemistry, College of Agriculture, Engineering and Science, University of KwaZulu-Natal, for the degree of Doctor of Philosophy.

This thesis has been prepared according to **Format 4** as outlined in the guidelines from the College of Agriculture, Engineering and Science which states:

This is a thesis in which chapters are written as a set of discrete research papers, with an overall introduction and final discussion, where one (or all) of the chapters have either been submitted for publication or already been published. Typically, these chapters will have been published in internationally recognized, peer- reviewed journals.

// Shree Ganeshaya Namah: //



Vakratunda Mahakaya Suryakoti Samaprabha /

Nirvighnam Kuru Mey Deva Sarva Karyeshu Sarvada //

Preface

I hereby declare that the thesis entitled “Synthesis, characterization and bioactivity of quinoxaline and benzimidazole derivatives” submitted to the University of KwaZulu-Natal for the award of the degree of Doctor of Philosophy in Chemistry under the supervision of Professor Neil A. Koorbanally represents original work by the author and has not been submitted in full or part for any degree or diploma at this or any other University. Where use was made of the work of others it has been duly acknowledged in the text. This work was carried out in the School of Chemistry and Physics, University of KwaZulu-Natal, Westville campus, Durban, South Africa.

Signed: _____

Suhas Ashok Shintre, M. Sc

As the candidate’s supervisor, I have approved this dissertation for submission

Signed: _____

Prof. Neil A. Koorbanally, Ph. D (Natal)

Declaration – Plagiarism

I, Suhas Ashok Shintre, declare that:

1. The research reported in this thesis, except where otherwise indicated is my original research.
2. This thesis has not been submitted for any degree or examination at any other university.
3. This thesis does not contain other persons' data, pictures, graphs or other information, unless specifically acknowledged as being sourced from other persons.
4. This thesis does not contain other persons' writing, unless specifically acknowledged as being sourced from other researchers. Where other written sources have been quoted, then:
 - a) their words have been re-written but the general information attributed to them has been referenced.
 - b) or, where their exact words have been used, then their writing has been placed in italics and inside quotation marks, and referenced.
5. This thesis does not contain text, graphics or tables copied and pasted from the internet, unless specifically acknowledged, and the source being detailed in the thesis and in the references sections.

Signed

Suhas. A. Shintre

Acknowledgements

The work presented in this thesis would not have been possible without my close association with many people who were always there when I needed them the most. I take this opportunity to acknowledge them and extend my sincere gratitude for helping me make this **Ph.D. thesis** a possibility.

I would like to express my special appreciation and thanks to my advisor **Prof. N. A. Koorbanally** you have been a tremendous mentor to me. I would like to thank you for encouraging my research and for allowing me to grow as a research scientist. Your advice on both research as well as on my career have been invaluable.

I express my sincere gratitude to my co-supervisor **Prof. Deresh Ramjugernath**, who has provided me financial support for this research and encouragement to fulfil my research work. For this I am extremely grateful.

A very special thank you to my best friend and my better half, **Dr Pradnya**. She was always stood by me, without her love, encouragement and assistance, I would not have finished this thesis.

Thank you to **Dr. Pravesh Singh** for his contribution and advice with my Computational chemistry studies. I am grateful to **Dr. Rajshekhar Karpoormath** for his assistance with my microwave reactions, and also I am grateful for your advice and moral support throughout my studies.

My sincere thanks to **Dr Chunderika Mocktar** for guiding me with my antibacterial activity studies, and **Dr Shahidul Islam** and **Dr Mopuri Ramgopal** for their help with my anti-diabetic and anti-oxidant testing.

I am pleased to express my gratitude to **Mr D. Jagjivan** for his assistance with recording NMR spectra. I extend my sincere thanks to **Dr. Bernard Omondi** for X-ray crystallography studies

I express my heart-felt gratitude to **Dr. Suhas Ramesh, Dr. Devender, Adele, Girish, and Kaalin** for helping me with theoretical studies and fruitful discussions and suggestions.

Especially to all the colleagues of the laboratory, **Adele, Abubaker, Asif, Christina, Devendar, Fitsum, Kaalin, Lamla, Mrs H Govender, Neha, Pramod, Thrineshen, Saba, Samuel, Shirveen, Sunayna, Srinivasulu** and **Victoria** with whom I've had the pleasure to work with during all these years, for all the good times we've had together in and outside the lab and for every wonderful day we've spent together. Also to all the visitors who have been at our lab. My time at UKZN was made enjoyable in a large part due to the many friends and "**NPRG** group" that became a part of my life.

I am grateful for time spent with roommates **Pramod and Ramesh**, as well as my friends **Aziz, Sachin, Sunayana, Swapnali, Nazia** for being my backpacking buddies for creating my most memorable trips and moments. For hospitality as I finished up my degree, and for many other people and memories.

I express my special and sincere thanks to **Mrs Malini Padyachee, Mrs Anita Naidoo, Mr Kishore Singh, Mrs Vashti Reddy, Mr Gregory Moodley, Mr Miler Nundkumar** and **Mr Shannon Soodeyal** for their support, and always willing to help me with even the smallest of things during the course of this work.

I would like to acknowledge all the teachers I learnt from since my childhood, I would not have been here without their guidance, blessing and support.

My special thanks to **Dr. Naren Rana** and **Dr. Kala Rana** for being role models in my life. I would never be able to pay back the love and affection showered upon by them. They have taught me how a person can succeed in achieving what seems impossible to begin with...thanks Uncle and Aunty for everything.

I would like to acknowledge the people who mean the world to me, my father **Mr Ashok Shintre** and mother **Lata**, my brother **Sunil** and sister **Sangita**. I extend my respect to my parents, my paternal and maternal grandparents and all elders to me in the family. I cannot imagine a life without their love and blessings. Thank you mom, pappa for showing faith in me and giving me liberty to choose what I desired. I consider myself the luckiest in the world to have such a supportive family, standing behind me with their love and support.

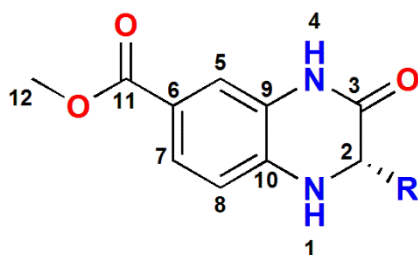
Finally, I thank my God, for letting me through all the difficulties. I have experienced your guidance day by day. You are the one who let me finish my degree. I will keep on trusting you for my future. Thank you, Lord.

To my **mother Lata** and memory of my beloved **Grandmother Sonabai**. This thesis is dedicated to you - for all of the above and much, much more. If there are feelings that can only be understated with words, this is definitely one of them. I could not expect more or be more grateful to anyone. You have always been there for me, either at a distance or visiting every time you could, and always did your best to make my life run as “smoothly” and happily as possible. I know how proud you are of me and let me just say that I am equally proud of having such great parents and, above all, best friends. My accomplishments in life reflect all of this! Thank You

Any future success that I may enjoy will be built on the educational foundation laid by all of those mentioned above. The extent to which I feel indebted to them is enormous, and as I emerge from my formal education and look to start contributing to the world in earnest, I will never forget the large debt I owe to these benefactors and to society. I am eager to start paying everyone back.

Suhas Ashok Shintre

Structures of synthesized compounds reported in chapters 4 and 5

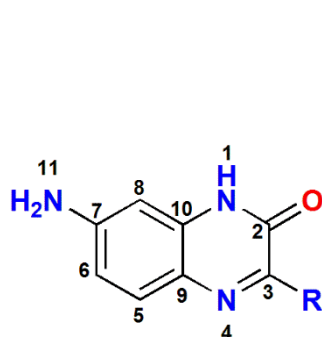


Quinoxaline-amino acid A6a-n

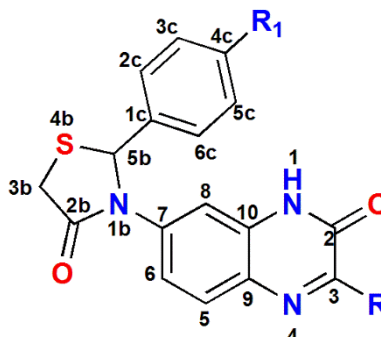
No.	R	No.	R
A6a		A6h	
A6b		A6i	
A6c		A6j	
A6d		A6k*	
A6e		A6l	
A6f		A6m	
A6g		A6n	

*Fragment fused with the quinoxaline framework. **N** belongs to the quinoxaline skeletal framework.

Structures of synthesized compounds reported in chapter 6



B5a-c

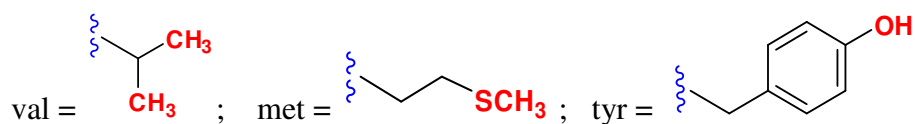


B6a-l

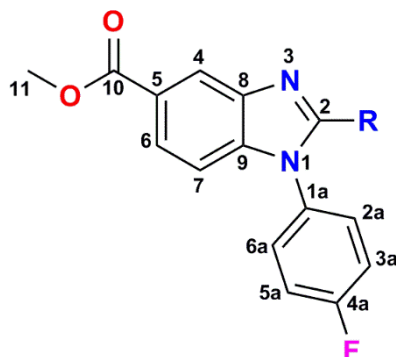
Quinoxaline-thiazolidine-amino acid

No.	R	R ₁
B5a	val	-
B5b	met	-
B5c	tyr	-
B6a	val	H
B6b	val	F
B6c	val	OMe
B6d	val	NO ₂
B6e	met	H
B6f	met	F
B6g	met	OMe
B6h	met	NO ₂
B6i	tyr	H
B6j	tyr	F
B6k	tyr	OMe
B6l	tyr	NO ₂

R = amino acid side chain;



Structures of synthesized compounds reported in Chapter 7



2-Substituted benzimidazoles C5a-v

No.	R	No.	R
C5a	Ph	C5l	4-S(CH ₃) Ph
C5b	4-F Ph	C5m	2-Naphthyl
C5c	4-Cl Ph	C5n	α -(<i>E</i>)-prop-1-en-1-yl Ph
C5d	4-Br Ph	C5o	2-(6-Chloroquinoliny)
C5e	4-CF ₃ Ph	C5p	2-OH-4,6-(OCH ₃) ₂ Ph
C5f	4-NO ₂ Ph	C5q	3,4-(OH) ₂ Ph
C5g	4-CH ₃ Ph	C5r	2,3,4-(OH) ₃ Ph
C5h	4-OCH ₃ Ph	C5s	2-Thiophenyl
C5i	4-NH ₂ Ph	C5t	2-Furanyl
C5j	4-OH Ph	C5u	<i>n</i> -Butyl
C5k	4-N(CH ₃) ₂ Ph	C5v	<i>n</i> -Heptyl

Abstract

A total of 51 compounds, including 17 quinoxaline-amino acid hybrids (**A6a-n** and **B5a-c**), 12 quinoxaline-amino acid-thiazolidine hybrids (**B6a-l**) and 22 2-phenyl substituted benzimidazoles (**C5a-v**) were successfully synthesized in yields in excess of 75%. Of these compounds, only 8 of the quinoxaline-amino acid hybrids were previously reported. All the other compounds synthesized in this work were novel. A thermal study was carried out on the quinoxaline-amino acid hybrids **A6a-n** to determine the hydrogen bonding capabilities of the molecules, important in deciding whether or not the molecules can act as good ligands. It was found that of the three centers studied for their hydrogen bonding, NH-1 and NH-4 had very poor hydrogen bonding capability whereas the best hydrogen bonding capability was seen by H-2. This study was supported by DFT and MD calculations on **A6d** since a crystal structure was also obtained for this molecule. The results supported the thermal study in showing that H-2 was highly involved in hydrogen bonding.

Certain steps in the synthesis of compounds **B6a-l** and **C5a-v** were carried out under microwave conditions, which have the advantage of short reaction times and good yields compared to conventional methods. We report here for the first time the synthesis of thiazolidines with quinoxaline-amino acids under microwave conditions. All the synthesized compounds were characterized using instrumental techniques such as 1D and 2D NMR and Mass spectrometry. X-Ray crystallography was carried out on selected samples to confirm the structures and to determine the configuration of stereocentres in the molecules. The crystal structures indicated that the quinoxaline-amino acid hybrids were synthesized in the *S*-configuration at C-2, while the quinoxaline-amino acid-thiazolidine hybrids were all synthesized as racemates.

The synthesized compounds were tested in three different assays; antimicrobial, antioxidant and antidiabetic. Compounds **B6f**, **B6j** and **B6k**, showed broad spectrum activity in the

antimicrobial assays with minimum bactericidal concentration (MBC) values comparable to that of ciprofloxacin. **B6f** and **B6j** was active at <100 μM against all the strains tested against and **B6k** were active at <100 μM against *Staphylococcus aureus*, Methicillin-resistant *S. aureus* (MRSA) and *Escherichia coli* as well as the fungal strain, *Candida albicans*. **B6f** was highly active against *S. aureus* (23.4 μM) and *Klebsiella pneumonia* (11.7 μM), **B6j** against *Pseudomonas aeruginosa* (21.7 μM) and **B6k** against *S. aureus* (15.9 μM) and *E. coli* (21.2 μM). The thiazolidine moiety was essential for antimicrobial activity. In the first series of compounds without the thiazolidine group, the activity was much less (in the mM range), with only **A6g** having a MBC of 80 μM against *E. coli*. The antimicrobial activity of the benzimidazoles was also not good, with only **C5p** and **C5r** being notably active against *K. pneumoniae* (MBCs of 14.5 and 25.5 μM).

The quinoxaline amino acids **A6a**, **A6d** and **A6f** showed better α -glucosidase inhibitory activity with IC_{50} values of 0.056, 0.012 and 0.042 mM, respectively compared to acarbose IC_{50} of 0.088 mM. Their activity against α -amylase was not as good, being higher than that for acarbose. The thiazolidine hybrids were less active than the quinoxaline amino acids in the antidiabetic assay with only a few compounds being 2-3 fold higher than the acarbose standard. Molecular docking of the two most active anti-diabetic compounds (**A6d** and **A6f**) in the binding site of *Saccharomyces cerevisiae* α -glucosidase indicated predominant hydrophobic and hydrogen bonding interactions, which could be responsible for their activity in the antidiabetic assay. The best antioxidant activity was shown by **B6k** and **B6l** with IC_{50} values of 19.60 and 10.53 μM respectively in comparison to ascorbic acid (IC_{50} 16.86 μM).

List of Abbreviations

¹H NMR - Proton nuclear magnetic resonance spectroscopy
¹³C NMR - Carbon-13 nuclear magnetic resonance spectroscopy
¹⁹F NMR – Fluorine-19 nuclear magnetic resonance spectroscopy
ACN - Acetonitrile
AcOH - Acetic acid
AMPA receptor - α -amino-3-hydroxy-5-methyl-4-isoxazolepropionic acid receptor
Br₂-HAC - Bromo acetic acid
CCDC - Cambridge Crystallographic Data Centre
CDCl₃ - Deuterated chloroform
COSY - Correlated nuclear magnetic resonance spectroscopy
d - Doublet
dd - Double doublet
DD - Disc diffusion
ddd - Doublet of doublet of doublets
DCM - Dichloromethane
DFT - Density functional theory
DIPEA - *N,N*-diisopropylethylamine
DMA - Dimethylacetamide
DMF - Dimethylformamide
DMSO - Dimethyl sulfoxide
DMSO-*d*₆ - Deuterated dimethyl sulfoxide
DNS - Dinitrosalicylic acid
DPPH - 2,2'-diphenyl-1-picrylhydrazyl
DS - Discovery studio
dt - Doublet of triplets
EtOAc - Ethyl acetate
EtOH - Ethanol
FT-IR - Fourier Transform - Infrared Spectroscopy
HIV - Human Immuno-deficiency virus
HMBC - Heteronuclear multiple bond coherence
HOMO - Highest occupied molecular orbital
HPLC - High pressure liquid chromatography

HRMS - High resolution mass spectrometry
HSQC - Heteronuclear multiple quantum coherence
Hz - Hertz
IBX - 2-Iodoxybenzoic acid
IC₅₀ - Half maximal inhibitory concentration
LUMO - Lowest unoccupied molecular orbital
m - Multiplet
MBC- Minimum bactericidal concentration
MD - Molecular dynamics
MeOH - Methanol
MeOH- *d*₄ - Deuterated methanol
MHA - Mueller-Hinton agar
MHB - Mueller-Hinton Broth
MIC - Minimum inhibitory concentration
MRSA - Methicillin-resistant *Staphylococcus aureus*
NaHMDS - Sodium bis(trimethylsilyl)amide
NMR - Nuclear magnetic resonance spectroscopy
NOESY - Nuclear Overhauser effect spectroscopy
PDB - Protein data bank
PPA - Polyphosphoric acid
PTSA - *p*-Toluenesulfonic acid
RMS - Root mean square
s - Singlet
t - Triplet
td - Triplet of doublets
TGA – Thioglycolic acid
THF - Tetrahydrofuran
TLC - Thin Layer chromatography
TMS - Tetramethylsilane
UV - Ultraviolet spectroscopy

Table of Contents

Chapter 1. Introduction.....	1
1.1 Quinoxalines.....	4
1.2 Benzimidazoles	5
1.3 Hypothesis.....	8
1.4 Aim.....	8
1.5 Objectives.....	9
1.6 References	9
 Chapter 2. Advanced synthetic methods and pharmacological potential of quinoxaline derivatives	15
2.1 Introduction	16
2.2 Synthesis.....	17
2.3 Pharmacological Importance of Quinoxaline Derivatives	39
2.4 Conclusion.....	47
2.5 References	47
 Chapter 3. The synthesis, antimicrobial and antidiabetic activity of benzimidazole scaffolds	53
3.1 Introduction	54
3.2 Synthesis.....	56
3.3 Applications of benzimidazole derivatives as antimicrobial and antidiabetic agents... ..	65
3.4 Conclusion.....	73
3.5 References	78
 Chapter 4. Synthesis and structure elucidation using 2D-NMR and thermal coefficient investigation on amino acid tethered quinoxalines.....	83
4.1 Introduction	84
4.2 Experimental	85
4.3 Results and Discussion.....	94
4.4 Conclusion.....	117
4.5 References	117

Chapter 5.	Biological evaluation and docking study of synthesized amino acid tethered quinoxalines	122
5.1	Introduction	123
5.2	Experimental	125
5.3	Results and Discussion.....	128
5.4	Conclusion.....	138
5.5	References	141
Chapter 6.	Synthesis, <i>in vitro</i> antimicrobial, antioxidant and antidiabetic activities of amino acid linked thiazolidine-quinoxaline derivatives	146
6.1	Introduction	147
6.2	Experimental	148
6.3	Results and discussion.....	162
6.4	Conclusion.....	169
6.5	References	170
Chapter 7.	Expedient synthesis, antimicrobial, antioxidant activities and docking study of 2-substituted methyl 1-(4-fluorophenyl)-1 <i>H</i> -benzimidazole-5-carboxylates	174
7.1	Introduction	175
7.2	Experimental	177
7.3	Results and Discussion.....	197
7.4	Conclusion.....	210
7.5	References	210
Chapter 8.	Conclusion	214

List of Schemes

Scheme 1-1. Synthesis of benzimidazole (1 and 2)	7
Scheme 1-2 Benzimidazole synthesized by the “Phillips method”	7
Scheme 1-3 Benzimidazole (4) synthesized using triethyl orthoformate	7
Scheme 2-1 Mechanism of synthesis of quinoxaline-2,3-diones (5).....	18
Scheme 2-2 Derivatization of quinoxaline-2,3-diones (5).....	19
Scheme 2-3 Reactions of <i>o</i> -diamine with one leaving group containing compound	20
Scheme 2-4 Mechanism for synthesis of 3-aminoquinoxalin-2(1 <i>H</i>)-one (14)	21
Scheme 2-5 Reactions of <i>o</i> -diamine with two poor leaving group-containing compound.....	22
Scheme 2-6 Mechanism of formation of quinoxaline (15).....	23
Scheme 2-7 Synthesis of benzimidazole fused quinoxaline compounds (21-29).....	23
Scheme 2-8 Synthesis and mechanism of pyrrolo quinoxaline	24
Scheme 2-9 Synthesis and mechanism of pyrazolo quinoxalines	25
Scheme 2-10 Mechanism of formation of imidazole quinoxaline (34)	26
Scheme 2-11 Synthesis and mechanism of pyrazolo quinoxaline (35)	27
Scheme 2-12 Reaction and mechanism of quinoxaline <i>via</i> azalactones with diamines	28
Scheme 2-13 Synthesis of quinoxalines from 1,2-dialdehydes with diamines.....	28
Scheme 2-14 Mechanism of preparation of intermediate (39)	29
Scheme 2-15 Mechanism of formation of quinoxaline (40).....	29
Scheme 2-16 Mechanism of formation of quinoxaline (41).....	30
Scheme 2-17 Mechanism of formation of quinoxaline (43).....	30
Scheme 2-18 Mechanism for synthesis of quinoxaline using IBX.....	31
Scheme 2-19 Synthesis of benzofurazan oxide (46).....	32
Scheme 2-20 Synthesis of <i>N</i> -oxide quinoxaline derivatives.....	32
Scheme 2-21 Synthesis of different <i>N</i> -oxide quinoxaline derivatives.....	33
Scheme 2-22 Mechanism of the Beirut reaction.....	34
Scheme 2-23 Reactions of benzofurazan oxide with different dicarbonyl compounds.....	35
Scheme 2-24 Synthesis of <i>N</i> -oxide quinoxaline urea and carbamate derivatives	35
Scheme 2-25 Synthesis of different quinoxaline ligands.....	36
Scheme 2-26 Synthesis of metal complexes of quinoxaline.....	37
Scheme 2-27 Synthesis of quinoxaline metal complexes	37
Scheme 2-28 Metal complexes prepared from quinoxaline schiff bases.....	38
Scheme 2-29 Quinoxaline metal complexes prepared from thiosemicarbazide ligand.....	38
Scheme 3-1 General scheme of synthesis of benzimidazole	56
Scheme 3-2 Synthesis of 2-substituted benzimidazoles using various carboxylic acid	57
Scheme 3-3 Synthesis of 2-substituted benzimidazoles using various carboxylic acid	58
Scheme 3-4 Mechanism of synthesis of benzimidazole (161).....	58
Scheme 3-5 Synthesis of benzimidazole using different reaction conditions.....	59
Scheme 3-6 Synthesis of 2-substituted benzimidazoles using various aldehydes.....	59
Scheme 3-7 Mechanism of synthesis of benzimidazole (184).....	59
Scheme 3-8 Synthesis of thiobenzimidazole (185).....	60

Scheme 3-9 Synthesis with possible mechanism of formation of thiobenzimidazole using hydrazine carbothiamide.....	61
Scheme 3-10 Synthesis with mechanism of benzimidazole (190).....	62
Scheme 3-11 Synthesis and mechanism of benzimidazole (192).....	62
Scheme 3-12 Formation of benzimidazole using <i>o</i> -phenylenediamine and urea	63
Scheme 3-13 Synthesis of benzimidazole using <i>o</i> -phenylenediamine and cyanogen bromide	64
Scheme 3-14 Synthesis of Benzimidazo-isoindol-ones (195)	65
Scheme 3-15 Synthesis and mechanism of benzimidazol-2-benzenesulphonamides (196)...	66
 Scheme 4-1 Synthesis of amino acids derived quinoxalines;	 94
 Scheme 6-1 Synthesis of amino acid linked thiazolidine-quinoxaline compounds.....	 149
 Scheme 7-1 Synthesis of fluorinated benzimidazoles C5a-v.....	 178
Scheme 7-2 The proposed mechanism for the final step of the benzimidazole synthesis....	199

List of Figures

Figure 1-1	Drugs containing a quinoxaline scaffold.....	2
Figure 1-2	Quinoxaline compounds as AMPA receptor antagonists.....	2
Figure 1-3	Drugs containing a benzimidazole scaffold	3
Figure 1-4	Structures isomeric with quinoxaline.....	4
Figure 1-5	Biologically active quinoxaline scaffold containing compounds	5
Figure 1-6	Benzimidazole core structure	5
Figure 1-7	Structure of kealiiquinone	6
Figure 2-1	The general structure of a quinoxaline with nomenclature included	16
Figure 2-2	Biologically active simple quinoxaline compounds	40
Figure 2-3	Second class of quinoxaline compounds.....	43
Figure 2-4	Unique quinoxaline compounds.....	45
Figure 3-1	The general structure of a benzimidazole with nomenclature included.....	55
Figure 3-2	Tautomeric forms of benzimidazoles.....	55
Figure 3-3	Biologically active N-1 substituted benzimidazoles	67
Figure 3-4	Biologically active C-2 substituted simple benzimidazoles.....	68
Figure 3-5	Biologically active C-2 substituted complex benzimidazoles	69
Figure 3-6	Biologically active C-2 substituted complex benzimidazoles	69
Figure 3-7	Biologically active N-1 and C-2 substituted complex benzimidazoles	70
Figure 3-8	Biologically active N-1, N-3 and C-2 substituted complex benzimidazoles	71
Figure 3-9	Biologically active benzimidazoles.....	71
Figure 4-1	¹ H NMR spectrum of (<i>S</i>)-methyl 2-(4-hydroxybenzyl)3-oxo-1,2,3,4-tetrahydroquinoxaline-6-carboxylate (A6b).....	98
Figure 4-2	¹³ C NMR spectrum of (<i>S</i>)-methyl 2-(4-hydroxybenzyl)3-oxo-1,2,3,4-tetrahydroquinoxaline-6-carboxylate (A6b).....	99
Figure 4-3	Selected HMBC correlations for (<i>S</i>)-methyl 2-(4-hydroxybenzyl)-3-oxo-1,2,3,4-tetrahydroquinoxaline-6-carboxylate (A6b).....	99
Figure 4-4	ORTEP diagram of compound A6d	108
Figure 4-5	Intermolecular hydrogen bonding in A6d	109
Figure 4-6	¹ H spectral traces showing the shift of amide, sec. amine and chiral carbon containing proton at variable temperature in DMSO- <i>d</i> ₆	113
Figure 4-7	Overlay of X-ray structure (in red sticks) of A6d with its DFT predicted conformer1 (in green sticks) and conformer 2 (in blue sticks), performed using DS Software (2013).....	115
Figure 4-8	Optimized geometry of A6d displaying natural charge distribution on each atom	115
Figure 4-9	The electron density distribution in HOMO of compound A6d	116
Figure 4-10	The electron density distribution in LUMO of compound A6d.....	116
Figure 4-11	Progress of selected inter-atomic distances (in Å) during MD simulation for compound A6d	116

Figure 5-1	The core structure of amino acid tethered quinoxalines	128
Figure 5-2	Superimposition of the conformation of ciprofloxacin.....	137
Figure 5-3	Docked conformation of A6g in the binding cavity of the bacterial protein	138
Figure 5-4	Docked conformation of A6n and ciprofloxacin in the binding cavity of the bacterial protein.....	139
Figure 5-5	Docked conformation of A6d and A6f in the binding cavity of the α -glucosidase	140
Figure 6-1	Selected HMBC correlations of compound B6j (H \rightarrow C)	165
Figure 7-1	Selected HMBC correlations of compound C5i (H \rightarrow C)	202
Figure 7-2	The orientation of C5r and C5h in the active site of topoisomerase II DNA-gyrase.	208
Figure 7-3	The orientation of ciprofloxacin in the active site of topoisomerase II DNA-gyrase.	209
Figure 7-4	Ortep diagram for C5k	209

List of Tables

Table 2-1	Antimicrobial activity of simple quinoxaline compounds	41
Table 2-2	Antimicrobial activity of simple quinoxaline compounds (continued).....	42
Table 2-3	Antimicrobial activity of second class of quinoxaline compounds.....	44
Table 2-4	Antimicrobial activity of unique quinoxaline compounds	46
Table 3-1	Antimicrobial activity of benzimidazole compounds (197-216).....	72
Table 3-2	Antimicrobial activity of benzimidazole compounds (217-238).....	73
Table 3-3	Antimicrobial activity of benzimidazole compounds (239-261).....	74
Table 3-4	Antimicrobial activity of benzimidazole compounds (262-285).....	75
Table 3-5	Antimicrobial activity of benzimidazole compounds (286-300).....	76
Table 3-6	Antimicrobial activity of benzimidazole compounds (301-316).....	77
Table 3-7	α -Glucosidase inhibitory enzyme activity	78
Table 4-1	Physical data of the synthesized compounds	88
Table 4-2	Yields and times of completion of reaction with different solvents for the formation of the intermediate A5.....	96
Table 4-3	The effect on yields and time of completion of reaction with different bases in the formation of the intermediate A5.....	97
Table 4-4	^1H NMR data (δ in ppm) for compounds A6a-g (J is given in Hz).....	100
Table 4-5	^1H NMR data (δ in ppm) for compounds A6h-n (J is given in Hz).....	101
Table 4-6	^{13}C NMR data (δ in ppm) for compounds A6a-6n.....	102
Table 4-7	Geometry of hydrogen bonding in molecule A6d ($\text{\AA},^\circ$).....	108
Table 4-8	$-\Delta\delta/\Delta T$ values of shielded and deshielded proton from compound A6a-n.....	112
Table 5-1	Side chains of compounds A6a-n	130
Table 5-2	Minimum Bactericidal Concentration (MBC in mM) of compounds A6a-n	131
Table 5-3	Antioxidant activity of the synthesized compounds A6a-n (mM)	133
Table 5-4	<i>In vitro</i> α -Glucosidase and α -amylase activity of A6a-n (IC_{50} in mM)	134
Table 6-1	Yields and duration of microwave synthesis for the amino acid linked quinoxaline-thiazolidinones	164
Table 6-2	Antimicrobial activity of the synthesized compounds, MBCs in μM	166
Table 6-3	Antioxidant activity of the synthesized compounds, IC_{50} (μM)	168
Table 6-4	α - Glucosidase and α -amylase inhibition of the synthesized compounds, IC_{50} (μM)	169
Table 7-1	Comparison of the yields and duration of the final step in the benzimidazole synthesis using three methods.....	201
Table 7-2	Antimicrobial activity of the synthesized compounds, MBCs in μM	204
Table 7-3	Antioxidant activity of the synthesized compounds from the DPPH assay.....	205
Table 7-4	Hydrogen bond interactions for C5k.....	207

Chapter 1. Introduction

Quinoxalines and benzimidazoles are two important classes of heterocyclic compounds, with major applications in the pharmaceutical industry. Currently, there are several drugs containing a quinoxaline core unit such as echinomycin, levomycin and quinacillin (antibiotics), varenicline (nicotinic receptor agonist), brimonidine (eye drop), chloroquinoxaline sulfonamide (CQS, NSC 339004), XK469 (NSC697887) (anticancer agents), and sulfaquinoxaline (used in veterinary medicine) (**Figure 1-1**) (Bailly et al., 1999; Campbell et al., 2008; Baumann et al., 2013; Nageswar et al., 2013; Ali et al., 2015). In addition, there are several other quinoxaline compounds presently used as AMPA (α -amino-3-hydroxy-5-methyl-4-isoxazolepropionic acid) receptor antagonists such as YM90K, CNQX, DNQX, YM872, LU112313 and NBQX (**Figure 1-2**) (Sasaki and Kaneko, 1996; Kodama et al., 1999; Loscher et al., 1999; Takahashi et al., 2002; Olayiwola et al., 2007; Seidl et al., 2014; Deng et al., 2016; Zuo et al., 2016).

Several drugs used in the pharmaceutical industry also contain a benzimidazole scaffold in their structure. Examples of these are omeprazole (used for gastric ulcers and acid reflux), clemizole and astemizole (antihistamines), mebendazole and thiabendazole (anthelmintics), pimobendan (inodilator), bezitramide (analgesic), cambendazole (veterinary anthelmintic), Imet-3393 (cancer), pimozide (antipsychotic drug) and diabazole (diabetes) (**Figure 1-3**) (Lieberman et al., 2009; Ingle and Magar, 2011; Khokra et al., 2011; Raghunath et al., 2014; Zhang et al., 2015). In addition, benomyl, thiabendazole and carbendazim are used as fungicides (Si et al., 2016).

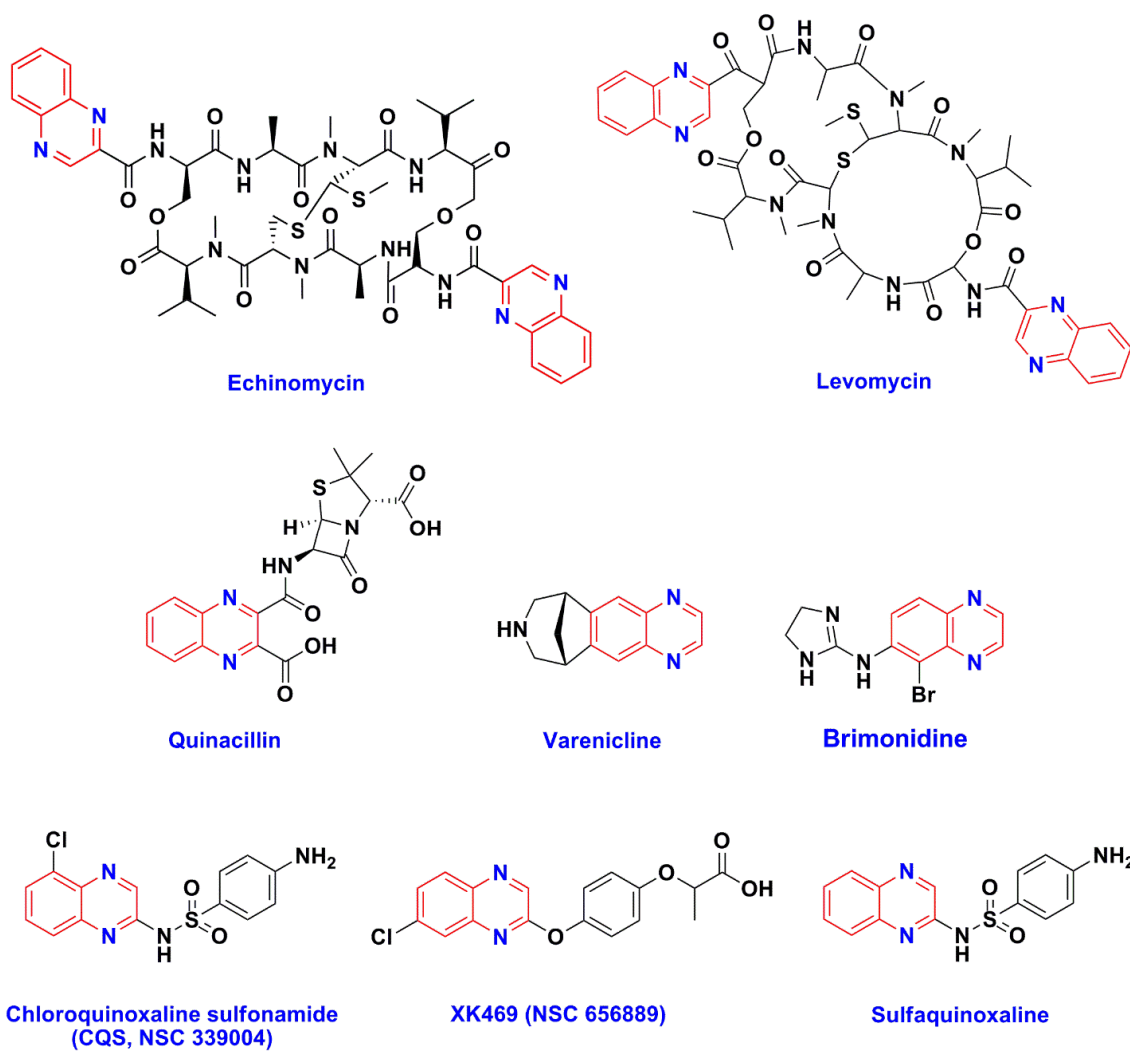


Figure 1-1 Drugs containing a quinoxaline scaffold

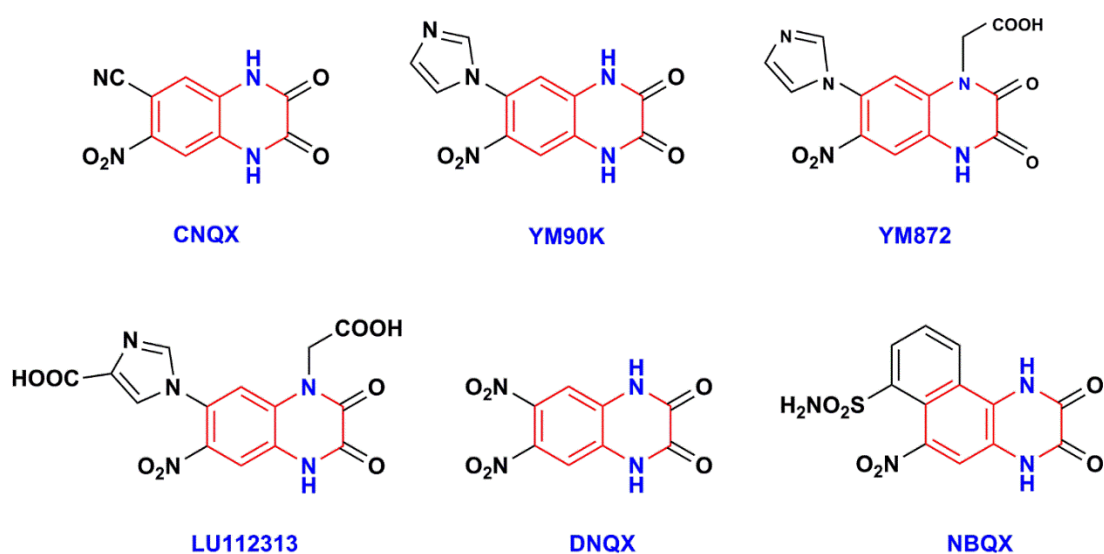


Figure 1-2 Quinoxaline compounds as AMPA receptor antagonists

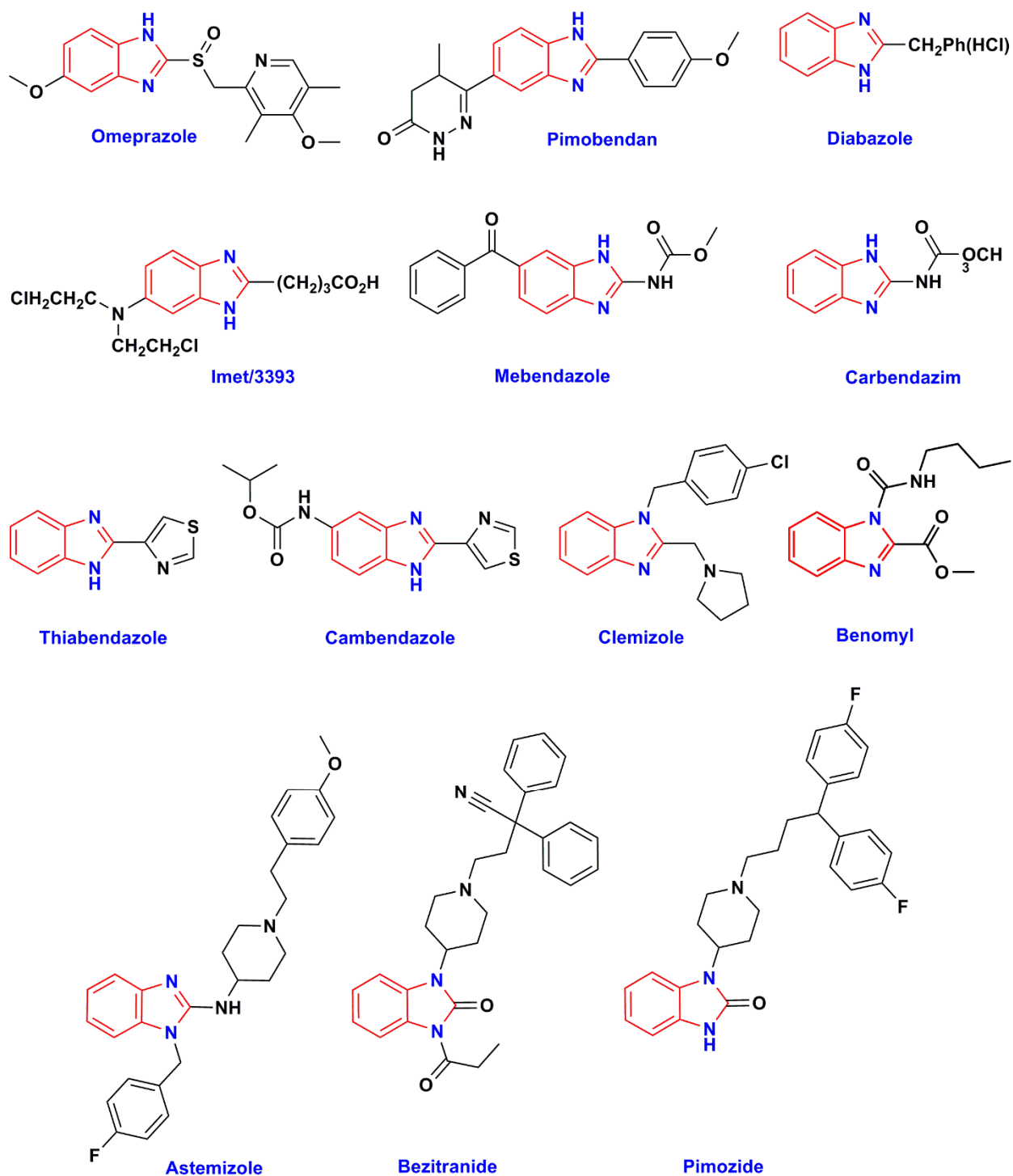


Figure 1-3 Drugs containing a benzimidazole scaffold

1.1 Quinoxalines

Quinoxaline is isomeric with other naphthyridines including quinazoline, phthalazine and cinnoline (**Figure 1-4**). It consists of two aromatic rings; a benzene ring fused to a second six membered ring containing two nitrogen atoms.

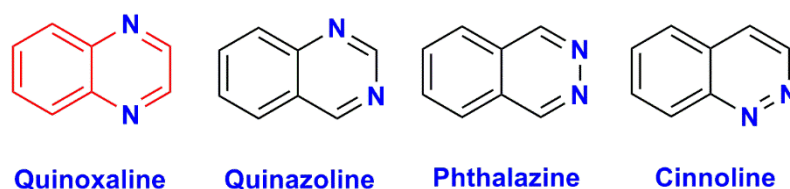


Figure 1-4 Structures isomeric with quinoxaline

The quinoxaline scaffold occurs in many naturally occurring compounds such as riboflavin (Vitamin B2) (**Figure 1-5**), flavoenzymes, molybdopterines and antibiotics of *Streptomyces* (Saito et al., 1967; Yoshida and Katagiri, 1969; Cornish et al., 1985; Hirose et al., 2011; Mu et al., 2014; Sheraz et al., 2014). Riboflavin is involved in a variety of biochemical processes in the body such as antibody production and red blood cell formation (Hardwick et al., 2004). In addition, they have potential industrial application, being able to inhibit metal corrosion, being used as dyes, and in organic semiconductors, cavitands and dehydroannulenes (O'Brien et al., 1996; Koti et al., 2000; Dailey et al., 2001; Sessler et al., 2002; Castro et al., 2004; Sascha and Faust, 2004; Chang et al., 2011; Zarrok et al., 2012; Tayebi et al., 2014). They have also been used as a ligand in a catalytic system (Wu et al., 2007).

The first report of a quinoxaline compound having antimalarial activity was reported by Haworth in 1948 (Haworth et al., 1948). In 1949, Crowther and his co-workers synthesized a series of dialkylaminoquinoxaline derivatives and tested them for their antimalarial activity. They obtained results similar to that of Haworth (Crowther et al., 1949). The antitumoral

properties of quinoxaline compounds was first noticed by Renault in 1981 (Renault et al., 1981).

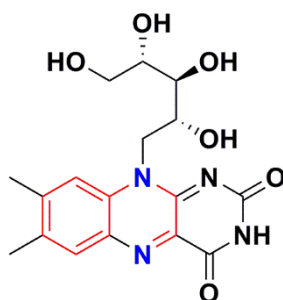


Figure 1-5 Biologically active quinoxaline scaffold containing compounds

Subsequently, there has much interest in the synthesis and bioactivity of quinoxaline derivatives. This is elaborated on further in Chapter 2.

1.2 Benzimidazoles

Benzimidazoles consist of a benzene ring fused to a diazole ring, where both nitrogen atoms are adjacent to the benzene ring (**Figure 1-6**). They are also known as 1,3-benzodiazoles, benziminazoles or benzoglyoxalines. In 1948, benzimidazole was recognised as an integral part of **vitamin B12** (α -(5,6-dimethylbenzimidazolyl)cobamidcyanide) available in nature (Barker et al., 1960).

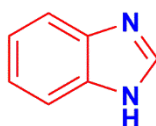


Figure 1-6 Benzimidazole core structure

Benzimidazole-derived alkaloids are rare in nature, and only a few examples of these natural products can be found in the literature such as kealiiquinone (**Figure 1-7**) (Faulkner et al.,

1992; Jin, 2011). In 1889, Fischer reported the bacteriostatic and fungicidal properties of the parent benzimidazole (Fischer et al., 1889).

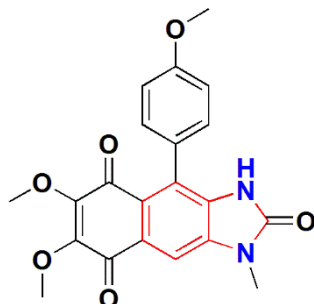
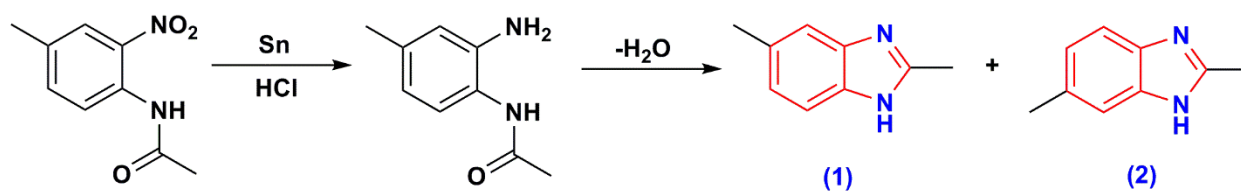


Figure 1-7 Structure of kealiquinone

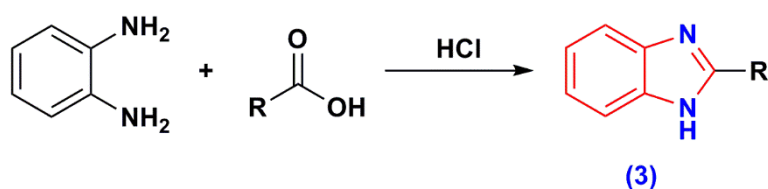
Beside their pharmaceutical application, benzimidazoles have played a role in organocatalysis, ligands for organometallic reactions, in semiconductors, the textile industry, dyes, the photographic industry, cosmetics and materials (Johnson et al., 1966; Overman, 1974; Hegngi et al., 1999; Berrada et al., 2002; Robert et al., 2004; Malathi et al., 2009; Mamada et al., 2011; Kim et al., 2012; Jain et al., 2013; Tozlu et al., 2013; Ahmed et al., 2014; Fleischmann et al., 2015; Mănescu et al., 2015; Nájera et al., 2015; Bodedla et al., 2016; Sánchez et al., 2016). 5-Methyl benzimidazole has also been used as camphor substitute (Wright, 1951). A number of salts of benzimidazole sulfonic acid are said to be of value in preparations for dental care (Rehman et al., 2013).

The first benzimidazole was prepared by Hobreck in 1872 (Wright, 1951), who obtained a mixture of 2,5- and 2,6-dimethyl-benzimidazole (**1** and **2**) by the reduction of 2-nitro-4-methylacetanilide (**Scheme 1-1**). Three years later Ladenburg obtained the same benzimidazole (**4**) by refluxing 3,4-diaminotoluene, with acetic acid (Wright, 1951).



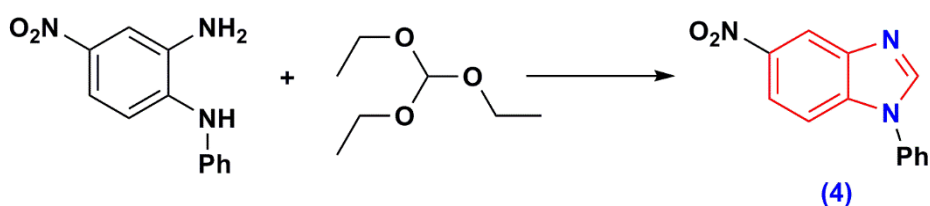
Scheme 1-1. Synthesis of benzimidazole (1 and 2)

The traditional synthesis of benzimidazoles (3) involves the reaction between an *o*-phenylenediamine and a carboxylic acid or its derivatives under harsh dehydrating reaction conditions (**Scheme 1-2**) (Phillips, 1928). As such, this is known as the “Phillips method”.



Scheme 1-2 Benzimidazole synthesized by the “Phillips method”

The first use of triethyl orthoformate for the preparation of 2-substituted benzimidazoles (4) was done by Walther and Kessler in 1906 (**Scheme 1-3**) (Wright, 1951).



Scheme 1-3 Benzimidazole (4) synthesized using triethyl orthoformate

Subsequent to these early studies, a range of synthetic pathways and reactions to synthesize benzimidazole derivatives were carried out. This is elaborated on further in **chapter 3**.

This thesis focuses on the synthesis and bioactivity of derivatives of these two scaffolds. The quinoxalines are combined with amino acids and thiazolidines resulting in hybrid molecules and the benzimidazoles contain substituted benzene moieties in their core structure. Hybrid molecules can either enhance or diminish the activity of either of the two scaffolds alone (Aiyelabola et al., 2012; Saxena et al., 2014; Tripathi et al., 2014; Demmer et al., 2015; Mickevičienė et al., 2015; Srivastava et al., 2015; Napoleon et al., 2016). Both amino acids and thiazolidines, are each bioactive molecules in their own right and hence are both capable of enhancing the effect of the quinoxalines (Hughes et al., 2007; Singh et al., 2011; Vinay and Lakshika, 2011; Bayram et al., 2015; Camacho et al., 2016; Gupta et al., 2016; Pânzariu et al., 2016). Different substituents attached to the core structure of many organic molecules alter their bioactivity. Hence derivatising benzimidazoles with aromatic groups containing different substituents can be used to identify lead compounds for the pharmaceutical industry.

1.3 Hypothesis

It is hypothesized that since quinoxalines and benzimidazole scaffolds are contained in known drugs, new molecules based on these scaffolds may lead to new drugs with either enhanced bioactivity or fewer side effects. Furthermore, it is hypothesized that the activity of each of the molecules can be enhanced by combining each of these scaffolds with another bioactive scaffold.

1.4 Aim

To identify lead compounds with quinoxaline and benzimidazole core structures, which can be developed into pharmaceuticals.

1.5 Objectives

Broad objective: To synthesize novel hybrid frameworks of amino acid tethered quinoxalines, amino acid-quinoxaline-thiazolidine hybrids and fluorinated benzimidazole derivatives and test them for their antimicrobial, antidiabetic and antioxidant activities.

Specific objective

1. To synthesize a small library of novel:
 - a) amino acid tethered quinoxalines;
 - b) amino acid-quinoxaline-thiazolidine hybrids and
 - c) fluorinated benzimidazoles.
2. To carry out a structural elucidation of all the synthesized compounds by 2D NMR spectroscopy and X-ray crystallography.
3. To screen the synthesized hybrid compounds for their antibacterial, antifungal, antioxidant and antidiabetic activities.

1.6 References

- Ahmed, N., Riaz, M., Singh, A., Malik, S. Synthesis, spectral and biological behavior of bivalent transition metal complex of tridentate (NNO donor) Schiff base ligand. *Int. J. Chem. Phys. Sci.*, **2014**, 5(4), 80-85.
- Aiyelabola, T. O., Ojo, I. A., Adebajo, A. C., Ogunlusi, G. O., Oyetunji, O., Akinkunmi, E. O., Adeoye, A. O. Synthesis, characterization and antimicrobial activities of some metal(II) amino acids' complexes. *Adv. Biol. Chem.*, **2012**, 2, 268-273.
- Ali, A., Hashem, A. Synthesis, reactions and biological activity of quinoxaline derivatives. *Am. J. Org. Chem.*, **2015**, 5(1), 14-56.
- Bailly, C., Echepare, S., Gago, F., Waring, M. J. Recognition elements that determine affinity and sequence-specific binding to DNA of 2QN, a biosynthetic bis-quinoline analogue of echinomycin. *Anticancer Drug Des.*, **1999**, 14(3), 291-303.
- Barker, H. A., Smyth, R. D., Weissbach, H., Toohey, J. I., Ladd, J. N., Volcanicani, B. E. Isolation and properties of crystalline cobamide coenzymes containing benzimidazole or 5,6-dimethylbenzimidazole. *J. Biol. Chem.*, **1960**, 235(2), 480-488.

- Baumann, M., Baxendale, I. R. An overview of the synthetic routes to the best selling drugs containing 6-membered heterocycles. *Beilstein J. Org. Chem.*, **2013**, 9, 2265-2319.
- Bayram, E. E. O., Buran, K., Durmaz, I., Berk, B., Cetin-Atalay, R. 3-Propionyl-thiazolidine-4-carboxylic acid ethyl esters: a family of antiproliferative thiazolidines. *Med. Chem. Commun.*, **2015**, 6, 90-93.
- Berrada, M., Carriere, F., Abboud, Y., Abourriche, A., Benamara, A., Lajrhed, N., Kabbaj, M., Berrada, M. Preparation and characterization of new soluble benzimidazole-imide copolymers. *J. Mater. Chem.*, **2002**, 12, 3551-3559.
- Bodedla, G. B., Thomas, K. R. J., Fan, M. S., Ho, K. C. Benzimidazole-branched isomeric dyes: effect of molecular constitution on photophysical, electrochemical, and photovoltaic properties. *J. Org. Chem.*, **2016**, 81(2), 640-653.
- Camacho, C. C., Oviedo, I. R., Ortiz, A. G., Toscano, R. A., Sánchez, L. S., Cardenas, J., Muñoz, H. L. Tributyltin(IV) Schiff base complexes with amino acid derivatives: synthesis, characterization and biological activity. *Appl. Organometal. Chem.*, **2016**, 30, 199-207.
- Campbell, W. C. History of the discovery of sulfaquinoxaline as a coccidiostat. *J. Parasitol.*, **2008**, 94(4), 934-945.
- Castro, P. P., Zhao, G., Masangkay, G. A., Hernandez, C., Tunstad, L. M. G. Quinoxaline excision: A novel approach to tri- and diquinoxaline cavitands. *Org. Lett.*, **2004**, 6 (3), 333-336.
- Chang, D. W., Lee, H. J., Kim, J. H., Park, S. Y., Park, S. M., Dai, L., Baek, J. B. Novel quinoxaline-based organic sensitizers for dye-sensitized solar cells. *Org. Lett.*, **2011**, 13(15), 3880-3883.
- Cornish, A., Fox, K. R., Santikarn, S., Waring, M. J., Williams, D. H. Incorporation of fluorotryptophan into triostin antibiotics by *Streptomyces triostinicus*. *J. Gen. Microbiol.*, **1985**, 131, 561-570.
- Crowther, A. F., Curd, F. H. S., Davey, D. G., Stacey, G. J. Synthetic antimalarials. Part XXXIX. Dialkylaminoalkylaminoquinoxalines. *J. Chem. Soc.*, **1949**, 1260-1271.
- Dailey, S., Feast, W. J., Peace, R. J., Sage, I. C., Till, S., Wood, E. L. Synthesis and device characterization of side-chain polymer electron transport materials for organic semiconductor applications. *J. Mater. Chem.*, **2001**, 11, 2238-2243.
- Demmer, C. S., Møller, C., Brown, P. M. G. E., Han, L., Pickering, D. S., Nielsen, B., Bowie, D., Frydenvang, K., Kastrop, J. S., Bunch, L. Binding mode of an α -amino acid-linked quinoxaline-2,3-dione analogue as glutamate receptor subtype gluk1. *ACS Chem. Neurosci.*, **2015**, 6, 845-854.
- Deng, P. Y., Klyachko, V. A. Genetic upregulation of BK channel activity normalizes multiple synaptic and circuit defects in a mouse model of fragile X syndrome. *J. Physiol.*, **2016**, 594(1), 83-97.
- Faulkner, D. J. Marine Natural Products. *Nat. Prod. Rep.*, **1992**, 323-364.
- Fischer, O. Ueber Harmin und Harmalin. II *Berichte der deutschen chemischen Gesellschaft*, **1889**, 22(1), 637-645. <http://onlinelibrary.wiley.com/doi/10.1002/cber.188902201146/abstract>.

- Fleischmann, C., Lievenbrück, M., Ritter, H. Polymers and dyes: Developments and applications. *Polymers*, **2015**, 7, 717-746.
- Gupta, A., Singh, R., Sonar, P. K., Saraf, S. K. Novel 4-thiazolidinone derivatives as anti-infective agents: Synthesis, characterization, and antimicrobial evaluation. *Biochem. Res. Int.*, **2016**, Article ID 8086762, 8 pages. <http://dx.doi.org/10.1155/2016/8086762>.
- Hardwick, C. C., Herivel, T. R., Hernandez, S. C., Ruane, P. H., Goodrich, R. P. Separation, identification and quantification of riboflavin and its photoproducts in blood products using high-performance liquid chromatography with fluorescence detection: A method to support pathogen reduction technology. *Photochem. Photobiol.*, **2004**, 80, 609-615.
- Haworth, R. D., Robinson, S. Synthetic antimalarials. Part XX VII. Some derivatives of phthalaxine, quinoxaline, and isoquinoline. *J. Chem. Soc.*, **1948**, 777-782.
- Hegngi, F. N., Doerr, J., Cummings, T. S., Schwartz, R. D., Saunders, G., Zajac, A., Larsen, C. T., Pierson, F. W. The effectiveness of benzimidazole derivatives for the treatment and prevention of histomonosis (blackhead) in turkeys. *Veterinary Parasitol.*, **1999**, 81, 29-37.
- Hirose, Y., Watanabe, K., Minami, A., Nakamura, T., Oguri, H., Oikawa, H. Involvement of common intermediate 3-hydroxy-L-kynurenine in chromophore biosynthesis of quinomycin family antibiotics. *J. Antibiot.*, **2011**, 64, 117-122.
- Hughes, R. A., Moody, C. J. From amino acids to heteroaromatic-thiopeptide antibiotics, nature's heterocyclic peptides. *Angew. Chem. Int. Ed.*, **2007**, 46, 7930-7954.
- Ingle, R. G., Magar, D. D. Heterocyclic chemistry of benzimidazoles and potential activities of derivatives. *Int. J. Drug Res. Tech.*, **2011**, 1(1), 26-32.
- Jain, Z. J., Gide, P. S., Kankate, R. S. Biphenyls and their derivatives as synthetically and pharmacologically important aromatic structural moieties. *Arabian J. Chem.*, **2013**. <http://dx.doi.org/10.1016/j.arabjc.2013.07.035>.
- Jin, Z. Muscarine, imidazole, oxazole, and thiazole alkaloids. *Nat. Prod. Rep.*, **2011**, 28, 1143-1191.
- Johnson, H. E., Charleston, S., Va, W. Process for the preparation of 2-(acylamidoalkyl) benzimidazoles. US Patent US3255202, **1966**.
- Khokra, S. L., Choudhary, D. Benzimidazole, an important scaffold in drug discovery. *Asian J. Biomed. Pharm. Sci.*, **2011**, 3(1), 476-486.
- Kim, S. K., Ko, T., Choi, S. W., Park, J. O., Kim, K. H., Pak, C., Chang, H., Lee, J. C. Durable cross-linked copolymer membranes based on poly(benzoxazine) and poly(2,5-benzimidazole) for use in fuel cells at elevated temperatures. *J. Mater. Chem.*, **2012**, 22, 7194-7205.
- Kodama, M., Yamada, N., Sato, K., Kitamura, Y., Koyama, F., Sato, T., Morimoto, K., Kuroda, S. Effects of YM90K, a selective AMPA receptor antagonist, on amygdala-kindling and long-term hippocampal potentiation in the rat. *Eur. J. Pharmacol.*, **1999**, 374, 11-19.

- Koti, A. S. R., Bhattacharjee, B., Haram, N. S., Das, R., Periasamy, N., Sonawane, N. D., Rangnekar, D. W. Photophysics of some styryl thiazolo quinoxaline dyes in organic media. *J. Photochem. Photobiol. A.*, **2000**, 137, 115-123.
- Lieberman, L. A., Higgins, D. E. A small-molecule screen identifies the antipsychotic drug pimozide as an inhibitor of *Listeria monocytogenes* infection. *Antimicrob. Agents Chemother.*, **2009**, 53(2), 756-764.
- Loscher, W., Lehmann, H., Behl, B., Seemann, D., Teschendorf, H. J., Hofmann, H. P., Lubisch, W., Hoget, T., Lemaire, H., Grob, G. A new pyrrolyl-quinoxalinedione series of non-NMDA glutamate receptor antagonists: pharmacological characterization and comparison with NBQX and valproate in the kindling model of epilepsy. *Eur. J. Neurosci.*, **1999**, 11, 250-262.
- Malathi, M., Mohan, P. S., Butcher, R. J., Venil, C. K. Benzimidazole quinoline derivatives - An effective green fluorescent dye for bacterial imaging. *Can. J. Chem.*, **2009**, 87, 1692-1703.
- Mamada, M., Bolivar, C. P., Anzenbacher, P. Green synthesis of polycyclic benzimidazole derivatives and organic semiconductors. *Org. Lett.*, **2011**, 13(18), 4882-4885.
- Mănescu, I. G., Badea, G., Iscrulescu, L., Iovu, M., Balaci, T. Incorporation of new benzimidazole compounds into lipid nanostructures in order to obtain photoprotective formulations. *Farmacia*, **2015**, 63(4), 518-525.
- Mickevičienė, K., Baranauskaitė, R., Kantminienė, K., Stasevych, M., Porokhnyavets, O. K., Novikov, V. Synthesis and antimicrobial activity of *N*-substituted- β -amino acid derivatives containing 2-hydroxyphenyl, benzo[*b*]phenoxazine and quinoxaline moieties. *Molecules*, **2015**, 20, 3170-3189.
- Mu, P., Zheng, M., Xu, M., Zheng, Y., Tang, X., Wang, Y., Wu, K., Chen, Q., Wang, L., Deng, Y. *N*-Oxide reduction of quinoxaline-1,4-dioxides catalyzed by porcine aldehyde oxidase SsAOX1. *Drug Metab. Dispos.*, **2014**, 42(4), 511-519.
- Nageswar, Y. V. D., Reddy, K. H. V., Ramesh, K., Murthy, S. N. Recent developments in the synthesis of quinoxaline derivatives by green synthetic approaches. *Org. Prep. Proced. Int.*, **2013**, 45, 1-27.
- Nájera, C., Yus, M. Chiral benzimidazoles as hydrogen bonding organocatalysts. *Tetrahedron Lett.*, **2015**, 56, 2623-22633.
- Napoleon, A. A. Review on recent developments and biological activities of 2,4-thiazolidinediones. *Int. J. PharmTech Res.*, **2016**, 9(3), 429-443.
- O'Brien, D., Weaver, M. S., Lidzey, D. G., Bradley, D. D. C. Use of poly(phenyl quinoxaline) as an electron transport material in polymer light-emitting diodes. *Appl. Phys. Lett.*, **1996**, 69(7), 881-883.
- Olayiwola, G., Obafemi, C. A., Taiwo, F. O. Synthesis and neuropharmacological activity of some quinoxalinone derivatives. *Afr. J. Biotechnol.*, **2007**, 6(6), 777-786.
- Overman, J. D. W. Photographic emulsions and developers containing 2-mercapto heterocyclic compounds. US Patent US3785822, **1974**.

- Pânzariu, A. T., Apotrosoaei, M., Vasincu, L. M., Drăgan, M., Constantin, S., Buron, F., Routier, S., Profire, L., Tuchilus, C. Synthesis and biological evaluation of new 1,3-thiazolidine-4-one derivatives of nitro-1-arginine methyl ester. *Chem. Cent. J.*, **2016**, 10(6), 1-14.
- Phillips, M. A. The formation of 8-substituted benzimidazole. *J. Chem. Soc.*, **1928**, 2393-2399.
- Raghunath, M., Viswanathan, C. L. Benzimidazole-2-carbamic acid as a privileged scaffold for antifungal, anthelmintic and antitumor activity: A review. *Int. J. Pharm. Pharm. Sci.*, **2014**, 6(5), 17-25.
- Rehman, M., Imran, M., Arif, M., Farooq, M. Mannich base derivatives of benzimidazole: Synthesis & antimicrobial properties – A short review. *World Appl. Programming*, **2013**, 3(12), 558-564.
- Renault, J., Baron, M., Mailliet, P. Heterocyclic quinones. 2. Quinoxaline-5,6-(and 5,8)-diones-potential antitumoral agents. *Eur. J. Med. Chem.*, **1981**, 16(6), 545-550.
- Robert, T. S., Lobanov, M. V., Schugar, H. J., Potenza, J. A. A geometrically constraining bis(benzimidazole) ligand and its nearly tetrahedral complexes with Fe(II) and Mn(II). *Inorg. Chem.*, **2004**, 43, 1472-1480.
- Saito, I., Matsuura, T. Chemical studies on riboflavin and related compounds. I. oxidation of quinoxaline-2,3-diols as a possible model for the biological decomposition of riboflavin. *Biochem. J.*, **1967**, 6(11), 3602-3608.
- Sánchez, D. S., Baeza, A., Alonso, D. A. Organocatalytic asymmetric-chlorination of 1,3-dicarbonyl compounds catalyzed by 2-aminobenzimidazole derivatives. *Symmetry*, **2016**, 8(1), Article 3. 10 pages, doi:10.3390/sym8010003.
- Sascha, O., Faust, R. Quinoxalinodehydroannulenes: A novel class of carbon-rich materials. *Synlett*, **2004**, 9, 1509-1512.
- Sasaki, T., Kaneko, A. L-Glutamate-induced responses in OFF type bipolar cells of the cat retina. *Vision. Res.*, **1996**, 36(6), 787-795.
- Saxena, C. M., Saxena, A., Shukla, N. V. Synthesis and biological activities of some new amides of amino acid. *Am. Int. J. Res. Formal, Appl. Nat. Sci.*, **2014**, 7(1), 88-90.
- Seidl, A. H., Rubel, E. W., Barría, A. Differential conduction velocity regulation in ipsilateral and contralateral collaterals innervating brainstem coincidence detector neurons. *J. Neurosci.*, **2014**, 34(14), 4914-4919.
- Sessler, J. L., Maeda, H., Mizuno, T., Lynch, V. M., Furuta, H. Quinoxaline-bridged porphyrinoids. *J. Am. Chem. Soc.*, **2002**, 124 (45), 13474-13479.
- Sheraz, M. A., Kazi, S. H., Ahmed, S., Anwar, Z., Ahmad, I. Photo, thermal and chemical degradation of riboflavin. *Beilstein J. Org. Chem.*, **2014**, 10, 1999-2012.
- Si, W., Zhang, T., Li, Y., She, D., Pan, W., Gao, Z., Ning, J., Mei, X. Synthesis and biological activity of novel benzimidazole derivatives as potential antifungal agents. *J. Pest Sci.*, **2016**, 41(1), 1-5.
- Singh, R., P., Dhankar, R., Bhardwaj, S., Gupta, M., Kumar, R. Synthesis and antimicrobial studies of novel benzimidazole derivatives. *J. Appl. Pharm. Sci.*, **2011**, 1(4), 127-130.

- Srivastava, J. K., Awatade, N. T., Bhat, H. R., Kmit, A., Mendes, K., Ramos, M., Amaral, M. D., Singh, U. P. Pharmacological evaluation of hybrid thiazolidin-4-one-1,3,5-triazines for NF- κ B, biofilm and CFTR activity. *RSC Adv.*, **2015**, 5, 88710-88718.
- Takahashi, M., Kohara, A., Shishikura, J., Yatsugi, S. K., Ni, J. W., Yatsugi, S. I., Sakamoto, S., Okada, M., Sasamata, M. S., Yamaguchi, T. YM872: A selective, potent and highly water-soluble α -amino-3-hydroxy-5-methylisoxazole-4-propionic acid receptor antagonist. *CNS Drug Rev.*, **2002**, 8(4), 337-352.
- Tayebi, H., Bourazmi, H., Himmi, B., Assyry, A. E., Ramli, Y., Zarrouk, A., Geunbour, A., Hammouti, B. Combined electrochemical and quantum chemical study of new quinoxaline derivative as corrosion inhibitor for carbon steel in acidic media. *Der Pharma Chemica.*, **2014**, 6(5), 220-234.
- Tripathi, A. C., Gupta, S. J., Fatima, G. L., Sonar, P. K., Verma, A., Saraf, S. K. 4-Thiazolidinones: The advances continue. *Eur. J. Med. Chem.*, **2014**, 72, 52-77.
- Tozlu, C., Ela, S. E., Singh, T. B., Sariciftic, N. S., Icli, S. Comparative study of arylene bisimides substituted with imidazole side group for different dielectrics on the OFET application. *Synth. Met.*, **2013**, 172, 5-10.
- Vinay, V., Lakshika, K. A review on antimicrobial activity of 4-thiazolidinone derivatives. *Int. J. Res. Pharm. Sci.*, **2011**, 1(1), 17-27.
- Wright, J. B. The Chemistry of the Benzimidazoles. *Chem. Rev.*, **1951**, 48(3), 397-541.
- Wu, X., Gorden, A. E. V., Tonks, S. A., Vilseck, J. Z. Regioselective synthesis of asymmetrically substituted 2-quinoxalinol salen ligands. *J. Org. Chem.*, **2007**, 72(23), 8691-8699.
- Yoshida, T., Katagiri, K. Biosynthesis of the quinoxaline antibiotic, triostin, by *Streptomyces* s-2-210L. *Biochem. J.*, **1969**, 8(6), 2645-2651.
- Zarrok, H., Zarrouk, A., Salghi, R., Oudda, H., Hammouti, B., Touhami, M. E., Bouachrine, M., Pucci, O. H. A combined experimental and theoretical study on the corrosion inhibition and adsorption behavior of quinoxaline derivatives during carbon steel corrosion in hydrochloric acid. *Portugaliae Electrochim. Acta*, **2012**, 30, 405-417.
- Zhang, Y., Islam, M. A., McAlpine, S. R. Synthesis of the natural product marthiapeptide A. *Org. Lett.*, **2015**, 17, 5149-5151.
- Zuo, W., Zhang, Y., Xie, G., Gregor, D., Bekker, A., Ye, J. H. Serotonin stimulates lateral habenula *via* activation of the postsynaptic serotonin 2/3 receptors and transient receptor potential channels. *Neuropharmacol.*, **2016**, 101, 449-459.

Chapter 2. Advanced synthetic methods and pharmacological potential of quinoxaline derivatives

Abstract

Quinoxalines, including those with additional fused heterocyclic rings are an important class of compounds with diverse pharmacological properties such as anticancer, antiviral, antibacterial and antifungal properties amongst others. This review reports on the different methods used to synthesize quinoxalines and comments on the reactants used to produce different types of quinoxalines, together with proposed mechanisms for their synthesis. Modification at the 2, 3 and 6 positions of the basic quinoxaline core structure demonstrated good antibacterial and antifungal activity.

Keywords: quinoxaline, synthesis, mechanisms.

2.1 Introduction

Quinoxaline is a heterocyclic molecule containing a benzene ring fused to a pyrazine ring (**Figure 2-1**). It is also known as 1,4-diazanaphthalene or benzopyrine. The chemistry and pharmacological activity of quinoxalines have been recently reviewed (Ajani et al., 2014), which shows their potential to be used widely in the field of pharmacy and medicine. In addition, there have also been reports of them used in industrial applications (Kono et al., 2012; Keshtov et al., 2015).

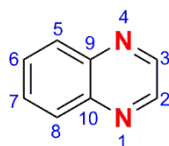


Figure 2-1 The general structure of a quinoxaline with nomenclature included

Quinoxaline derivatives possess a wide range of pharmacological properties such as antimicrobial (Alasmari et al., 2015; Chaudhary et al., 2015; Issa et al., 2015; Manchal et al., 2015), antifungal (Castro et al., 2015; Issa et al., 2015; Manchal et al., 2015), antioxidant (Manta et al., 2014; Burguete et al., 2011), anticancer (Neckel et al., 2015; Thabit et al., 2015; Ma et al., 2014, 2015), antidiabetic (Kulkarni et al., 2015), antitubercular (Puratchikody et al., 2011; Achutha et al., 2013), antimalarial (Chandra Shekhar et al., 2014), anti-inflammatory (Burguete et al., 2011), antiviral (Selvam et al., 2011; Henen et al., 2012), and anti-HIV (Gris et al., 2008). The quinoxaline framework was also part of various antibiotics such as echinomycin, levomycin and actinolutin, known to inhibit growth of Gram +ve bacteria (Katagiri et al., 1975).

In this review, we focus on the different routes for synthesizing quinoxaline molecules and highlight the reactants used in each of these routes. We also attempt to provide some mechanistic information on the formation of these molecules from their precursors.

2.2 Synthesis

A common procedure for the synthesis of these molecules makes use of *ortho* diamines, which undergo substitution or addition reactions with dicarbonyl compounds or carbonyl derivatives forming the quinoxalines (Ingle and Wadher, 2014; Chandra Shekhar et al., 2014; Alasmari et al., 2015; Demmer et al., 2015). Various carbonyl compounds such as oxalic acid (Pradeep et al., 2015; Thabit et al., 2015), pyruvic acid (Noolvi et al., 2011) and acetic acid (Kumar et al., 2013; Neckel et al., 2015) all result in different quinoxalines being formed, each with different groups at C-2 and C-3. In addition, quinoxalines were synthesized from α,β -unsaturated carbonyl compounds (Arimondo et al., 2001; Vekariya et al., 2003; Karki et al., 2009; Hossain et al., 2012; Manta et al., 2014), α -chloro carbonyl compounds (Gavara et al., 2010) and 1,4-dialdehydes (Diana et al., 2008; Parrino et al., 2015), all using *o*-phenylenediamines. There are also some miscellaneous routes to synthesizing quinoxalines, which involve nucleophilic substitution reactions of fluorinated nitrobenzenes and fluorinated amines (Moarbess et al., 2008; Khier et al., 2010). Quinoxaline *N*-oxides were also reported to be synthesized from benzofurazan (Ismail et al., 2010; Barea et al., 2013; Torres et al., 2013; Gil et al., 2014).

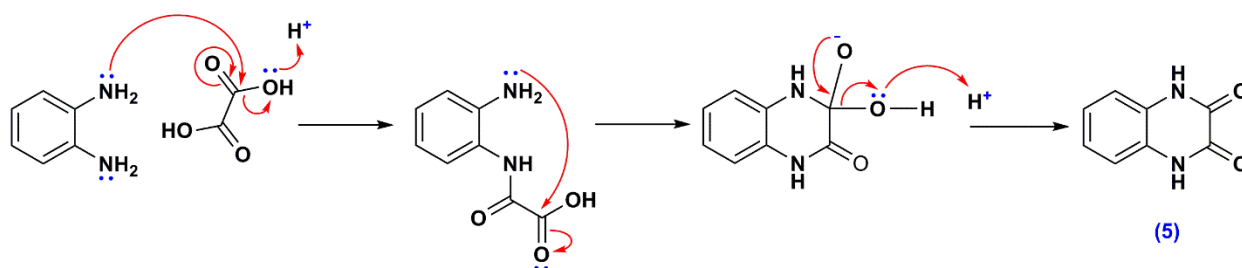
2.2.1 Quinoxalines synthesized from *o*-phenylenediamines and 1,2-dicarbonyl compounds

In this particular synthesis, the amino group first reacts with one carbonyl group by either a substitution reaction (if the leaving group is good) or an addition reaction (with a poor leaving

group). A second nucleophilic addition to the second carbonyl group in an intramolecular reaction leads to the formation of the quinoxaline.

2.2.2 The reaction of *ortho* diamines with 1,2-dicarbonyl compounds with leaving groups at both carbonyl centers

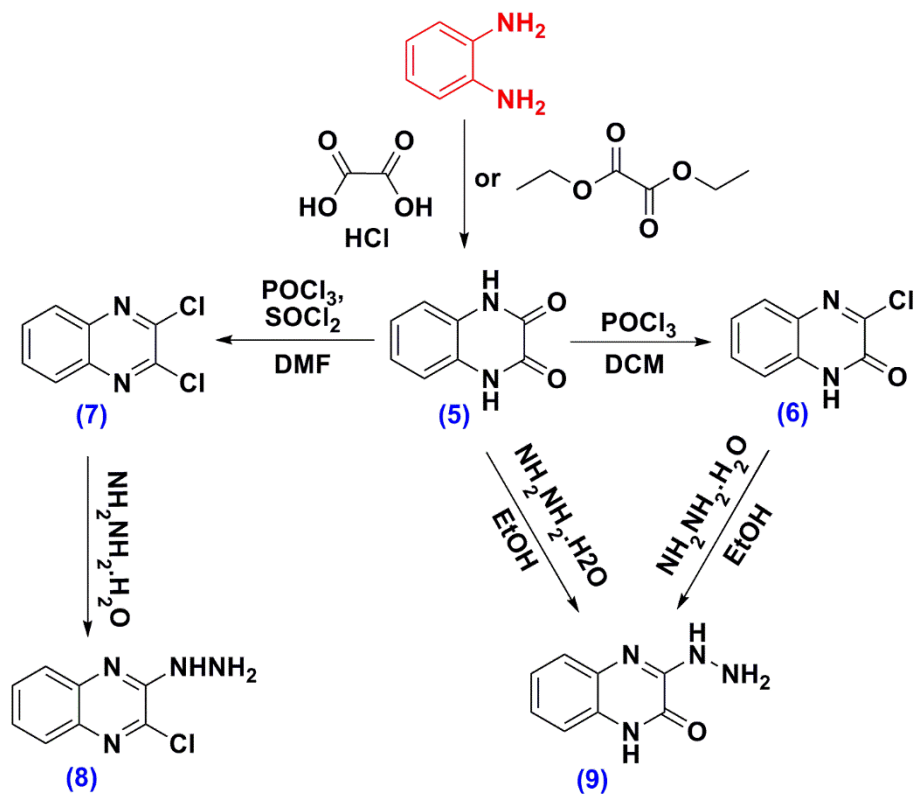
There have been several reports of quinoxalines being synthesized from oxalic acid resulting in quinoxaline-2,3-dione (**5**) (Alasmari et al., 2015; Thabit et al., 2015; Pradeep et al., 2015). These intermediates were synthesized en route to other quinoxaline derivatives, which make use of the reactivity of the two amide bonds formed in the reaction. The lone pair of the amine of the diamine initially adds to the carbonyl carbon of the carboxylic acid, forming the alkoxide anion, followed by the same mechanism occurring with the other amino group and carboxylic group, the latter being an intramolecular reaction. The hydroxyl group in the intermediate then picks up a proton, and reformation of the carbonyl group at C-2 occurs forming the quinoxaline-2,3-diones (**5**) (Scheme 2-1). The same mechanism takes place with diethyloxalate and this reagent can be used for the synthesis of quinoxaline-2,3-dione instead of oxalic acid (Demmer et al., 2015).



Scheme 2-1 Mechanism of synthesis of quinoxaline-2,3-diones (**5**)

Once formed, the intermediate **5** can be chlorinated at both C-2 and C-3 with phosphoryl chloride (POCl_3) in DCM or with POCl_3 and thionyl chloride (SOCl_2) leading to the 3-chloro-2-ketoquinoxaline (**6**) or dihalogenated quinoxaline (**7**). These halogenated quinoxalines can

then be substituted with strong bases for example hydrazine hydrate resulting in the hydrazine derivative **8** and **9** (**Scheme 2-2**) (Suresh et al., 2010; Galal et al., 2011, 2013; Alswah et al., 2013; Alasmari et al., 2015).

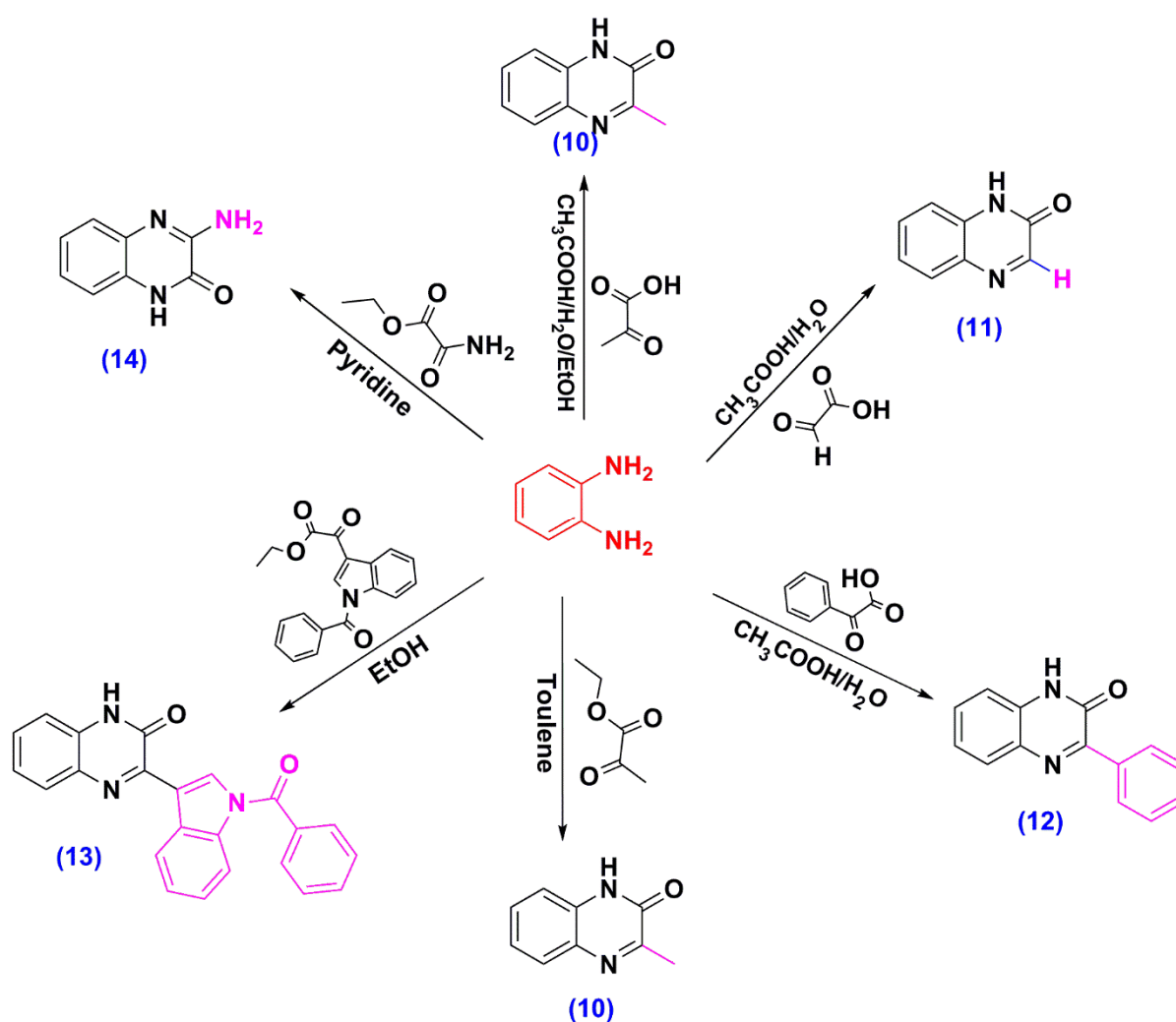


Scheme 2-2 Derivatization of quinoxaline-2,3-diones (5)

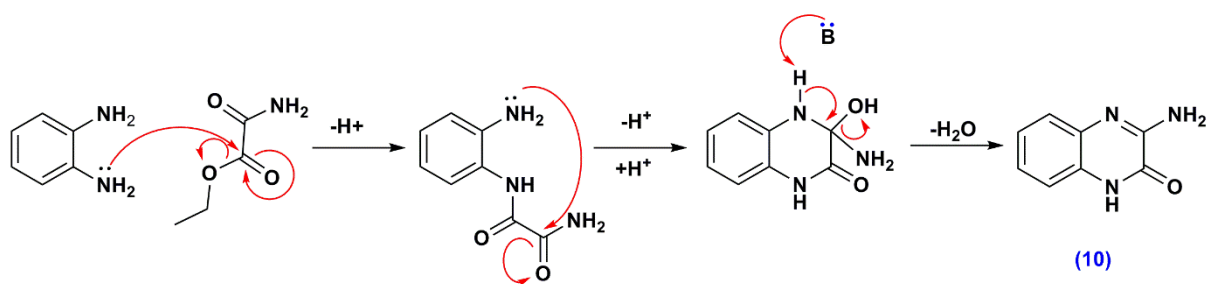
2.2.3 The reaction of *ortho* diamines with 1,2-dicarbonyl compounds with leaving groups at only one carbonyl centre

Pyruvic acid (Noolvi et al., 2011; Andres et al., 2013; Chaudhary et al., 2015), 2-oxoacetic acid (Rodrigues et al., 2014), 2-oxo-2-phenylacetic acid (Corona et al., 2008, 2009), ethyl-2-oxopropanoate (Andres et al., 2013), ethyl 2-(1-benzoyl-1*H*-indol-3-yl)-2-oxoacetate (El-Sawy et al., 2010) and ethyl oxamate (Galal et al., 2011) all have one good leaving group (or a hydroxyl group capable of being protonated) and one poor leaving group attached to each of the carbonyl centres (**Scheme 2-3**). After nucleophilic attack by the amino group of the diamino phenyl reagent, the leaving group departs from the tetrahedral intermediate after a

proton is abstracted from the secondary amine, forming an amide bond. Nucleophilic attack of the second amine intramolecularly results in a tetrahedral hydroxy intermediate, which undergoes elimination of water after a base abstracts a proton from the secondary amine, forming the imine. The product of the reaction with 1,2-dicarbonyl compounds with one leaving group is a 3-substituted quinoxaline-2-one (14) (Scheme 2-4).



Scheme 2-3 Reactions of *o*-diamine with one leaving group containing compound



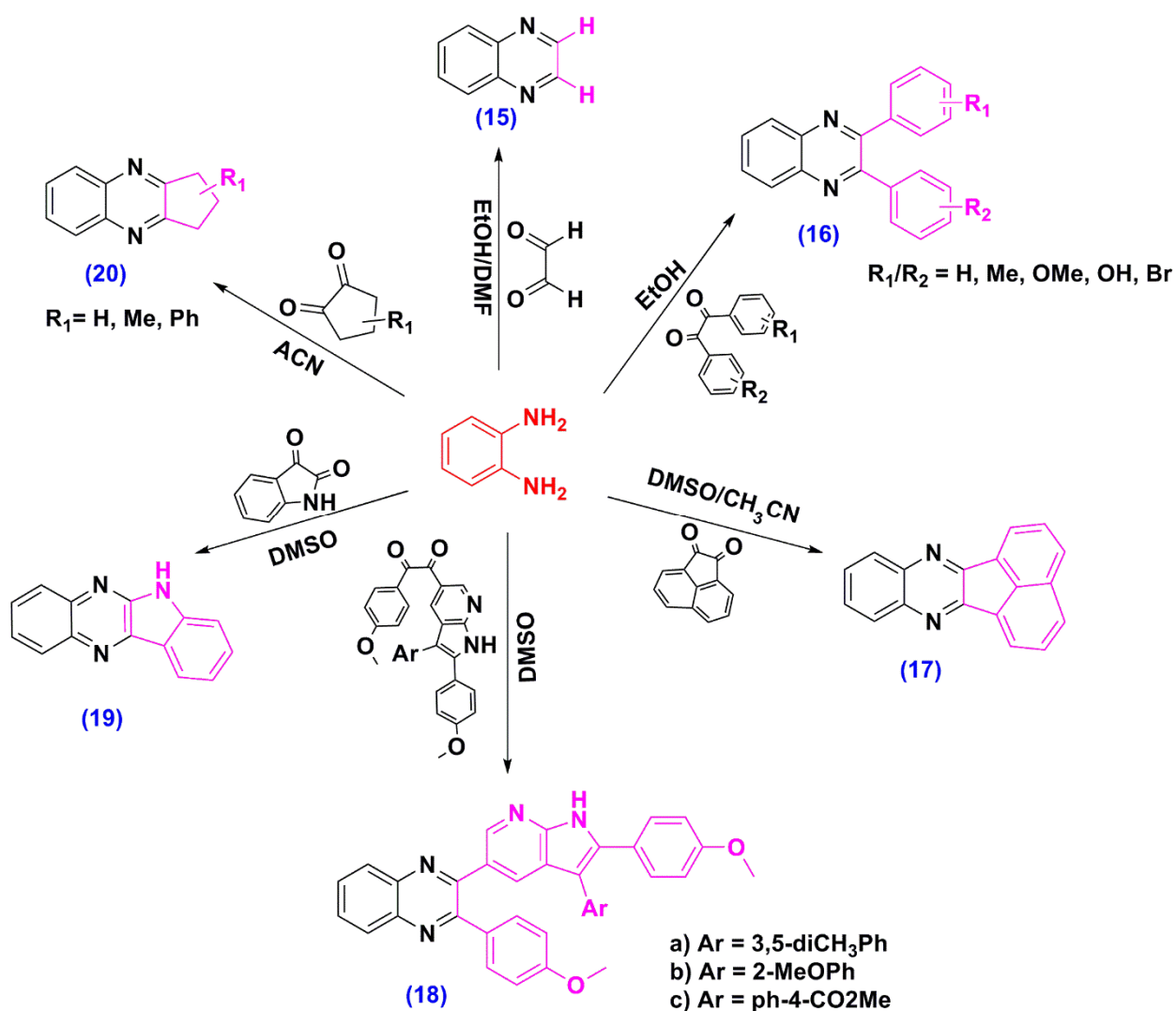
Scheme 2-4 Mechanism for synthesis of 3-aminoquinoxalin-2(1*H*)-one (**14**)

2.2.4 The reaction of *ortho* diamines with 1,2-dicarbonyl compounds with two poor leaving groups (1,2-diketones and 1,2-dialdehyde)

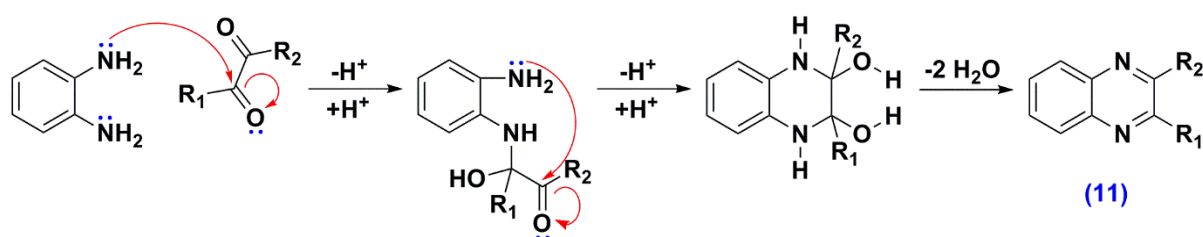
Two types of 1,2-diketones are reported to react with the diamines. The first consists of alkyl groups which are not joined together (open chain diketones) (Gavara et al., 2010; Isikdag et al., 2011; Rajule et al., 2012; Chandra Shekhar et al., 2014; Piras et al., 2014) and the second contains the diketone as part of a ring (mainly five membered and six membered rings) (Gavara et al., 2010; Isikdag et al., 2011; Alasmari et al., 2015).

Examples of these precursors to the quinoxalines include simple 1,2-diketones such as hexane-3,4-dione (Gavara et al., 2010) as well as aromatic diketones such as substituted benzils (Ingle and Marathe, 2012; Ingle et al., 2013; Ingle and Wadher, 2014). The substituents on the dicarbonyl compound could even be heterocyclic rings such as pyrrolopyridine (Leboho et al., 2015). When the diacarbonyl compounds are contained in heterocyclic rings such as indoline-2,3-dione (Arimondo et al., 2001; Karki et al., 2009; Sridevi et al., 2011; Hossain et al., 2012; Srinivas et al., 2013) or carbocyclic rings such as cyclopentane-1,2-diones (Gavara et al., 2010; Alasmari et al., 2015), a heterocyclic or carbocyclic ring occurs at the 2 and 3 positions of the quinoxaline molecule after addition of the diamine (**Scheme 2-5**).

The mechanism for these reactions consist of the amino groups adding to the carbonyl carbon, forming an alcohol after which the same mechanism occurs intramolecularly to form the quinoxalines. Elimination of two water molecules results in the formation of the substituted quinoxaline molecule (15) (Scheme 2-6), with both substituents adjacent to the carbonyl groups retained after imine formation. With glyoxal (Melero et al., 2004; Huang et al., 2009; Mielcke et al., 2012; Neckel et al., 2015), butenedioane (Melero et al., 2004), a two-carbon compound containing two aldehyde groups (Melero et al., 2004), an unsubstituted quinoxaline occurs where R₁ and R₂ is hydrogen (Scheme 2-6).



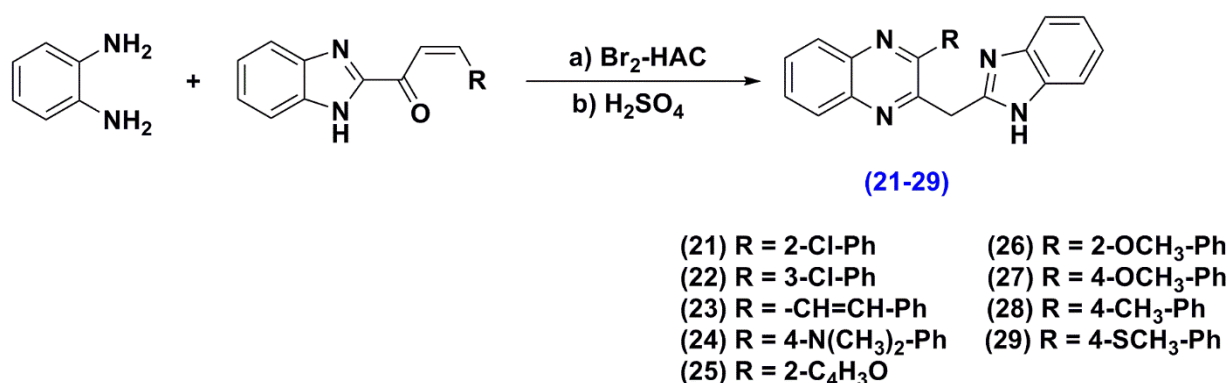
Scheme 2-5 Reactions of *o*-diamine with two poor leaving group-containing compound



Scheme 2-6 Mechanism of formation of quinoxaline (15)

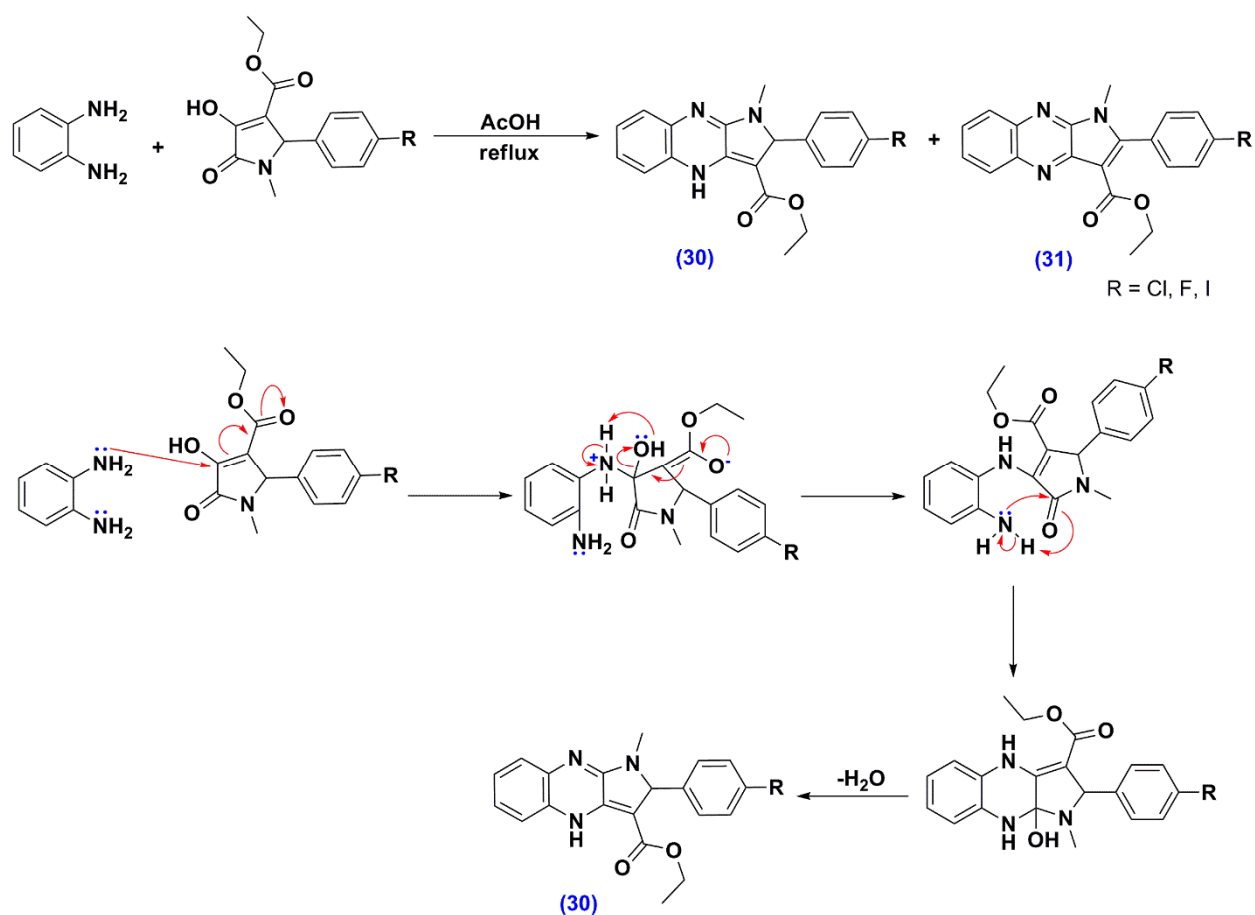
2.2.5 The reaction of diamines with α,β -unsaturated carbonyl compounds

There are two reports of quinoxalines forming from α,β -unsaturated carbonyl compounds, however the mechanisms for these reactions are not clear. In the first instance, bromoacetic acid is used together with the α,β -unsaturated carbonyl compound producing a quinoxaline where the two nitrogen atoms from the diamine add across the double bond and the carbonyl group is reduced in the process. It is reported that the product forms through a dibromo intermediate, but this is not further clarified (Vekariya et al., 2003). This leads to the quinoxalines **21-29** in **Scheme 2-7**.



Scheme 2-7 Synthesis of benzimidazole fused quinoxaline compounds (21-29)

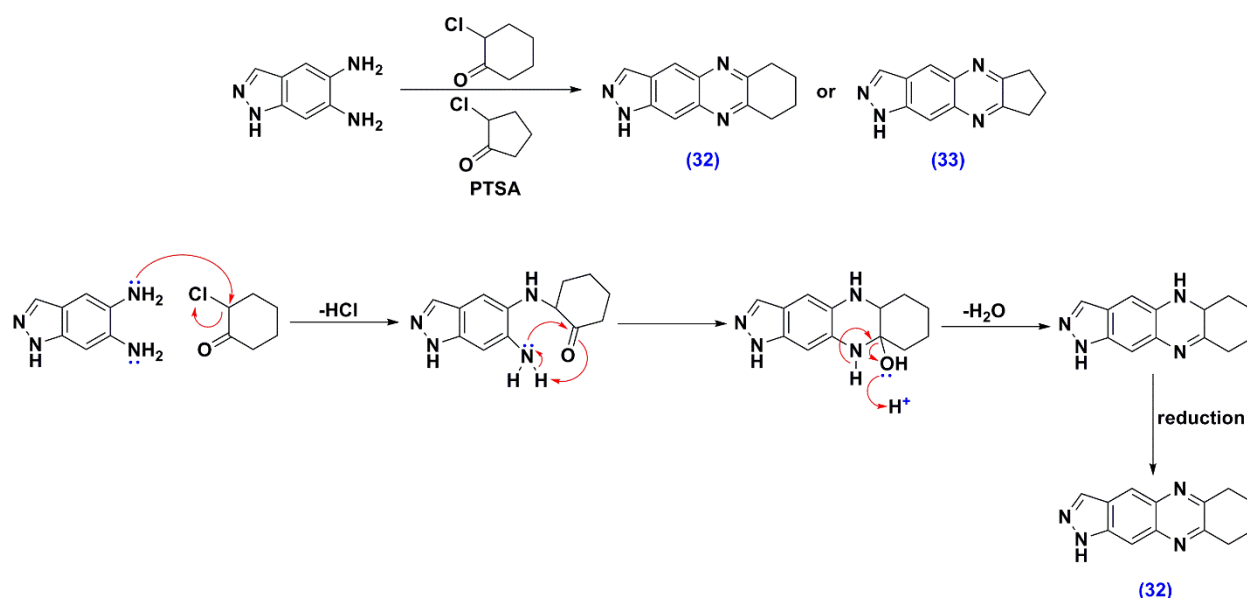
The second example contains an α,β -unsaturated amide group reacting with a hydroxy and ester substituted double bond in the reagent. A complete mechanism is not reported in the literature (Manta et al., 2014), however it is proposed that **30** occurs through a nucleophilic attack on the α -carbon of the double bond, resulting an enolate ion, which eliminates H_2O on reformation of the α,β -unsaturated group, placing the double bond adjacent to the ester carbonyl. A second nucleophilic attack on the amide carbonyl and elimination of water leads to the quinoxalines **30** (Scheme 2-8). Compound **31** is formed by reduction since this is energetically favourable due to the formation of a fully conjugated system.



Scheme 2-8 Synthesis and mechanism of pyrrolo quinoxaline

2.2.6 The reaction of diamines with α -chloro ketones

The reaction of diamines with α -chloro ketones probably occurs *via* a direct nucleophilic substitution of the chloro group with an amino group of the diamine followed by nucleophilic attack by the second amino group on the carbonyl carbon producing an aminol, which dehydrates to an imine forming the quinoxaline **32**. PTSA is used as a catalyst in the reaction. The products reported in Gavara et al. (2010) is speculated to be due to a subsequent reduction step after formation of the quinoxaline, since formation of **32** leads to aromaticity into the nitrogen-containing ring (**Scheme 2-9**) (Gavara et al., 2010).



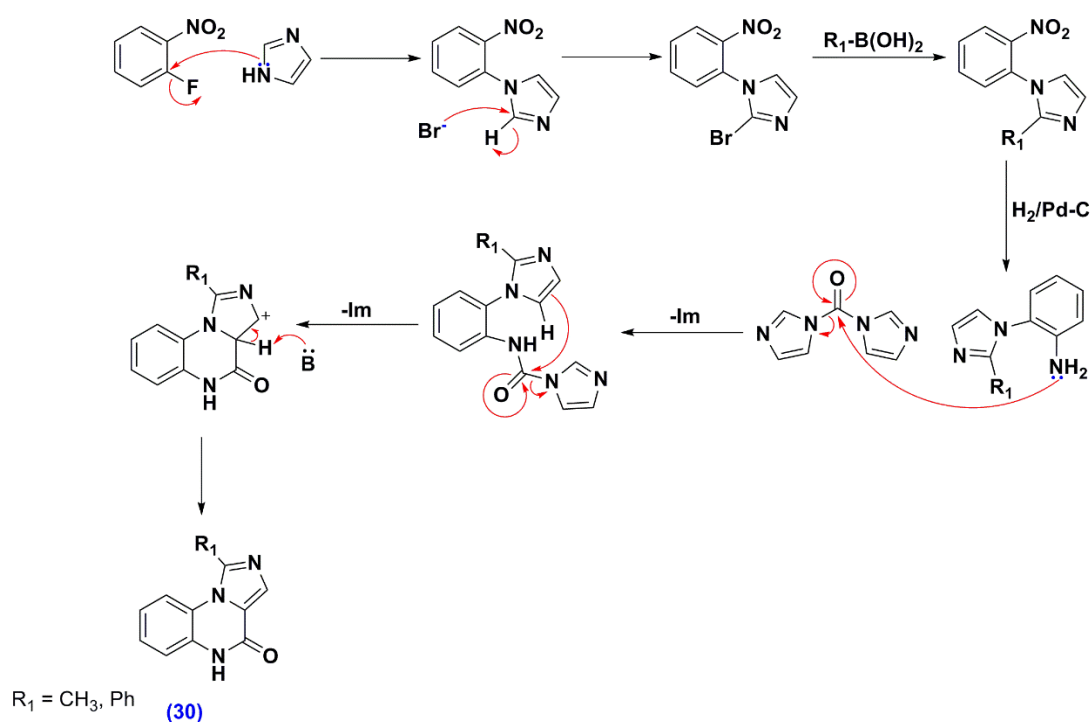
Scheme 2-9 Synthesis and mechanism of pyrazolo quinoxalines

2.2.7 Formation of quinoxalines by nucleophilic substitution of *ortho* nitrofluorobenzenes and *ortho* aminofluorobenzenes

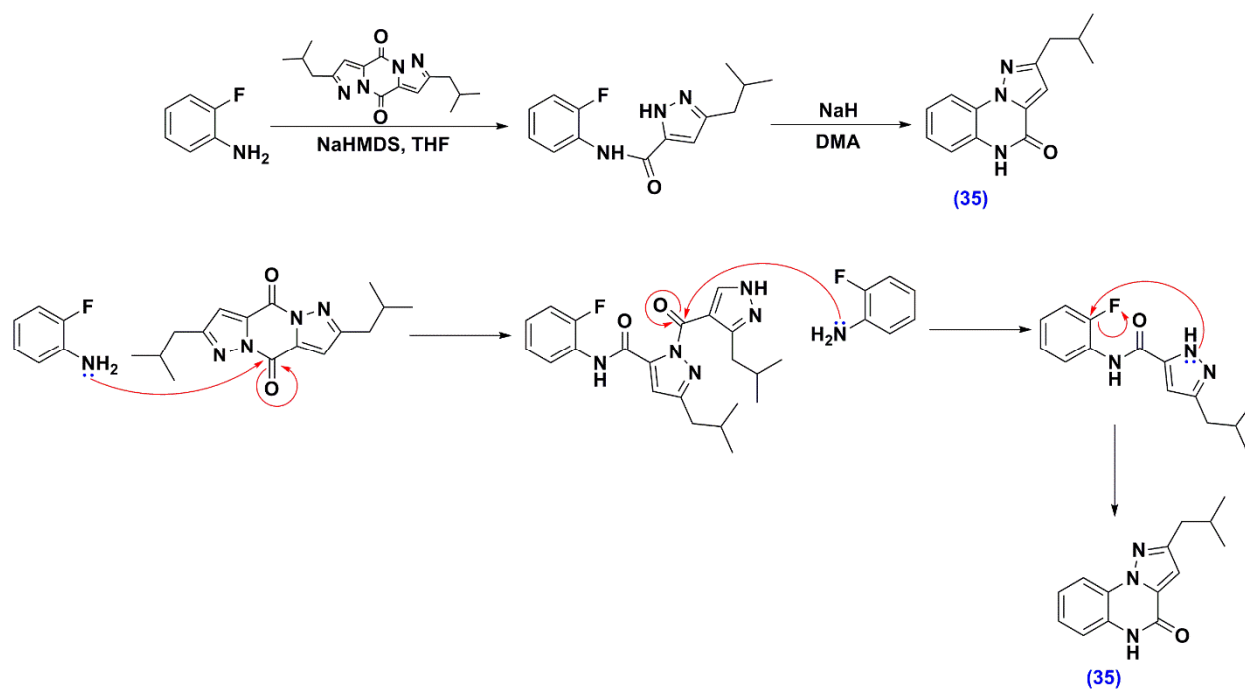
Ortho nitrofluorobenzenes were subjected to a nucleophilic substitution reaction with imidazole. Reduction of the nitro group to the amine follows and then formation of the quinoxaline with di-imidazolymethanone. This occurred by attack of the amine on the di-imidazolymethanone carbonyl group with a concomitant loss of one imidazole group and then

an intramolecular attack on the same carbonyl group by the imidazolyl group *ortho* to the amide resulting in formation of the quinoxaline (**34**) and departure of the second imidazole group (Scheme 2-10) (Moarbess et al., 2008).

With imidazole and pyrazole dimers formed through their carboxylic acids, the amino group of the *ortho* aminofluorobenzene attacks the carbonyl group of the dimer resulting in cleavage of the imidazole group. Attack at the other carbonyl group in a similar fashion leads to two molecules of the fluorinated intermediate being formed. The imidazole nitrogen then replaces the fluorine on the aromatic ring leading to formation of the quinoxalines (**35**) (Scheme 2-11) (Moarbess et al., 2008; Khier et al., 2010).



Scheme 2-10 Mechanism of formation of imidazole quinoxaline (**34**)



Scheme 2-11 Synthesis and mechanism of pyrazolo quinoxaline (35)

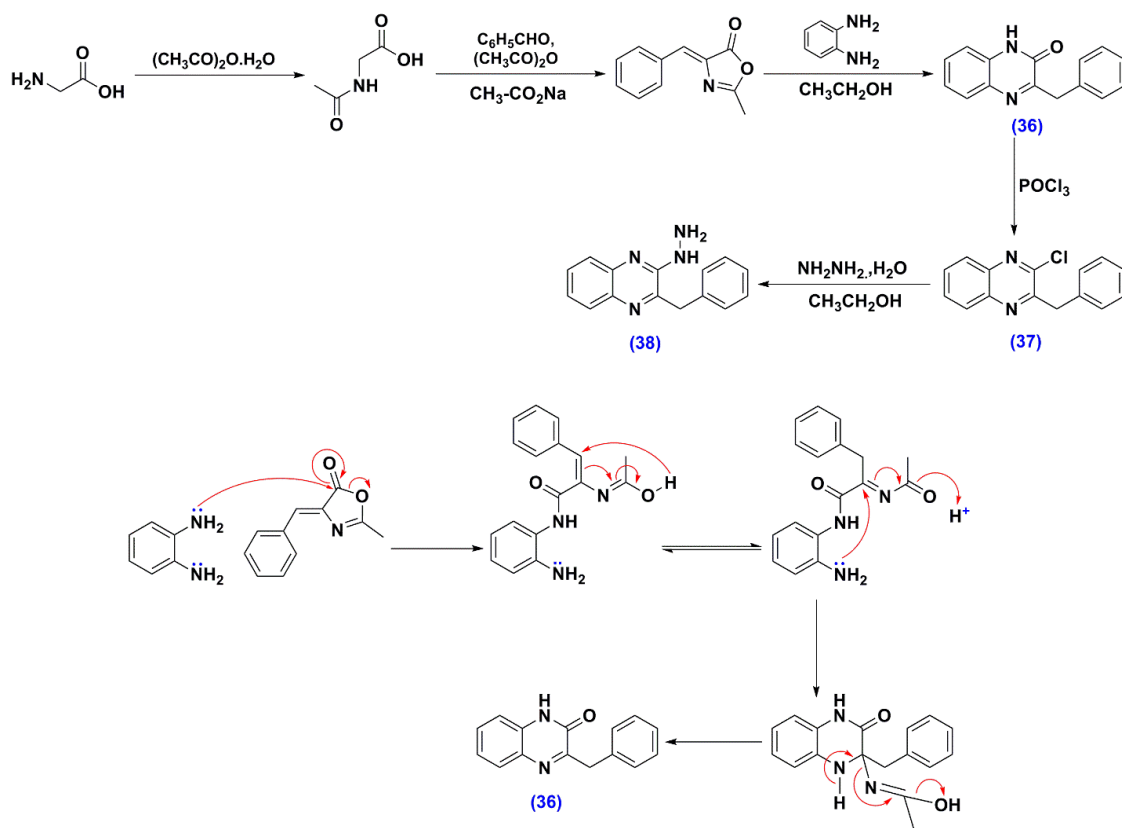
2.2.8 Reaction of azalactones with diamines

The cinnamate azalactone was prepared by the reaction of *N*-acetyl glycine with benzaldehydes, which when added to the *ortho* diamine forms quinoxaline (36) (Issa et al., 2015). It is speculated that the reaction occurs through a nucleophilic attack by the amine on the lactone carbonyl, which rearranges to the keto tautomer before attack on the imine carbon occurs by a pictet-spengler like reaction. Removal of an acetonitrile group then leads to the quinoxaline 36 (**Scheme 2-12**).

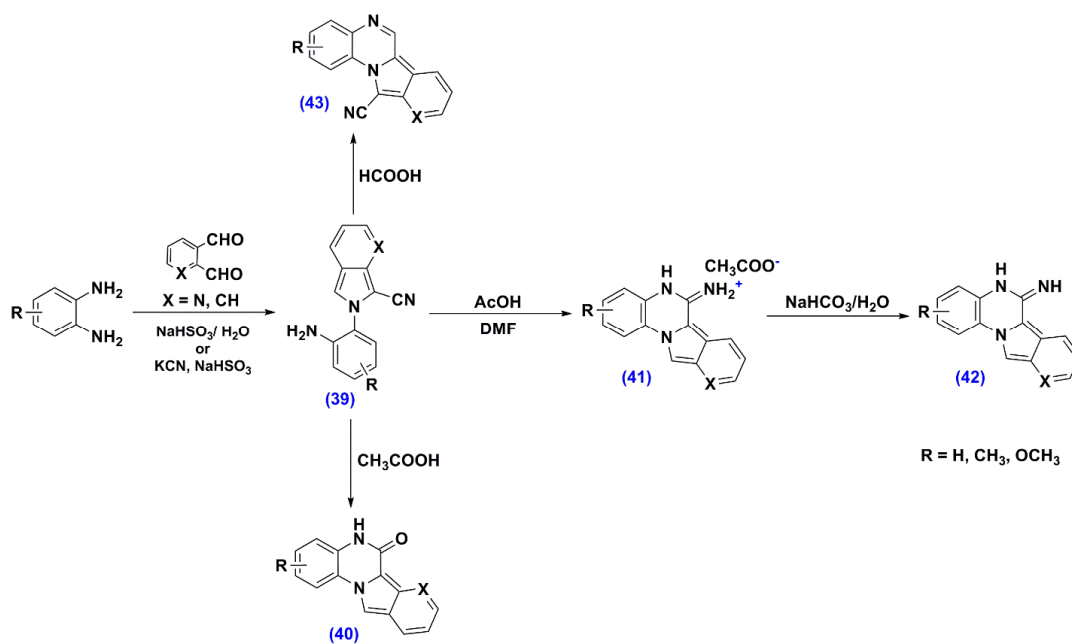
2.2.9 Reaction of 1,2-dialdehydes with diamines

Diamines react with 1,2-dialdehydes in the presence of a cyanide ion and acid, producing a cyano intermediate (39) which further cyclises to three different quinoxalines (40-43) (**Scheme 2-13**) (Diana et al., 2008; Parrino et al., 2015). In the synthesis of the intermediate, one of the amino groups first adds to the aldehyde forming an imine, which is activated by acid and

attacked by a cyanide ion. The secondary amine formed then attacks the second aldehyde resulting in pyrrole formation to which a nitrile is attached (**39**) (**Scheme 2-14**).

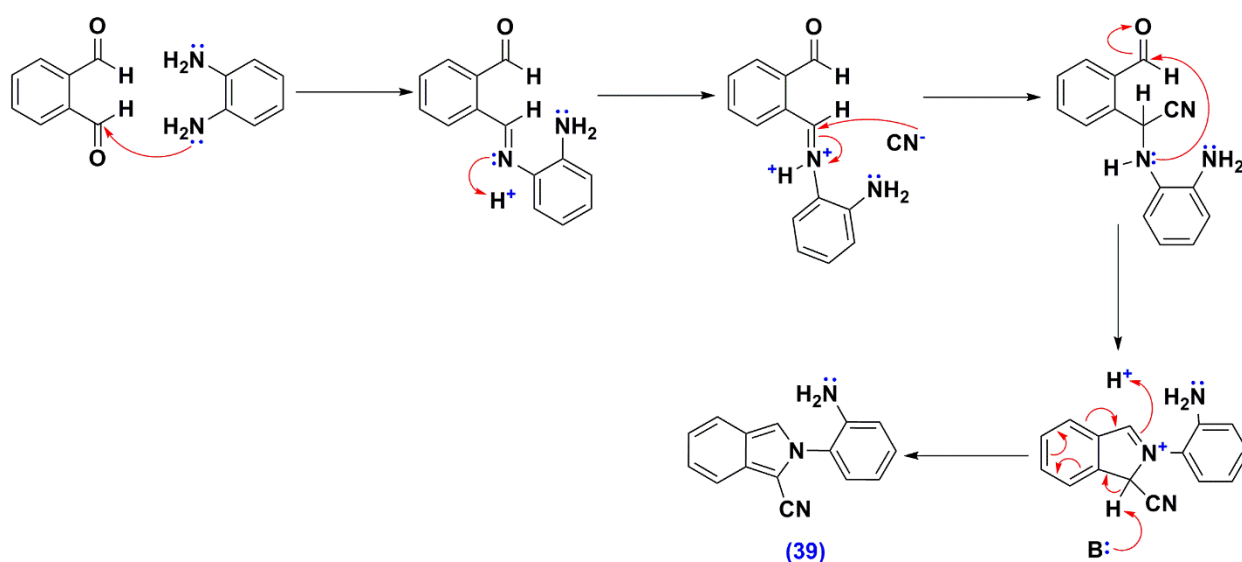


Scheme 2-12 Reaction and mechanism of quinoxaline *via* azalactones with diamines

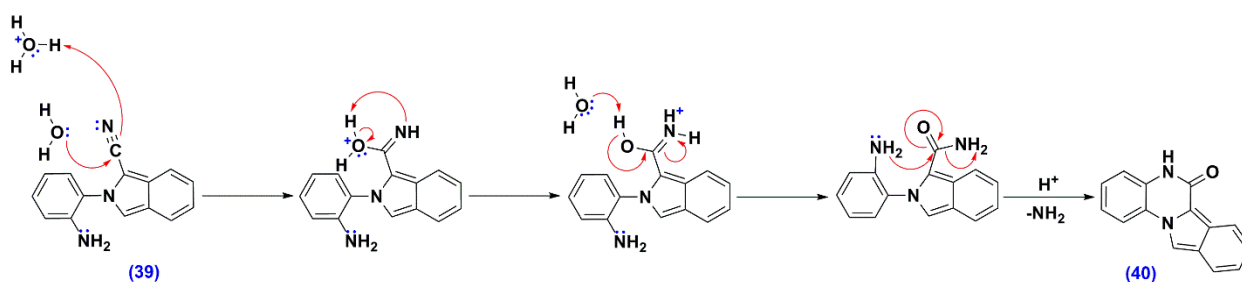


Scheme 2-13 Synthesis of quinoxalines from 1,2-dialdehydes with diamines

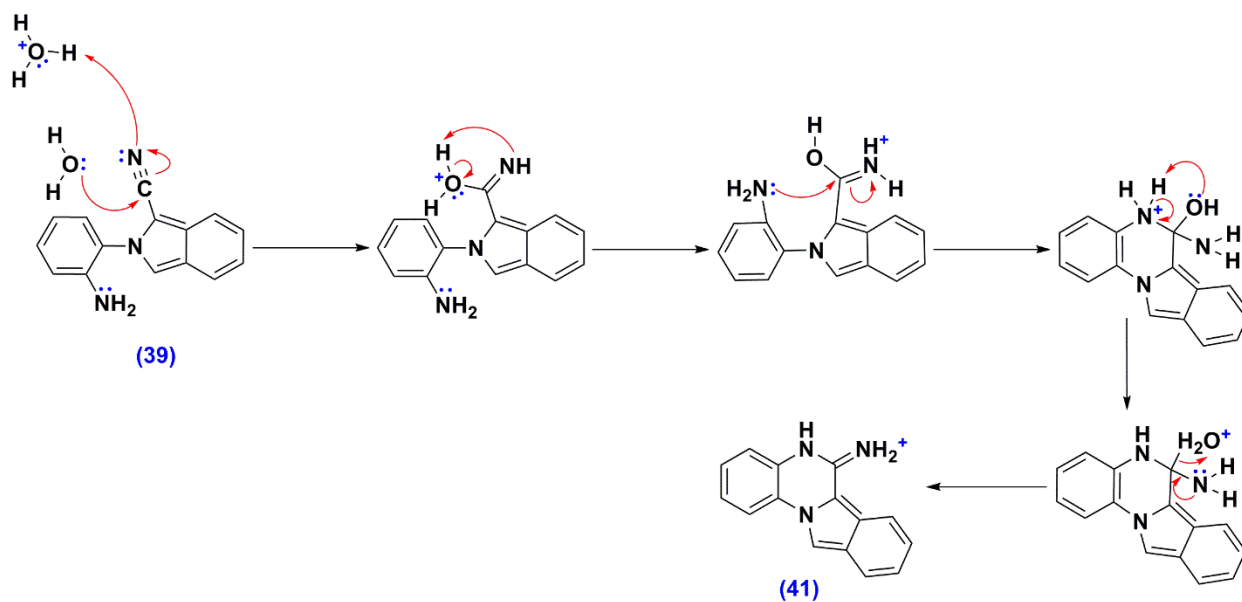
In formation of the first quinoxaline (**40**), H₂O adds to the nitrile carbon and the nitrile nitrogen is protonated by acid, resulting in an imide, which is further protonated, resulting in collapse of the imide to the amide. Intramolecular amide formation then occurs under acidic conditions, hydrolysing the free amide and forming a cyclic amide resulting in the quinoxaline (**40**) (Scheme 2-15). In the second quinoxaline (**41**), collapse of the imide to the amide does not occur, but instead the second amino group adds to the activated iminium carbon, forming the quinoxaline after elimination of water, resulting in an iminium quinoxaline (**41**) (Scheme 2-16).



Scheme 2-14 Mechanism of preparation of intermediate (**39**)

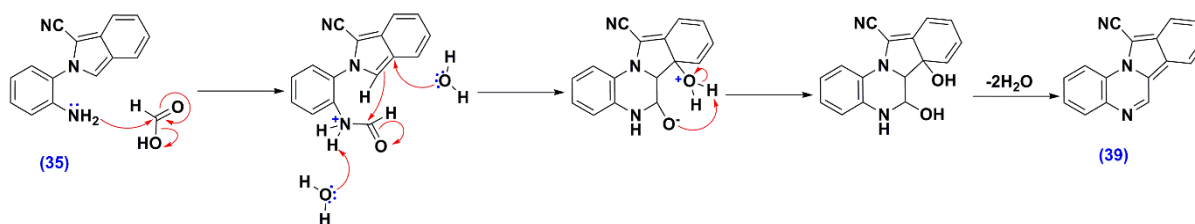


Scheme 2-15 Mechanism of formation of quinoxaline (**40**)



Scheme 2-16 Mechanism of formation of quinoxaline (41)

The third quinoxaline forms by the amine of the nitrile intermediate (39) reacting with formic acid and producing a protonated intermediate to which a water molecule adds resulting in ring closure. Loss of two water molecules leading to the stable aromatic quinoxaline (43) then occurs (Scheme 2-17).

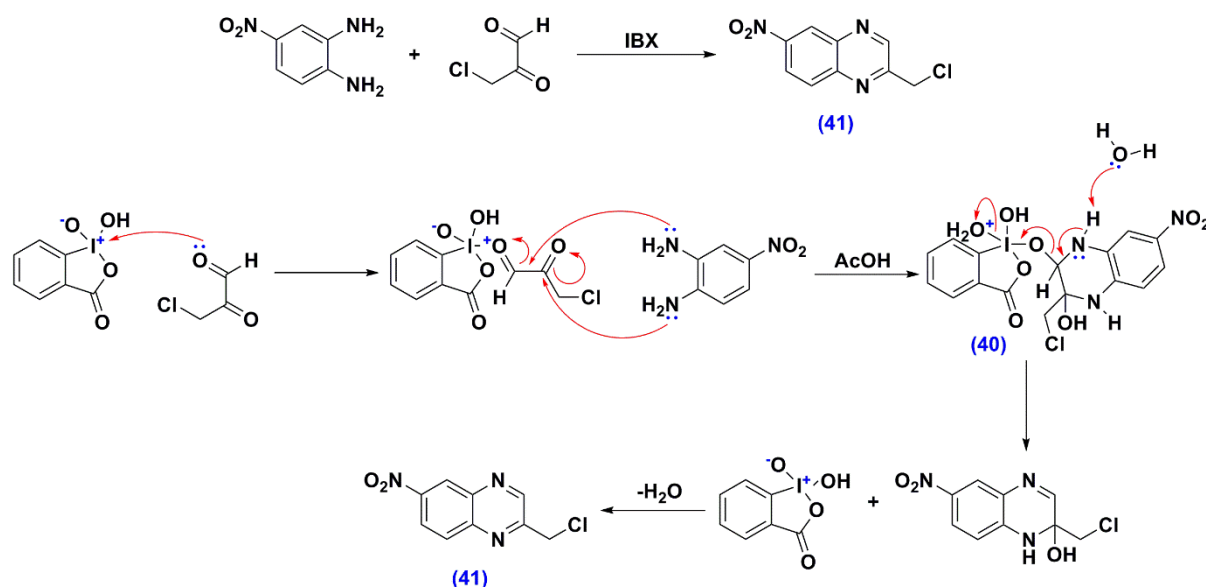


Scheme 2-17 Mechanism of formation of quinoxaline (43)

2.2.10 Reaction of diamines with 3-chloro-2-oxopropanal and iodoxybenzoic acid

3-chloro-2-oxopropanal and iodoxybenzoic acid first reacts to activate the aldehydic carbonyl group. Thereafter the two amino groups attack each of the carbonyl groups forming a hydroxy

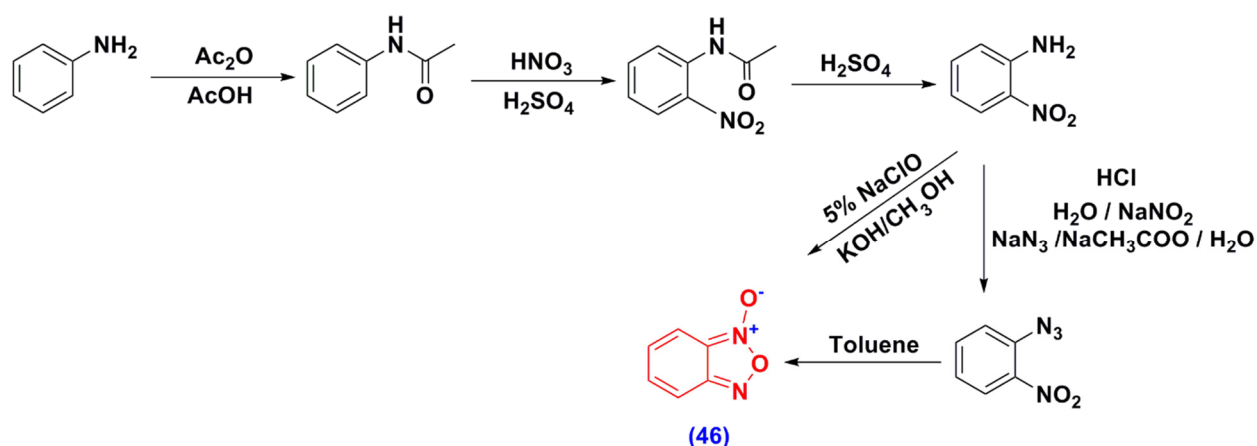
intermediate (**44**). The first double bond forms when the iodo complex is eliminated and the quinoxaline (**45**) forms after the elimination of water (**Scheme 2-18**) (Elshihawy et al., 2013).



Scheme 2-18 Mechanism for synthesis of quinoxaline using IBX

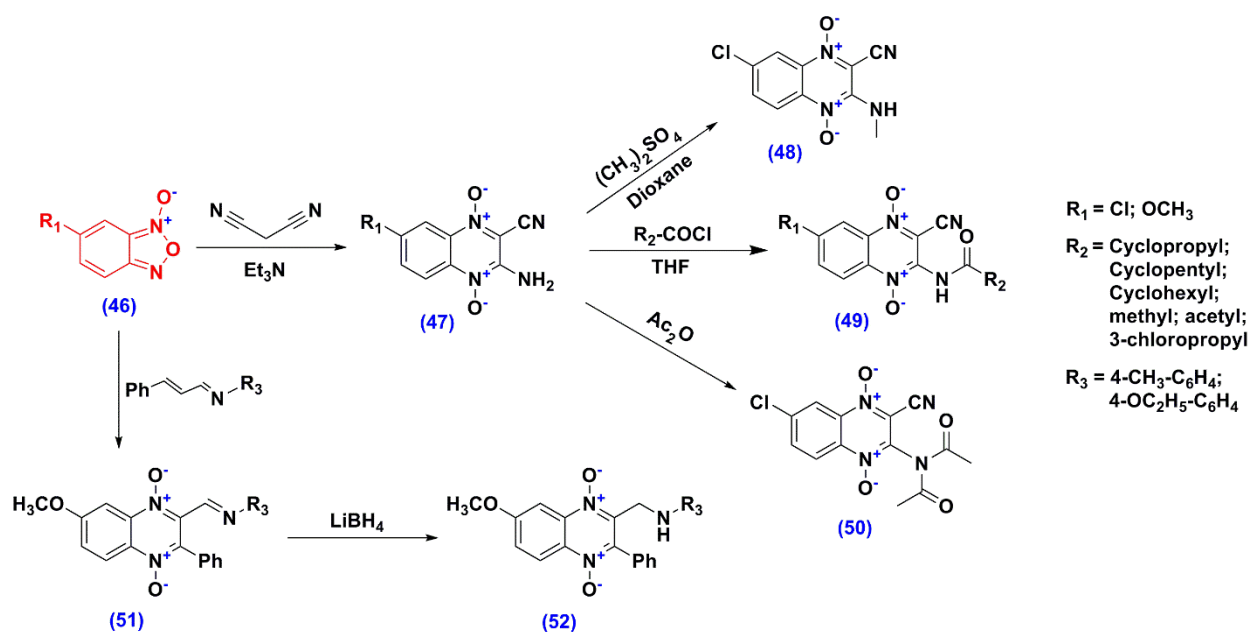
2.2.11 Synthesis of 1,4-di-*N*-oxide quinoxaline derivatives

The benzofurazan oxide **46** is an important intermediate in the synthesis of 1,4-di-*N*-oxide quinoxaline derivatives, which can react with nitrile, carbonyl or dicarbonyl compounds with acidic α hydrogens or with conjugated double bonds. This benzofurazan oxide (**46**) intermediate was synthesized from 2-nitroaniline by reacting it with either sodium nitrite, sodium azide (Monge et al., 1995) or sodium hypochlorite (Sheng et al., 2007) (**Scheme 2-19**). 2-Nitroaniline is commercially available, however it can also be synthesized from aniline by first protecting the aniline and then nitrating it. Depending on the reagent used, different functionalities become available on the quinoxaline ring, which can be reacted further to create a multitude of organic products. Some of these reactions are shown in **Scheme 2-20** to **Scheme 2-24**.



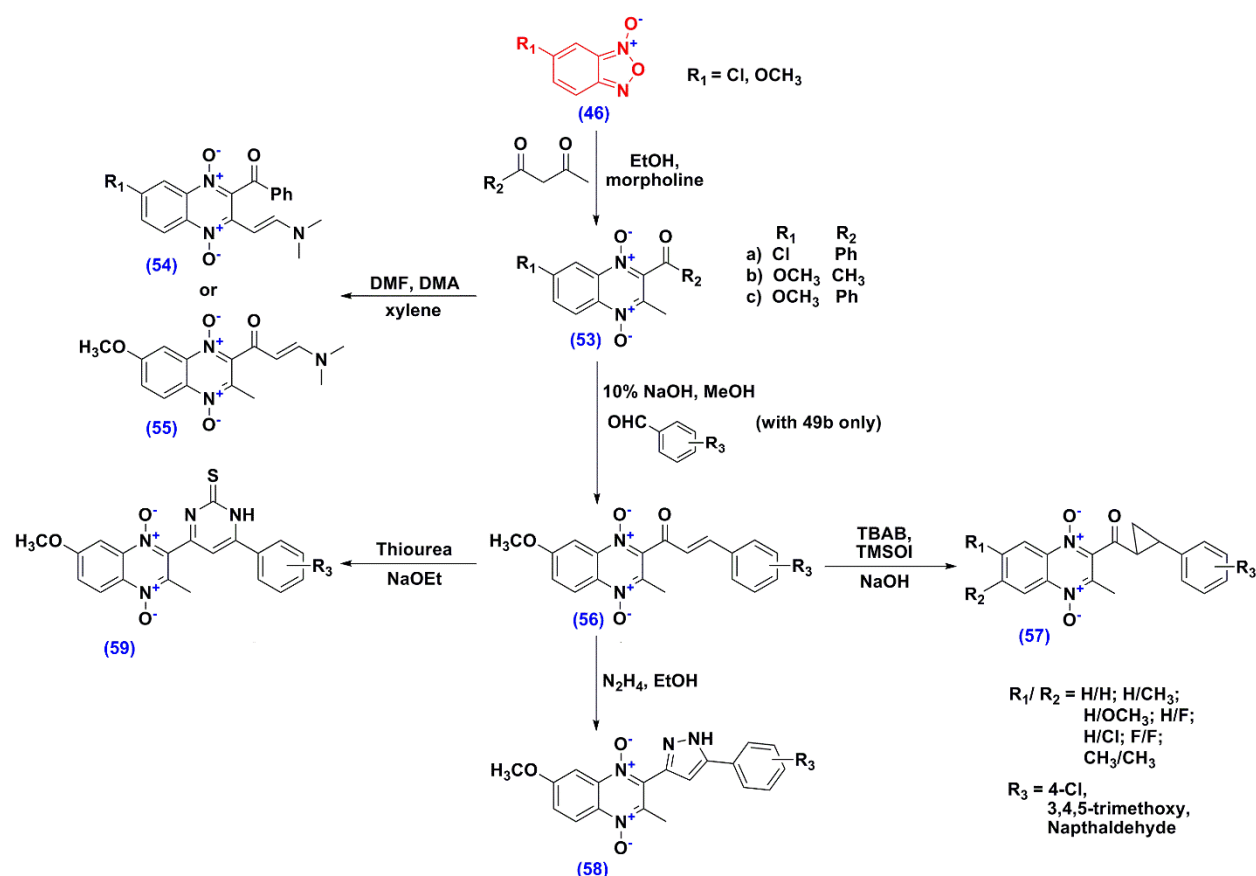
Scheme 2-19 Synthesis of benzofurazan oxide (**46**)

By the reaction of **46** with malonitrile, *N*-oxide quinoxalines **47** (Monge et al., 1995) with cyano and amino groups result where the amino group is reacted further with dimethyl sulphoxide producing *N*-methyl derivatives **48** (Ismail et al., 2010), acid chlorides producing *N* acyl derivatives **49** (Barea et al., 2013) and acetic anhydride producing *N* acetyl derivatives **50** (Ismail et al., 2010) (**Scheme 2-20**). With styrene imines, the intermediate **46** produces *N*-oxide quinoxalines with imino groups **51**, which can be reduced with LiBH_4 to yield amines **52** (**Scheme 2-20**) (Ismail et al., 2010).



Scheme 2-20 Synthesis of *N*-oxide quinoxaline derivatives

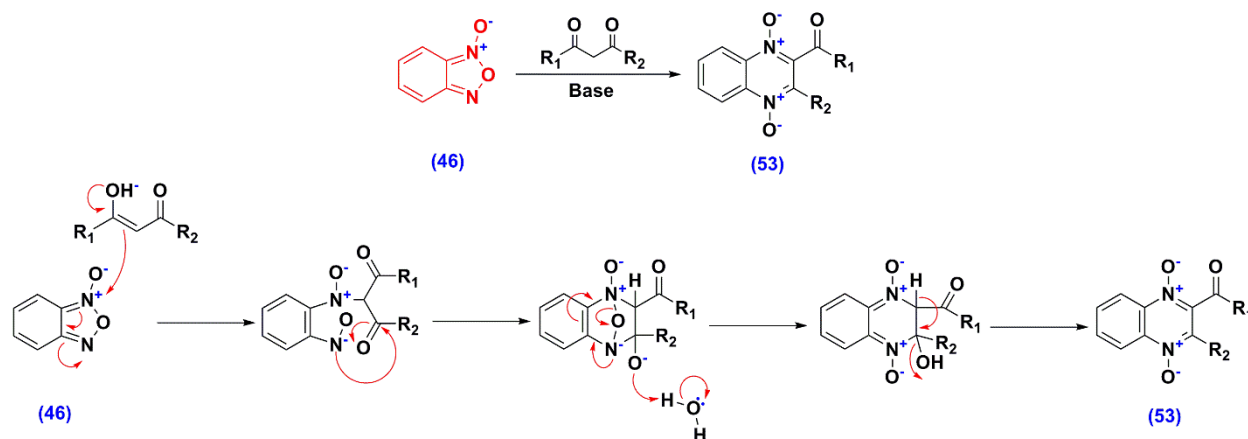
Substituted 2-keto-3-methylquinoxaline-1,4-dioxides (**53**) were prepared by the Beirut reaction (reacting 1,3-dicarbonyl compounds, ethanol, morpholine and the benzofurazan oxide **46**). These intermediates were further reacted with DMA (a strong base) and DMF in xylene yielding the enamines (**54**) or the enaminone derivative (**55**). The intermediate quinoxaline-*N*-oxide acetophenone (**53b**) underwent Claisen-Schmidt condensation reactions with various substituted aldehydes yielding chalcones (**56**) which were used as precursors for the synthesis of three, five and six membered cyclic compounds **57**, **58** and **59** respectively (Amin et al 2006; Gil A et al., 2014) (Scheme 2-21).



Scheme 2-21 Synthesis of different *N*-oxide quinoxaline derivatives

The mechanism of the Beirut reaction involves the enol form of the 1,3-dicarbonyl compound attacking the electrophilic *N*-oxide nitrogen of the benzofurazan *N*-oxide (**46**), forming an anion on the other nitrogen, which subsequently adds to the carbonyl of the ketone forming an

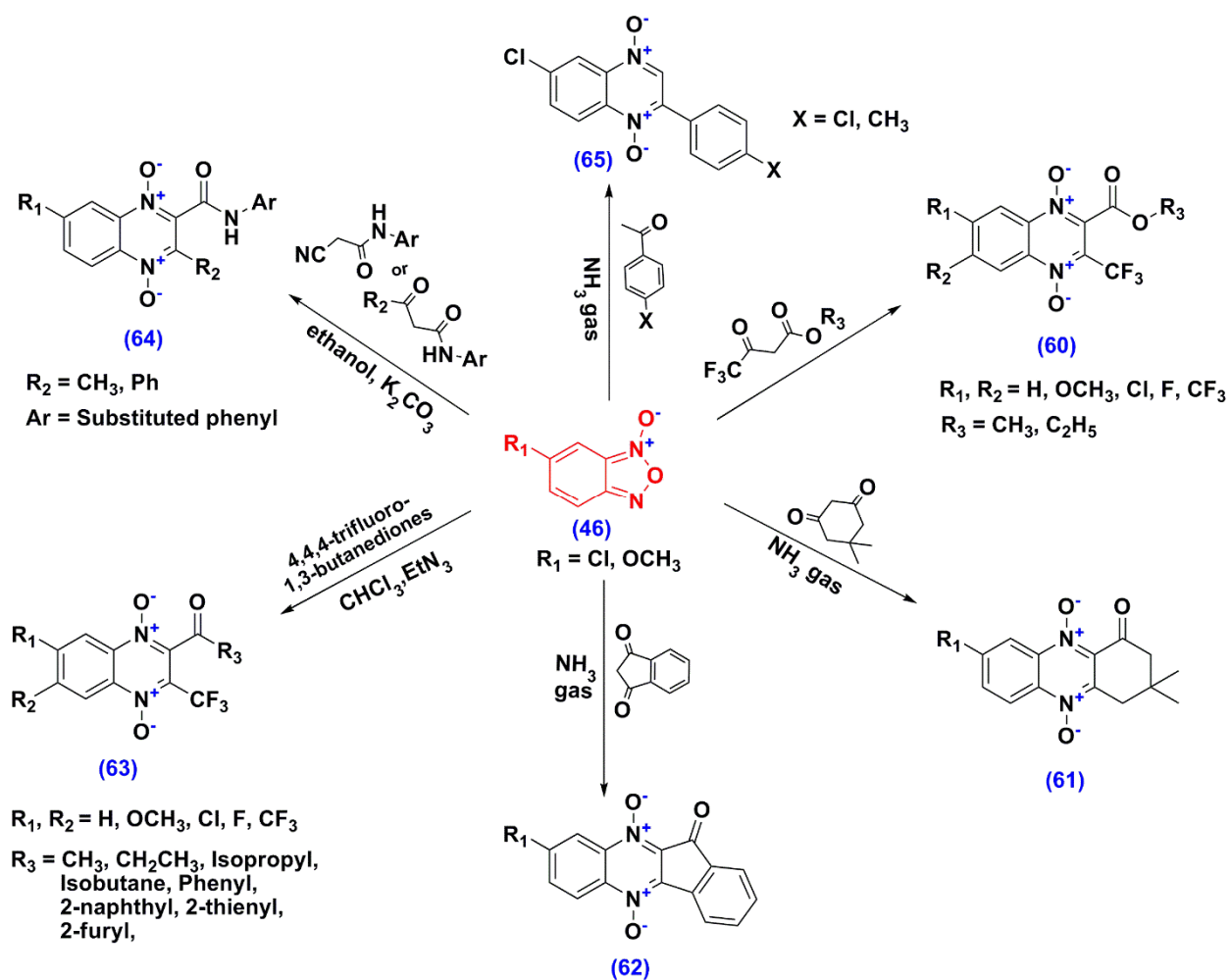
alcohol intermediate. Rearrangement of the benzofurazan *N*-oxide and elimination of water results in the 1,4-di-*N*-oxides (**53**) (**Scheme 2-22**).



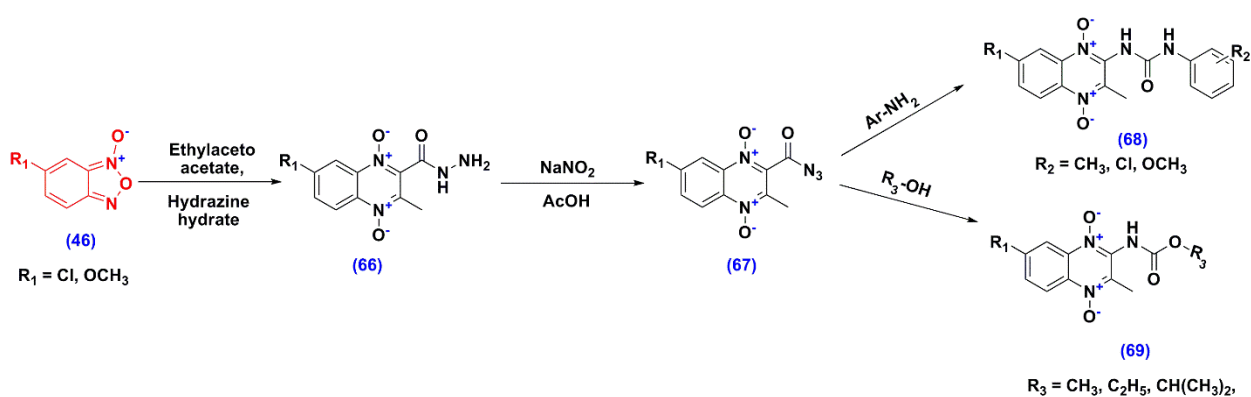
Scheme 2-22 Mechanism of the Beirut reaction

The benzofurazan *N*-oxide **46** reacts with various other 1,3-dicarbonyl reagents or a β -cyanocarbonyl reagent yielding quinoxaline alkyl esters **60**, ketones (**61-63**) or caboxamides (**64**) (Zarranz et al., 2004; Amin et al., 2006; Solano et al., 2007; Torres et al., 2013) (**Scheme 2-23**). The bubbling of ammonia gas in a warm alcoholic solution of **46** and substituted acetophenones for 3 h yielded **65**, a phenylene quinoxaline derivative in high yields (Amin et al., 2006) (**Scheme 2-23**).

The reaction of **46** with hydrazine hydrate and ethyl acetoacetate produced the intermediate **66**, which upon treatment with sodium nitrite produced the keto azides **67**, which were reacted further with aryl amines and alkyl alcohols to produce quinoxaline *N*-oxide ureas (**68**) or carbamates (**69**) (**Scheme 2-24**) (Ismail et al., 2010).



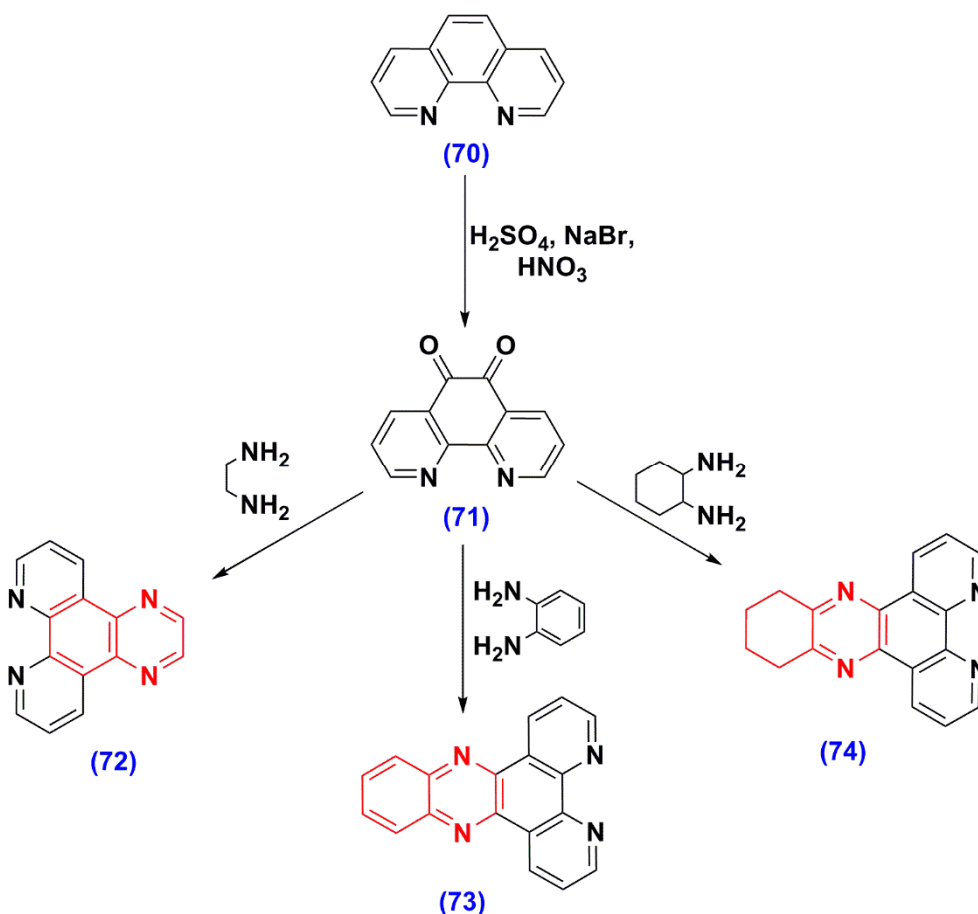
Scheme 2-23 Reactions of benzofurazan oxide with different dicarbonyl compounds



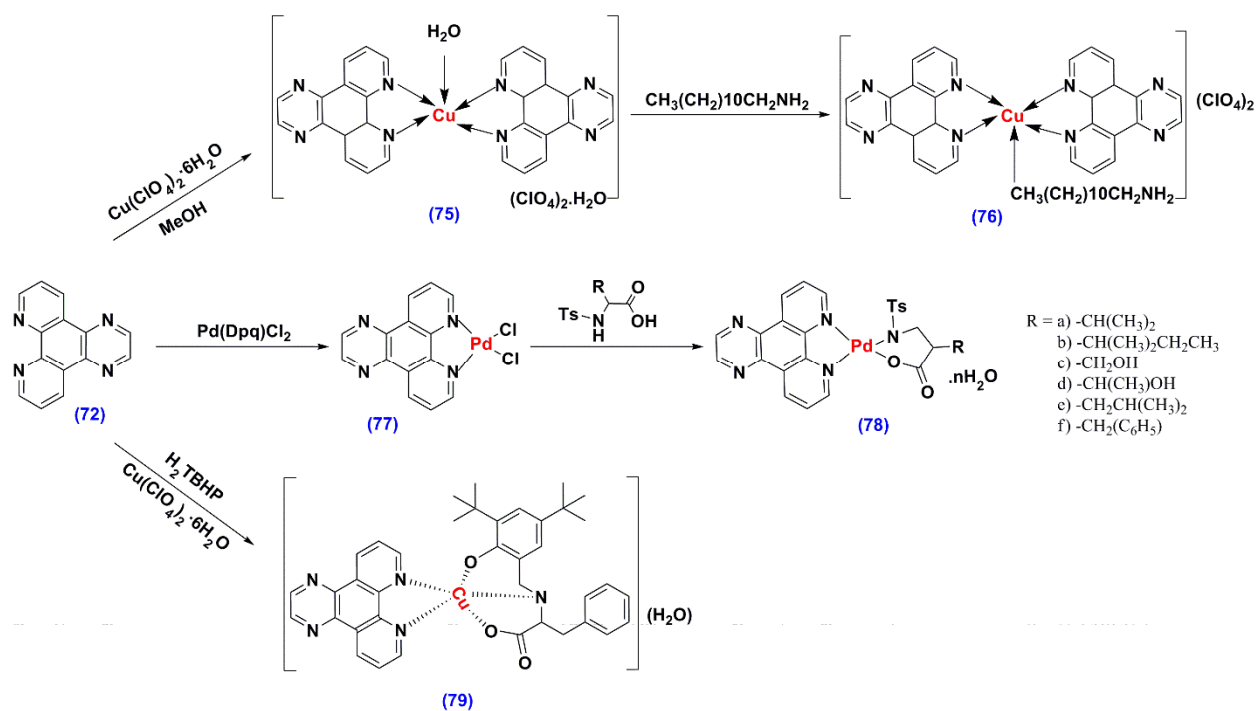
Scheme 2-24 Synthesis of *N*-oxide quinoxaline urea and carbamate derivatives

2.2.12 Synthesis of quinoxaline ligands starting with phenanthroline and subsequent complex formation

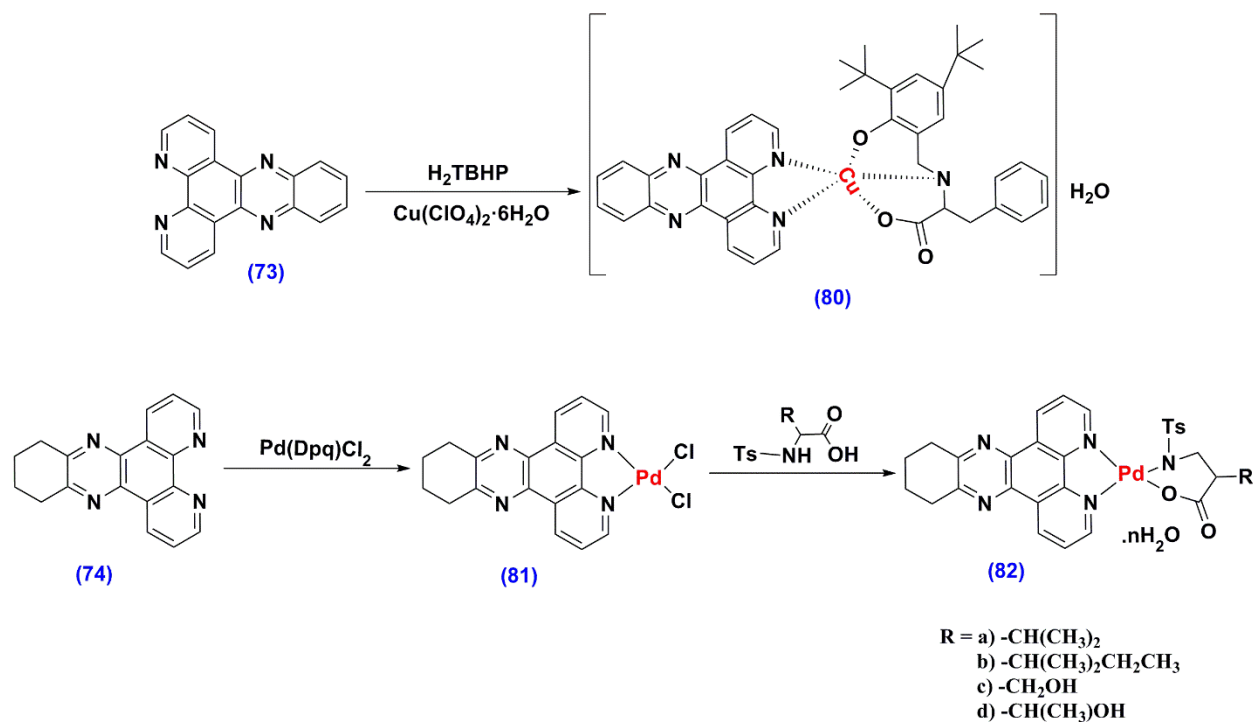
Quinoxaline based ligands were synthesized by oxidation of phenanthroline (**70**) using sulphuric and nitric acids along with sodium bromide to yield 2,10-phenanthroline-5,6-dione (**71**). This diketo intermediate, **71** was further reacted with various di-amino compounds such as ethylene diamine, *o*-phenylenediamine and cyclohexane-1,2-diamine to yield dipyrido[3,2-*d*:2',3'-*f*] quinoxaline (**72**), dipyrido[3,2-*a*:2',3'-*c*]phenazine (**73**) and dipyrido[3,2-*a*:2',3'-*c*](6,7,8,9-tetrahydro)phenazine (**74**) respectively (Scheme 2-25). These derivatives **72**, **73** and **74** were bidentate ligands, which were shown to co-ordinate to Cu and Pd metals *via* the nitrogen lone pairs of the phenanthroline ring resulting in the quinoxaline metal complexes **75-82** (Nagaraj et al., 2015; Ma et al., 2014, 2015) (Scheme 2-26 and Scheme 2-27).



Scheme 2-25 Synthesis of different quinoxaline ligands

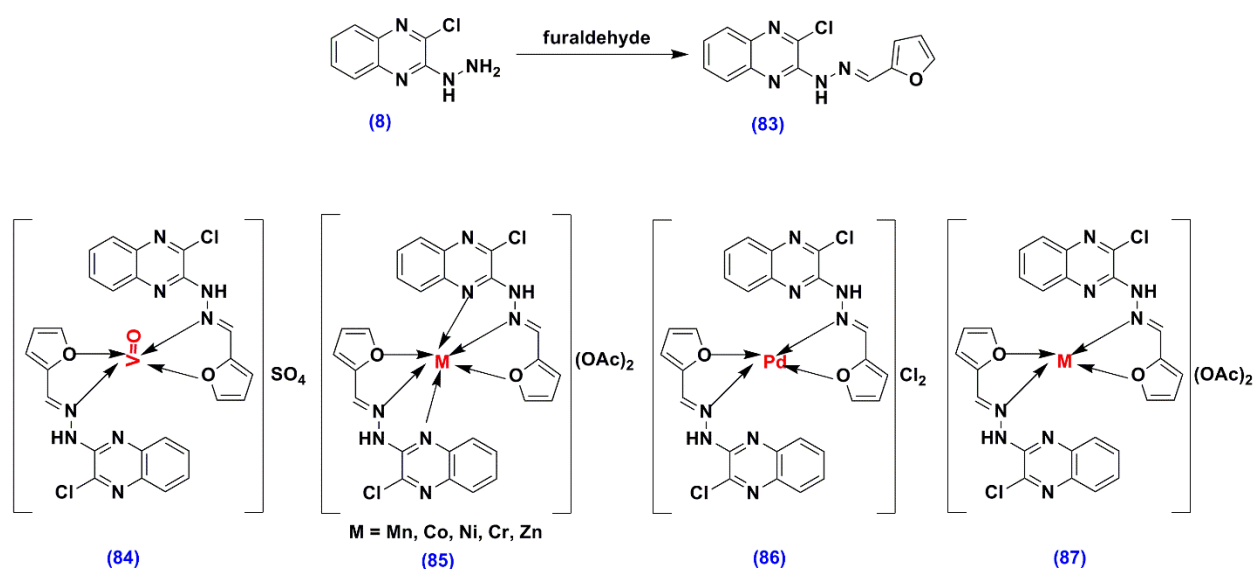


Scheme 2-26 Synthesis of metal complexes of quinoxaline



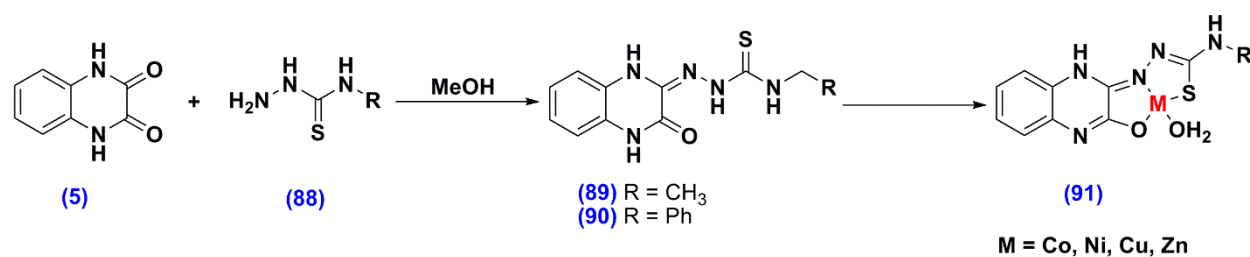
Scheme 2-27 Synthesis of quinoxaline metal complexes

Manchal *et al.* (2015) reported various metal complexes (**84-87**) prepared from the quinoxaline schiff base (**83**) obtained from commercially available 3-chloro-2-hydrazinequinoxaline (**8**) and furfuraldehyde (Manchal et al., 2015). This ligand **83** co-ordinates to the metal *via* the nitrogen atoms of the quinoxaline and imine and the oxygen atom of the furan ring (**Scheme 2-28**).



Scheme 2-28 Metal complexes prepared from quinoxaline schiff bases

Quinoxaline dione (**5**) treated with substituted hydrazine carbothioamides (**88**) yielded the thiosemicarbazide ligand **89-90** which was shown to complex with various metals *via* both sulfur and nitrogen to form the complexes **91** (Kulkarni et al., 2012) (**Scheme 2-29**).



Scheme 2-29 Quinoxaline metal complexes prepared from thiosemicarbazide ligand

2.3 Pharmacological Importance of Quinoxaline Derivatives

Derivatives of quinoxaline have shown activity in a vast array of biological assays including antioxidant, antimicrobial, anticancer, antitubercular, antimalarial, analgesic, anti-inflammatory, anticonvulsant, anti-epileptic and anti-HIV and have been reviewed extensively in the last three years (Ajani et al., 2014; Ali et al., 2015; Newahie et al., 2016). Synthetic quinoxalines form part of antibiotics such as echinomycin, levomycin and actinomycin (Katagiri et al., 1975). This short review focusses on the antimicrobial and antidiabetic activities of quinoxalines, since these two biological assays were carried out in this thesis.

2.3.1 Antimicrobial activity

Table 2-1 to **Table 2-4** contains quinoxaline derivatives with reported MIC values of $<100 \mu\text{g mL}^{-1}$ and zones of inhibition $>25 \text{ mm}$. These quinoxalines fall into several classes of substituted quinoxalines ranging from simple quinoxalines to more complex dimers.

The simple quinoxalines contain substituents at the nitrogen, C-2 and C-3 and various positions on the aromatic ring (**Figure 2-2**). These quinoxalines contain thioketo groups at C-2 and alkyl groups at N-1 (**92, 93**) (Caleb et al., 2011), carboxylic acids at C-3 along with methoxy or ethoxy groups (**94-96**) (Kumar et al., 2013), a 2-chloro-3-alkyl-3-carboxylate (**97**) (Kumar et al., 2013), C-6 amino acid linked quinoxalines (**98-109**) (Chaudhary et al., 2015), and a 6-methyl-2-piperidiny quinoxaline (**110**) (Henen et al., 2012), 2,3-diphenyl-6-sulphonyl quinoxalines (**111-118**) (Ingle and Wadher, 2014), 3-hydrazino-2-benzylquinoxaline (**119**) (Issa et al., 2015) and 2-hetrocyclic-3-alkyl or aromatic substituted quinoxalines (**21-29, 120-124**) (Vekariya et al., 2003; El-Sawy et al., 2010; Issa et al., 2015). Among these compounds, the best antimicrobial activity was seen by the C-6 amino acid linked quinoxalines **98-109**

(Table 2-1 and Table 2-2) ranging from 6 to 25 $\mu\text{g mL}^{-1}$ and **96-97** and **121-122** showing zones of inhibition > 30 mm (Table 2-1 and Table 2-2).

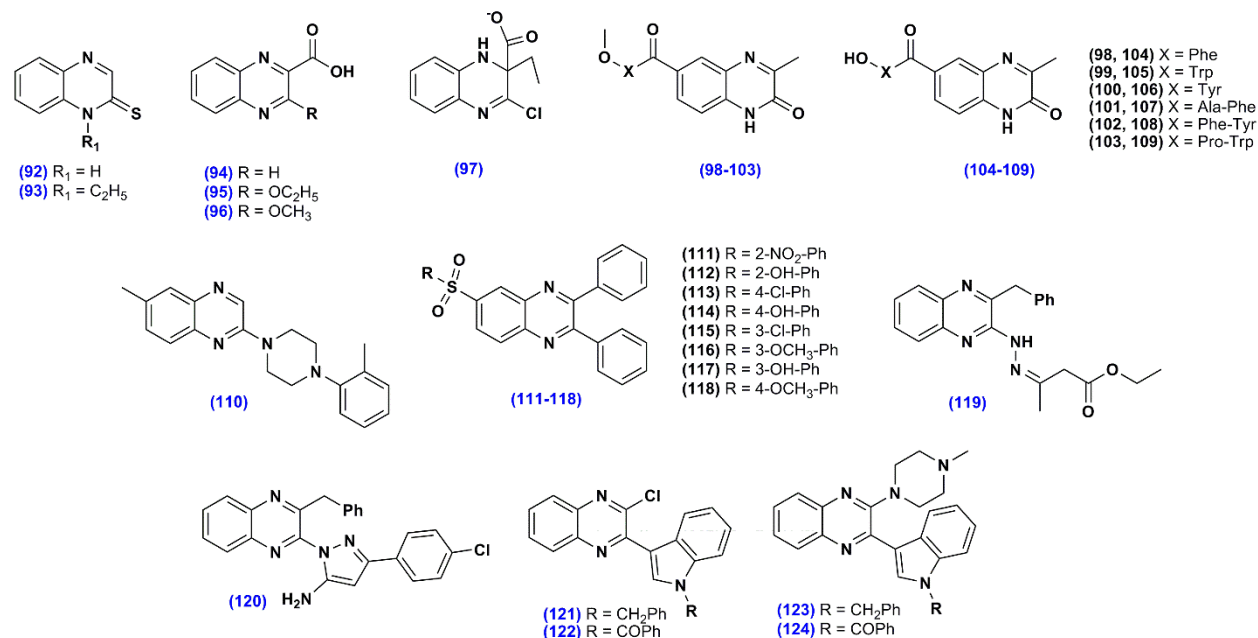


Figure 2-2 Biologically active simple quinoxaline compounds

The second class of bioactive quinoxalines are the 2-substituted C-3-N-4 fused triazolo quinoxalines. Compounds **125-133** contain a benzyl-substituted group at C-2 and a triazolo group fused at C-3-N-4 (Issa et al. 2015). The triazolo moiety in turn has C-3' substituted alkyl (**126**), phenyl (**127**, **128**), keto (**129**), ester (**130**, **131**), alkyl acid (**132**) or phenyl acid (**133**) group attached to it, providing further variation within this class. Further compounds **134-145** contains chloro, methoxy, thioacids, piperazine, anilines and thiotriazoles at the 2-position (Figure 2-3) (Suresh et al., 2010; Henen et al., 2012).

Table 2-1 Antimicrobial activity of simple quinoxaline compounds

Comp. No.	Gram Positive						Gram Negative				Fungi				
	S.A		B.S		B.M	R.F	E.C	P.V	K.P	P.A	C.A	A.N		M.A	P.C
	DD	MIC	DD	MIC	DD	MIC	DD	DD	MIC	MIC	MIC	DD	MIC	MIC	DD
21	18-25	-	-	-	-	-	18-25	-	-	-	-	-	-	-	-
22	18-25	-	-	-	18-25	-	18-25	18-25	-	-	-	-	-	-	-
23	-	-	-	-	18-25	-	-	-	-	-	-	18-25	-	-	-
24	18-25	-	-	-	-	-	-	-	-	-	-	18-25	-	-	-
25	18-25	-	-	-	-	-	-	-	-	-	-	18-25	-	-	-
26	-	-	-	-	-	-	18-25	18-25	-	-	-	18-25	-	-	-
27	-	-	-	-	-	-	18-25	-	-	-	-	18-25	-	-	-
28	-	-	-	-	-	-	-	18-28	-	-	-	-	-	-	-
29	-	-	-	-	-	-	-	18-25	-	-	-	-	-	-	-
92*	-	32	-	-	-	16	-	-	-	-	-	-	-	-	-
93*	-	64	-	-	-	-	-	-	-	-	-	-	-	-	-
94	-	-	-	-	-	-	-	-	-	-	-	29	-	-	-
95	-	-	-	-	-	-	-	-	-	-	-	27	-	-	-
96	-	-	35	-	-	-	-	-	-	-	-	33	-	-	-
97											-	30	-	-	-
98	-	12.5	-	6	-	-	-	-	12.5	6	6	-	12.5	25	6
99	-	25	-	12.5	-	-	-	-	12.5	6	12.5	-	12.5	12.5	12.5
100	-	12.5	-	6	-	-	-	-	12.5	6	6	-	25	25	6
101	-	12.5	-	6	-	-	-	-	25	12.5	12.5	-	12.5	25	6
102	-	25	-	12.5	-	-	-	-	25	6	6	-	12.5	12.5	6
103	-	12.5	-	6	-	-	-	-	12.5	6	25	-	25	6	25

S.A = *Staphylococcus aureus*; B.S = *Bacillus subtilis*; B.C = *Bacillus cereus*; B.M = *Bacillus magaterium*; R.F = *Rhodococcus fascians*; E.C = *Escherichia coli*; P.V = *Proteus vulgaris*; K.P = *Klebsiella pneumoniae*; P.A = *Pseudomonas aeruginosa*; C.A = *Candida albicans*; A.N = *Aspergillus niger*; M.A = *Microsporum audouinii*; P.C = *Penicillium chrysogenum*; DD = Disc diffusion method, zone of inhibition in mm; MIC = Minimum inhibitory concentration in $\mu\text{g ML}^{-1}$; * = MIC value in mg ML^{-1} . Highlighted values show the most best results.

Table 2-2 Antimicrobial activity of simple quinoxaline compounds (continued)

Comp. No.	Gram Positive			Gram Negative				Fungi				
	<i>S. aureus</i>	<i>B. subtilis</i>	<i>B. cereus</i>	<i>E. coli</i>	<i>K. pneumoniae</i>	<i>P. aeruginosa</i>		<i>C. albicans</i>		<i>A. niger</i>	<i>M. audouinii</i>	<i>P. chrysogenum</i>
	MIC	MIC	DD	MIC	MIC	DD	MIC	DD	MIC	MIC	MIC	DD
104	12.5	6	-	-	6	-	6	-	6	12.5	25	6
105	12.5	6	-	-	6	-	6	-	6	25	12.5	6
106	25	6	-	-	6	-	12.5	-	6	12.5	12.5	6
107	12.5	12.5	-	-	6	-	6	-	6	12.5	12.5	6
108	25	6	-	-	6	-	6	-	6	12.5	12.5	6
109	12.5	6	-	-	6	-	6	-	6	12.5	12.5	6
110	-	-	-	85	-	-	-	-	-	-	-	-
111	23	-	-	36	-	-	-	-	-	-	-	-
112	32	-	-	35	-	-	-	-	-	-	-	-
113	50	-	-	40	-	-	-	-	-	-	-	-
114	12	-	-	67	-	-	-	-	-	-	-	-
115	35	-	-	25	-	-	-	-	-	-	-	-
116	19	-	-	21	-	-	-	-	-	-	-	-
117	22	-	-	27	-	-	-	-	-	-	-	-
118	24	-	-	29	-	-	-	-	-	-	-	-
119	100	50	-	50	-	-	100	-	50	-	-	-
120	100	100	-	100	-	-	50	-	50	-	-	-
121	-	-	-	-	-	-	-	32	-	-	-	-
122	-	-	-	-	-	-	-	32	-	-	-	-
123	-	-	28	-	-	25	-	-	-	-	-	-
124	-	-	28	-	-	25	-	-	-	-	-	-

DD = Disc diffusion method, zone of inhibition in mm; **MIC** = Minimum inhibitory concentration in $\mu\text{g ML}^{-1}$. Highlighted values show the most best results.

Compounds **125**, **127**, **132** and **133** showed MIC values of 25 $\mu\text{g mL}^{-1}$ or less against bacterial strains, whilst **128**, **130-131** and **133** showed MICs of 25 $\mu\text{g mL}^{-1}$ against *C. albicans*. Compounds **136**, **139** and **142** showed zones of inhibition of > 30 mm against bacterial strains with **136** showing a broad spectrum of activity being active against both Gram +ve and Gram -ve bacteria. Compounds **138**, **140-143** all showed zones of inhibition > 30 mm against the fungal species, *A. niger* and *P. chrysogenum* (Table 2-3).

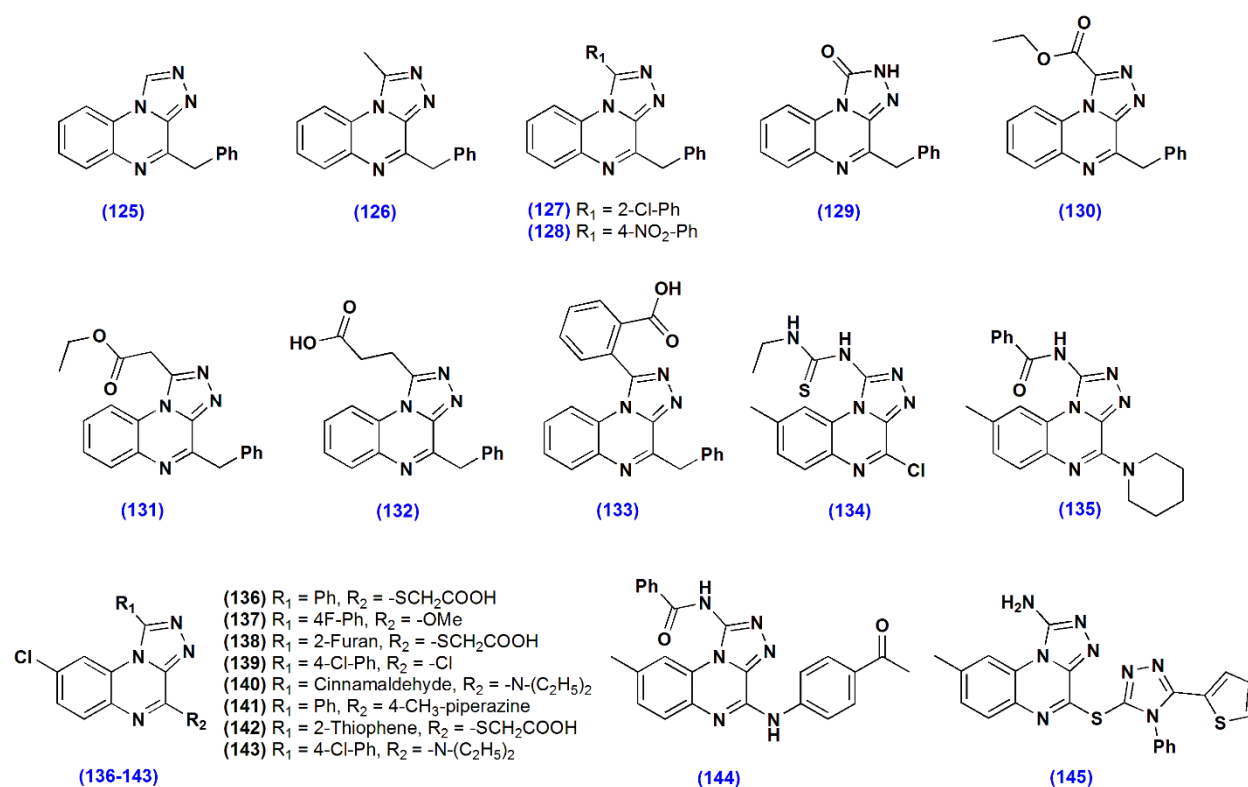


Figure 2-3 Second class of quinoxaline compounds

A set of unique quinoxalines with a C-2-C-3 fused imidazo thiadiazole group also showed good bioactivity (**146-152**) (Teja et al., 2013). Compounds **146-147** showed MICs of 15.63 $\mu\text{g mL}^{-1}$ against Gram +ve and Gram -ve bacteria as well as the fungal *A. fumigatus*.

Table 2-3 Antimicrobial activity of second class of quinoxaline compounds

Comp. No.	Gram Positive				Gram Negative				Fungi		
	<i>S. aureus</i>		<i>B. subtilis</i>		<i>E. coli</i>	<i>P. Vulgaris</i>	<i>K. pneumoniae</i>	<i>P. aeruginosa</i>	<i>C. albicans</i>	<i>A. niger</i>	<i>P. chrysogenum</i>
	DD	MIC	DD	MIC	MIC	DD	DD	MIC	MIC	DD	DD
125	-	50	-	50	25	-	-	50	100	-	-
126	-	50	-	50	50	-	-	100	100	-	-
127	-	100	-	25	25	-	-	50	100	-	-
128	-	50	-	100	100	-	-	50	25	-	-
129	-	100	-	100	100	-	-	100	50	-	-
130	-	50	-	50	50	-	-	100	25	-	-
131	-	50	-	100	100	-	-	100	25	-	-
132	-	25	-	12.5	12.5	-	-	25	50	-	-
133	-	100	-	100	25	-	-	100	25	-	-
134	-	-	-	-	87	-	-	-	89	-	-
135	-	84	-	-	-	-	-	-	-	-	-
136	31	-	30	-	-	31	35	-	-	-	-
137	25	-	-	-	-	-	-	-	-	26	26
138	-	-	-	-	-	-	-	-	-	31	-
139	32	-	27	-	-	-	36	-	-	-	25
140	26	-	26	-	-	-	-	-	-	25	30
141	-	-	-	-	-	-	-	-	-	30	26
142	28	-	31	-	-	-	-	-	-	31	28
143	25	-	-	-	-	-	-	-	-	33	34
144	-	94	-	-	67	-	-	-	-	-	-
145	-	-	-	91	98	-	-	-	78	-	-

DD = Disc diffusion method, zone of inhibition in mm; MIC = Minimum inhibitory concentration in $\mu\text{g ML}^{-1}$. Highlighted values show the best results.

The best activity was seen by the 2-hydroxyphenyl derivative **149**, which showed MIC values of $7.81 \mu\text{g mL}^{-1}$ against these same bacterial and fungal strains (**Table 2-4**). Three molecules with a six membered triazine ring fused at C-3-N-4 (**153-155**) also showed activity $< 100 \mu\text{g mL}^{-1}$ with **153** showing a MIC of $25 \mu\text{g mL}^{-1}$ against *P. aeruginosa* and $12.5 \mu\text{g mL}^{-1}$ against *C. albicans* (**Figure 2-4; Table 2-4**) (Issa et al., 2015).

Compounds **156-158** contained a methylene linker bridging two quinoxalines (Srinivas et al., 2013) (**Figure 2-4**). The *para* chloro and fluoro derivatives **157** and **158** showed MIC values of $8\text{-}16 \mu\text{g mL}^{-1}$ against both Gram +ve and -ve bacterial strains (**Table 2-4**).

Two metal chelated quinoxalines (**75, 76**) synthesized from phenanthroline and ethylenediamine precursors (discussed above, **Scheme 2-27**) showed zones of inhibition of 26 and 29 mm respectively against an unspecified fungal *Aspergillus* species (**Table 2-4**) (Nagaraj et al., 2015).

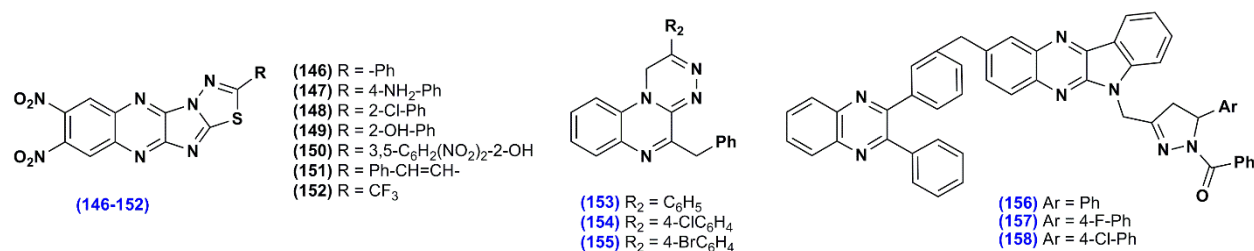


Figure 2-4 Unique quinoxaline compounds

Table 2-4 Antimicrobial activity of unique quinoxaline compounds

Comp. No.	Gram Positive			Gram Negative			Fungi			
	<i>S. aureus</i>	<i>B. subtilis</i>	<i>B. cereus</i>	<i>E. coli</i>	<i>P. vulgaris</i>	<i>P. aeruginosa</i>	<i>C. albicans</i>	<i>A. niger</i>	<i>A. fumigatus</i>	<i>Aspergillus</i>
	MIC ($\mu\text{g ML}^{-1}$)									DD
75	-	-	-	-	-	-	-	-	-	26
76	-	-	-	-	-	-	-	-	-	29
146	31.25	-	15.63	31.25	-	15.63	-	31.25	15.63	-
147	31.25	-	15.63	31.25	-	31.25	-	31.25	15.63	-
148	31.25	-	-	31.25	-	-	-	-	-	-
149	7.81	-	7.81	31.25	-	7.81	-	31.25	7.81	-
150	-	-	31.25	-	-	-	-	31.25	31.25	-
151	-	-	-	31.25	-	31.25	-	31.25	-	-
152	31.25	-	31.25	-	-	31.25	-	-	-	-
153	50	25	-	50	-	25	12.5	-	-	-
154	50	100	-	50	-	50	25	-	-	-
155	50	50	-	50	-	100	50	-	-	-
156	-	64	-	-	-	-	-	-	-	-
157	8	8	-	16	8	-	-	-	-	-
158	8	16	-	16	16	-	-	-	-	-

DD = Disc diffusion method, zone of inhibition in mm; **MIC** = Minimum inhibitory concentration in $\mu\text{g ML}^{-1}$. Highlighted values show the best results.

2.3.2 Antidiabetic Activity

Antidiabetic activity of quinoxalines were limited to the quinoxaline–thiosemicarbazone ligands (**89-90**) and their metal complexes (**91**) (Kulkarni et al., 2012) (**Scheme 2-29**). This was evaluated by a blood-glucose and oral glucose tolerance test (OGTT). These compounds showed a notable reduction in the blood glucose level and promising activity in the OGTT. In addition, they possessed low toxicity with a high safety profile (Kulkarni et al., 2012).

2.4 Conclusion

Quinoxalines can be easily synthesized using a variety of methods, most of which contain an *ortho*-diamine with oxalic acid derivatives. There are however some other more specific syntheses, also contained in this review. This literature survey identifies many quinoxaline molecules with promising antibacterial and antifungal activity such as C-6 amino acid linked quinoxalines (MIC 6-12.5 $\mu\text{g mL}^{-1}$), 7,8-dinitro-2-(2-hydroxy-phenyl)[1,3,4]thiadiazolo[2',3':2,3]imidazo[4,5-b]quinoxaline (MIC 7.81 $\mu\text{g mL}^{-1}$), (5-(4-fluorophenyl)-3-((2-(3-(3-phenylquinoxalin-2-yl)benzyl)-6H-indolo[2,3-b]quinoxalin-6-yl)methyl)-4,5-dihydro-1*H*-pyrazol-1-yl)(phenyl)methanone (MIC 8-16 $\mu\text{g mL}^{-1}$) and 3-(4-benzyl-[1,2,4]triazolo[4,3-a] quinoxalin-1-yl)propanoic acid (MIC 12.5-50 $\mu\text{g mL}^{-1}$). These compounds can be considered lead compounds for antibiotics since they show better activity than gatifloxacin, ampicillin and clotrimazole (currently used antibiotics).

2.5 References

- Achutha, L., Parameshwar, R., Reddy, B. M., Babu, V. H. Microwave-assisted synthesis of some quinoxaline-incorporated schiff bases and their biological evaluation. *J. Chem.*, **2013**, Article ID 578438, 5 pages. <http://dx.doi.org/10.1155/2013/578438>.
- Ajani, O. O. Present status of quinoxaline motifs: Excellent pathfinders in therapeutic medicine. *Eur. J. Med. Chem.*, **2014**, 85, 688-715.

- Alasmari, F. A. S., Aljaber, N. A. Synthesis and antimicrobial activities of some novel quinoxaline derivatives. *Int. J. Adv. Res. Chem. Sci.*, **2015**, 2(1), 14-23.
- Alswah, M., Ghiaty, A., El-Morsy, A., El-Gamal, K. Synthesis and biological evaluation of some [1,2,4]triazolo[4,3-*a*]quinoxaline derivatives as novel anticonvulsant agents. *Int. Scholarly Res. Notices Org. Chem.*, **2013**, Article ID 587054, 7 pages. <http://dx.doi.org/10.1155/2013/587054>.
- Amin, K. M., Ismail, M. M. F., Noaman, E., Soliman, D. H., Ammar, Y. A. New quinoxaline 1,4-di-*N*-oxides. Part 1: Hypoxia-selective cytotoxins and anticancer agents derived from quinoxaline 1,4-di-*N*-oxides. *Bioorg. Med. Chem.*, **2006**, 14, 6917-6923.
- Ali, A., Hashem, A. Synthesis, reactions and biological activity of quinoxaline derivatives. *Am. J. Org. Chem.*, **2015**, 5(1), 14-56.
- Andrés, J. I., Buijnsters, P., Angelis, M. D., Langlois, X., Rombouts, F., Trabanco, A. A., Vanhoof, G. Discovery of a new series of [1,2,4]triazolo[4,3-*a*]quinoxalines as dual Phosphodiesterase 2/phosphodiesterase 10 (PDE2/PDE10) inhibitors. *Bioorg. Med. Chem. Lett.*, **2013**, 23, 785-790.
- Arimondo, P. B., Baldeyrou, B., Laine, W., Bal, C., Alphonse, F. A., Routier, S., Coudert, G., Me´rour, J. Y., Colson, P., Houssier, C., Bailly, C. DNA interaction and cytotoxicity of a new series of indolo[2,3-*b*]quinoxaline and pyridopyrazino[2,3-*b*]indole derivatives. *Chem. Biol. Interact.*, **2001**, 138, 59-75.
- Barea, C., Pabón, A., Silanes, S. P., Galiano, S., Gonzalez, G., Monge, A., Deharo, E., Aldana, I. New amide derivatives of quinoxaline 1,4-di-*N*-oxide with leishmanicidal and antiplasmodial activities. *Molecules*, **2013**, 18, 4718-4727.
- Burguete, A., Pontiki, E., Litina, D. H., Ancizu, S., Villar, R., Solano, B., Moreno, E., Torres, E., Pe´rez, S., Aldana, I., Monge, A. Synthesis and biological evaluation of new quinoxaline derivatives as antioxidant and anti-inflammatory agents. *Chem Biol. Drug Des.*, **2011**, 77, 255-267.
- Castro, M. A., Gamito, A. M., Tangarife-Castano, V., Roa-Linares, V., Corral, J. M. M. D., Mesa-Arango, A. C., Betancur-Galvis, L., Francesch, A. M., Feliciano, A. S. New 1,4-anthracenedione derivatives with fused heterocyclic rings: synthesis and biological evaluation. *RSC Adv.*, **2015**, 5, 1244-1261.
- Chandra Shekhar, A., Shanthan Rao, P., Narsaiah, B., Allanki, A. D., Sijwali, P. S. Emergence of pyrido quinoxalines as a new family of antimalarial agents. *Eur. J. Med. Chem.*, **2014**, 77, 280-287.
- Chaudhary, S., Kumar, S. Synthesis and biological activity of peptide derivatives of 1,2-dihydro-3-methyl-2-oxoquinoxaline-6-carboxylic acid. *Der Pharma Chemica.*, **2015**, 7(9), 210-220.
- Corona, P., Loriga, M., Costi, M. P., Ferrari, S., Paglietti, G. Synthesis of *N*-(5,7-diamino-3-phenyl-quinoxalin-2-yl)-3,4,5-substituted anilines and *N*-[4[(5,7-diamino-3-phenylquinoxalin-2-yl)amino]benzoyl]-*L*-glutamic acid diethyl ester: Evaluation of *in vitro* anti-cancer and anti-folate activities. *Eur. J. Med. Chem.*, **2008**, 43, 189-203.
- Corona, P., Carta, A., Loriga, M., Vitale, G., Paglietti, G. Synthesis and *in vitro* antitumor activity of new quinoxaline derivatives. *Eur. J. Med. Chem.*, **2009**, 44, 1579-1591.
- Caleb, A. A., Ballo, D., Rachid, B., Amina, H., Mostapha, B., Abdelfettah, Z., Rajae, E. A., Mokhtar, E. E. Synthesis and antibacterial activity of new spiro[thiadiazoline-quinoxaline] derivatives. *ARKIVOC*, **2011**, 2, 217-226.

- Demmer, C. S., Møller, C., Brown, P. M. G. E., Han, L., Pickering, D. S., Nielsen, B., Bowie, D., Frydenvang, K., Kastrop, J. S., Bunch, L. Binding mode of an α -amino acid-linked quinoxaline-2,3-dione analogue at glutamate receptor subtype GluK1. *ACS Chem. Neurosci.*, **2015**, 6, 845–854.
- Diana, P., Martorana, A., Barraja, P., Montalbano, A., Dattolo, G., Cirrincione, G., Acqua, F. D., Salvador, A., Vedaldi, D., Basso, G., Viola, G. Isoindolo[2,1-*a*]quinoxaline derivatives, novel potent antitumor agents with dual inhibition of tubulin polymerization and topoisomerase I. *J. Med. Chem.*, **2008**, 51, 2387-2399.
- El-sawy, E., Bassyouni, F. A., Abu-bakr, S. H., Rady, H. M., Abdlla, M. M. Synthesis and biological activity of some new 1-benzyl and 1-benzoyl-3-heterocyclic indole derivatives. *Acta Pharm.*, **2010**, 60, 55-71.
- Elshihawy, H., Hammad, M. Molecular modeling studies and synthesis of novel quinoxaline derivatives with potential anti-cancer activity as inhibitors of methionine synthase. *Med. Chem. Res.*, **2013**, 22, 3405-3415.
- Galal, S. A., Abdelsamie, A. S., Tokuda, H., Suzuki, N., Lida, A., ElHefnawi, M. M., Ramadan, R. A., Atta, M. H. E., Diwani, H. I. E. Part I: Synthesis, cancer chemopreventive activity and molecular docking study of novel quinoxaline derivatives. *Eur. J. Med. Chem.*, **2011**, 46, 327-340.
- Galal, S. A., Abdelsamie, A. S., Soliman, S. M., Mortier, J., Wolber, G., Ali, M. M., Tokuda, H., Suzuki, N., Lida, A., Ramadan, R. A., Diwani, H. I. E. Design, synthesis and structure-activity relationship of novel quinoxaline derivatives as cancer chemopreventive agent by inhibition of tyrosine kinase receptor. *Eur. J. Med. Chem.*, **2013**, 69, 115-124.
- Gavara, L., Saugues, E., Alves, G., Debiton, E., Anizon, F., Moreau, P. Synthesis and biological activities of pyrazolo[3,4-*g*]quinoxaline derivatives. *Eur. J. Med. Chem.*, **2010**, 45, 5520-5526.
- Gil, A., Pabón, A., Galiano, S., Burguete, A., Silanes, S. P., Deharo, E., Monge, A., Aldana, I. Synthesis, biological evaluation and structure-activity relationships of new quinoxaline derivatives as anti-*plasmodium falciparum* agents. *Molecules*, **2014**, 19, 2166-2180.
- Gris, J., Glisoni, R., Fabian, L., Fernánde, B., Moglioni, A. G. Synthesis of potential chemotherapeutic quinoxalinone derivatives by biocatalysis or microwave-assisted Hinsberg reaction. *Tetrahedron Lett.*, **2008**, 49, 1053-1056.
- Henen, M. A., El Bialy, S. A. A., Goda, F. E., Nasr, M. N. A., Eisa, H. M. [1,2,4]Triazolo [4,3-*a*]quinoxaline: synthesis, antiviral, and antimicrobial activities. *Med. Chem. Res.*, **2012**, 21, 2368-2378.
- Hossain, M. M., Muhib, M. H., Mia, M. R., Kumar, S., Wadud, S. A. *In vitro* antioxidant potential study of some synthetic quinoxalines. *Bangladesh Med. Res. Counc. Bull.*, **2012**, 38, 47-50.
- Huang, H. S., Chen, T. C., Chen, R. H., Huang, K. F., Huang, F. C., Jhan, J. R., Chen, C. L., Lee, C. C., Lo, Y., Lin, J. J. Synthesis, cytotoxicity and human telomerase inhibition activities of a series of 1,2-heteroannelated anthraquinones and anthra[1,2-*d*]imidazole-6,11-dione homologues. *Bioorg. Med. Chem.*, **2009**, 17, 7418-7428.
- Ingle, R. G., Marathe, R. P. Sulfonamido quinoxalines - Search for anti-inflammatory agents. *Int. J. Pharm. Res. Allied Sci.*, **2012**, 1(4), 46-51.
- Ingle, R., Marathe, R., Magar, D., Patel, H. M., Surana, S. J. Sulphonamido-quinoxalines: Search for anticancer agent. *Eur. J. Med. Chem.*, **2013**, 65, 168-186.
- Ingle, R., Wadher, S. Synthetic development of antimicrobial novel quinoxaline derivatives. *Int. J. Pharm. Chem.*, **2014**, 4(1), 34-38.

- Işıkdağ, I., Ozkay, Y., Incesu, Z. Synthesis and anticancer activity of some bisquinoxaline derivatives. *Turk. J. Pharm. Sci.*, **2011**, 8 (2), 179-188.
- Ismail, M. M. F., Amin, K. M., Noaman, E., Soliman, D. H., Ammar, Y. A. New quinoxaline 1,4-di-*N*-oxides: Anticancer and hypoxia-selective therapeutic agents. *Eur. J. Med. Chem.*, **2010**, 45, 2733-2738.
- Issa, D. A. E., Habib, N. S., Abdel Wahab, A. E. Design, synthesis and biological evaluation of novel 1,2,4-triazolo and 1,2,4-triazino[4,3-*a*] quinoxalines as potential anticancer and antimicrobial agents. *Med. Chem. Commun.*, **2015**, 6, 202-211.
- Karki, S. S., Hazare, R., Kumar, S., Bhadauria, V. S., Balzarini, J., Clercq, E. D. Synthesis, anticancer and cytostatic activity of some 6*H*-indolo[2,3-*b*]quinoxalines. *Acta Pharm.*, **2009**, 59, 431-440.
- Katagiri, K., Yoshida, T., Sato, K. Mechanism of action of antimicrobial and antitumor agents. *Antibiotics*, **1975**, 3, 234-251.
- Keshtov, M. L., Kuklin, S. A., Chen, F. C., Khokhlov, A. R., Peregudov, A. S., Siddiqui, S. A., Sharma, G. D. Two new D–A conjugated polymers P(PTQD-T) and P(PTQD-2T) with same 9-(2-octyldodecyl)-8*H*-pyrrolo[3,4-*b*]bisthieno[2,3-*f*:30,20-*h*]quinoxaline-8,10(9*H*)-dione acceptor and different donor units for BHJ polymer solar cells application. *Org. Electron.*, **2015**, 24, 137-146.
- Khier, S., Masquéfa, C. D., Moarbess, G., Gattacceca, F., Margout, D., Solassol, I., Cooper, J. F., Pinguet, F., Bonnet, P. A., Bressolle, F. M. M. Pharmacology of EAPB0203, a novel imidazo[1,2-*a*]quinoxaline derivative with anti-tumoral activity on melanoma. *Eur. J. Pharm. Sci.*, **2010**, 39, 23-29.
- Kono, T., Murakami, T. N., Nishida, J., Yoshida, Y., Hara, K., Yamashita, Y. Synthesis and photo-electrochemical properties of novel thienopyrazine and quinoxaline derivatives, and their dye-sensitized solar cell performance. *Org. Electron.*, **2012**, 13, 3097-3101.
- Kulkarni, N. V., Revankar, V. K., Kirasur, B. N., Hugar, M. H. Transition metal complexes of thiosemicarbazones with quinoxaline hub: an emphasis on antidiabetic property. *Med. Chem. Res.*, **2012**, 21, 663-671.
- Kumar, N., Sharma, P., Kaur, N., Pareek, A. An efficient synthesis and biological activity of quinoxaline-2-carboxylic acid and its derivatives. *J. Appl. Chem.*, **2013**, 2(2), 143-149.
- Leboho, T. C., Giri, S., Popova, I., Cock, I., Michael, J. P., Koning, C. B. D. Double Sonogashira reactions on dihalogenated aminopyridines for the assembly of an array of 7-azaindoles bearing triazole and quinoxaline substituents at C-5: Inhibitory bioactivity against *Giardia duodenalis* trophozoites. *Bioorg. Med. Chem.*, **2015**, 23, 4943-4951.
- Ma, L., Ge, K., Zhang, R., Fu, W., Li, S., Wang, S., Zhou, G., Qin, X., Zhang, J. Synthesis, characterization, cytotoxicity of mixed ligand complexes of palladium(II) with dipyrrodo[3,2-*d*:20,30-*f*]quinoxaline/dipyrrodo[3,2-*a*:20,30-*c*](6,7,8,9-tetrahydro)phenazine and 4-toluenesulfonyl-*L*-amino acid dianion. *Eur. J. Med. Chem.*, **2014**, 87, 624-630.
- Ma, T., Xu, J., Wang, Y., Yu, H., Yang, Y., Liu, Y., Ding, W., Zhu, W., Chen, R., Ge, Z., Tan, Y., Jia, L., Zhu, T. Ternary copper(II) complexes with amino acid chains and heterocyclic bases: DNA binding, cytotoxic and cell apoptosis induction properties. *J. Inorg. Biochem.*, **2015**, 144, 38-46.
- Manchal, R., Kasula, M., Muthadi, S., Kumari, K. V. N. G., Somu, S. Synthesis and testing of metal complexes of quinoxaline based schiff bases for antimicrobial and anticancer activities. *Int. J. Pharm. Sci. Res.*, **2015**, 6(2), 698-704.

- Manta, S., Gkaragkouni, D. N., Kaffesaki, E., Gkizis, P., Hadjipavlou-Litina, D., Pontiki, E., Balzarini, J., Dehaen, W., Komiotis, D. A novel and easy two-step, microwave-assisted method for the synthesis of halophenyl pyrrolo[2,3-b]quinoxalines *via* their pyrrolo precursors. Evaluation of their bioactivity. *Tetrahedron Lett.*, **2014**, 55, 1873-1876.
- Melero, C. P., Maya, A. B. S., Rey, B. D., Pelaez, R., Caballero, E., Medarde, M. A new family of quinoline and quinoxaline analogues of combretastatins. *Bioorg. Med. Chem. Lett.*, **2004**, 14, 3771-3774.
- Mielcke, T. R., Mascarello, A., Chiela, E. F., Zanin, R. F., Lenz, G., Leal, P. C., Chirardia, L. D., Yunes, R. A., Nunes, R. J., Battastini, A. M. O., Morrone, F. B., Campos, M. M. Activity of novel quinoxaline-derived chalcones on *in vitro* glioma cell proliferation. *Eur. J. Med. Chem.*, **2012**, 48, 255-264.
- Moarbess, G., Masquef, C. D., Bonnard, V., Paniagua, S. G., Vidal, J. R., Bressolle, F., Pinguet, F., Bonnet, P. A. *In vitro* and *in vivo* anti-tumoral activities of imidazo[1,2-*a*]quinoxaline, imidazo[1,5-*a*]quinoxaline, and pyrazolo[1,5-*a*]quinoxaline derivatives. *Bioorg. Med. Chem.*, **2008**, 16, 6601-6610.
- Monge, A., Palop, J. A., Cerain, A. L., Senador, V., Martinez-Crespo, F. J., Sainz, Y., Narro, S., Garcia, E., Migue, C. D., Gonzalez, B. M., Hamilton, E., Barker, A. J., Clarke, E. D., Greenhow, D. T. Hypoxia-selective agents derived from quinoxaline 1,4-di-*N*-oxides. *J. Med. Chem.*, **1995**, 38, 1786-1792.
- Nagaraj, K., Ambika, S., Arunachalam, S. Synthesis, CMC determination, and intercalative binding interaction with nucleic acid of a surfactant-copper(II) complex with modified phenanthroline ligand (dpq). *J. Biomol. Struct. Dyn.*, **2015**, 33(2), 274-288.
- Neckel, G. L., Bicca, M. A., Leal, P. C., Mascarello, A., Siqueira, J. M., Calixto, J. B. *In vitro* and *in vivo* anti-glioma activity of a chalcone-quinoxaline hybrid. *Eur. J. Med. Chem.*, **2015**, 90, 93-100.
- Newahie, A. M. E., Ismail, N. S. M., El Ella, D. A. A., Abouzid, K. A. M. Quinoxaline-based scaffolds targeting tyrosine kinases and their potential anticancer activity. *Arch. Pharm. Chem. Life Sci.*, **2016**, 349, 1-18.
- Noolvi, M. N., Patel, H. M., Bhardwaj, V., Chauhan, A. Synthesis and *in vitro* antitumor activity of substituted quinazoline and quinoxaline derivatives: Search for anticancer agent. *Eur. J. Med. Chem.*, **2011**, 46, 2327-2346.
- Parrino, B., Carbone, A., Spano, V., Montalbano, A., Giallombardo, D., Barraja, P., Attanzio, A., Tesoriere, L., Sissi, C., Palumbo, M., Cirrincione, G., Diana, P. Aza-isoindolo and isoindolo-azaquinoxaline derivatives with antiproliferative activity. *Eur. J. Med. Chem.*, **2015**, 94, 367-377.
- Piras, S., Carta, A., Briguglio, I., Corona, P., Paglietti, G., Luciani, R., Costi, M. P., Ferrari, S. 2-[*N*-Alkyl(*R*-phenyl)-aminomethyl]-3-phenyl-7-trifluoromethylquinoxalines as anticancer agents inhibitors of folate enzymes. *Eur. J. Med. Chem.*, **2014**, 75, 169-183.
- Pradeep, K., Kotra, V., Priyadarshini, R. L., Pratap, V. Synthesis, characterization and anti-inflammatory activity of novel quinoxaline derived chalcones. *Int. J. Pharm. Pharm. Sci.*, **2015**, 7(1), 243-246.
- Puratchikody, A., Natarajan, R., Jayapal, M., Doble, M. Synthesis, *in vitro* antitubercular activity and 3D-QSAR of novel quinoxaline derivatives. *Chem. Biol. Drug Des.*, **2011**, 78, 988-998.
- Rajule, R., Bryant, V. C., Lopez, H., Luo, X., Natarajan, A. Perturbing pro-survival proteins using quinoxaline derivatives: A structure-activity relationship study. *Bioorg. Med. Chem.*, **2012**, 20, 2227-2234.
- Rodrigues, F. A. R., Bomfim, I. D. S., Cavalcanti, B. C., Pessoa, C. D. O., Wardell, J. L., Wardell, S. M. S. V., Pinheiro, A. C., Kaiser, C. R., Nogueira, T. C. M., Low, J. N., Gomes, L. R., De Souza, M. V. N. Design,

- synthesis and biological evaluation of (*E*)-2-(2-arylhydrazinyl)quinoxalines, a promising and potent new class of anticancer agents. *Bioorg. Med. Chem. Lett.*, **2014**, 24, 934-939.
- Selvam, P., Chandramohan, M., Christophe, P., Clercq, D. Studies on antiviral activity of 2,3-diphenylquinoxaline. *Int. J. Pharm & Ind. Res.*, **2011**, 1(2), 138-140.
- Sheng, R., Xu, Y., Weng, Q., Xia, Q., He, Q., Yang, B., Hu, Y. Synthesis and cytotoxic activity of 3-phenyl-2-thio-quinoxaline 1,4-dioxide derivatives in hypoxia and in normoxia. *Drug Discov Ther.*, **2007**, 1(2), 119-123.
- Solano, B., Junnotula, V., Mari'n, A., Villar, R., Burguete, A., Vicente, E., Silanes, S. P., Aldana, I., Monge, A., Dutta, S., Sarkar, U., Gates, K. S. Synthesis and biological evaluation of new 2-arylcarbonyl-3-trifluoromethylquinoxaline 1,4-di-*N*-oxide derivatives and their reduced analogues. *J. Med. Chem.*, **2007**, 50, 5485-5492.
- Sridevi, C., Balaji, K., Naidu, A. Synthesis and pharmacological evaluation of some phenyl-pyrazolo indoquinoxaline derivatives. *E-J. Chem.*, **2011**, 8(2), 924-930.
- Srinivas, M., Tejasri, A., Anjaneyulu, N., Satyanarayana, K. Microwave assisted synthesis and antimicrobial activity of some novel quinoxaline compounds. *Int. J. Pharma. Sci.*, **2013**, 3(1), 142-146.
- Suresh, M., Lavanya, P., Sudhakar, D., Vasu, K., Rao, C. V. Synthesis and biological activity of 8-chloro-[1,2,4]triazolo[4,3-*a*]quinoxalines. *J. Chem. Pharm. Res.*, **2010**, 2(1), 497-504.
- Teja, R., Kapu, S., Kadiyala, S., Dhanapal, V., Raman, A. N. Heterocyclic systems containing bridgehead nitrogen atom: Synthesis and antimicrobial activity of thiadiazolo[20,30:2,3]imidazo[4,5-*B*]quinoxaline. *J. Saudi Chem. Soc.*, **2013**. doi:10.1016/j.jscs.2012.12.011.
- Thabit, M. G., El Bialy, S. A. A., Nasr, M. N. A. Synthesis and biological evaluation of new 3-(4-substituted phenyl)aminoquinoxaline derivatives as anticancer agents. *Heterocycl. Commun.*, **2015**, 21(1), 25-35.
- Torres, E., Viguri, E. M., Galiano, S., Devarapally, G., Crawford, P. W., Azqueta, A., Arbillaga, L., Varela, J., Birriel, E., Maio, R. D., Cerecetto, H., González, M., Aldana, I., Monge, A., Pérez-Silanes, S. Novel quinoxaline 1,4-di-*N*-oxide derivatives as new potential antichagasic agents. *Eur. J. Med. Chem.*, **2013**, 66, 324-334.
- Vekariya, N. A., Khunt, M. D., Parikh, A. R. Synthesis of isoxazoles and quinoxalines as potential anticancer agents. *Indian J. Chem., Sect B.*, **2003**, 42B, 421-424.
- Zarranz, B., Jaso, A., Aldana, I., Monge, A. Synthesis and anticancer activity evaluation of new 2-alkylcarbonyl and 2-benzoyl-3-trifluoromethylquinoxaline 1,4-di-*N*-oxide derivatives. *Bioorg. Med. Chem.*, **2004**, 12, 3711-3721.

Chapter 3. The synthesis, antimicrobial and antidiabetic activity of benzimidazole scaffolds

Abstract

Molecules with a benzimidazole scaffold are regarded as an important class of heterocyclic compounds with a wide spectrum of biological activities. We report on the latest synthetic methods and mechanisms of these reactions as well as their antibacterial, antifungal and antidiabetic activities. The present review covers more than 60 of the latest references, which focused on the synthesis of the benzimidazole scaffold using various synthetic strategies.

Keywords: Benzimidazole, synthesis, mechanism, antibacterial, antifungal, antidiabetic.

3.1 Introduction

Benzimidazoles are the benzo derivatives of imidazole, also known as 1*H*-benzimidazole or 1,3-benzodiazole (**Figure 3-1**). Benzimidazole and thiobenzimidazole both exist in two equivalent tautomeric forms (**Figure 3-2**). In 1944, Woolley proved that benzimidazoles showed similar therapeutic potential to purines in eliciting optimum biological responses (Woolley et al., 1944). In recent years, benzimidazoles have gained much importance, having applications in the pharmaceutical industry (Chaudhari et al., 2014; Yadav et al., 2015; Preethi et al., 2015; Aboul-Enein et al., 2015; Verma et al., 2016), in agriculture as fungicides (Yang et al., 2011; Raghunath et al., 2014) and in industry (Tang et al., 2013; Finšgar et al., 2014; Zhang et al., 2014). In addition, benzimidazoles are applied as important intermediates in many organic reactions (Sánchez et al., 2016). There are currently a number of drugs in the market containing a benzimidazole scaffold, such as omeprazole (proton pump inhibitors), albendazole (anthelmintic), mebendazole (antimicrobial) and envirodine (antiviral) (Bansal et al., 2015; Yadav et al., 2015).

Benzimidazoles have been prepared most commonly from the reaction of *o*-phenylenediamine with carbonyl-containing compounds such as carboxylic acids, acid chlorides and aldehydes, under harsh dehydrating conditions using strong acids such as polyphosphoric and hydrochloric acids (Chen et al., 2014; Fang et al., 2016; Khairunissa et al., 2016; Weijie et al., 2016). When *o*-phenylenediamine was reacted with carbon disulphide (Reddy et al., 2016) or hydrazinecarbothioamide (El Ashry et al., 2010), 1*H*-benzo[*d*]imidazole-2-thiols were produced. In addition, *o*-phenylenediamines reacted with cyanogen bromide or urea produced 1*H*-benzo[*d*]imidazol-2-amines and 1*H*-benzo[*d*]imidazol-2(3*H*)-ones respectively (Abbas et al., 2013; Reddy et al., 2016).

There have also been reports of the preparation of benzimidazole isoindolones from *o*-phenylenediamines and phthalic anhydride (Deshmukh et al., 2015; Mehta et al., 2015) as well as 2-(*o*-sulfamoylphenyl) benzimidazoles with *o*-phenylenediamine and saccharin (Ashraf et al., 2016). Such reactions provide convenient strategies for the synthesis of hybrid benzimidazoles, which have the potential to be further derivatized. Beside *o*-phenylenediamines, *o*-nitro arylamines were also used to synthesize benzimidazoles, producing 2-cyclohexyl-1*H*-benzimidazoles with cyclohexanecarbonyl chloride (Park et al., 2014).

This mini review covers the literature from 2014 to May 2016 focusing on the various pathways for the synthesis of the benzimidazole nucleus under different reaction conditions. In addition, we attempt to explain a mechanistic pathway for the formation of the benzimidazole nucleus from *o*-phenylenediamine. The antibacterial, antifungal and antidiabetic activity of benzimidazole derivatives are also highlighted in this review.

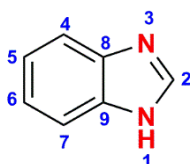


Figure 3-1 The general structure of a benzimidazole with nomenclature included

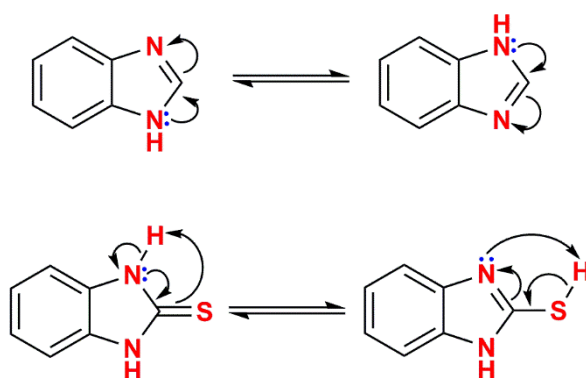


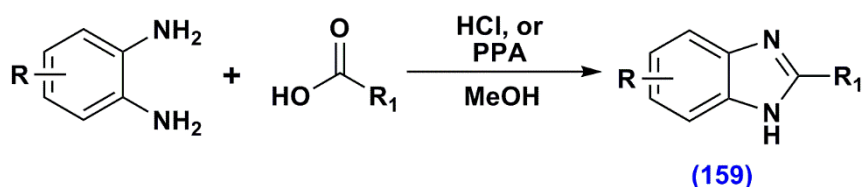
Figure 3-2 Tautomeric forms of benzimidazoles

3.2 Synthesis

There are two common methods for the synthesis of benzimidazoles. The first is the coupling of *o*-phenylenediamine with carboxylic acids or their derivatives and the second involves a two-step reaction that includes oxidative cyclo-dehydrogenation of Schiff bases generated from the condensation of *o*-phenylenediamine and aldehydes. Since a vast number of acids and aldehydes are available, a large number of benzimidazoles have been prepared from these precursors.

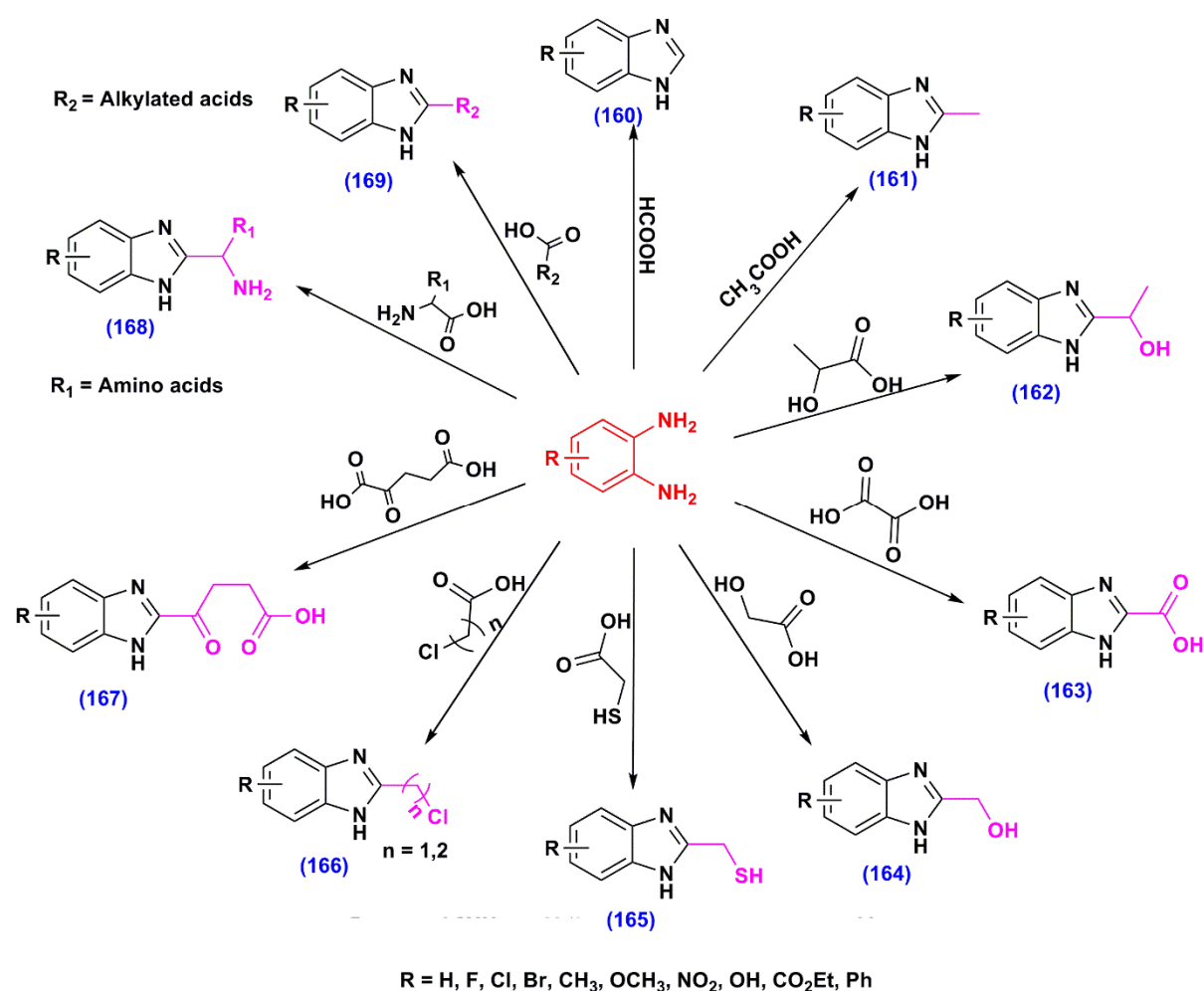
3.2.1 Benzimidazoles synthesized from substituted *o*-phenylenediamine with carboxylic acids

2-Substituted benzimidazoles (**159-174**) were prepared in good yields from *o*-phenylenediamines and different types of carboxylic acids in the presence of hydrochloric or polyphosphoric acid (**Scheme 3-1** to **Scheme 3-3**) (Chinnappadu et al., 2014; Harkala et al., 2014; Huizhen et al., 2014; Madabhushi et al., 2014; Rao et al., 2014; Alasmary et al., 2015; Chandra et al., 2015; Elagab et al., 2015; Gobis et al., 2015; Kankate et al., 2015; Mariappan et al., 2015; Rashid et al., 2015; Fang et al., 2016; Gaballah et al., 2016; Govindaraj et al., 2016; Mehta et al., 2016; Reddy et al., 2016; Tien et al., 2016; Wu et al., 2016; Zhang et al., 2016).

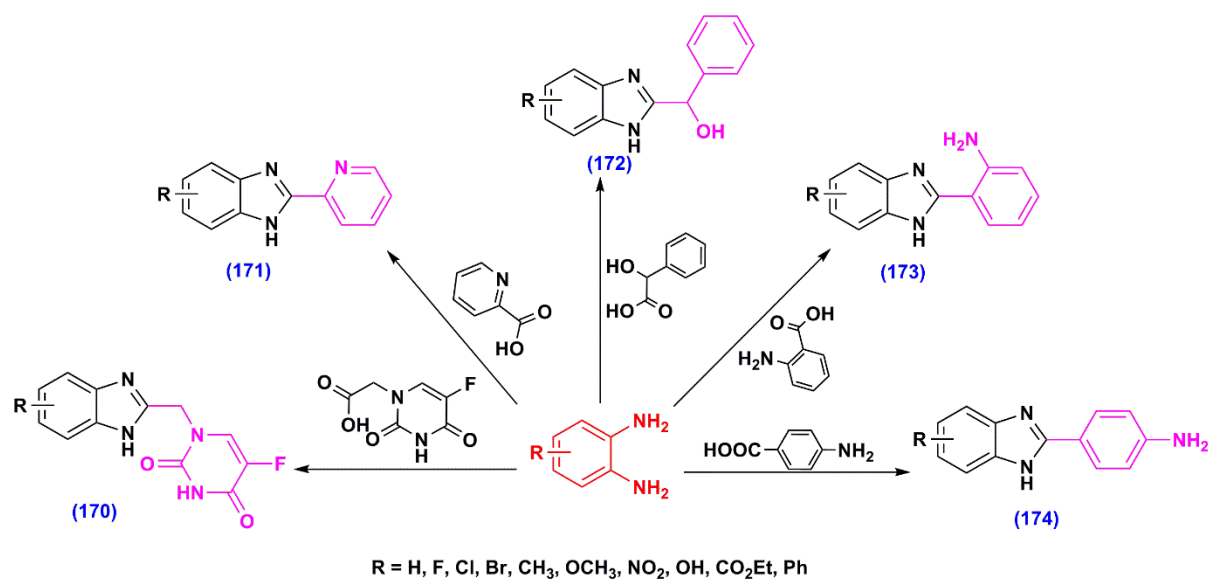


Scheme 3-1 General scheme of synthesis of benzimidazole

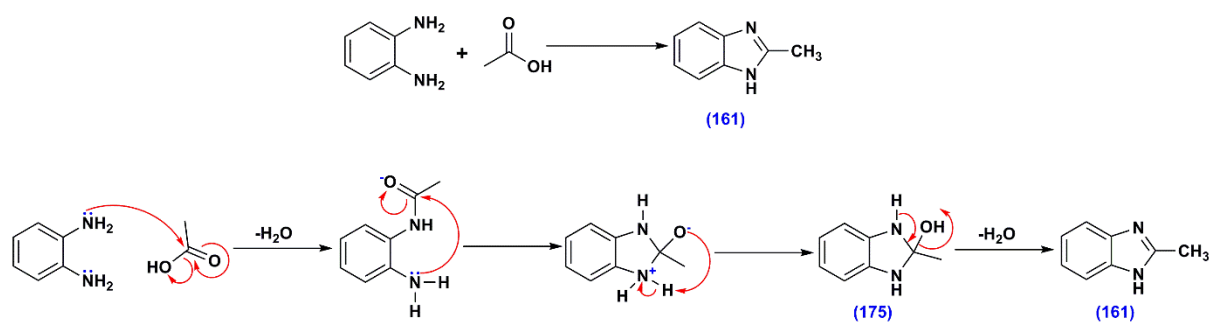
The mechanism for this reaction involves nucleophilic addition of the amino group to the carbonyl carbon of the carboxylic acid, forming the amide, after which a second nucleophilic step involving the other amino group resulted in the alcohol addition intermediate (**175**), which formed the benzimidazole (**161**) upon dehydration (**Scheme 3-4**). The reaction is catalysed by either polyphosphoric or hydrochloric acid, whose function is to activate the carboxylic acid, making the carbonyl group more susceptible to nucleophilic attack.



Scheme 3-2 Synthesis of 2-substituted benzimidazoles using various carboxylic acid



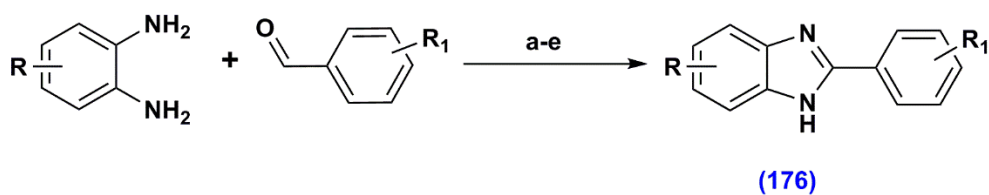
Scheme 3-3 Synthesis of 2-substituted benzimidazoles using various carboxylic acid



Scheme 3-4 Mechanism of synthesis of benzimidazole (161)

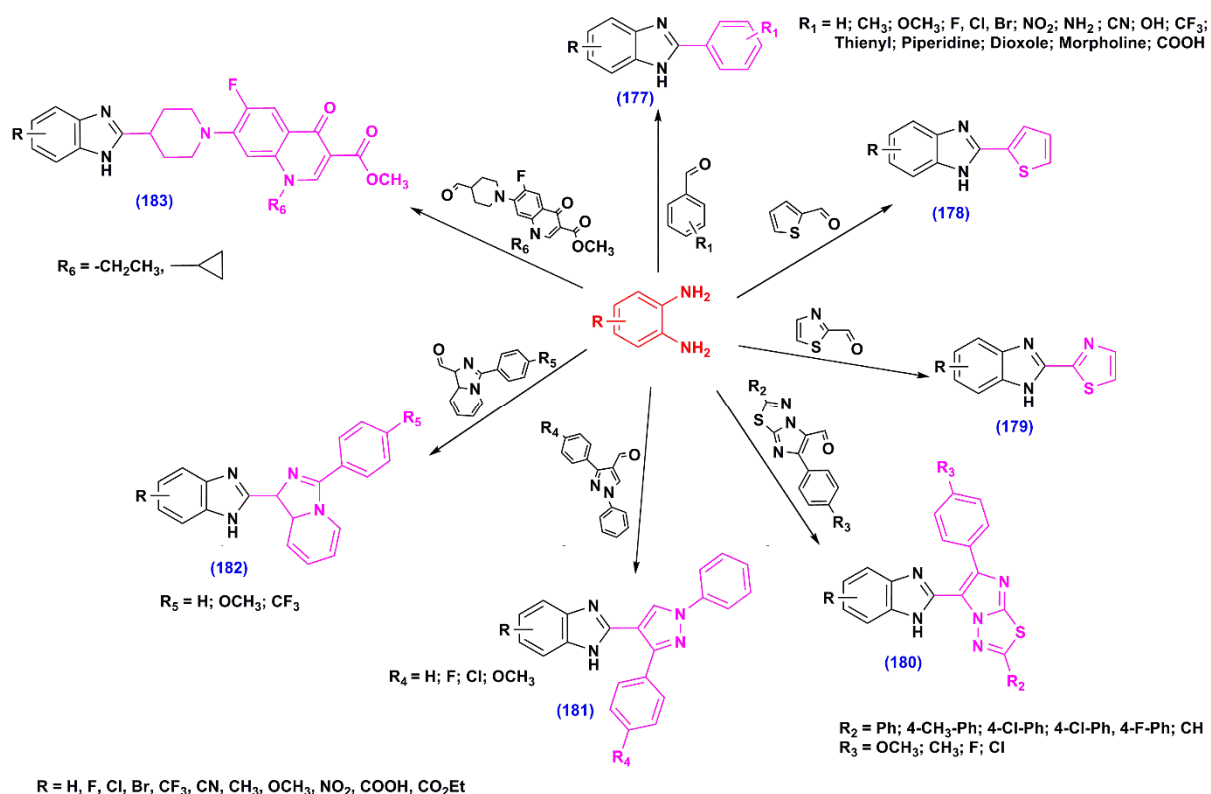
Benzimidazoles synthesized from substituted *o*-phenylenediamine and aldehydes

Aldehydes react with *o*-phenylenediamines in the presence of a catalyst such as sodium dithionite (Kamal et al., 2014; Kumar et al., 2015), sodium metabisulfite (Taha et al., 2014; Kamal et al., 2015; Ramprasad et al., 2015; Khairunissa et al., 2016), sodium bisulfite (Weijie et al., 2016), copper sulfate (Zhang et al., 2016), ammonium chloride (Al-ebaist et al., 2015), zinc oxide or magnesium oxide (Dinparastast et al., 2016), resulting in 2-substituted benzimidazoles (176-183) (**Scheme 3-5** and **Scheme 3-6**).

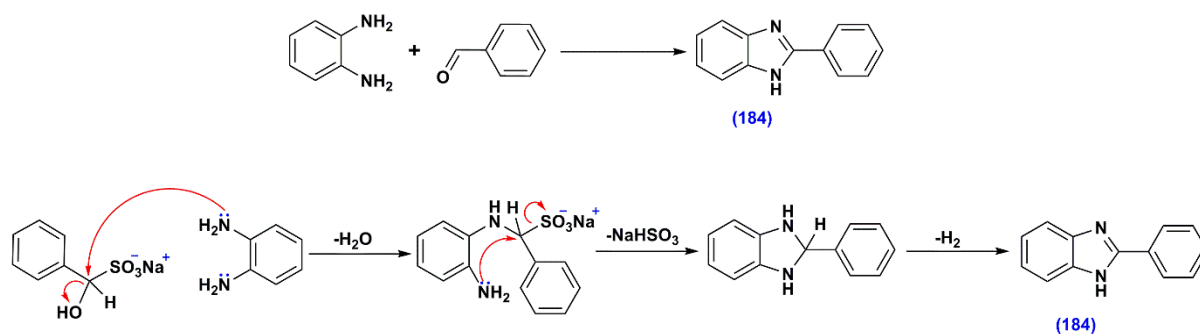


Reaction conditions: (a) Na₂S₂O₄, EtOH/ DMSO; (b) Na₂S₂O₅, EtOH/ DMF/ MeOH:H₂O; (c) NaHSO₃, EtOH,H₂O; (d) CuSO₄, 1,4-dioxane; (e) NH₄Cl, CHCl₃; (f) Nano-ZnO/Mgo, [bmim]Cl

Scheme 3-5 Synthesis of benzimidazole using different reaction conditions



Scheme 3-6 Synthesis of 2-substituted benzimidazoles using various aldehydes



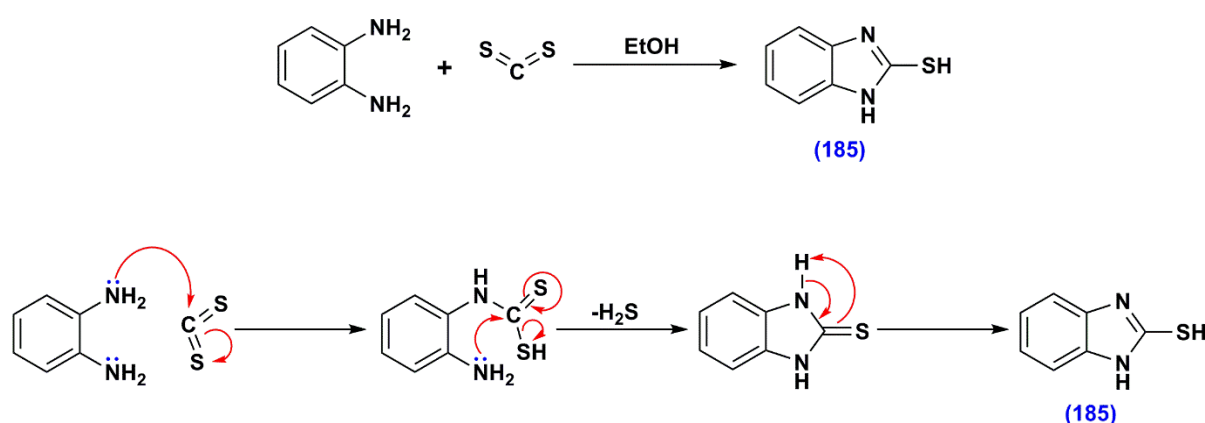
Scheme 3-7 Mechanism of synthesis of benzimidazole (184)

Eren et al. (2014) reports a plausible mechanism for this reaction in which sodium sulphite adds to the aldehyde intermediate forming the hydroxy sulphite, which is then attacked by one of the amino groups of the *o*-phenylenediamine. This first substitutes the hydroxy group and subsequently the sulphite group when the second amino group adds to the same carbon, forming the benzimidazole (**184**) after the release of H₂ (**Scheme 3-7**) (Eren et al., 2014).

3.2.2 1*H*-benzo[*d*]imidazole-2-thiols synthesized from substituted *o*-phenylenediamine with carbondisulfide or hydrazinecarbothioamide

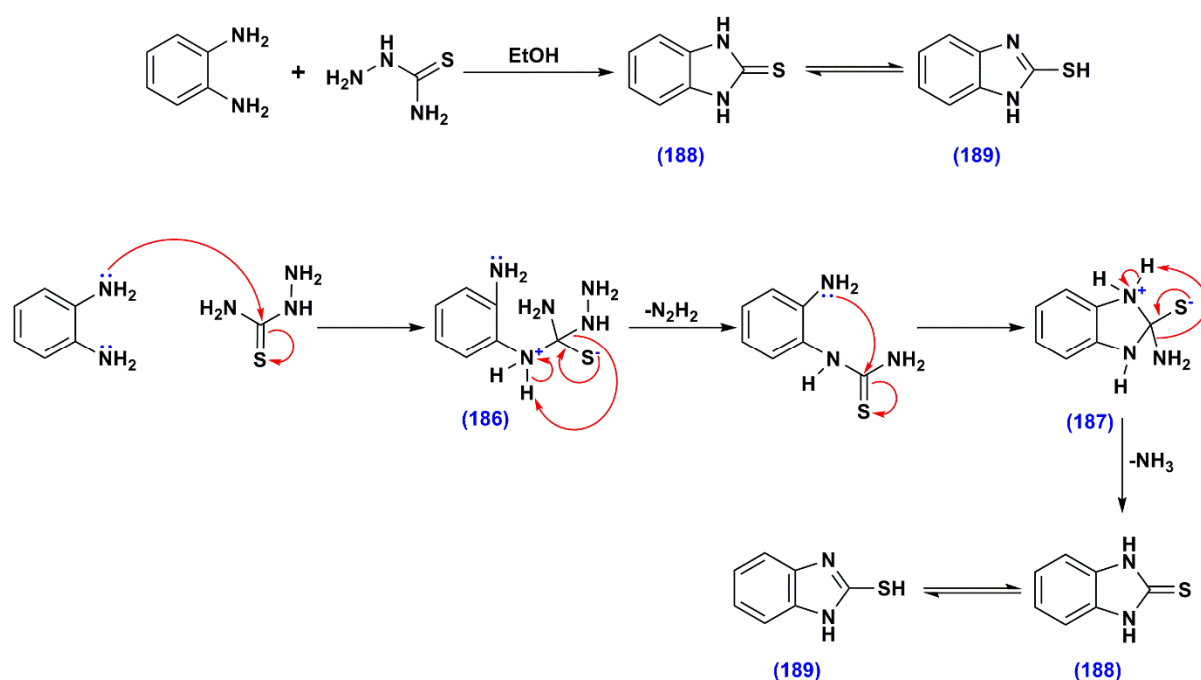
Both carbon disulphide and carbothioamide were used to synthesize benzimidazole-2-thiols with *o*-phenylenediamine, however no mechanisms are reported in the literature (El Ashry et al., 2010; Reddy et al., 2016). We postulate mechanisms for each of the reactions below.

With carbon disulphide, the amino group from *o*-phenylenediamine adds to the carbon of CS₂ forming a thiol intermediate, which is attacked by the second amino group, substituting the thiol group, eliminating H₂S and forming the benzimidazole thiol (**185**) (**Scheme 3-8**).



Scheme 3-8 Synthesis of thiobenzimidazole (**185**)

Using hydrazine carbothiamide, the amino group of *o*-phenylenediamine attacks the electrophilic carbon in the usual manner, forming a tetrahedral sulphide intermediate (186), which then collapses eliminating hydrazine and forming a trigonal planar thiourea like intermediate, which is again attacked by the second amino group forming a tetrahedral sulphide intermediate again (187), which this time collapses eliminating ammonia and forming the thiobenzimidazole (188-189) (Scheme 3-9).

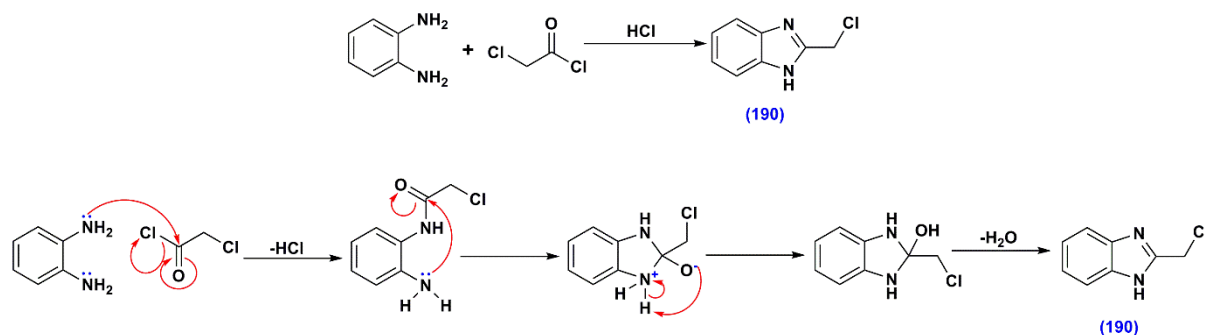


Scheme 3-9 Synthesis with possible mechanism of formation of thiobenzimidazole using hydrazine carbothiamide

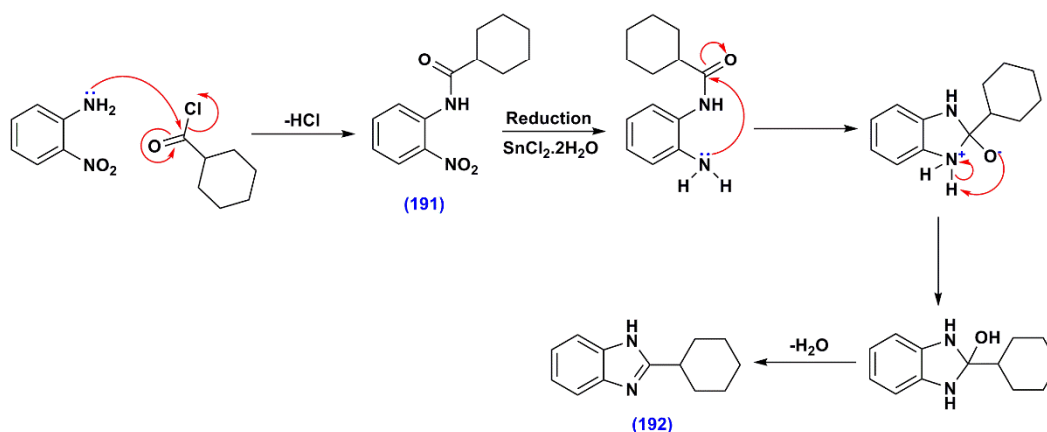
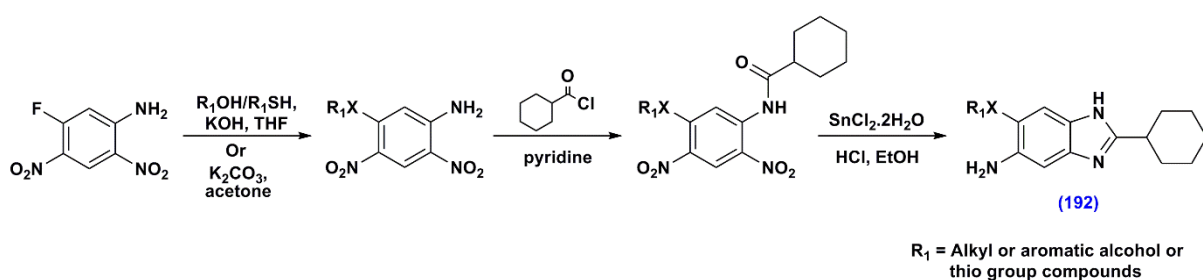
3.2.3 Benzimidazoles synthesized from *o*-phenylenediamine or *o*-nitroaniline and acid chlorides

Benzimidazoles are formed in good yields using *o*-phenylenediamine with acid chlorides (Chen et al., 2014; Park et al., 2014). This reaction forms *via* nucleophilic acyl substitution of the chloro group with the amino group on the *o*-phenylenediamine, first forming the amide, which is attacked further by the second amino group forming a tetrahedral intermediate, which

ultimately forms the benzimidazole (**190**) by elimination of water (**Scheme 3-10**). When *o*-nitroanilines are used instead of *o*-phenylenediamines, an additional reduction step is needed after the formation of the amide intermediate (**191**) (**Scheme 3-11**).



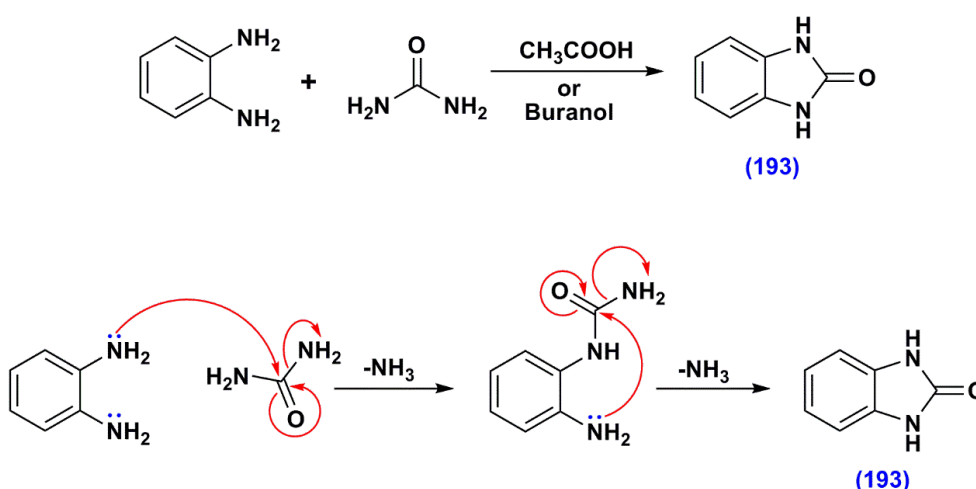
Scheme 3-10 Synthesis with mechanism of benzimidazole (**190**)



Scheme 3-11 Synthesis and mechanism of benzimidazole (**192**)

3.2.4 Benzimidazoles synthesized from *o*-phenylenediamine and urea

O-phenylenediamines react with urea in acidic condition producing 1*H*-benzo[*d*]imidazol-2(3*H*)-one in good yields (Abbas et al., 2013; Srinivas Rao et al., 2014; Benali et al., 2015). In this mechanism, the lone pair on the amino group attacks the carbonyl group of urea forming an amide bond and eliminating ammonia. The lone pair on the second amine then repeats this process to produce the benzimidazol-2(3*H*)-one (**193**) (Scheme 3-12).

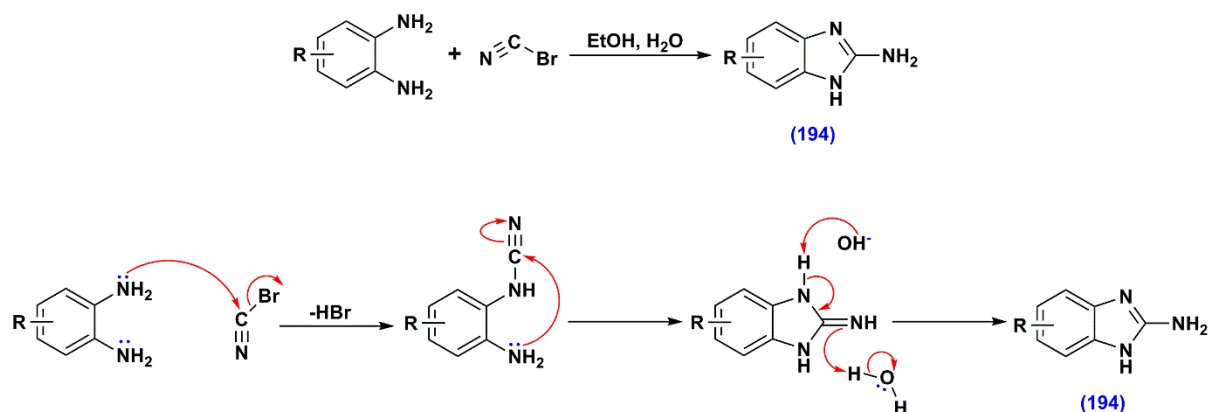


Scheme 3-12 Formation of benzimidazole using *o*-phenylenediamine and urea

3.2.5 Benzimidazoles synthesized from substituted *o*-phenylenediamine and cyanogen bromide

Benzimidazole-2-amines (**194**) are synthesized from the reaction of substituted *o*-phenylenediamines and cyanogen bromide in the presence of ethanol and water (Garg et al., 2014; Bansal et al., 2015; Reddy et al., 2016). The postulated mechanism for this reaction is attack of the lone pair of one of the amino groups from *o*-phenylenediamine on the cyanogen carbon. This occurs with a concomitant loss of HBr. The lone pair of the second amino group then attacks the same nitrile carbon, forming an imine. Proton transfers then produce the

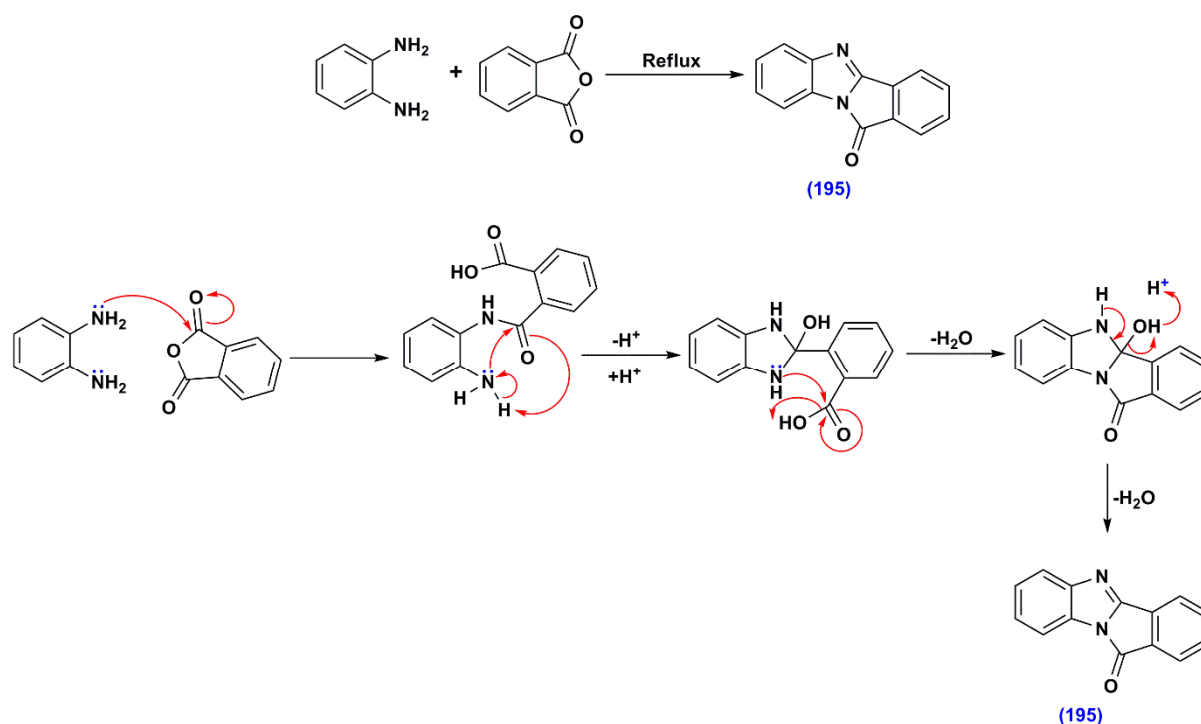
benzimidazole-2-amines (**194**) (**Scheme 3-13**). The presence of an amino group at C-2 makes a variety of derivatisation involving amino groups possible.



Scheme 3-13 Synthesis of benzimidazole using *o*-phenylenediamine and cyanogen bromide

3.2.6 Benzimidazo-indol-ones synthesized from *o*-phenylenediamine and phthalic anhydride

Benzimidazole-indole (**195**) hybrid scaffolds are formed in good yields by the reaction of *o*-phenylenediamines and phthalic anhydride (Deshmukh et al., 2015; Mehta et al., 2015). In this mechanism, the anhydride is cleaved after the amine attacks the carbonyl group of the anhydride, forming an amide bond at one end and an acid at the other. The lone pair of the second amino group then attacks the amide carbonyl group, forming an imidazole ring with a hydroxy group at C-2. A further attack of the lone pair of one of the NH groups on the imidazole moiety then reacts with the carboxylic acid forming the benzimidazo-indol-one (**195**) after a dehydration step (**Scheme 3-14**).



Scheme 3-14 Synthesis of Benzimidazo-isoindol-ones (**195**)

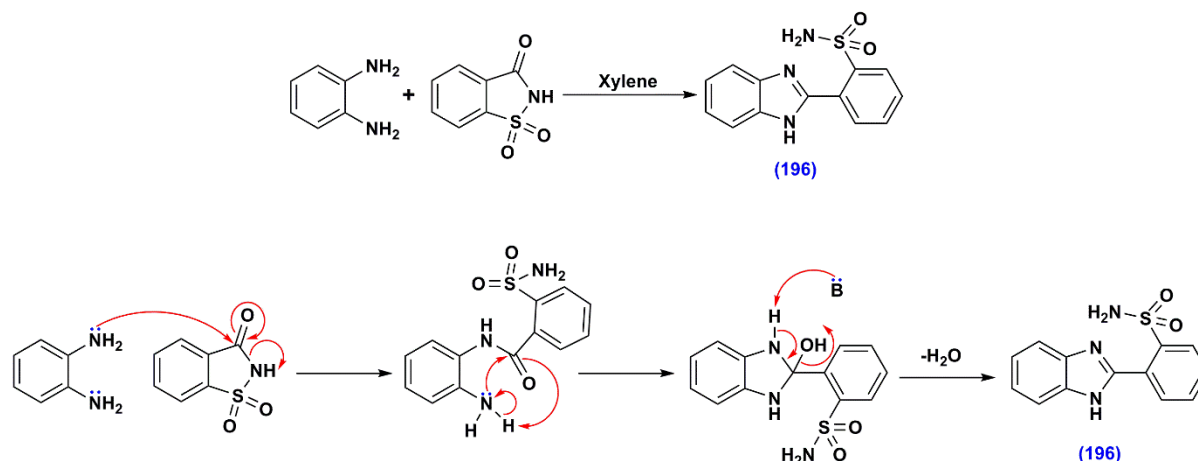
3.2.7 Benzimidazol-2-benzenesulphonamides synthesized from *o*-phenylenediamine and saccharin

The reaction of *o*-phenylenediamine and benzene sulphonamide (saccharin) produced 2-(1*H*-benzo[*d*]imidazol-2-yl)benzenesulfonamide (**196**) (Ashraf et al., 2016), probably by the lone pair of the amino group attacking the carbonyl group of saccharin, hydrolysing the amide bond. The second amino group of *o*-phenylenediamine then reacts with the newly formed amide bond, forming the benzimidazol-2-benzene sulphonamide (**196**) after a dehydration step (Scheme 3-15).

3.3 Applications of benzimidazole derivatives as antimicrobial and antidiabetic agents

Benzimidazole derivatives have shown a number of different biological activities including antimicrobial, antidiabetic, antioxidant, anticancer, anti-tubercular, anti-HIV, anti-inflammatory, antiviral, antihypertensive, antiprotozoal, anticonvulsant and analgesic activity (Keri et al., 2015; Singla et al., 2015; Khairunissa et al., 2016; Verma et al., 2016; Zhang et al.,

2016). The benzimidazole scaffold can be functionalised at a variety of positions, however the most common positions found to be derivatised are N-1, C-2, C-5 and C-6.



Scheme 3-15 Synthesis and mechanism of benzimidazol-2-benzenesulphonamides (**196**)

This short review focus on the antimicrobial and antidiabetic activities of benzimidazole derivatives since these two biological assays were carried out in this thesis.

3.3.1 Antimicrobial activity

Outlined below is a summary of benzimidazole structures with reported MIC values of $<10 \mu\text{g mL}^{-1}$ and $>30 \text{ mm}$ zones of inhibition against one or more bacterial and fungal strains (**Table 3-1** to **Table 3-6**). Essentially, these benzimidazoles were substituted at C-2 and N-1.

Compounds **197-199** contains substitution on N-1 only, with C-2 left unsubstituted. These substituents were propanoate esters. The benzene ring in these compounds were either unsubstituted (**199**), contained methyl groups at C-5 and C-6 (**197**) or a chloro group at C-6 (**198**) (**Figure 3-3**). Compounds **197** and **198** showed strain specific activity to *Bacillus*.

proteus and **199** showed activity against *Staphylococcus aureus*, all having MIC values of 8 $\mu\text{g mL}^{-1}$ (Wen et al., 2016).

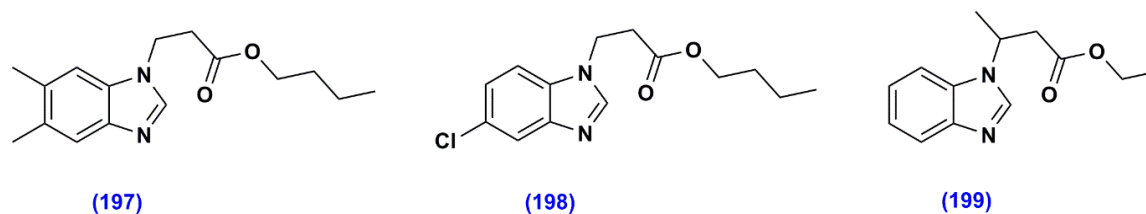


Figure 3-3 Biologically active N-1 substituted benzimidazoles

Benzimidazoles **200-204** contain hydroxy, methyl, amino and nitro groups on the phenyl ring substituted at C-2 and bromo, nitro and methyl groups on the benzene ring of benzimidazole (Al-Ebaisat et al., 2015; Govindaraj et al., 2016). Compounds **205** and **206** contain a 2-benzamide group at C-2, with the benzene ring of the benzimidazole being unsubstituted in **205** and substituted with a bromo group at C-6 in **206** (Govindaraj et al., 2016; Reddy et al., 2016). Compound **207** also contained a phenyl group at C-2, but with a phenyl tetrazolo moiety attached at the *ortho* position (Reddy et al., 2016). Compound **208** contains a fluoro group at C-5 and a methyl-5-fluorouracil moiety at C-2, while compounds **209-214** contains a thio-6-methyl pyrimidine moiety with fluoro, chloro, bromo, methyl, methoxy and trifluoromethyl groups (**209-214**) (Chen et al., 2014; Fang et al., 2016). Compounds **215-216** contains a phenyl substituted thiourea moiety at C-2, with trifluoromethyl groups on the phenyl ring and propyl and butyl groups substituted at the nitrogen of the thiourea group (**Figure 3-4**) (Madabhushi et al., 2014). Compounds **208** and **210** showed excellent MIC values of 2 $\mu\text{g mL}^{-1}$ against the fungal strain (*Candida albicans*) and Gram –ve strain (*Stenotrophomonas maltophilia*).

Benzimidazoles **217-327** all contained an imidazo-thiadiazol group attached to C-2 through C-5' of the imidazole ring in the substituent. These substituents further contained fluoro, chloro

and methoxy groups on the phenyl ring at C-4' of the imidazole group (Ramprasad et al., 2015). Compounds **238-249** contained thiomethyl-1,2,3-triazol-1-ylarylethylideneaceto-hydrazide groups at C-2, where the phenyl group was substituted with halogens, hydroxy, methoxy, isopropyl or dimethylamino groups (Youssif et al., 2014).

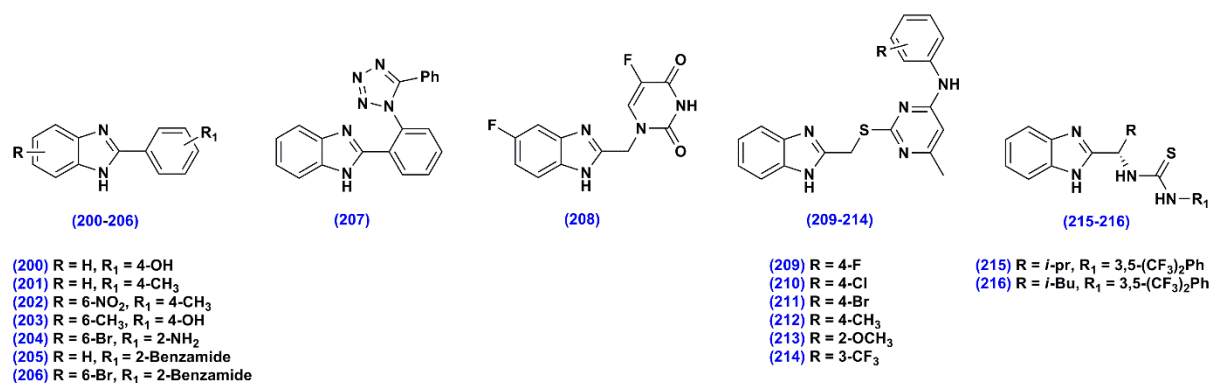


Figure 3-4 Biologically active C-2 substituted simple benzimidazoles

Compounds **250-267** each contained fluoroquinolones attached to C-2 through a piperidine linker, either directly (**250** and **251**) or through a methylene (**252-261**), ethylene (**262-263**), ethylamine (**264-265**) or imine group (**266-267**) (Zhang et al., 2016). The nitrogen of the fluoroquinoline moiety was substituted either with an ethyl group or with a cyclopropyl group and the benzene ring of the benzimidazole moiety was either unsubstituted or contained halogens (Br, Cl and F) or a nitro group. In addition, compound **268** contained an ethylidene-pyridine-6-arylimino-3,5-dicarbonitrile-4-nitrophenyl group at C-2 (**Figure 3-5** and **Figure 3-6**) (Desai et al., 2014). Among these, compounds **257** and **259** showed the best antimicrobial activity with MIC values ranging from 0.125-1 $\mu\text{g mL}^{-1}$ against Gram +ve and -ve bacterial strains. The other compounds also showed good MIC values of between 0.5-10 $\mu\text{g mL}^{-1}$.

The next class of benzimidazoles contain substitution at both N-1 and C-2. Compounds **269-272** contain ethyl, propyl, butyl and 3-F-benzyl groups at N-1, while C-2 is attached to a substituted 5-fluorouracil moiety (Fang et al., 2016).

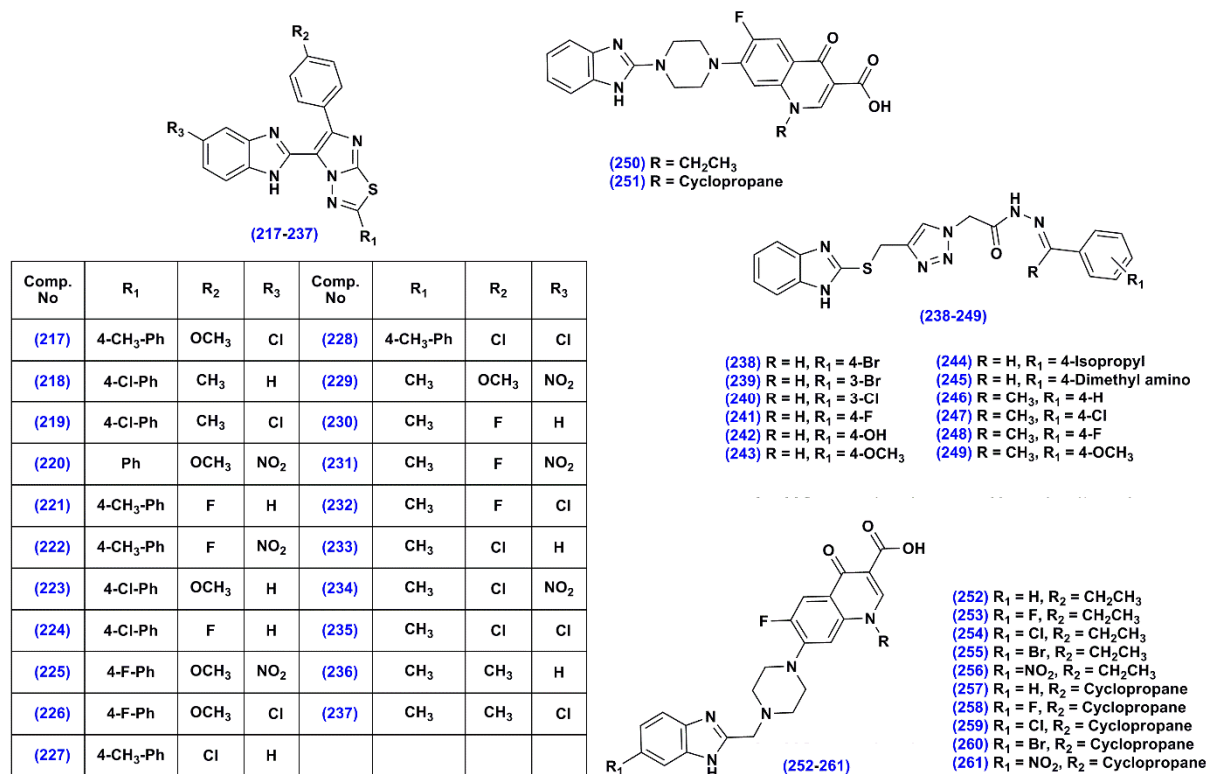


Figure 3-5 Biologically active C-2 substituted complex benzimidazoles

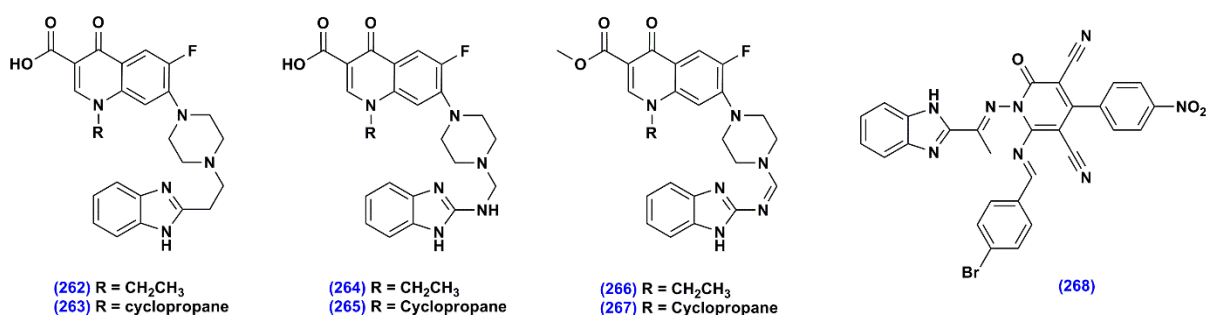


Figure 3-6 Biologically active C-2 substituted complex benzimidazoles

Compounds **273-274** contains a 2,4-difluorobenzyl group at N-1 and a 3,5-ditrifluoromethyl methylaminophenyl group at C-2 (Huizhen et al., 2014). In addition, **275** and **276** has a *N*-benzyl-*N*-methyl-5-fluorouracil group at C-2 and a substituted benzyl group at N-1 (Fang et

al., 2016). Compounds **277-301** all contain a piperidine linked fluoroquinolone linked to C-2 similar to **250-267**, but now with either an ethyl group or a substituted benzyl group at N-1 (**Figure 3-7**) (Zhang et al., 2016). Of these, compounds **292**, **295** and **299** showed the best activity against Gram +ve and Gram –ve bacterial strains and fungal strains with MIC values ranging from 0.03-8 $\mu\text{g mL}^{-1}$. Other compounds also showed good antimicrobial activity against certain bacteria.

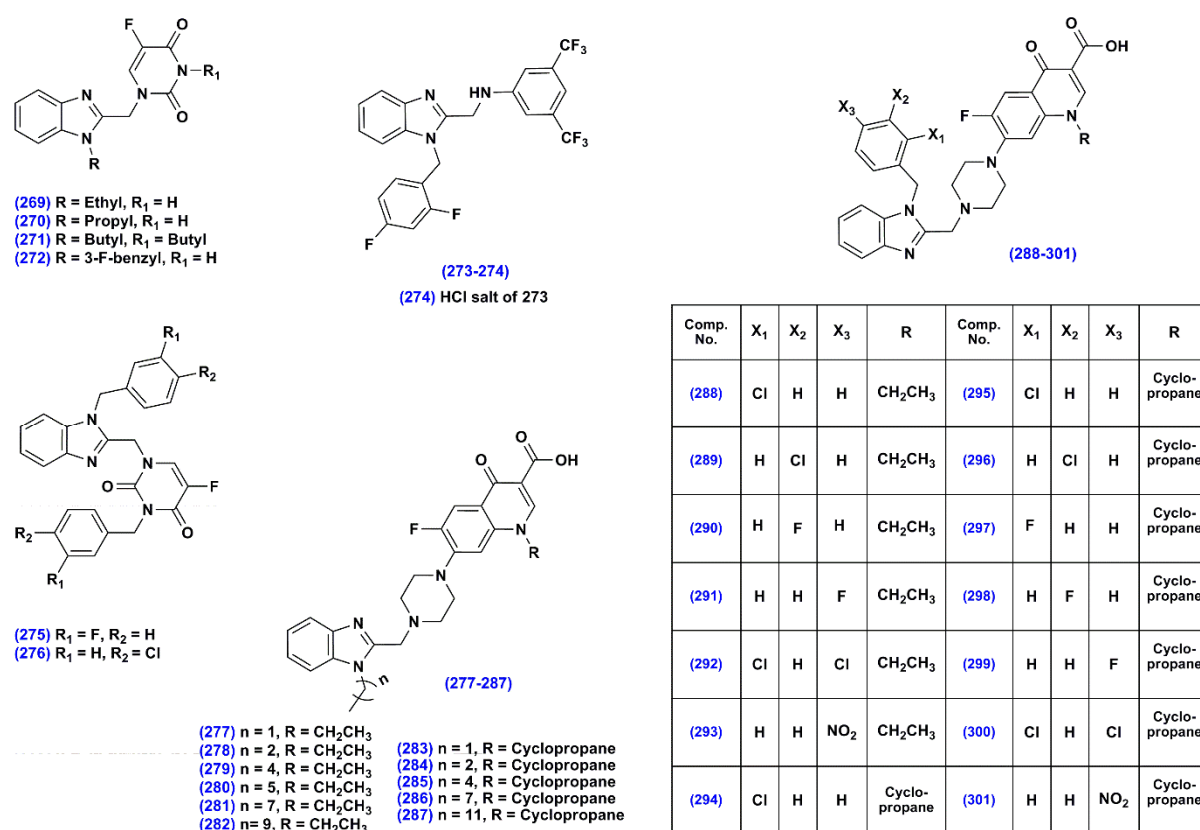


Figure 3-7 Biologically active N-1 and C-2 substituted complex benzimidazoles

Compounds **302-316** were slightly different to all the other compounds discussed previously. Compounds **302-304** contained an imine at C-2 and either phenylpropyl or 2-oxo-2-phenylethyl groups at N-1 and N-3 (Mavrova et al., 2015). Compounds **305-316** contain a propyl chain at N-1, a 2,4-dichlorophenyl moiety at C-2 and substituted benzilidene hydrazones at C-5 (**Figure 3-8**) (Kumar et al., 2015). Most of these compounds showed good activity

against the fungal strain, *Aspergillus niger* with MIC values of 3.12-6.25 $\mu\text{g mL}^{-1}$. Compound **315** showed broad spectrum antimicrobial activity with MIC values of 3.12 to 6.25 $\mu\text{g mL}^{-1}$.

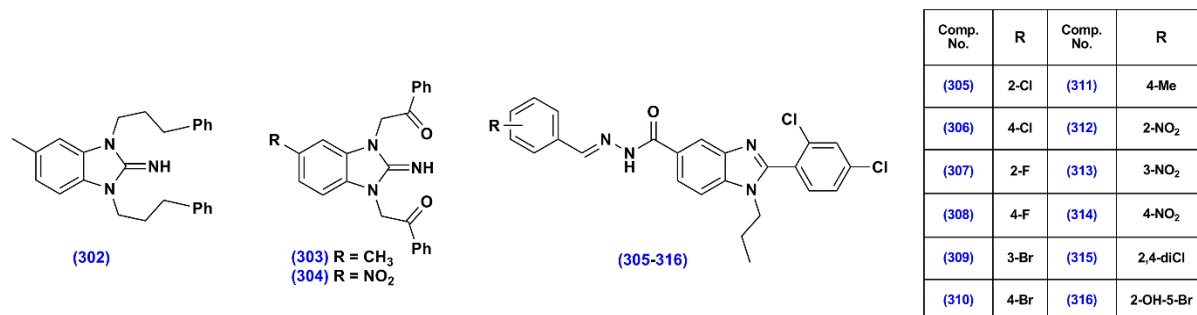


Figure 3-8 Biologically active N-1, N-3 and C-2 substituted complex benzimidazoles

3.3.2 Antidiabetic activity

Two types of benzimidazoles showed α -glucosidase inhibition with reported IC_{50} values of $<25 \mu\text{g mL}^{-1}$ (**Table 3-7**). This includes benzimidazole **318** with a 4-cyanophenyl moiety at C-2 and a 4-cyanobenzyl moiety at N-1 and compounds **319-333** with methyl groups at C-5 and C-6 and a substituted benzohydrazide group at C-2 containing hydroxy, methoxy, chloro, and methyl groups. The most active of these compounds were **319, 321, 324-325** and **333** with IC_{50} values of $<9 \mu\text{g mL}^{-1}$ (**Figure 3-9; Table 3-7**) (Dinparast et al., 2016; Khairunissa et al., 2016). In addition, 2,3-dihydro-3-(4-nitrobenzensulfonyl)-2-oxo-1H-benzimidazole (**317**) (**Figure 3-9**) coupled to hydroxyethyl starch (HES) resulted in a 67% reduction in blood glucose levels of rats (Abbas et al., 2015).

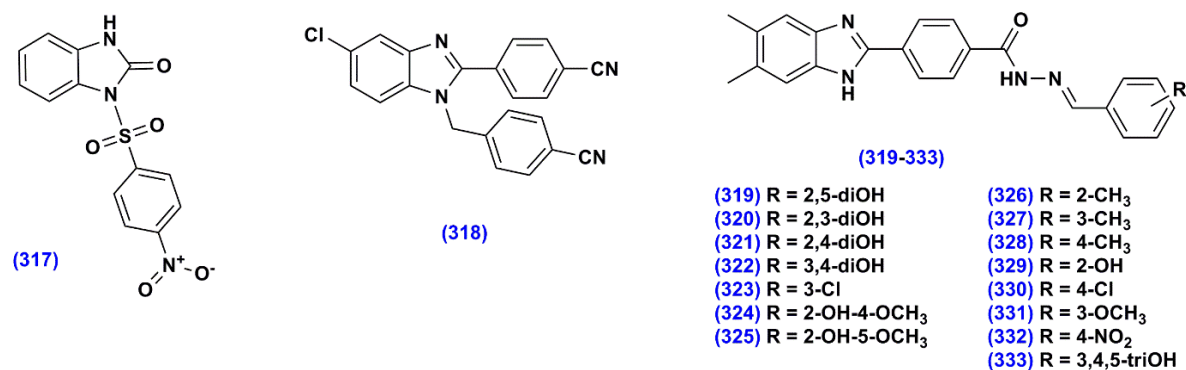


Figure 3-9 Biologically active benzimidazoles

Table 3-1 Antimicrobial activity of benzimidazole compounds (197-216)

Comp. No.	Gram +ve			Gram -ve				Fungi			
	<i>M. luteus</i>	<i>S. aureus</i>		<i>B. proteus</i>	<i>E. coli</i>	<i>P. aeruginosa</i>	<i>S. maltophilia</i>	<i>C. albicans</i>	<i>S. cerevisiae</i>	<i>C. glabrata</i>	<i>C. krusei</i>
	MIC	MIC	DD	MIC	DD	MIC					
197	-	-	-	8	-	-	-	-	-	-	-
198	-	-	-	8	-	-	-	-	-	-	-
199	-	8	-	-	-	-	-	-	-	-	-
200	-	-	-	-	-	-	-	-	-	6.25	6.25
201	-	-	-	-	-	-	-	-	-	-	6.25
202	-	-	-	-	-	-	-	-	-	-	6.25
203	-	-	-	-	-	-	-	-	-	-	6.25
204	-	-	-	-	30	-	-	-	-	-	-
205	-	-	-	-	30	-	-	-	-	-	-
206	-	-	32	-	36	-	-	-	-	-	-
207	-	-	32	-	36	-	-	-	-	-	-
208	-	8	-	-	-	-	-	2	8	-	-
209	-	-	-	-	-	-	-	8	-	-	-
210	-	8	-	-	-	-	2	-	-	-	-
211	-	-	-	-	-	-	4	8	-	-	-
212	-	-	-	-	-	-	8	-	-	-	-
213	-	-	-	-	-	-	8	-	-	-	-
214	-	-	-	-	-	-	8	-	-	-	-
215	-	-	-	-	-	6.25	-	-	-	-	-
216	6.25	-	-	-	-	-	-	-	-	-	-

MIC = Minimum inhibitory concentration in $\mu\text{g mL}^{-1}$; DD = Disc diffusion method, zone of inhibition in mm

M. luteus = *Micrococcus luteus*; *E. coli* = *Escherichia coli*; *P. aeruginosa* = *Pseudomonas aeruginosa*; *S. cerevisiae* = *Saccharomyces cerevisiae*; *C. glabrata* = *Candida glabrata*; *C. krusei* = *Candida krusei*.

Table 3-2 Antimicrobial activity of benzimidazole compounds (217-238)

Comp. No.	Gram +ve	Gram -ve			Fungi		
	<i>S. aureus</i>	<i>E. coli</i>	<i>P. aeruginosa</i>	<i>S. typhi</i>	<i>A.flavus</i>	<i>C.albicans</i>	<i>C. Keratinophilum</i>
	MIC ($\mu\text{g mL}^{-1}$)						
217	6	4	7	3	3	3	4
218	4	5	4	5	5	4	5
219	3	4	4	3	3	4	3
220	4	4	5	6	3	3	4
221	-	-	-	-	6	6	5
222	4	4	3	4	5	5	4
223	3	3	2	3	-	-	-
224	7	5	8	3	4	3	4
225	5	5	6	4	5	5	4
226	4	5	2	3	4	5	4
227	3	4	6	4	-	6	-
228	5	4	3	-	5	2	3
229	-	-	-	-	2	2	3
230	2	4	3	2	3	-	4
231	3	4	1	2	-	9	-
232	9	-	-	10	7	6	8
233	4	4	5	3	6	-	7
234	9	6	8	6	-	4	-
235	3	4	4	4	3	-	5
236	5	5	3	6	-	4	-
237	-	8	9	8	3	-	2
238	-	-	-	-	-	6.25*	-

MIC = Minimum inhibitory concentration in $\mu\text{g mL}^{-1}$; *= MIC in μM

3.4 Conclusion

Benzimidazoles can easily be prepared from substituted *o*-phenylenediamine with a variety of carboxylic acid or aldehyde derivatives. Due to the variety of substituted precursors available, a vast number of benzimidazoles were able to be prepared, however there is still scope for the synthesis of many more. Many of these compounds showed promising antimicrobial and anti-diabetic activity and can be considered lead compounds for antibiotics and anti-diabetic agents since some have shown better activity than miconazole, fluconazole and acarbose (currently used drugs).

Table 3-3 Antimicrobial activity of benzimidazole compounds (239-261)

Comp. No.	Gram +ve				Gram –ve					Fungi
	<i>B. subtilis</i>	MRSA	<i>M. luteus</i>	<i>S. aureus</i>	<i>B. proteus</i>	<i>E. coli</i>	<i>P. aeruginosa</i>	<i>S. dysenteriae</i>	<i>S. Enterica</i>	<i>C. albicans</i>
	MIC ($\mu\text{g mL}^{-1}$)									
239	-	-	-	-	-	3.12*	-	-	-	6.25*
240	-	-	-	-	-	6.25*	-	-	-	3.12*
241	-	-	-	-	-	-	-	-	-	6.25*
242	-	-	-	-	-	-	-	-	-	6.25*
243	-	-	-	-	-	6.25*	-	-	-	6.25*
244	-	-	-	-	-	3.12*	-	-	-	3.12*
245	-	-	-	-	-	-	-	-	-	3.12*
246	-	-	-	-	-	6.25*	-	-	-	6.25*
247	-	-	-	-	-	-	-	-	-	6.25*
248	-	-	-	-	-	-	-	-	-	6.25*
249	-	-	-	-	-	6.25*	-	-	-	6.25*
250	2	4	4	2	1	2	2	4	2	-
251	2	0.5	1	1	2	1	0.5	0.5	1	-
252	1	1	1	2	0.5	0.5	1	2	0.5	-
253	8	-	0.5	-	2	-	4	8	8	-
254	-	1	1	2	0.5	0.5	1	1	0.5	-
255	8	-	2	-	4	-	2	-	8	-
256	8	8	1	-	2	8	2	4	4	-
257	0.125	0.125	0.125	0.25	0.125	0.125	0.5	1	0.125	-
258	0.5	2	2	4	1	1	2	2	1	-
259	0.5	0.5	0.25	0.5	0.5	0.5	0.5	0.5	0.5	-
260	-	4	-	-	8	8	1	-	4	-
261	8	2	8	--	4	4	0.5	4	4	-

MIC = Minimum inhibitory concentration in $\mu\text{g mL}^{-1}$; * = MIC in μM ; *B. subtilis* = *Bacillus subtilis*

Table 3-4 Antimicrobial activity of benzimidazole compounds (262-285)

Comp. No.	Gram +ve				Gram –ve						Fungi				
	<i>B. subtilis</i>	<i>MRSA</i>	<i>M. luteus</i>	<i>S. aureus</i>	<i>B. proteus</i>	<i>B. typhi</i>	<i>E. coli</i>	<i>P. aeruginosa</i>	<i>S. dysenteriae</i>	<i>S. enterica</i>	<i>A. flavus</i>	<i>C. albicans</i>	<i>C. mycoderma</i>	<i>C. utilis</i>	<i>S. cerevisiae</i>
	MIC ($\mu\text{g mL}^{-1}$)														
262	2	-	-	-	-	-	-	-	-	-	-	-	-	-	-
263	-	4	1	4	2	-	4	0.5	0.5	1	-	-	-	-	-
264	8	0.5	4	2	8	-	1	1	0.5	2	-	-	-	-	-
265	1	0.25	1	1	1	-	1	0.5	0.25	1	-	-	-	-	-
266	4	-	-	-	-	-	-	8	-	-	-	-	-	-	-
267	2	-	4	-	4	-	8	2	8	4	-	-	-	-	-
268	-	6.25	-	-	-	-	-	-	-	-	-	-	-	-	-
269	-	-	-	-	-	-	8	-	-	-	-	2	-	-	4
270	-	-	-	-	-	-	-	-	-	-	-	2	-	-	8
271	-	-	-	-	8	-	-	-	-	-	-	-	8	-	8
272	8	-	-	4	2	-	2	-	-	-	-	-	-	-	4
273	-	-	-	-	-	-	8	-	-	-	-	-	-	8	-
274	8	-	8	8	-	-	-	-	-	-	8	-	8	-	8
275	-	2	-	4	4	8	2	-	-	-	8	-	-	-	1
276	-	-	-	-	-	-	-	-	-	-	-	4	-	-	-
277	2	8	4	-	1	-	4	-	-	0.5	-	-	-	-	-
278	2	-	8	-	-	-	-	-	-	-	-	-	-	-	-
279	-	-	-	-	8	-	8	-	-	-	-	-	-	-	-
280	-	-	4	-	4	-	4	-	-	8	-	-	-	-	-
281	-	2	4	-	4	-	8	2	-	4	-	-	-	-	-
282	4	8	-	-	8	-	0.5	4	8	8	-	-	-	-	-
283	0.5	-	2	-	0.5	-	2	2	8	0.5	-	-	-	-	-
284	-	2	1	-	-	-	1	1	4	4	-	-	-	-	-
285	4	-	4	-	2	-	1	2	8	4	-	-	-	-	-

MIC = Minimum inhibitory concentration in $\mu\text{g mL}^{-1}$;

Table 3-5 Antimicrobial activity of benzimidazole compounds (286-300)

Comp. No	Gram +ve				Gram –ve				
	<i>B. subtilis</i>	MRSA	<i>M. luteus</i>	<i>S. aureus</i>	<i>B. proteus</i>	<i>E. coli</i>	<i>S. dysenteriae</i>	<i>S. enterica</i>	<i>P. aeruginosa</i>
	MIC ($\mu\text{g mL}^{-1}$)								
286	-	1	1	-	0.5	0.5	4	4	1
287	4	-	4	-	4	8	2	-	4
288	-	0.125	0.5	8	4	2	-	0.5	1
289	-	2	2	-	-	8	-	4	2
290	-	-	-	-	4	-	1	8	8
291	8	-	8	8	-	-	-	8	8
292	8	0.125	0.25	4	1	1	2	0.25	1
293	2	8	4	4	-	-	4	4	4
294	0.5	4	4	-	1	2	-	2	2
295	4	0.5	0.125	8	0.5	0.5	4	0.25	0.125
296	8	0.25	0.25	-	1	1	4	0.25	2
297	-	8	-	-	-	-	-	4	-
298	8	4	-	-	-	-	-	-	8
299	4	0.125	0.0625	8	0.03	0.125	1	0.03	0.5
300	4	2	8	4	8	-	8	-	4

Table 3-6 Antimicrobial activity of benzimidazole compounds (**301-316**)

Comp. No.	Gram +ve		Gram -ve			Fungi			
	<i>B. subtilis</i>	<i>S. aureus</i>	<i>E. coli</i>	<i>K. pneumonia</i>	<i>S. abony</i>	<i>A. niger</i>	<i>C. albicans</i>	<i>C. tropicalis</i>	<i>P. notatum</i>
	MIC ($\mu\text{g mL}^{-1}$)								
301	0.125*	0.016*	0.50*	-	0.50*	-	-	-	-
302	0.50*	0.50*	-	-	-	-	-	-	-
303	1*	-	-	-	-	-	-	-	-
304	-	-	-	-	-	6.25	-	6.25	-
305	-	-	6.25	-	-	-	-	-	-
306	6.25	-	6.25	-	-	3.12	6.25	6.25	-
307	6.25	6.25	6.25	6.25	-	6.25	6.25	6.25	-
308	-	6.25	-	-	-	3.12	-	-	-
309	6.25	-	3.12	-	-	6.25	-	-	-
310	-	6.25	-	6.25	-	3.12	-	6.25	6.25
311	6.25	-	-	-	-	-	-	-	-
312	-	-	-	-	-	6.25	6.25	3.12	-
313	-	-	-	-	-	6.25	-	-	-
314	-	-	-	-	-	6.25	-	-	-
315	3.12	3.12	3.12	6.25	-	3.12	3.12	6.25	6.25
316	-	-	6.25	-	-	6.25	-	-	-

* = Minimum inhibitory concentration (MIC) in mg mL^{-1}

Table 3-7 α -Glucosidase inhibitory enzyme activity

Comp. No.	IC ₅₀ $\mu\text{g mL}^{-1}$	Comp. No.	IC ₅₀ $\mu\text{g mL}^{-1}$
318	22.4	326	84.84
319	8.74	327	23.53
320	9.99	328	18.30
321	8.74	329	18.21
322	12.49	330	24.82
323	22.36	331	15.06
324	8.44	332	19.35
325	8.44	333	8.40

3.5 References

- Abbas, M. A., Hameed, S., Kressler, J. Preparation of 2(3*H*)-Benzimidazolone and its derivative under aqueous condition as a potential agent for antidiabetic compounds. *Asian J. Chem.*, **2013**, 25(1), 509-511.
- Abbas, M. A., Hameed, S., Farman, M., Kressler, J., Mahmood, N. Conjugates of degraded and oxidized hydroxyethyl starch and sulfonylureas: Synthesis, characterization, and *in vivo* antidiabetic activity. *Bioconjugate Chem.*, **2015**, 26, 120-127.
- Aboul-Enein, H. Y., El Rashedy, A. A. Benzimidazole derivatives as antidiabetic agents. *Med. Chem.*, **2015**, 5(7), 318-325.
- Alasmay, F. A. S., Snelling, A. M., Zain, M. E., Alafeefy, A. M., Awaad, A. S., Karodia, N. Synthesis and evaluation of selected benzimidazole derivatives as potential antimicrobial agents. *Molecules*, **2015**, 20, 15206-15223.
- Al-Ebaisat, H. S. Evaluation of biological activity of some benzimidazole derivatives as antifungal. *Int. Res. J. Pure Appl. Chem.*, **2015**, 8(1), 19-25.
- Ashraf, A., Siddiqui, W. A., Akbar, J., Mustafa, G., Krautscheid, H., Ullah, N., Mirza, B., Sher, F., Hanif, M., Hartinger, C. G., Metal complexes of benzimidazole derived sulfonamide: Synthesis, molecular structures and antimicrobial activity. *Inorg. Chim. Acta.*, **2016**, 443, 179-185.
- Bansal, Y., Kaur, M., Silakari, O. Benzimidazoleibuprofen/mesalamine conjugates: Potential candidates for multifactorial diseases. *Eur. J. Med. Chem.*, **2015**, 89, 671-682.
- Benali, B., El Assyry, A., Boucetta, A., Lazar, Z., Lakhrissi, B. Thermal, structural, and conformational study of the benzimidazolone molecule. *Res. Chem. Intermed.*, **2015**, 41, 821-830.
- Chandra, J. K., Srinivasan, R., Vasavi, G., Lakshmi, P. V., Swathi, S., Latarose, K., Radhika, M., Swathi, N. Synthesis and biological evaluation of benzimidazole derivatives. *World J. Pharm. Pharm. Sci.*, **2015**, 4(6), 990-997.

- Chaudhari, V. K., Pathak, D., Singh, S. Benzimidazole: As potential biologically active agent. *Int. Res. J. Pharm.*, **2014**, 5(12), 861-875.
- Chen, P., Yang, A., Gu, Y., Zhang, X., Shao, K., Xue, D., He, P., Jiang, T., Zhang, Q., Liu, H. Synthesis, *in vitro* antimicrobial and cytotoxic activities of novel pyrimidine–benzimidazole combinations. *Bioorg. Med. Chem. Lett.*, **2014**, 24, 2741-2743.
- Chinnappadu, B., Chandra, S. S., Prasanna, V. S., Veeranjanyulu, P., Sumanth, M. Synthesis and evaluation of 2-substituted benzimidazoles. *World J. Pharm. Pharm. Sci.*, **2014**, 3(10), 1538-1549.
- Desai, N. C., Shihory, N. R., Kotadiya, G. M., Desai, P. Synthesis, antibacterial and antitubercular activities of benzimidazole bearing substituted 2-pyridone motifs. *Eur. J. Med. Chem.*, **2014**, 82, 480-489.
- Deshmukh, M. S., Bhagwat, A. A., Sekar, N. A. combined experiment and computation study of the fused polycyclic benzimidazole derivatives. *J. Fluoresc.*, **2015**, 25, 127-136.
- Dinparast, L., Valizadeh, H., Bahadori, M. B., Soltani, S., Asghari, B., Rashidi, M. R. Design, synthesis, α -glucosidase inhibitory activity, molecular docking and QSAR studies of benzimidazole derivatives. *J. Mol. Struct.*, **2016**, 1114, 84-94.
- El Ashry, E. S., Aly, A., Aouad, M. R., Amer, M. R. Revisit to the reaction of *o*-phenylene diamine with thiosemicarbazide to give benzimidazole-2-thione rather than benzotriazine-2-thione and its glycosylation. *Nucleosides, Nucleotides Nucleic Acids*, **2010**, 29(9), 698-706.
- Elagab, H. A., Alt, H. G. Titanium, zirconium and vanadium complexes of 2-(benzimidazolyl, benzothiazolyl, and benzoxazolyl) pyridine as catalyst precursors for ethylene polymerization. *Inorg. Chim. Acta.*, **2015**, 431, 266-275.
- Eren, B., Bekdemir, Y. Simple, mild, and highly efficient synthesis of 2-substituted benzimidazoles and bis-benzimidazoles. *Quim. Nova*, **2014**, 37(4), 643-647.
- Fang, X., Jeyakumar, P., Avula, S. R., Zhou, Q., Zhou, C. Design, synthesis and biological evaluation of 5-fluorouracil-derived benzimidazoles as novel type of potential antimicrobial agents. *Bioorg. Med. Chem. Lett.*, **2016**, 26(11), 2584-2588.
- Finšgar, M., Jackson, J. Application of corrosion inhibitors for steels in acidic media for the oil and gas industry: A review. *Corros. Sci.*, **2014**, 86, 17-41.
- Gaballah, S. T., El-nezhawy, A. O. H., Amer, H., Ali, M. M., Mahmoud, A. E. E., Horvath, A. H. Synthesis and antiproliferative activities of benzimidazole-based sulfide and sulfoxide derivatives. *Sci. Pharm.*, **2016**, 84, 1-18.
- Garg, K., Bansal, Y., Bansal, G., Goel, R. K. Design, synthesis, and PASS-assisted evaluation of novel 2-substituted benzimidazole derivatives as potent anthelmintics. *Med. Chem. Res.*, **2014**, 23, 2690-2697.
- Gobis, K., Foks, H., Suchan, K., Augustynowicz-Kopec, E., Napiorkowska, A., Bojanowski, K. Novel 2-(2-phenalkyl)-1*H*-benzo[d]imidazoles as antitubercular agents. Synthesis, biological evaluation and structure–activity relationship. *Bioorg. Med. Chem.*, **2015**, 23, 2112-2120.

- Govindaraj, M., Vijayakumar, K., Nair, V. N., Simon, A. V. Synthesis characterization and biological activity of benzimidazole derivatives. *Int. J. Eng. Res. & Mod. Educ.*, **2016**, 1(1), 75-79.
- Harkala, K. J., Eppakayala, L., Maringanti, T. C. Synthesis and biological evaluation of benzimidazole-linked 1,2,3-triazole congeners as agents. *Org. Med. Chem. Lett.*, **2014**, 4(14), 1-4.
- HuiZhen, Z., JianMei, L., Syed, R., ChengHe, Z. Design, synthesis, and biological evaluation of novel benzimidazole derivatives and their interaction with calf thymus DNA and synergistic effects with clinical drugs. *Sci. China Chem.*, **2014**, 57(6), 807-822.
- Kamal, A., Rao, A. V. S., Nayak, V. L., Reddy, N. V. S., Swapna, K., Ramakrishna, G., Alvala, M. Synthesis and biological evaluation of imidazo-[1,5-a]pyridine-benzimidazole hybrids as inhibitors of both tubulin polymerization and PI3K/Akt pathway. *Org. Biomol. Chem.*, **2014**, 12, 9864-9880.
- Kamal, A., Nagaseshadri, B., Nayak, V. L., Srinivasulu, V., Sathish, M., Kapure, J. S., Reddy, C. S. Synthesis and biological evaluation of benzimidazole-oxindole conjugates as microtubule-targeting agents. *Bioorg. Chem.*, **2015**, 63, 72-84.
- Kankate, R. S., Gide, P. S., Belsare, D. P. Design, synthesis and antifungal evaluation of novel benzimidazole tertiary amine type of fluconazole analogues. *Asian J. Chem.*, **2015**. in press, <http://dx.doi.org/10.1016/j.arabjc.2015.02.002>.
- Keri, R. S., Hiremathad, A., Budagumpi, S., Nagaraja, B. M., Comprehensive review in current developments of benzimidazole-based medicinal chemistry. *Chem. Biol. Drug Des.*, **2015**, 86, 19-65.
- Khairunissa, N., Zawawi, N. A., Taha, M., Ahmat, N., Wadood, A., Ismail, N. H., Rahim, F., Azam, S. S., Abdullah, N. Benzimidazole derivatives as new α -glucosidase inhibitors and in silico studies. *Bioorg. Chem.*, **2016**, 64, 29-64.
- Kumar, V., Basavarajaswamy, G., Rai, M. V., Poojary, B., Pai, V. R., Shruthi, N., Bhat, M. Rapid 'one-pot' synthesis of a novel benzimidazole-5-carboxylate and its hydrazone derivatives as potential anti-inflammatory and antimicrobial agents. *Bioorg. Med. Chem. Lett.*, **2015**, 25, 1420-1426.
- Madabhushi, S., Reddy Mallu, K. K., Vangipuram, V. S., Kurva, S., Poornachandra, V., Kumar, C. G. Synthesis of novel benzimidazole functionalized chiral thioureas and evaluation of their antibacterial and anticancer activities. *Bioorg. Med. Chem.*, **2014**, 24, 4822-4825.
- Mariappan, G., Hazarika, R., Alam, F., Karki, R., Patangia, U., Nath, S. Synthesis and biological evaluation of 2-substituted benzimidazole derivatives. *Asian J. Chem.*, **2015**, 8, 715-719.
- Mavrova, A. T., Yancheva, D., Anastassova, N., Anichina, K., Zvezdanovic, J., Djordjevic, A., Markovic, D., Smelcerovic, A. Synthesis, electronic properties, antioxidant and antibacterial activity of some new benzimidazoles. *Bioorg. Med. Chem.*, **2015**, 23, 6317-6326.
- Mehta, P., Chovatiya, P., Joshi, H. S. Synthesis, characterization and antimicrobial evaluation of some novel benzenesulfonylhydrazone derivatives of benzimidazole. *Chem. Sin.*, **2015**, 6(2), 29-34.
- Mehta, M. R., Batra, S., Synthesis of benzothiazole-benzimidazole thiazolidin derivatives as anti-inflammatory and analgesic. *J. Chem. Bio. Phy. Sci. Sec. A.*, **2016**, 6(2), 410-418.

- Park, B., Awasthi, D., Chowdhury, S. R., Melief, E. H., Kumar, K., Knudson, S. E., Slayden, R. A., Ojima, I. Design, synthesis and evaluation of novel 2,5,6-trisubstituted benzimidazoles targeting FtsZ as antitubercular agents. *Bioorg. Med. Chem.*, **2014**, 22, 2602-2612.
- Preethi, P. J., Karthikeyan, E., Lohita, M., Teja, P. G., Subhash, M., Shaheena, P., Prashanth, Y., Sai Nandhu, K. Benzimidazole: An important scaffold in drug discovery. *Asian J. Pharm. Tech.*, **2015**, 5(3), 138-152.
- Raghunath, M., Viswanathan, C. L. Benzimidazole-2-carbamic acid as a privileged scaffold for antifungal, anthelmintic and antitumor activity a review. *Int. J. Pharm. Pharm. Sci.*, **2014**, 6(5), 17-25.
- Rao, K. G., Chakraborty, D. Synthesis, characterization and antibacterial evaluation of some potent 2-substituted benzimidazole analogues. *Int. J. Pharm. Sci. Drug Res.*, **2014**, 6(1), 67-69.
- Rashid, M., Husain, A., Mishra, R., Karim, S., Khan, S., Ahmad, M., Al-wabel, N., Husain, A., Ahmad, A., Khan, S. A. Design and synthesis of benzimidazoles containing substituted oxadiazole, thiadiazole and triazolothiadiazines as a source of new anticancer agents. *Arabian J. Chem.*, **2015**. <http://dx.doi.org/10.1016/j.arabjc.2015.08.019>.
- Ramprasad, J., Nayak, N., Dalimba, U., Yogeewari, P., Sriram, D., Peethambar, S. K., Achur, R., Kumar, H. S. S. Synthesis and biological evaluation of new imidazo[2,1-*b*][1,3,4]thiadiazole-benzimidazole derivatives. *Eur. J. Med. Chem.*, **2015**, 95, 49-63.
- Reddy S. R. S. R., Rao, V. S., Kanchana, S. N. Synthesis, characterization and biological activity of some novel benzimidazole derivatives. *Pharm. Lett.*, **2016**, 8(2), 59-72.
- Sánchez, D. S., Baeza, A., Alonso, D. A. Organocatalytic asymmetric α -chlorination of 1,3-dicarbonyl compounds catalyzed by 2-aminobenzimidazole derivatives. *Symmetry*, **2016**, 8 (1), Article 3, 10 pages. doi:10.3390/sym8010003.
- Singla, M., Ranjan, R., Mahiya, K., Mohapatra, S. C., Ahmad, S. Nitric oxide inhibition, antioxidant, and antitumour activities of novel copper(II) bis-benzimidazole diamide nanocoordination complexes. *New J. Chem.*, **2015**, 39, 4316-4327.
- Srinivas Rao, S., Reddy, C. V., Dubey, P. K. A green approach for the synthesis of 1-methyl-2-(alkylthio)-1*H*-benzimidazoles. *Asian J. Chem.*, **2014**, 26(18), 5995-5997.
- Tang, Y., Zhang, F., Hu, S., Cao, Z., Wu, Z., Jing, W. Novel benzimidazole derivatives as corrosion inhibitors of mild steel in the acidic media. Part I: Gravimetric, electrochemical, SEM and XPS studies. *Corros. Sci.*, **2013**, 74, 271-282.
- Taha, M., Ismail, N. H., Jamil, W., Rashwan, H., Kashif, S. M., Sain, A. A., Adenan, M. I., Anouar, E., Ali, M., Rahim, F., Khan, K. M. Synthesis of novel derivatives of 4-methylbenzimidazole and evaluation of their biological activities. *Eur. J. Med. Chem.*, **2014**, 84, 731-738.
- Tien, C. N., Cam, D. T. T., BuiManh, H., Dang, D. N. Synthesis and antibacterial activity of some derivatives of 2-methylbenzimidazole containing 1,3,4-oxadiazole or 1,2,4-triazole heterocycle. *J. Chem.*, **2016**, Article ID 1507049, 6 pages. <http://dx.doi.org/10.1155/2016/1507049>.

- Verma, N., Singh, R. B., Srivastava, S., Dubey, P. Benzimidazole: A plethora of biological load. *J. Chem. Pharm. Res.*, **2016**, 8(3), 365-374.
- Weijie, S., Zhang, T., Li Y., She, D., Pan, W., Gao, Z., Ning, J., Mei, X. Synthesis and biological activity of novel benzimidazole derivatives as potential antifungal agents. *J. Pestic. Sci.*, **2016**, 41(1), 15-19.
- Wen, J., Luo, Y. L., Zhang, H. Z., Zhao, H. H., Zhou, C. H., Cai, G. X. A green and convenient approach toward benzimidazole derivatives and their antimicrobial activity. *Chin. Chem. Lett.*, **2016**, 27, 391-394.
- Woolley, D. W. Some biological effects produced by benzimidazole and their reversal by purines. *J. Biol. Chem.*, **1944**, 152, 225-232.
- Wu, L., Jiang, Z., Shen, J., Yi, H., Zhan, Y., Sha, M., Wang, Z., Xue, S., Li, Z. Design, synthesis and biological evaluation of novel benzimidazole-2-substituted phenyl or pyridine propyl ketene derivatives as antitumor agents. *Eur. J. Med. Chem.*, **2016**, 114, 328-336.
- Yadav, G., Ganguly, S. Structure activity relationship (SAR) study of benzimidazole scaffold for different biological activities: A mini-review. *Eur. J. Med. Chem.*, **2015**, 97, 419-443.
- Yang, C., Hamel, C., Vujanovic, V., Gan, Y. Fungicide: Modes of action and possible impact on nontarget microorganisms. *Int. Scholarly Res. Network Ecol.*, **2011**, Article ID 130289, 8 pages. doi:10.5402/2011/130289.
- Youssif, B. G. M., Moty, S. G. A., Sayed, I. M. Synthesis and biological evaluation of some novel 1,2,3-triazol-*N*-arylidene acetohydrazide incorporating benzimidazole ring moiety as potential antimicrobial agents. *J. Curr. Chem. Pharm. Sci.*, **2014**, 4(2), 54-64.
- Zhang, L., Addla, D., Ponmani, J., Wang, A., Xie, D., Wang, Y., Zhang, S. L., Geng, R. X., Cai, G., Li, S., Zhou, C. H. Discovery of membrane active benzimidazole quinolones-based topoisomerase inhibitors as potential DNA-binding antimicrobial agents. *Eur. J. Med. Chem.*, **2016**, 111, 160-182.
- Zhang, M., Perry, Z., Park, J., Zhou, H. Stable benzimidazole-incorporated porous polymer network for carbon capture with high efficiency and low cost. *Polymers*, **2014**, 55, 335-339.

Chapter 4. Synthesis and structure elucidation using 2D-NMR and thermal coefficient investigation on amino acid tethered quinoxalines

* The compounds referred to in the chapter are referred to elsewhere in the thesis with an **A** preceding the number of the compound. For example **6a-n** is referred to as **A6a-n** elsewhere in the thesis.

Abstract

A chiral library of amino acid tethered quinoxalines (**A6a-A6n**) was synthesized *via* a 4-step synthesis using a S_NAr reaction mediated by reduction and cyclization steps at ambient temperature. The synthesized compounds were characterized with the use of instrumental techniques such as 2D NMR spectroscopy and X-ray crystallography. Hydrogen bonding in the molecules was determined by thermal coefficient investigations and X-ray crystallography. We herein report the elucidation of the series of quinoxalines (**A6a-n**) by NMR spectroscopy and X-ray crystallography and report on the thermal coefficient investigations. Density functional theory (DFT) and molecular dynamic (MD) studies were additionally conducted to support the experimental hydrogen bonding and conformational flexibility of these compounds.

Keywords: quinoxalines; amino acids; 1H & ^{13}C NMR; X-ray crystallography; thermal coefficient investigations

4.1 Introduction

The structure of quinoxalines are characterised by a benzene ring fused to a 6 membered heterocyclic ring incorporating two nitrogen atoms, both of which are bonded to the aromatic ring. These compounds play an important role in the field of medicine (Reddy et al., 1999; Lu et al., 2011; Cholo et al., 2012; Ajani et al., 2014; Demmer et al., 2015), industrial (Keshtov et al., 2015; Podsiadly et al., 2011; Kono et al., 2012).

Quinoxaline units are present in a number of natural and pharmacological compounds and are found to display a wide array of biological activity (Deepika et al., 2011), such as anticancer (Vázquez et al., 2015; Issa et al., 2015; Parrino et al., 2015), anti-HIV (Ajani et al., 2014; Ramli et al., 2014; Balasubramanian et al., 2014), antituberculosis (Vicente et al., 2011; Puratchikody et al., 2011; Ramli et al., 2014; Ajani et al., 2014), antibacterial (Chandra Shekhar et al., 2015; Raju et al., 2015; Manchal et al., 2015), fungicidal (Naga Raju et al., 2015; Zhang et al., 2014; Ramli et al., 2014), insecticidal (Gil et al., 2014; Ninfa et al., 2014), anti-inflammatory (Achutha et al., 2013; Ingle and Marathe, 2012b; Patidar et al., 2011), antioxidant (Kotra et al., 2013; Sridevi et al., 2011; Burguete et al., 2011), antimalarial (Gil et al., 2014; Chandra Shekhar et al., 2014; Barea et al., 2013), anti-tumor (Neckel et al., 2015; Huang et al., 2015; Bříza et al., 2015), and other pharmacological activities. They have therefore become an interesting scaffold to for the synthetic chemists (Ameen et al., 2015; Ingle and Marathe, 2012a).

Bioactive compounds show enhanced activity when linked to amino acids (Suhas et al., 2011; Sharma et al., 2013). Amino acids are good building blocks to incorporate into quinoxalines since they have low toxicity and biocompatibility (Shantharam et al., 2014). Currently there is huge tendency of conjugating amino acid/peptide residues with small bioactive heterocyclic

motifs in the field of biomedical research (Sharma et al., 2013; Suhas et al., 2012, Suhas et al., 2011).

We herein report the NMR elucidation of a series of amino acid tethered quinoxalines, of which six are novel. Their structural elucidation is slightly more complicated because of the amino acid moiety linked to the quinoxaline, which has an effect on the resonances of the quinoxaline moiety. Extensive 2D NMR studies, X-ray crystallography and thermal coefficient investigations were used to provide a full structural elucidation of these amino acid tethered quinoxalines. Additionally, the density functional theory (DFT) and molecular dynamic (MD) simulations were employed to explain the hydrogen bonding tendency and conformational flexibility of these compounds.

4.2 Experimental

4.2.1 Chemistry

All the chemicals were supplied by Sigma-Aldrich *via* Capital Lab, South Africa. Organic solvents were redistilled and dried according to standard procedure. Silica gel 60F₂₅₄ plates (Merck) were used for thin layer chromatography. Purifications were carried out by column chromatography using silica gel (60-120 mesh) with an EtOAc : Hexane mobile phase. Melting points were recorded using a Stuart Scientific SMP3 apparatus. UV spectra were obtained on a Varian Cary UV-VIS spectrometer in MeOH. IR spectra were recorded on a Perkin Elmer 100 FT-IR spectrometer with universal attenuated total reflectance sampling accessory. ¹H, ¹³C and all 2D NMR spectra were recorded at 298 K with 5- to 10-mg samples dissolved in 0.5 ml of DMSO-*d*₆ in 5-mm NMR tubes using a Bruker Avance 400 MHz instrument and ¹H NMR for thermal analysis was performed on a Bruker Avance 600 MHz instrument (9.4 T; Bruker, Germany) (400.22 MHz for ¹H, 100.63 MHz for ¹³C). The digital digitizer resolution

was set at 22 for both the ^1H and ^{13}C NMR experiments. Chemical shifts are reported in δ values (ppm) and coupling constants (J) in Hz relative to the internal standard, tetramethylsilane (TMS) and referenced to the solvent line of DMSO- d_6 ($\delta_{\text{H}} = 2.5$, $\delta_{\text{C}} = 39.52$). For the ^1H NMR analyses, 16 transients were acquired with a 1-s relaxation delay using 32 K data points. The 90° pulse duration was 10.0 μs , and the spectral width was 8223.68 Hz. The ^{13}C NMR spectra were obtained with a spectral width of 24 038.46 Hz using 64 K data points. The 90° pulse duration was of 8.40 μs . For the 2D experiments including COSY, NOESY, HSQC and HMBC, all data were acquired with 4 K \times 128 data points ($t_2 \times t_1$). The mixing time for the NOESY experiment was 0.3 s, and the long range coupling time for the HMBC experiment was 65ms. All data were analysed using Bruker Topspin 2.1 (2008) software. High-resolution mass data were obtained using a Bruker micro TOF-Q II ESI instrument operating at ambient temperature. Optical rotations were recorded using a Perkin ElmerTM model 341 polarimeter with a 10 cm flow tube in MeOH. The purity of the compounds were determined by analytical HPLC on a Shimadzu-20A5 fitted with a C8 (150mm \times 5 μm \times 4.6) column using a mobile phase (A) of 0.1M KHPO_4 buffer and (B) acetonitrile with a linear gradient of 0 to 30% over a period of 60 minutes at a flow rate of 1 mL/min.

General procedure for the preparation of amino acid methyl ester hydrochloride (A4)

Methanol (20 mL) was added to different amino acids (**A3a-n**) (0.1 mol) followed by the gradual addition of thionyl chloride (0.3 mol) at room temperature. The resulting solution was stirred at 70°C for 4h and the reaction mixture concentrated on a rotary evaporator producing the respective amino acid ester hydrochlorides in yields of >90%.

General procedure for the preparation of methyl 4-fluoro-3-nitrobenzoate (**A2**)

4-Fluoro-3-nitrobenzoic acid (5g, 27 mmol) was refluxed in methanol (50 mL) and conc. H_2SO_4 (5 mL) for 8h. After completion of the reaction (as evident from TLC), the methanol was evaporated under reduced pressure and the aqueous layer extracted with ethyl acetate (25 mL x 3). The EtOAc layer was dried over anhydrous Na_2SO_4 and concentrated under reduced pressure to yield **A2** as a cream-colored powder in a yield of 95%.

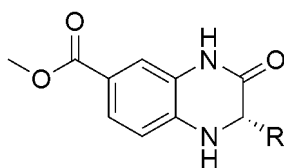
General procedure for the preparation of compound (**A5**)

Methyl-4-fluoro-3-nitrobenzoate **A2** (0.5g, 2.34 mmol), the hydrochloride salt of the amino acid ester **A4** (3.51 mmol) and NaHCO_3 (0.005g, 4.68 mmol) were mixed in THF (10 mL). The reaction mixture was stirred overnight at room temperature. After completion of the reaction (monitored by TLC), the reaction mixture was washed with water (10 mL x 2), followed by 10% Na_2CO_3 solution (10 mL). The organic layer was separated and dried over anhydrous Na_2SO_4 and concentrated under reduced pressure to afford **A5**, which was purified by column chromatography (hexane/ethyl acetate) to afford the desired product in good yields (80-90%).

General procedure for the preparation of compound (**A6**)

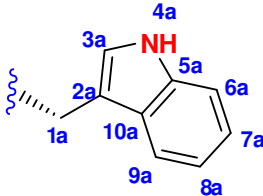
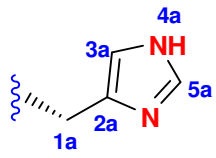
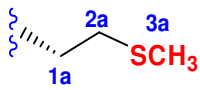
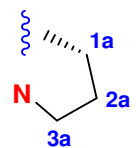
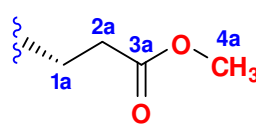
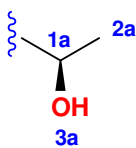

4-(Substituted amino)-3-nitro-methyl benzoate **A5** (1 mmol) was added to methanol (10 mL), to which 10% Pd/C (50 mg) was added. The reaction mixture was stirred for 4h at room temperature under H_2 atmosphere. The reaction mixture was then filtered through Celite 545 to remove the catalyst. The filtrate was evaporated under reduced pressure and the obtained solid was purified by column chromatography (hexane/ethyl acetate) to afford the desired products (**Table 4-1**) in moderate to good yield (60-85%).

Table 4-1 Physical data of the synthesized compounds



A6

Entry	R	Appearance	Melting Point	Yield ^a	Purity ^b
A6a		Orange solid	212-214	80	92
A6b		Cream solid	218-220	77	94
A6c		Yellow solid	158-160	75	98
A6d		White solid	216-218	85	98
A6e		White solid	204-206	83	90
A6f		White solid	206	75	85
A6g		Cream solid	166-168	93	87

A6h		Orange solid	102	84	96
A6i		Black solid	206-208	76	93
A6j		Cream solid	140-142	90	98
A6k**		Yellow solid	135-137	88	97
A6l		Cream solid	168-170	86	92
A6m		Cream solid	184-186	78	80
A6n		Black solid	102-104	75	80

^aPurified sample yield (%); ^bPurity determined by HPLC; **Proline and quinoxaline conjugated together

(S)-Methyl-2-methyl-3-oxo-1,2,3,4-tetrahydroquinoxaline-6-carboxylate (A6a), UV λ_{\max} nm (log ϵ): 316 (3.75), 253 (3.89), 220 (4.01); IR ν_{\max} (cm⁻¹): 3342 (NH), 3188 (CH aromatic), 3098 (NH amide), 1746 (C=O ester), 1670 (C=O amide); $[\alpha]^{25}_D = +12^\circ$ (c = 10, MeOH); LRMS m/z 243.0843 [M + Na]⁺.

(S)-Methyl-2-(4-hydroxybenzyl)-3-oxo-1,2,3,4-tetrahydroquinoxaline-6-carboxylate (A6b), UV λ_{\max} nm (log ϵ): 319 (4.01), 257 (4.12), 223 (4.37); IR ν_{\max} (cm⁻¹): 3365 (OH), 3337

(NH), 3198 (CH aromatic), 3099 (NH amide), 1776 (C=O ester), 1662 (C=O amide); $[\alpha]^{25}_{\text{D}} = -108.3^{\circ}$ ($c = 10$, MeOH); HRMS m/z 335.0992 $[\text{M} + \text{Na}]^{+}$ (calcd. for $\text{C}_{17}\text{H}_{16}\text{N}_2\text{O}_4\text{Na}$ 335.1008).

(S)-Methyl-2-(2-methoxy-2-oxoethyl)-3-oxo-1,2,3,4-tetrahydroquinoxaline-6-carboxylate (A6c), UV λ_{max} nm (log ϵ): 315 (4.01), 254 (4.18), 220 (4.32); IR ν_{max} (cm^{-1}): 3337 (NH), 3144 (CH aromatic), 3025 (NH amide), 1776 (C=O ester), 1676 (C=O amide); $[\alpha]^{25}_{\text{D}} = -49.50^{\circ}$ ($c = 10$, MeOH); HRMS m/z 301.0786 $[\text{M} + \text{Na}]^{+}$ (calcd. for $\text{C}_{13}\text{H}_{14}\text{N}_2\text{O}_5\text{Na}$ 301.0800).

(S)-Methyl-2-isobutyl-3-oxo-1,2,3,4-tetrahydroquinoxaline-6-carboxylate (A6d), UV λ_{max} nm (log ϵ): 317 (3.95), 254 (4.07), 221 (4.17); IR ν_{max} (cm^{-1}): 3344 (NH), 3217 (CH aromatic), 2958 (NH amide), 1748 (C=O ester), 1696 (C=O amide); $[\alpha]^{25}_{\text{D}} = +23.50^{\circ}$ ($c = 10$, MeOH); LRMS m/z 285.1573 $[\text{M} + \text{Na}]^{+}$.

(S)-Methyl-2-isopropyl-3-oxo-1,2,3,4-tetrahydroquinoxaline-6-carboxylate (A6e), UV λ_{max} nm (log ϵ): 320 (3.84), 257 (3.95), 221 (4.08); IR ν_{max} (cm^{-1}): 3331 (NH), 3139 (CH aromatic), 3017 (NH amide), 1727 (C=O ester), 1678 (C=O amide); $[\alpha]^{25}_{\text{D}} = +36.50^{\circ}$ ($c = 10$, MeOH); LRMS m/z 271.1412 $[\text{M} + \text{Na}]^{+}$.

(S)-Methyl-2-((S)-sec-butyl)-3-oxo-1,2,3,4-tetrahydroquinoxaline-6-carboxylate (A6f), UV λ_{max} nm (log ϵ): 321 (3.84), 257 (3.95), 221 (4.22); IR ν_{max} (cm^{-1}): 3338 (NH), 3206 (CH aromatic), 2960 (NH amide), 1746 (C=O ester), 1698 (C=O amide); $[\alpha]^{25}_{\text{D}} = +30.50^{\circ}$ ($c = 10$, MeOH); LRMS m/z 285.1579 $[\text{M} + \text{Na}]^{+}$.

(S)-Methyl-2-benzyl-3-oxo-1,2,3,4-tetrahydroquinoxaline-6-carboxylate (A6g), UV λ_{max} nm (log ϵ): 319 (3.73), 258 (3.89), 220 (4.11); IR ν_{max} (cm^{-1}): 3342 (NH), 3144 (CH aromatic),

3025 (NH amide), 1750 (C=O ester), 1695 (C=O amide); $[\alpha]^{25}_{\text{D}} = -67.50^{\circ}$ ($c = 10$, MeOH); HRMS m/z 319.1057 $[\text{M} + \text{Na}]^{+}$ (calcd. for $\text{C}_{17}\text{H}_{16}\text{N}_2\text{O}_3\text{Na}$ 319.1059).

(S)-Methyl-2-((1*H*-indol-3-yl)methyl)-3-oxo-1,2,3,4-tetrahydroquinoxaline-6-carboxylate (A6h), UV λ_{max} nm (log ϵ): 320 (3.79), 258 (3.94), 221 (4.38); IR ν_{max} (cm^{-1}): 3331 (NH), 3170 (CH aromatic), 2948 (NH amide), 1730 (C=O ester), 1671 (C=O amide); $[\alpha]^{25}_{\text{D}} = -47.0^{\circ}$ ($c = 10$, MeOH); HRMS m/z 358.1169 $[\text{M} + \text{Na}]^{+}$ (calcd. for $\text{C}_{19}\text{H}_{17}\text{N}_3\text{O}_3\text{Na}$ 358.1168).

(S)-Methyl-2-((1*H*-imidazol-4-yl)methyl)-3-oxo-1,2,3,4-tetrahydroquinoxaline-6-carboxylate (A6i), UV λ_{max} nm (log ϵ): 316 (3.61), 255 (3.77), 219 (4.00); IR ν_{max} (cm^{-1}): 3356 (NH), 3134 (CH aromatic), 2947 (NH amide), 1730 (C=O ester), 1671 (C=O amide); $[\alpha]^{25}_{\text{D}} = -16.0^{\circ}$ ($c = 10$, MeOH); LRMS m/z 309.1420 $[\text{M} + \text{Na}]^{+}$.

(S)-Methyl-2-(2-(methylthio)ethyl)-3-oxo-1,2,3,4-tetrahydroquinoxaline-6-carboxylate (A6j), UV λ_{max} nm (log ϵ): 317 (3.82), 255 (3.95), 220 (4.05); IR ν_{max} (cm^{-1}): 3345 (NH), 3181 (CH aromatic), 3089 (NH amide), 1720 (C=O ester), 1683 (C=O amide); $[\alpha]^{25}_{\text{D}} = -16.25^{\circ}$ ($c = 10$, MeOH); HRMS m/z 303.0766 $[\text{M} + \text{Na}]^{+}$ (calcd. for $\text{C}_{13}\text{H}_{16}\text{N}_2\text{O}_3\text{SNa}$ 303.0763).

(S)-Methyl-4-oxo-1,2,3,3a,4,5-hexahydropyrrolo[1,2-*a*]quinoxaline-7-carboxylate (A6k), UV λ_{max} nm (log ϵ): 321 (3.93), 257 (3.94), 224 (4.093); IR ν_{max} (cm^{-1}): 3189 (CH aromatic), 3095 (NH amide), 1701 (C=O ester), 1677 (C=O amide); $[\alpha]^{25}_{\text{D}} = -117.3^{\circ}$ ($c = 10$, MeOH); LRMS m/z 269.1239 $[\text{M} + \text{Na}]^{+}$.

(S)-Methyl-2-(3-methoxy-3-oxopropyl)-3-oxo-1,2,3,4-tetrahydroquinoxaline-6-carboxylate (A6l), UV λ_{max} nm (log ϵ): 317 (3.87), 255 (4.02), 221 (4.19); IR ν_{max} (cm^{-1}):

3348 (NH), 3185 (CH aromatic), 3095 (NH amide), 1734 (C=O ester), 1686 (C=O amide); $[\alpha]^{25}_D = -10.75^\circ$ ($c = 10$, MeOH); HRMS m/z 315.0952 $[M + Na]^+$ (calcd. for $C_{14}H_{16}N_2O_5Na$ 315.0957).

(S)-Methyl-2-((R)-1-hydroxyethyl)-3-oxo-1,2,3,4-tetrahydroquinoxaline-6-carboxylate (A6m), UV λ_{max} nm (log ϵ): 324 (3.50), 264 (3.77), 220 (4.14); IR ν_{max} (cm^{-1}): 3302 (OH), 3254 (NH), 3170 (CH aromatic), 2980 (NH amide), 1730 (C=O ester), 1699 (C=O amide); $[\alpha]^{25}_D = +22.50^\circ$ ($c = 10$, MeOH); HRMS m/z 273.0854 $[M + Na]^+$ (calcd. for $C_{12}H_{14}N_2O_4Na$ 273.0851).

(S)-Methyl-2-(hydroxymethyl)-3-oxo-1,2,3,4-tetrahydroquinoxaline-6-carboxylate (A6n) UV λ_{max} nm (log ϵ): 325 (3.45), 265 (3.69), 221 (4.06); IR ν_{max} (cm^{-1}): 3244 (OH), 3205 (NH), 3188 (CH aromatic), 2950 (NH amide), 1720 (C=O ester), 1668 (C=O amide); $[\alpha]^{25}_D = +24.50^\circ$ ($c = 10$, MeOH); HRMS m/z 259.0690 $[M + Na]^+$ (calcd. for $C_{11}H_{12}N_2O_4Na$ 259.0695).

4.2.2 Single Crystal X-ray Diffraction Analysis of compound A6d

A cube-shaped single crystal was selected and glued onto the tip of a glass fiber and mounted in a stream of cold nitrogen at 173 K and centered in the X-ray beam using a video camera. The crystal evaluation and data collection were performed on a Bruker Smart APEX II diffractometer with Mo $K\alpha$ radiation ($\lambda = 0.71073 \text{ \AA}$). The diffractometer to crystal distance was set at 4.00 cm. The initial cell matrix was obtained from three series of scans at different starting angles. Each series consisted of 12 frames collected at intervals of 0.5° in a 6° range with the exposure time of 10s per frame. The reflections were successfully indexed by an automated indexing routine built in the APEX II program suite. The final cell constants were calculated from a set of 3387 strong reflections from the actual data collection. Data collection method involved ω scans of width 0.5° . Data reduction was carried out using the program

System Administrator's Integrated Network Tool (SAINT+). The structure was solved by direct methods using SHELXS and refined. Non-H atoms were first refined isotropically and then by anisotropic refinement with full-matrix least-squares calculations based on F^2 using SHELXS. All H atoms were positioned geometrically and allowed to ride on their respective parent atoms. All H atoms were refined isotropically. The absorption correction was based on fitting a function to the empirical transmission surface as sampled by multiple equivalent measurements. The final least-squares refinement of 286 parameters against 5126 data points resulted in residuals R (based on F^2 for $I \geq 2\sigma$) and wR (based on F^2 for all data) of 0.0497 and 0.1358, respectively. The final difference Fourier map was featureless. The programs Olex-2 and Ortep-3 were used within the WinGX software package to prepare artwork representation (Farrugia et al., 2012; Spek et al., 2003). Crystallographic data (excluding structure factors) for the structure in this paper has been deposited with the Cambridge Crystallographic Data Centre, CCDC, 12 Union Road, Cambridge CB21EZ, UK. Copies of the data can be obtained free of charge on quoting the depository number CCDC 1451681 (Fax: +44-1223-336-033; E-Mail: deposit@ccdc.cam.ac.uk, <http://www.ccdc.cam.ac.uk>).

4.2.3 Computational methods

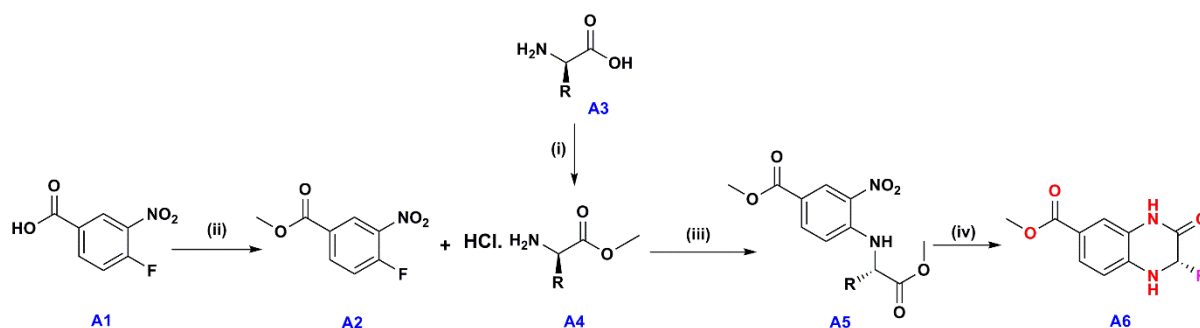
Different conformations of **A6d** were obtained using the "Generate Conformation" module in the Accelrys Discovery Studio (Accelrys Software, 2013). Conformation of **A6d** with lowest energy was further optimized using the Becke's (Becke et al., 1988) three parameter exchange-functional (B3) and gradient-corrected correlation functional of Lee, Yang and Parr (LYP) (Lee et al., 1988) with implementation of 6-311g+(2d,p) basis sets, with Gaussian 09 software (Frisch et al., 2009). The true energy minima was further verified by frequency calculations on the optimized geometry. HOMO-LUMO visualization was performed using the gauss view.

For MD, the optimized structure of **A6d** was explicitly solvated with water molecules using the “Solvation” algorithm embedded in the Discovery Studio (DS). The system was energetically minimized in DS using 1000 steps of the steepest descent algorithm followed by 1000 steps of Conjugant gradient, until the root mean square (RMS) gradient of 0.1 kcal mol⁻¹ was achieved in DS. The temperature of the system was raised to 300 K at constant volume. The equilibration step with a length of 10 picoseconds was used to create uniform density of the solvent around the compound at constant pressure and temperature. Finally, the MD simulation of 500 ps was performed using default parameters in DS.

4.3 Results and Discussion

4.3.1 Synthesis

Quinoxalines with various substituents at C-2 and with an ester group at C-6 were synthesized in a four- step reaction involving esterification of 4-fluoro-3-nitrobenzoic acid **A1** to methyl 4-fluoro-3-nitrobenzoate **A2**, which was then reacted with various amino acid hydrochloride esters **A4** prepared from amino acids themselves. This produced an intermediate **A5** which incorporates both the amino acid and the benzoate moieties. This intermediate was cyclised to the quinoxalines **A6a-n** following reduction of the nitro group with Pd/C and methanol (Scheme 4-1).



Scheme 4-1 Synthesis of amino acids derived quinoxalines; Reagents and conditions: (i) SOCl₂, MeOH, reflux, 4h; (ii) H₂SO₄, MeOH, reflux, 8h; (iii) NaHCO₃, THF, rt, 8h; (iv) 10% Pd/C, MeOH, rt, 4h

The most important step in the reaction sequence was the nucleophilic substitution of the fluorine in **A2** with the amino acid ester **A4a**. In order to determine the optimum conditions for step, we first examined the effect of solvent (**Table 4-2**), followed by base (**Table 4-3**). Various polar, non-polar, protic and non-protic solvents were investigated. The results indicated that the two polar non-protic solvents, THF and DMF reacted in the shortest time (8 h) and with the highest yield (80 and 68% respectively) (**Table 4-2**).

The role of the base in step 3 is to deprotonate the hydrochloride amino salt of the ester, allowing the amino ester to act as a nucleophile. From the results in **Table 4-3**, the moderate bases NaHCO_3 and Et_3N resulted in the best yields (78-80%) in the shortest time (8 h). From these two, NaHCO_3 has the advantages of being less expensive, available in the solid form and easy to handle as opposed to the pungent odour and comparatively more expensive organic liquid base of Et_3N .

4.3.2 Structural elucidation

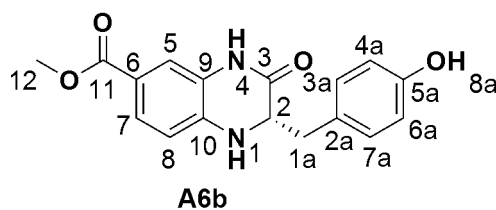
The full characterization (^1H and ^{13}C NMR) of amino acid derived tetrahydroquinoxalines **A6a-n** is presented in **Table 4-4**, **Table 4-5** and **Table 4-6** and the ^1H and ^{13}C NMR spectra of a representative tetrahydroquinoxaline (**A6b**) is presented in **Figure 4-1** and **Figure 4-2** respectively. With the aid of COSY, NOESY, HSQC and HMBC as well as multiplicity of the resonances, unambiguous chemical shift assignments were made.

Compounds **A6a-n** from this series were derived from various amino acids and hence these analogues contain a basic skeleton, 3-oxo-1,2,3,4-tetrahydroquinoxaline-6-carboxylate with different amino acid side chain functionalities at the chiral carbon C-2. Compound **A6b** was chosen for discussion, since this compound was the most interesting of the series.

Table 4-2 Yields and times of completion of reaction with different solvents for the formation of the intermediate **A5**^a

No.	Solvent	Time (h)	Yield ^b (%)
1	MeOH	16	48
2	DCM	14	35
3	Ethanol	12	64
4	Diethyl ether	18	40
5	DMF	8	68
6	THF	8	80
7	Water	24	NR
8	ACN	24	NR
9	EtOAc	24	NR
10	Toluene	24	NR

^a prepared from methyl-4-fluoro-3-nitrobenzoate (2.34 mmol) and (R)-methyl 2-amino-3-methylbutanoate (3.51 mmol), base: Et₃N (4.68 mmol), room temperature and 10 mL solvent; ^b Isolated yield, NR = No reaction



The core quinoxaline framework

The core quinoxaline structure contains seven proton resonances at δ 10.34 for the H-4 amino, δ 6.73 for the H-1 amino, δ 4.15 for H-2 (a triplet in this case with $J = 4.6$ Hz) and a singlet methyl resonance at δ 3.73 for the H-12 ester methyl group. The aromatic protons of the core skeleton, H-8, H-7 and H-5 appear between δ 6.64 to 7.35, H-8 appearing as a doublet at δ 6.64 ($J = 8.3$ Hz), H-7 as a double doublet at δ 7.35 ($J = 8.2, 1.5$ Hz) and H-5 at δ 7.22 as a doublet with $J = 1.5$ Hz. For **A6a-n**, H-2 shows different chemical shifts and splitting patterns, which is dependent on the groups at the 2-position. For **A6b** H-2 showed a COSY correlation with

NH-1, distinguishing it from NH-4. Furthermore, NH-4 also showed a HMBC correlation to C-5 and NH-1 to C-8 confirming these assignments.

Table 4-3 The effect on yields and time of completion of reaction with different bases in the formation of the intermediate **A5**^a

Sl. No.	Base	pKa	Time (h)	Yield ^b (%)
1	Pyridine	5.2	14	67
2	4-Methyl morpholine	7.38	18	59
3	DIPEA	40	12	60
4	DMAP	9.7	10	50
5	K ₂ CO ₃	10.25	24	55
6	NaHCO ₃	10.3	8	80
7	Et ₃ N	10.75	8	78
8	NaOH	13	24	NR
9	KOH	13.5	24	NR

^a Reaction condition: Methyl-4-fluoro-3-nitrobenzoate (2.34 mmol), (*R*)-methyl 2-amino-3-methylbutanoate (3.51 mmol), solvent: THF (10 mL), room temperature and base (2 eq.); ^b Isolated yield; NR = No reaction

The two carbonyl resonances in the core skeleton, the amide carbon resonance (C-3) and the ester carbonyl resonance (C-11) appear very close to each other in the ¹³C NMR spectrum at δ 166.1 and δ 166.0 and are interchangeable. These resonances also cannot be distinguished in compounds **A6h**, **A6k** and **A6l**. However, in other compounds, for example **A6a**, these can be distinguished due to HMBC correlations between C-2 with H-2, NH-4 and H-1a and C-11 with H-7, H-5 and the ester methyl H-12. The assignment of C-10 at δ 138.3 was made due to an HMBC correlation with H-7. C-9 and C-6 at δ 124.3 and δ 117.1 respectively were distinguished by C-9 showing a HMBC correlation to both H-8 and NH-1 and C-6 showing a HMBC correlation to H-8 only.

Side chain of quinoxaline **A6b**

For the benzyl moiety attached to C-2, the two diastereotopic protons of H-1a each appeared as a doublet of doublets at δ_H 2.84 ($J = 13.8, 6.2$ Hz) and δ_H 2.80 ($J = 13.8, 4.8$ Hz). These proton resonances showed a COSY correlation to H-2 and a HMBC correlation to the amide carbonyl C-3. The aromatic protons of benzyl group H-3a/7a and H-4a/6a, each occurred as doublets at δ_H 6.93 and δ_H 6.59 respectively with coupling constants of 8.2 Hz respectively. The assignment of H-3a/7a was made due to a HMBC correlation with C-1a. The hydroxyl proton attached to the *para* position of benzyl group appeared at δ_H 9.1 as a singlet. This hydroxyl proton (OH-8a) showed a long range COSY correlation with H-4a/6a. The singlet C-2a and C-5a resonances occurred at δ_C 126.6 and δ_C 155.8 respectively. C-2a showed HMBC correlations to H-2 and C-5a showed HMBC correlations to H-3a/7a. Selected HMBC correlations used in the structural elucidation of **A6b** are provided in **Figure 4-3**.

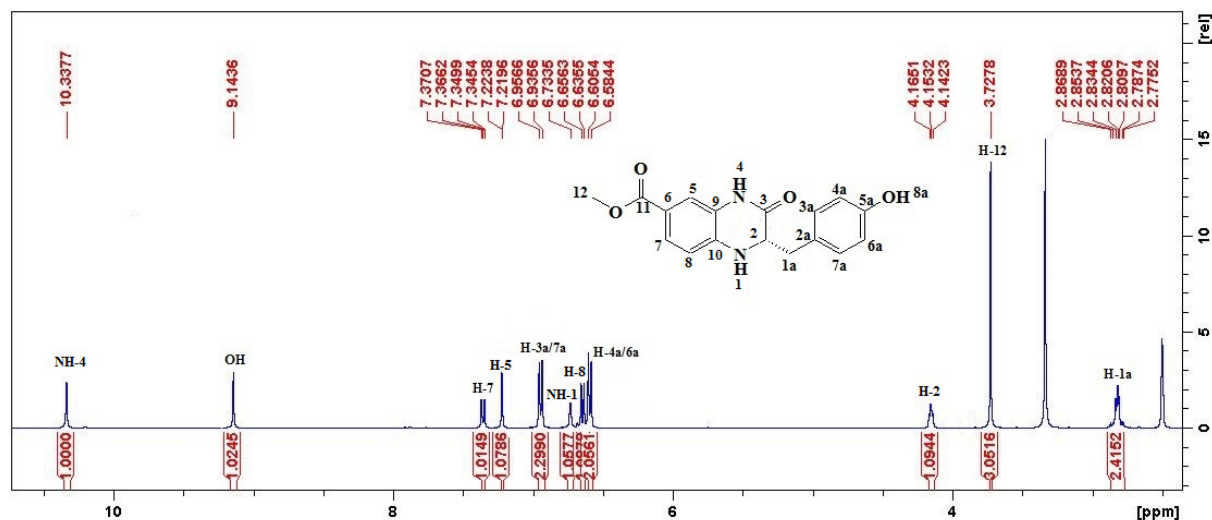


Figure 4-1 ^1H NMR spectrum of (*S*)-methyl 2-(4-hydroxybenzyl)3-oxo-1,2,3,4-tetrahydroquinoxaline-6-carboxylate (**A6b**)

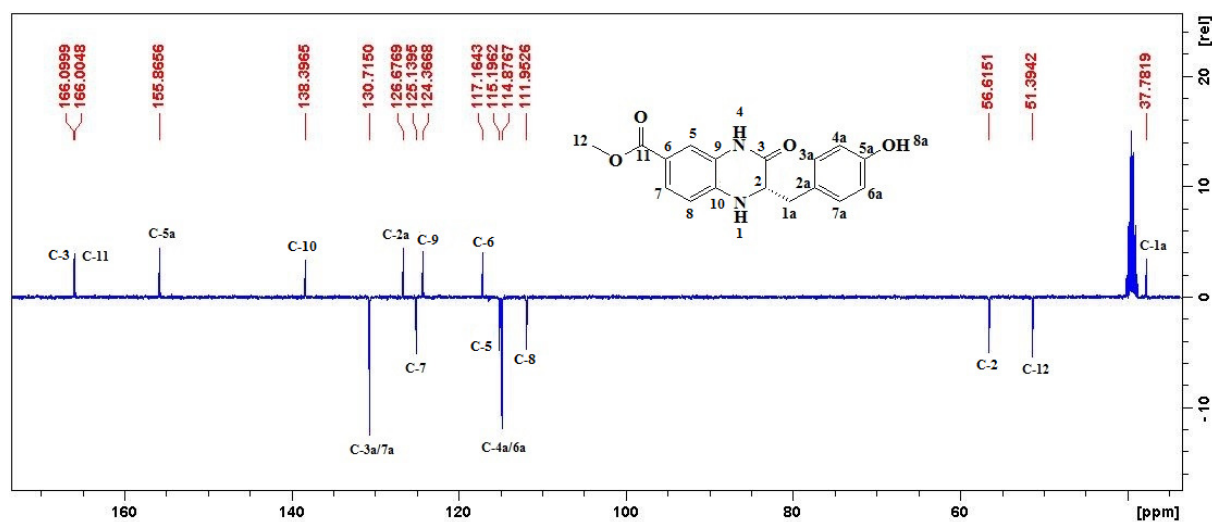


Figure 4-2 ^{13}C NMR spectrum of (*S*)-methyl 2-(4-hydroxybenzyl)-3-oxo-1,2,3,4-tetrahydroquinoxaline-6-carboxylate (**A6b**)

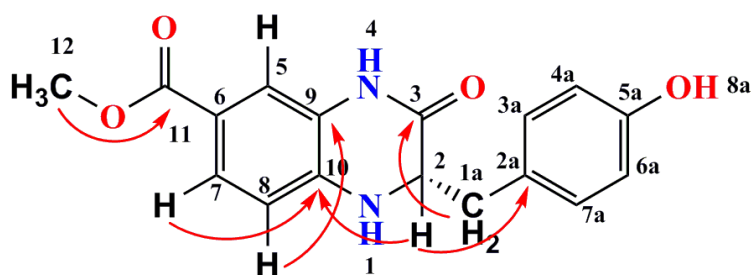


Figure 4-3 Selected HMBC correlations for (*S*)-methyl 2-(4-hydroxybenzyl)-3-oxo-1,2,3,4-tetrahydroquinoxaline-6-carboxylate (**A6b**)

The structural elucidation of each of the side chains in the quinoxalines are divided into three sections, (i) quinoxalines with aromatic side chains, (ii) quinoxalines with non-polar side chains and (iii) quinoxalines with polar side chains.

Table 4-4 ¹H NMR data (δ in ppm) for compounds **A6a-g** (*J* is given in Hz)

	A6a	A6b	A6c	A6d	A6e	A6f	A6g
1	6.81 s	6.73 s	6.86 s	6.82 s	6.84 s	6.84 s	6.80 s
2	3.95 (q, 6.6)	4.15 (t, 4.6) ¹	4.31 (td, 5.7, 1.2) ²	3.88 (ddd, 7.4, 5.5, 1.6)	3.77 (dd, 4.2, 2.0)	3.84 (dd, 4.0, 1.8)	4.25 (ddd, 6.6, 5.2, 1.6)
3	-	-	-	-	-	-	-
4	10.36 s	10.34 s	10.49 s	10.37 s	10.41 s	10.40 s	10.37 s
5	7.34 (d, 1.8)	7.22 (d, 1.5)	7.34 (d, 1.6)	7.33 (d, 1.6)	7.29 (d, 1.7)	7.29 (d, 1.6)	7.20 (d, 1.9)
6	-	-	-	-	-	-	-
7	7.40 (dd, 8.1, 1.8)	7.35 (dd, 8.2, 1.5)	7.40 (dd, 8.2, 1.6)	7.40 (dd, 8.3, 1.6)	7.38 (dd, 8.3, 1.7)	7.38 (dd, 8.2, 1.6)	7.36 (dd, 8.4, 1.9)
8	6.67 (d, 8.3)	6.64 (d, 8.3)	6.67 (d, 8.3)	6.73 (d, 8.3)	6.73 (d, 8.3)	6.70 (d, 8.3)	6.65 (d, 8.3)
9	-	-	-	-	-	-	-
10	-	-	-	-	-	-	-
11	-	-	-	-	-	-	-
12	3.75 s (3H)	3.73 s (3H)	3.75 s (3H)	3.74 s (3H)	3.73 s (3H)	3.73 s (3H)	3.72 s (3H)
1a	1.28 (d, 6.6, 3H)	2.84 (dd, 13.8, 6.2) 2.80 (dd, 13.8, 4.8)	2.78 (dd, 14.1, 3.2) 2.73 (dd, 14.1, 3.8)	1.40-1.52 m ³	2.06 (sep of d, 6.8, 2.0)	1.75-1.83 m	2.97 (13.7, 6.0)
2a	-	-	-	1.81 (sep, 6.6)	0.94 (d, 6.8, 3H)	1.37-1.44 m 1.06-1.16 m	-
3a	-	6.93 (d, 8.2)	3.58 s (3H)	0.87 (d, 6.6, 6H) ⁴	0.82 (d, 6.8, 3H)	0.90 (d, 7.0, 3H)	7.15-7.17 m
4a	-	6.59 (d, 8.2)	-	-	-	0.81 (t, 7.4, 3H) ¹	7.20-7.22 m
5a	-	-	-	0.87 (d, 6.6, 6H) ⁴	-	-	7.15-7.17 m
6a	-	6.59 (d, 8.2)	-	-	-	-	7.20-7.22 m
7a	-	6.93 (d, 8.2)	-	-	-	-	7.15-7.17 m
8a	-	9.1 s	-	-	-	-	-

¹ actually a dd appearing as a t due to 2nd order coupling; ² actually a ddd appearing as a td due to 2nd order coupling; ³ two overlapping ddd; ⁴ equivalent resonances integrating to 6H.

Table 4-5 ¹H NMR data (δ in ppm) for compounds **A6h-n** (*J* is given in Hz)

	A6h	A6i	A6j	A6k	A6l	A6m	A6n
1	6.75 s	6.71 s	6.88 s	-	6.85 (d, 1.1)	6.84 s	-
2	4.24 (td, 5.6, 1.4) ¹	4.15 (ddd, 7.7, 4.1, 1.6)	4.02 (ddd, 6.2, 4.4, 1.0)	3.86 (dd, 9.2, 7.2)	3.95 (td, 6.1, 1.6)	3.93 (dd, 6.4, 3.6)	3.97 (dd, 5.4, 3.5)
3	-	-	-	-	-	-	-
4	10.34 s	10.41 s	10.44 s	10.50 s	10.46 s	10.37 s	10.40 s
5	7.23 (d, 1.6)	7.31 (d, 1.7)	7.33 (d, 1.7)	7.40 (d, 1.8)	7.33 (d, 1.8)	7.26 (d, 1.8)	7.29 (d, 1.8)
6	-	-	-	-	-	-	-
7	7.34 (dd, 8.2, 1.7)	7.38 (dd, 8.3, 1.8)	7.41 (dd, 8.3, 1.8)	7.52 (dd, 8.3, 1.8)	7.40 (dd, 8.1, 1.9)	7.36 (dd, 8.2, 1.8)	7.37 (dd, 8.2, 1.7)
8	6.63 (d, 8.3)	6.69 (d, 8.3)	6.71 (d, 8.3)	6.59 (d, 8.3)	6.70 (d, 8.3)	6.72 (d, 8.3)	6.69 (d, 8.3)
9	-	-	-	-	-	-	-
10	-	-	-	-	-	-	-
11	-	-	-	-	-	-	-
12	3.72 s (3H)	3.74 s (3H)	3.74 s (3H)	3.76 s (3H)	3.73 s (3H)	3.73 s (3H)	3.73 s (3H)
1a	3.07 (d, 5.6) ²	2.97 (dd, 14.7, 4.1) 2.83 (dd, 14.7, 7.7)	1.81-1.98 m	2.00-2.20 m	1.81-1.97 m	3.71-3.73 m	3.66 (dd, 10.8, 5.4) 3.60 (dd, 10.8, 3.4)
2a	-	-	2.53-2.64 m	1.93-2.00 m	2.39-2.45 m	1.12 (d, 6.4)	-
3a	7.07 (d, 2.1)	6.79 s	2.03 s (3H)	3.25-3.47 m	-	-	-
4a	10.82 s	10.90 s	-	-	3.55 s (3H)	-	-
5a	-	7.58 s	-	-	-	-	-
6a	7.51 (d, 7.8)	-	-	-	-	-	-
7a	7.03 (t, 7.8) ³	-	-	-	-	-	-
8a	6.95 (t, 7.5) ³	-	-	-	-	-	-
9a	7.29 (d, 7.5)	-	-	-	-	-	-

¹actually a ddd collapsed due to 2nd order coupling. ² both resonances of 1a overlap. Each proton of 1a should be a dd, however this could not be detected since the 2nd order coupling is so strong that the outer peaks of the dd were too negligible to be detected. ³ actually a dd appearing as a t since both *J* values are the same.

Table 4-6 ^{13}C NMR data (δ in ppm) for compounds **A6a-6n**

	A6a	A6b	A6c	A6d	A6e	A6f	A6g	A6h	A6i	A6j	A6k	A6l	A6m	A6n
1	-	-	-	-	-	-	-	-	-	-	-	-	-	-
2	50.4	56.6	51.9	53.3	60.3	59.7	56.3	55.9	55.0	53.8	59.0	54.2	67.4	57.5
3	167.4	166.1	166.0	167.0	166.1	166.1	166.0	166.4	166.1	166.4	166.2	166.5	166.2	166.1
4	-	-	-	-	-	-	-	-	-	-	-	-	-	-
5	115.4	115.1	115.5	115.3	115.2	115.2	115.2	115.1	115.4	115.4	114.9	115.7	115.0	115.2
6	117.8	117.1	117.8	117.6	116.9	116.8	117.3	117.1	117.7	117.8	117.8	118.0	116.5	116.8
7	125.0	125.1	125.1	125.1	125.2	125.2	125.1	125.1	125.1	125.1	125.3	125.4	125.0	125.1
8	112.2	111.9	112.1	112.3	111.4	111.4	112.0	111.9	112.4	112.2	110.5	112.5	111.6	111.6
9	125.2	124.3	124.7	124.8	124.1	124.1	124.3	124.4	124.7	124.7	126.8	124.8	124.3	124.2
10	138.9	138.3	138.2	138.3	138.9	138.9	138.3	138.3	138.3	138.4	138.5	138.6	139.1	138.8
11	166.1	166.0	165.4	166.1	165.8	165.7	165.8	166.1	165.9	166.0	166.1	166.3	165.5	165.2
12	51.4	51.3	51.4	51.4	51.3	51.3	51.4	51.3	51.5	51.4	51.5	51.7	51.3	51.3
1a	18.2	37.7	37.0	41.4	32.1	39.0	38.5	28.7	29.4	31.8	27.0	27.9	61.3	62.8
2a	-	126.6	170.5	23.3	18.6	24.2	136.8	136.0	131.7	28.7	21.7	29.2	19.8	-
3a	-	130.7	51.5	22.9	17.2	15.1	129.9	124.2	117.3	14.4	46.0	173.1	-	-
4a	-	114.8	-	21.7	-	11.6	128.2	-	-	-	-	51.5	-	-
5a	-	155.8	-	-	-	-	126.3	127.5	134.4	-	-	-	-	-
6a	-	114.8	-	-	-	-	128.2	118.3	-	-	-	-	-	-
7a	-	130.7	-	-	-	-	129.9	120.8	-	-	-	-	-	-
8a	-	-	-	-	-	-	-	118.4	-	-	-	-	-	-
9a	-	-	-	-	-	-	-	111.2	-	-	-	-	-	-
10a	-	-	-	-	-	-	-	109.0	-	-	-	-	-	-

Quinoxalines with aromatic side chain

Compounds **A6b** and **A6g-i** contained aromatic amino acids, tyrosine (**A6b**), phenylalanine (**A6g**), tryptophan (**A6h**) and histidine (**A6i**). Tyrosine contains a polar hydroxyl group, tryptophan and histidine are basic whereas phenylalanine is non-polar.

All the functional groups of these amino acids contain a methylene group bonded directly to C-2 and hence, H-2 should appear as a ddd in each case, coupling with the two methylene protons and NH-1. However, this is only seen in two cases, **A6g** and **A6i** with $J = 6.6, 5.2, 1.6$ Hz for **A6g** and $J = 7.7, 4.1, 1.6$ Hz for **A6i**. For **A6b** we observe a triplet for H-2 at δ 4.15 ($J = 4.6$ Hz). This could be due to there being no coupling with the NH-1 proton and the protons of the diastereotopic methylene group occurring at the same resonance. For **A6h**, we observe a triplet of doublets at δ 4.24 for H-2, due to coupling with equivalent methylene protons ($J = 5.6$ Hz) and a small coupling with the NH-1 proton ($J = 1.4$ Hz). The diastereotopic proton resonances are clearly observed in **A6b** at δ 2.84 ($J = 13.8, 6.2$ Hz) and 2.80 ($J = 13.8, 4.8$ Hz) and **A6i** at δ 2.97 ($J = 14.7, 4.1$ Hz) and 2.83 ($J = 14.7, 7.7$ Hz). For **A6h**, this methylene group, H-1a is observed as a doublet at δ 3.07 ($J = 5.6$ Hz). We do not observe geminal coupling here and propose that due to second order coupling, the two outer peaks of each of the doublets have disappeared and that the inner peaks only are observed 5.6 Hz apart. Since no other coupling is observed, the dihedral angle between the two methylene protons and H-2 must be very close to 90° . For **A6g**, the two methylene protons overlap at δ 2.97 and both geminal (13.7 Hz) and vicinal (6.0 Hz) coupling is observed.

For the rest of the side chain, expected resonances were seen for **A6b**, two pairs of doublets at δ 6.93 (H-3a/7a) and 6.59 (H-4a/6a) with $J = 8.2$ Hz indicative of ortho coupling; for **A6g**, three

proton (at δ 7.15-7.17) and two proton (at δ 7.20-7.22) aromatic resonances were seen for the five aromatic protons; for **A6h** the six tryptophan proton resonances can be seen at δ 7.07 (d, $J = 2.1$ Hz, H-3a), δ 10.82 (s, NH-4a), δ 7.51 (d, $J = 7.8$ Hz, H-6a), δ 7.03 (t, $J = 7.3$ Hz, H-7a), δ 6.95 (t, $J = 7.5$ Hz, H-8a) and δ 7.29 (d, $J = 7.5$ Hz, H-9a); and for **A6i** the three imidazole protons can be seen at δ 6.79 (s, H-3a), δ 10.90 (s, NH-4a) and δ 7.58 (s, H-5a).

An NMR study on hydrogen bonding (see 4.3.4) indicated that amongst these aromatic side chain amino acid quinoxalines, the $-\Delta\delta/\Delta T$ value of H-2 for compound **A6b** is much higher at 3.8 than for compounds **A6g-A6i** (0.46, 0.28 and 0.19 respectively) (Table 4-8). This indicates strong hydrogen bonding for **A6g-i** and only moderate hydrogen bonding for **A6b** as H-2 in this case showed the largest change.

Quinoxalines with aliphatic non-polar side chain

The side chains of quinoxalines containing alanine (**A6a**), leucine (**A6d**), valine (**A6e**), isoleucine (**A6f**) and proline (**A6k**) are aliphatic and non-polar in nature. In the case of **A6a** (alanine quinoxaline) with a methyl group in its side chain, H-2 was observed as a quartet at δ 3.95 and the methyl group H-1a appeared at δ 1.28 with a J value of 6.6 Hz. For **A6d** (leucine quinoxaline) with a 2-methylpropyl side chain, H-2 appears as a ddd ($J = 7.4, 5.5, 1.6$ Hz), coupling with each of the diastereotopic methylene protons and the NH-1 proton. The two H-1a protons overlap and occur as a multiplet at δ 1.40-1.52. Interestingly, H-2a does not couple with either of the H-1a protons and occurs as a septet at δ 1.81 ($J = 6.6$ Hz) coupling only with the two equivalent methyl groups, which appear as a doublet at δ 0.87.

In **A6e**, H-2 appears as a double doublet at δ 3.77 ($J = 4.2, 2.0$ Hz), coupling with both NH-1 and H-1a. The H-1a resonance occurs as a multiplet at δ 2.03-2.11. The methyl groups appear as two separate doublets at δ 0.94 and 0.82. These methyl groups appear as separate resonances since they are close to the chiral H-2 proton. In **A6f** (isoleucine side chain), H-2 appears as a double doublet at δ 3.84 ($J = 4.0, 1.8$ Hz), H-1a and the two H-2a protons as multiplets at δ 1.75-1.83, 1.06-1.16 and δ 1.37-1.44 respectively. The methyl groups CH₃-3a and CH₃-4a appear as a doublet and triplet with $J = 7.0$ and 7.4 Hz respectively. In **A6k** with a proline side chain, the H-2 resonance occurs as a double doublet ($J = 9.2, 7.2$ Hz) and H-1a to H-3a all appear as multiplets at δ 2.00-2.20, δ 1.93-2.00 and δ 3.25-3.47 respectively, the latter resonance being deshielded since it is adjacent to nitrogen.

The $-\Delta\delta/\Delta T$ value of the H-2 proton (**Table 4-8**) for compounds **A6a**, **A6d-f** and **A6k** indicated that **A6d**, **A6f** and **A6k** are more strongly involved in hydrogen bonding than **A6a** and that **A6e** has the least intermolecular hydrogen bonding from this series.

Quinoxalines with ester, thiomethyl and hydroxyl functionality

Compounds **A6c** and **A6l** both have ester functional groups in its side chain. In **A6c**, the H-2 proton was split into a triplet of doublets (td), since H-2 was first split into a triplet by the H-1a protons and then into a td by NH-1. Even though both H-1a protons are diastereotopic, they behave as though they split H-2 equally, thus resulting in a triplet. Each of the diastereotopic H-1a resonances appear separately at δ 2.78 ($J = 14.1, 3.2$ Hz) and 2.73 ($J = 14.1, 3.8$ Hz). A similar splitting pattern for H-2 is seen in **A6l** which appears as a td. Since **A6l** has two methylene groups adjacent to each other in its side chain, each of H-1a and H-2a appear as two-proton multiplets at

δ 1.81-1.97 and δ 2.39-2.45 respectively. Each of the ester methyl groups for **A6c** and **A6l** appear as singlets at δ 3.58 and 3.55 respectively and the ester carbonyl resonances occur at δ 170.5 and 173.1 respectively. For **A6j** with a thiomethyl ester side chain, H-2 appears as a ddd, coupling with each of the diastereotopic H-1a protons and then NH-1 with J values of 6.2, 4.4 and 1.0 Hz. This is slightly different to H-2 of **A6c** and **A6l** above which occur as td. Both 1a and 2a appear as two-proton multiplets similar to **A6l** at δ 1.81-1.98 and δ 2.53-2.64 respectively and the thiomethyl group appears a singlet at δ 2.03.

For **A6m** and **A6n** derived from threonine and serine, containing hydroxy groups in its side chain, the H-2 splitting pattern and coupling constants were similar in both cases, occurring as dd at δ 3.93 ($J = 6.4, 3.6$ Hz) and δ 3.97 ($J = 5.4, 3.5$ Hz) respectively, even though H-2 in **A6m** was vicinal to a CH-O moiety and in **A6n** to a CH₂-O moiety. This could be due to there being no coupling to NH-1 in **A6n** and therefore the dd arises from coupling to each of the H-1a protons. The H-1a resonance in **A6m** overlaps with the ester methyl resonance and appears as a deshielded multiplet at δ 3.71-3.73. The methyl group CH₃-2a appears as a doublet as expected at δ 1.12 ($J = 6.4$ Hz). In **A6n**, each of the H-1a resonances occur separately as dd at δ 3.66 and 3.60 with geminal coupling of 10.8 Hz and smaller vicinal coupling to H-2 of 5.4 and 3.4 Hz respectively.

From the thermal study carried out, **A6c** is seen to have a larger $-\Delta\delta/\Delta T$ value for H-2 of 2.34 than **A6m**- **A6n**, **A6j** and **A6l** with a $-\Delta\delta/\Delta T$ value of less than 0.5 (**Table 4-8**), indicating that **A6c** has weaker intermolecular hydrogen bonding than the other compounds in this series.

4.3.3 Structure determination of A6d by single crystal X-Ray diffraction

In order to describe the structure of the series of compounds more fully, we obtained the crystal structure of **A6d** as a representative of the series (**Figure 4-4**). Compound **A6d** was solved in the orthorhombic space group $P2_1/c$, with one molecule in the asymmetric unit. The crystal structure of **A6d** indicated that the absolute stereochemistry at C-2 was in the *S* configuration and that the benzene and piperazine rings are contained in the same plane (the torsion angle for C5 - C9 - C10 - N1 is 177.7° and that of N4 - C9 - C10 - C8 is -175.3°) with the isobutyl moiety out of the plane, perpendicular to the benzene ring with the dihedral angle between C1a and C10 being 73.8° and C1a and N4 being -89.6° (**Figure 4-4**). The dihedral angle between the axial H-2 with axial H-1a^a is 124.8° , whereas the dihedral angle between the axial H-2 with equatorial H-1a^b is 4.5° . The six membered rings exist in a twist half boat conformation $\Phi = 42.1 (3)^\circ$, $\theta = 64.3 (3)^\circ$, $\Psi = 0.3703 (17)^\circ$. As expected the O(3)...NH(4) distance is 2.44 \AA and the O(3)...H(2) distance is 2.53 \AA , falling within the range of $2.30\text{--}3.10 \text{ \AA}$ required for hydrogen abstraction (Nishio et al., 2005). Interestingly the O(3)...H(1a^b) distance of 2.89 \AA also falls within this range, but the O(3)...H(1a^a) distance of 3.44 \AA falls out of this range. In general there was intermolecular hydrogen bonding between the NH protons and the oxygen of the carbonyl groups as well as between the chiral proton H-2 and the oxygen atoms of carbonyl groups (**Figure 4-5**; **Table 4-7**).

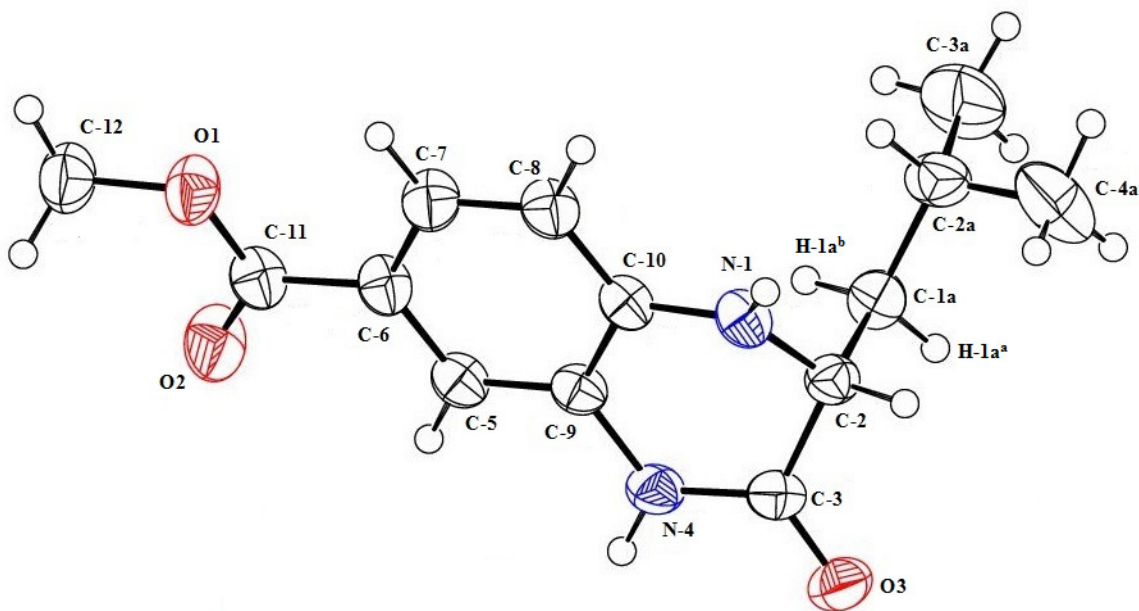


Figure 4-4 ORTEP diagram of compound **A6d**

Table 4-7 Geometry of hydrogen bonding in molecule **A6d** (Å,°)

<i>D</i> - H... <i>A</i>	<i>D</i> - H	H... <i>A</i>	<i>D</i> ... <i>A</i>	<i>D</i> - H... <i>A</i>
N1 – H1...O2	0.88	2.06	2.852 (2)	149
N4 – H4...O3	0.88	2.26	3.104 (2)	162
C2 – H2...O3	1.00	2.60	3.597 (2)	179

Symmetry codes: (i) $-x, -1/2+y, 3/2-z$; (ii) $-x, 1/2+y, 3/2-z$; (iii) $x, -1+y, z$

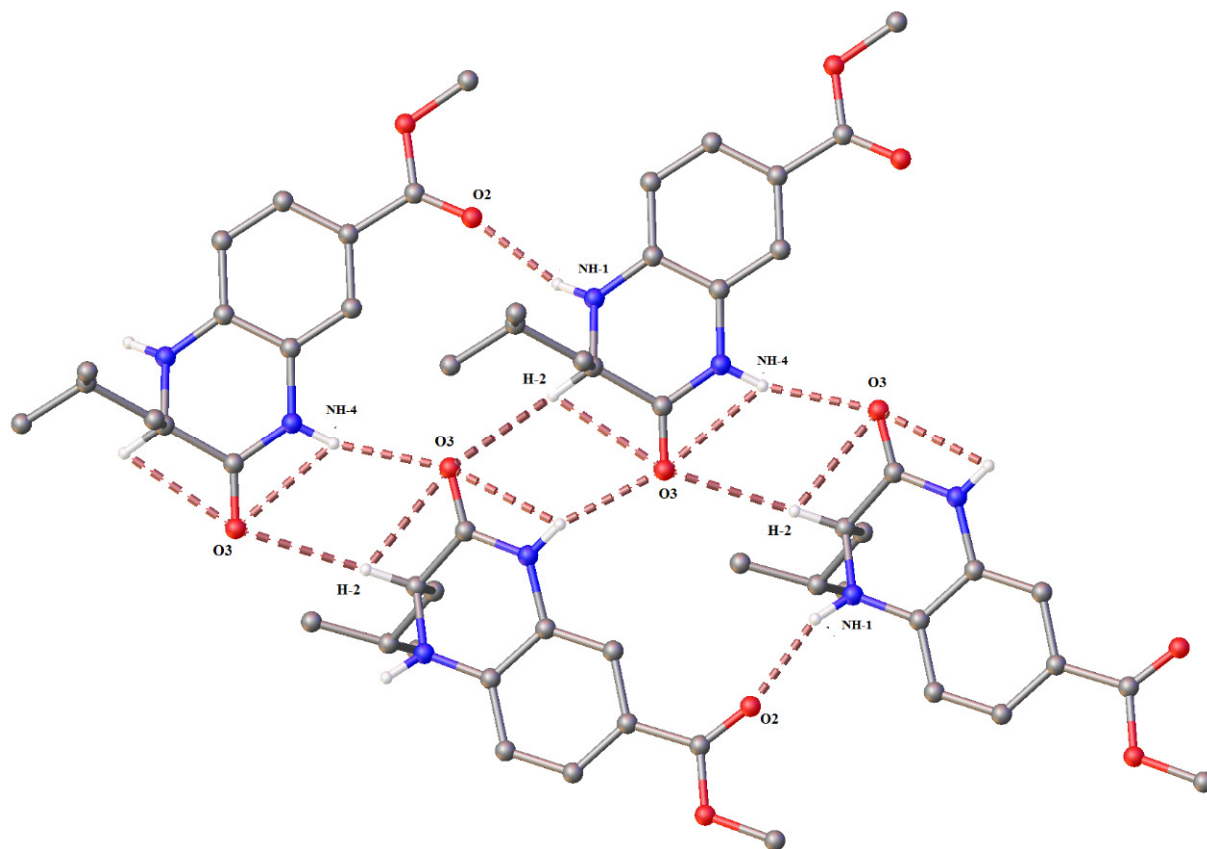


Figure 4-5 Intermolecular hydrogen bonding in **A6d**

4.3.4 Thermal coefficient shift NMR investigation

Amino acids have the tendency to be involved in hydrogen bonding, both intermolecular and intramolecular, especially the ones with polar functional groups. In order to investigate this hydrogen bonding in the molecules synthesized in this work, ^1H proton NMR thermal analysis was performed starting from 298 K and increasing the temperature in increments of 10 °C up to 328 K. At higher temperatures, the hydrogen bonding would be disrupted and as such the proton resonances involved in hydrogen bonding would be more shielded due to the N-H bond now being shorter.

Upon heating, a significant upfield shift of NH-4 and NH-1 in the tetrahydroquinoxalines was observed in the ^1H NMR spectra (**Figure 4-6**). The chemical shift of the chiral proton H-2 did not change much. In the crystal structure of **A6d**, intermolecular hydrogen bond interactions were evident between NH-1 and the carbonyl oxygen of the ester moiety (O2). For NH-4 both intramolecular and intermolecular hydrogen bonding was present to O3, the amide carbonyl oxygen, with greater intermolecular hydrogen bonding being present. Intramolecular and intermolecular hydrogen bonding also occurred with H-2 and O3 with greater intramolecular hydrogen bonding being present (**Figure 4-5**).

In aprotic solvents such as $\text{DMSO-}d_6$, $-\Delta\delta/\Delta T < 3 \text{ ppb K}^{-1}$ indicates the presence of hydrogen bonding and at $-\Delta\delta/\Delta T > 5 \text{ ppb K}^{-1}$ hydrogen bonding is not possible (Farahani et al., 2014). The $-\Delta\delta/\Delta T$ values for selected protons in **A6a-n** acquired in $\text{DMSO-}d_6$ are summarised in (**Table 4-8**). For the NH-4 proton our results indicate $-\Delta\delta/\Delta T$ values between 4.12 - 5.04 ppb K^{-1} . According to the definition above only **A6a** with $-\Delta\delta/\Delta T$ of 5.04 ppb K^{-1} would have no hydrogen bonding. All the other compounds show weak hydrogen bonding since its values are close to $-\Delta\delta/\Delta T$ of 5.0. For the NH₁ proton resonance, $-\Delta\delta/\Delta T$ range from 3.90 to 44.77, although only three values are in the high end of the range between 41.67-44.77 for **A6c** (esterified aspartic acid derivative), **A6d** (leucine derivative) and **A6e** (valine derivative). All other compounds have $-\Delta\delta/\Delta T$ less than 5.64. In two of the cases, NH₁ could not be observed and the $-\Delta\delta/\Delta T$ was not calculated. For the three compounds with very high $-\Delta\delta/\Delta T$ values for NH-1 (**A6c-e**) all hydrogen bonding involving this proton was totally absent upon heating. The fact that these three molecules deviated from the norm could be due to the fact that once heated, the interaction between the atoms involved in hydrogen bonding were totally absent. For the chiral proton H-2, hydrogen bonding

in **A6a-n** were conserved upon heating since the $-\Delta\delta/\Delta T$ values were present in the range of 0.04-3.80. This could be due to the conservation of the intramolecular hydrogen bonding between H-2 and the oxygen of the amide carbonyl group. NH-4 also had intramolecular hydrogen bonding, not as much as H-2, but more than NH₁. This supports our data in that the more intramolecular hydrogen bonding present, the smaller the $-\Delta\delta/\Delta T$ value.

4.3.5 Computational results

Conformational analysis and structure validation

The conformational profile with of **A6d** was explored using the Discovery studio programme, and the five lowest energy conformers obtained. These structures were re-optimized at DFT level using Gaussian software (Frisch et al., 2009). The computed electronic energies of conformer 1-5 were found to be -879.531657, -879.528114, -879.530716, -879.525673 and -879.529739 Hartree, respectively, indicating conformer 1 to be the energetically most favourable in comparison to other conformers. The most energetically favourable DFT predicted structure was further validated by monitoring the root mean square deviation (RMSD) of all five conformers relative to the X-ray structure of **A6d** considering all their atoms, using the Discovery Studio visualizer. The computed RMSD with values of 0.832 Å, 1.112 Å, 1.125 Å, 1.151 Å and 1.045 Å for conformers 1-5 respectively, indicated a close structural correlation between conformer 1 and the X-ray structure. Three dimensional structure comparison of conformer 1 and conformer 2 with the X-ray structure of **A6d** was performed using DS visualizer to indicate the similarity between conformer 1 and the X-Ray structure and the deviation from the X-Ray structure by conformer 2 (**Figure 4-7**). Conformer 1 (green) structurally fits very well on the X-ray structure (red). On the

other hand, conformer 2 (blue), was slightly more folded bringing the ester and alkyl chain inwards, accounting for higher RMSD (1.112Å) compared to conformer 1 (0.832Å).

Table 4-8 $-\Delta\delta/\Delta T$ values of shielded and deshielded proton from compound **A6a-n**

Entry	NH-1	NH-4	H-2	OH	NH-4a
A6a	4.50	5.04	1.59	-	-
A6b	5.64	4.57	3.8	5.43	-
A6c	44.77	4.54	2.34	-	-
A6d	43.81	4.75	0.45	-	-
A6e	41.67	4.79	3.53	-	-
A6f	3.90	4.81	0.25	-	-
A6g	4.51	4.30	0.46	-	-
A6h	5.15	4.27	0.26	-	3.64
A6i	4.21	4.70	0.19	-	-
A6j	4.03	4.67	0.23	-	-
A6k	-	4.68	0.57	-	-
A6l	4.12	4.71	0.04	-	-
A6m	5.09	4.12	0.12	1.28	-
A6n	-	4.42	0.26	-	-

Natural atomic charges and electronic properties

The effective atomic charges of chemical entities provide very useful information about their interactions in the molecular systems. Accordingly, the atomic charges of **A6d** were obtained using the Mulliken population analysis procedure, and are depicted in **Figure 4-8**. A closer inspection of **Figure 4-8** revealed that the negative (–ve) charge was predominantly distributed over the nitrogen (N4 and N1) and oxygen atoms (O1 and O2), imposing large positive charges on the directly bonded carbon atoms (C3, C2, C10, C9 and C11). Except for the nitrogen bonded hydrogen atoms (H4 and H1), no significant charge distribution was observed in the remaining hydrogen atoms of the molecule. The accumulation of a large positive charge on H4 (0.290) and H1 (0.258) was attributed to a large negative charge on the nitrogen atoms (N4 and N1, respectively). This indicates the participation of these atoms in hydrogen bonding, in agreement with the argument presented above.

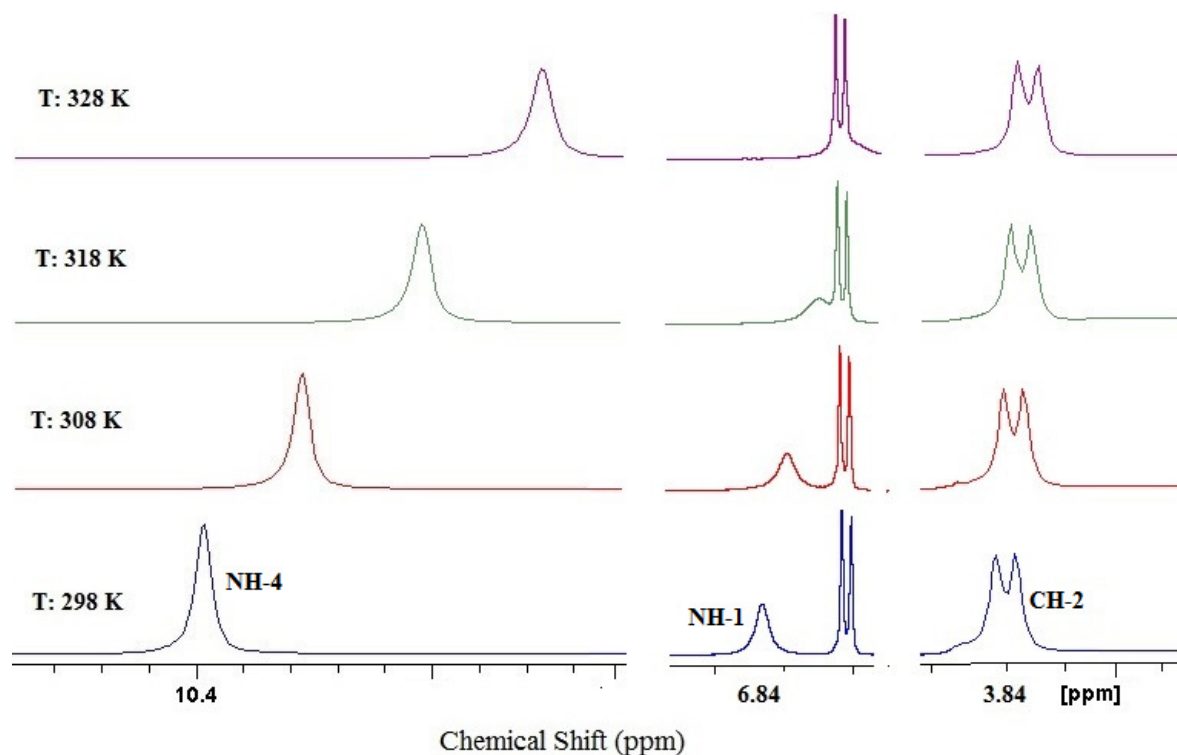


Figure 4-6 ^1H spectral traces showing the shift of amide, sec. amine and chiral carbon containing proton at variable temperature in $\text{DMSO-}d_6$

In order to substantiate these observations, the electron density plots for the highest occupied molecular orbital (HOMO) and the lowest unoccupied molecular orbital (LUMO) were visualized, and are depicted in **Figure 4-9** and **Figure 4-10** respectively. The electron density in HOMO was preferably localized on the piperazine and phenyl rings, whereas in LUMO it was distributed over the oxygens of the ester functionality and phenyl ring. This HOMO-LUMO electronic arrangement suggests an electron density exchange between the central part (piperazine and phenyl rings) and the edge (ester group) of the molecule, indicating the possibility of hydrogen bonding in these regions, in accordance with the X-ray structure. Moreover, the computed HOMO-LUMO gap was sufficiently low (4.4 eV) reflecting the chemical reactivity of the compound and resulting charge transfer interaction.

Molecular dynamics (MD) results

Finally, a molecular dynamics (MD) study was conducted to explain the structural flexibility of **A6d**, observed in NMR experiments (**Table 8**). A total of 500 different conformations of **A6d** were explored under explicit solvent conditions using the Standard Dynamics Cascade algorithm embedded in the Discovery Studio (Accelrys Software, 2013).

The evolution of four distances; distance 1 [(N1)H..H(C2a)], distance 2 [O3..H(C2a)], distance 3 [(N1)H..H(C1a)] and distance 4 [(N1)H..O3), was monitored during the progress of MD simulation, and is diagrammatically shown in **Figure 4-11**. These results revealed that the distance 1 (in black) fluctuates between 2-5 Å during the first half of simulation, but becomes stable (2.3 Å) during the next half, suggesting the formation of a hydrogen bond between atoms N1 and HC2a. On the other hand, the distance 2 (in red) exhibited an average fluctuation around 5 Å after 250 picoseconds, indicating the unstable nature of this interaction. The inter-atomic distances, 3 (in green) and 4 (in blue), exhibited larger deviations (>3.0 Å) in the majority of the sampled conformations. Overall, the MD results suggested that compound **A6d** is highly flexible in the presence of solvent molecules, and also indicates the role of N1 (quinoxaline) and HC2a in intramolecular and intermolecular hydrogen bonding.

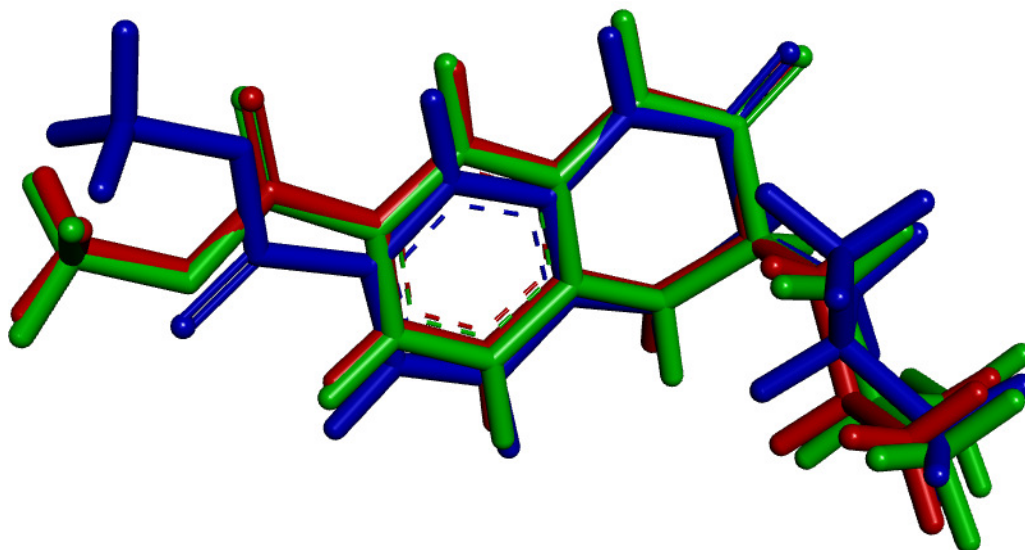


Figure 4-7 Overlay of X-ray structure (in red sticks) of **A6d** with its DFT predicted conformer1 (in green sticks) and conformer 2 (in blue sticks), performed using DS Software (2013)

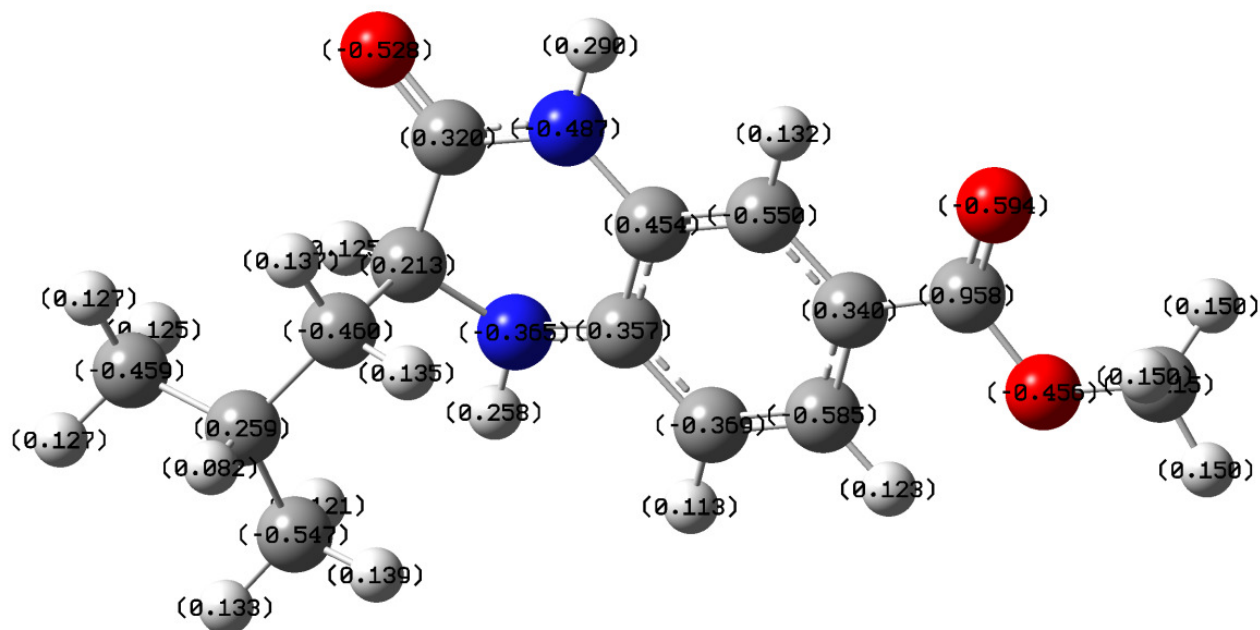


Figure 4-8 Optimized geometry of **A6d** displaying natural charge distribution on each atom

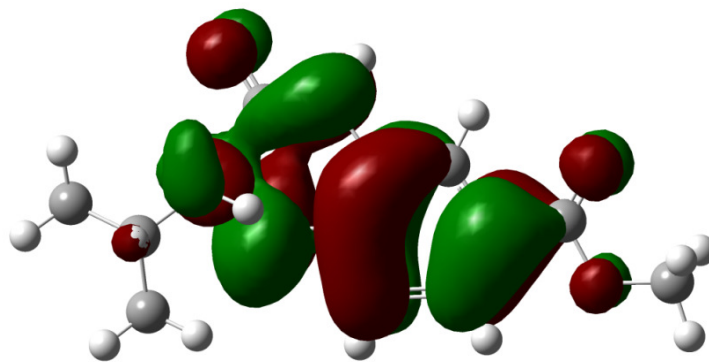


Figure 4-9 The electron density distribution in HOMO of compound **A6d**

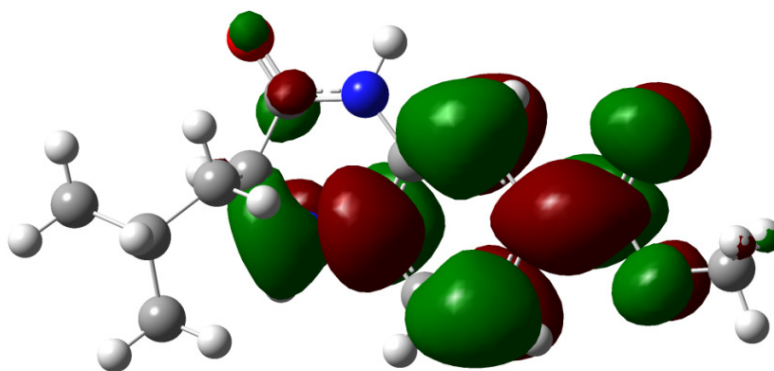


Figure 4-10 The electron density distribution in LUMO of compound **A6d**

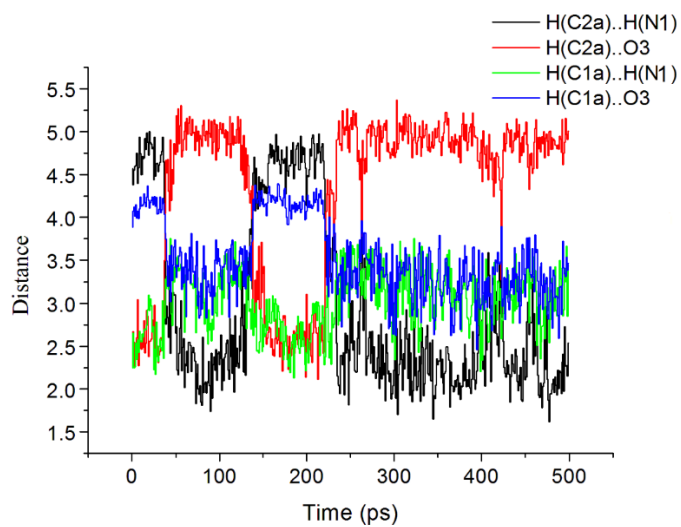


Figure 4-11 Progress of selected inter-atomic distances (in Å) during MD simulation for compound **A6d**

4.4 Conclusion

Fourteen quinoxaline derivatives were successfully synthesized and ^1H and ^{13}C NMR assignments of tetrahydroquinoxaline were made with the aid of HSQC and HMBC data and will provide a reference point for the structural elucidation of other tetrahydroquinoxalines synthesized. NMR studies appear to reveal that atoms on the tetrahydroquinoxaline core enforce intermolecular hydrogen bonding interactions. The stereochemistry of C-2 for **A6d** was shown to be in the *S* configuration for tetrahydroquinoxaline from X-Ray data. Thermal coefficient investigation studies revealed the presence of hydrogen bonding in these molecules. Additionally, DFT calculations of **A6d** revealed the role of the quinoxaline ring in hydrogen bonding and charge transfer. Moreover, MD studies explained the high flexible nature of **A6d** in the solvent phase, and supported the experimental observations. From the thermal coefficient shift, NMR investigation and X-ray crystal analysis of quinoxalines it can be described that the chiral carbon containing proton (H-2) is involved in low to strong hydrogen bonding. This could be due to different side chain functionalities of amino acid precursors, each having a different structure.

Acknowledgement

The authors acknowledge the facilities from the Centre for High Performance Computing, an initiative supported by the Department of Science and Technology of South Africa for software and cluster facilities to run the computations.

4.5 References

- Achutha, L., Parameshwar, R., Madhava Reddy, B., Harinadha Babu, V. Microwave-assisted synthesis of some quinoxaline-incorporated schiff bases and their biological evaluation. *J. Chem.*, **2013**, 1-6.
- Ameen, A., Hashe, A., Synthesis, reactions and biological activity of quinoxaline derivatives. *Am. J. Org. Chem.*, **2015**, 5(1), 14-56.

- Accelrys Software Inc., Discovery studio modeling environment, release 4.0, San Diego: *Accelrys Software Inc.*, **2013**.
- Ajani, O. O. Present status of quinoxaline motifs: Excellent pathfinders in therapeutic medicine. *Eur. J. Med. Chem.*, **2014**, 85, 688-715.
- Balasubramanian, S., Sasikumar, P., Velmurugan, D. *In-vitro* Evaluation and molecular docking calculation of tricyclic phthalimide quinoxaline analogues as novel inhibitors of HIV-1 integrase using GLIDE and GOLD. *Int. J. Pharm. Sci. Drug Res.*, **2014**, 6(1), 60-66.
- Becke, A. D. Density-functional exchange-energy approximation with correct asymptotic behaviour. *Phys. Rev. A.*, **1988**, 38(6), 3098-3100.
- Burguete, A., Pontiki, E., Hadjipavlou-Litina, D., Ancizu, S., Villar, R., Solano, B., Moreno, E., Torres, E., Rez, S., Aldana, I., Monge, A. Synthesis and biological evaluation of new quinoxaline derivatives as antioxidant and anti-inflammatory agents. *Chem. Biol. Drug Des.*, **2011**, 77, 255-267.
- Barea, C., Pabon, A., Perez-Silanes, S., Galiano, S., Gonzalez, G., Monge, A., Deharo, E., Aldana, I. New amide derivatives of quinoxaline 1,4-di-*N*-oxide with leishmanicidal and antiparasmodial activities. *Molecules*, **2013**, 18, 4718-4727.
- Briza, T., Kralova, J., Dolensky, B., Rimpelova, S., Kejik, Z., Ruml, T., Hajduch, M., Dzubak, P., Mikula, I., Martasek, P., Pouckova, P., Kral, V. Striking antitumor activity of a methinium system with incorporated quinoxaline unit obtained by spontaneous cyclization. *ChemBioChem.*, **2015**, 16(4), 555-558.
- Chandra Shekhar, A., Lingaiah, B. P. V., Shanthan Rao, P., Narsaiah, B., Allanki, A., Sijwali, P. S. Design, synthesis and biological evaluation of novel fluorinated heterocyclic hybrid molecules based on triazole & quinoxaline scaffolds lead to highly potent antimalarials and antibacterials. *Lett. Drug Des. Discovery*, **2015**, 12(5), 393-407.
- Chandra Shekhar, A., Shanthan Rao, P., Narsaiah, B., Allanki, A., Sijwali, P. S. Emergence of pyrido quinoxalines as new family of antimalarial agents. *Eur. J. Med. Chem.*, **2014**, 77, 280-287.
- Cholo, M. C., Steel, H. C., Fourie, P. B., Germishuizen, W. A., Anderson, R. Clofazimine: current status and future prospects. *J. Antimicrob. Chemother.*, **2012**, 67, 290-298.
- Demmer, C. S., Møller, C., Brown, P. M. G. E., Han, L., Pickering, D. S., Nielsen, B., Bowie, D., Frydenvang, K., Kastrup, J. S., Bunch, L. Binding mode of an α -amino acid-linked quinoxaline-2,3-dione analogue at glutamate receptor subtype GluK1. *ACS Chem. Neurosci.*, **2015**, 6, 845-854.
- Deepika, Y., Nath, P. S., Kumar, S., Sinha, S. Biological activity of quinoxaline derivatives. *Int. J. Curr. Pharm. Rev. Res.*, **2011**, 2(1), 33-46.
- Frisch, M. J., Trucks, G. W., Schlegel, H. B., Scuseria, G. E., Robb, M. A., Cheeseman, J. R., Scalmani, G., Barone, V., Mennucci, B., Petersson, G. A., Nakatsuji, H., Caricato, M., Li, X., Hratchian, H. P., Izmaylov, A. F., Bloino, J., Zheng, G., Sonnenberg, J. L., Hada, M., Ehara, M., Toyota, K., Fukuda, R., Hasegawa, J., Ishida,

- M., Nakajima, T., Honda, Y., Kitao, O., Nakai, H., Vreven, T., Montgomery Jr. J. A., Peralta, J. E., Ogliaro, F., Bearpark, M., Heyd, J. J., Brothers, E., Kudin, K. N., Staroverov, V. N., Kobayashi, R., Normand, J., Raghavachari, K., Rendell, A., Burant, J. C., Iyengar, S. S., Tomasi, J., Cossi, M., Rega, N., Millam, J. M., Klene, M., Knox, J. E., Cross, J. B., Bakken, V., Adamo, C., Jaramillo, J., Gomperts, R., Stratmann, R. E., Yazyev, O., Austin, A. J., Cammi, R., Pomelli, C., Ochterski, J. W., Martin, R. L., Morokuma, K., Zakrzewski, V. G., Voth, G. A., Salvador, P., Dannenberg, J. J., Dapprich, S., Daniels, A. D., Farkas, O., Foresman, J. B., Ortiz, J. V., Cioslowski, J., Fox, D. J. *Gaussian-09, Revision A.02, Gaussian Inc., Wallingford CT, 2009*.
- Farahani, M. D., Honarparvar, B., Albericio, F., Maguire, G. E. M., Govender, T., Arvidsson, P., Kruger, H. G. Proline *N*-oxides: modulators of the 3D conformation of linear peptides through “NO-turns”. *Org. Biomol. Chem.*, **2014**, 12, 4479–4490.
- Farrugia, L. J. WinGX and ORTEP for Windows: an update. *J. Appl. Cryst.*, **2012**, 45, 849–854.
- Gil, A., Pabón, A., Galiano, S., Burguete, A., Silanes, S. P., Deharo, E., Monge, A., Aldana, I. Synthesis, biological evaluation and structure-activity relationships of new quinoxaline derivatives as anti-*Plasmodium falciparum* agents. *Molecules*, **2014**, 19, 2166–2180.
- Huang, H., Zhang, P., Chen, H., Ji, L., Chao, H. Comparison between polypyridyl and cyclometalated ruthenium(II) complexes: anticancer activities against 2D and 3D cancer models. *Chem. Eur. J.*, **2015**, 21, 715–725.
- Ingle, R. G., Marathe, R. P. Review on literature study of quinoxaline. *Pharmacophore*, **2012a**, 3(2), 109–116.
- Ingle, R. G., Marathe, R. P. Sulfonamido quinoxalines - search for anti-inflammatory agents. *Int. J. Pharm. Res. Allied Sci.*, **2012b**, 1(4), 46–51.
- Issa, D. A. E., Habib, N. S., Abdel Wahab, A. E. Design, synthesis and biological evaluation of novel 1,2,4-triazolo and 1,2,4-triazino[4,3-*a*]quinoxalines as potential anticancer and antimicrobial agents. *Med. Chem. Commun.*, **2015**, 6, 202–211.
- Kotra, V., Pradeep, K., Vasanthi, R., Synthesis, characterization and pharmacological evaluation of some novel quinoxaline derived chalcones. *Pharma Chem.*, **2013**, 5(4), 301–307.
- Kono, T., Murakami, T. N., Nishida, J., Yoshida, Y., Hara, K., Yamashita, Y. Synthesis and photo-electrochemical properties of novel thienopyrazine and quinoxaline derivatives, and their dye-sensitized solar cell performance. *Org. Electron*, **2012**, 13, 3097–3101.
- Keshtov, M. L., Kuklin, S. A., Chen, F. C., Khokhlov, A. R., Peregudov, A. S., Siddiqui, S. A., Sharma, G. D. Two new D–A conjugated polymers P(PTQD-T) and P(PTQD-2T) with same 9-(2-octyldodecyl)-8*H*-pyrrolo[3,4-*b*]bisthieno[2,3-*f*:3',2'-*h*]quinoxaline-8,10(9*H*)-dione acceptor and different donor units for BHJ polymer solar cells application. *Org. Electron*, **2015**.

- Lu, Y., Zheng, M., Wang, B., Fu, L., Zhao, W., Li, P., Xu, J., Zhu, H., Jin, H., Yin, D., Huang, H., Upton, A. M., Ma, Z. Clofazimine analogs with efficacy against experimental tuberculosis and reduced potential for accumulation. *Antimicrob. Agents Chemother.*, **2011**, 55(11), 5185-5193.
- Lee, C., Yang, W., Parr, R. G. Development of the Colic-Salvetti correlation-energy formula into a functional of the electron density. *Phys. Rev. B.*, **1988**, 37(2), 785-789.
- Manchal, R., Kasula, M., Muthadi, S., Kumari, K.V.N.G., Somu, S. Synthesis and testing of metal complexes of quinoxaline based schiff bases for antimicrobial and anticancer activities. *Int. J. Pharm. Sci. Res.*, **2015**, 6(2), 698-704.
- Naga Raju, G., Bhavya Sai, K., Myneni, R. T., Navya, N., Yaraswini, R. S., Nadendla, R. Synthesis, characterization and antimicrobial evaluation of novel 2,3-diphenyl quinoxaline-1,4-di-N-oxide derivatives. *World J. Pharm. Res.*, **2015**, 4(5), 2625-2633.
- Ninfa, M. R. G., Mayorga, V. H., Martínez, M. M., Villegas-Mendoza, J. M., Rivera, G. Toxic activity of N-oxide derivatives against three Mexican populations of *spodoptera frugiperda*. *Southwest Entomol.*, **2014**, 39(4), 717-726.
- Neckel, G. L., Bicca, M. A., Leal, P. C., Mascarello, A., Siqueira, J. M., Calixto, J. *In vitro* and *in vivo* anti-glioma activity of a chalcone-quinoxaline hybrid. *Eur. J. Med. Chem.*, **2015**, 90, 93-100.
- Nishio, T., Tabata, M., Koyama, H., Sakamoto, M. Photochemistry of N-(2-Acylphenyl)-2-methylprop-2-enamides: Competition between photocyclization and long-range hydrogen abstraction. *Helv. Chim. Acta*, **2005**, 88, 78-86.
- Patidar, A. K., Jeyakandan, M., Mobiya, A. K., Selvam, G. Exploring potential of quinoxaline moiety. *Int. J. PharmTech Res.*, **2011**, 3(1), 386-392.
- Puratchikody, A., Natarajan, R., Jayapal, M., Doble, M. Synthesis, *in vitro* antitubercular activity and 3D-QSAR of novel quinoxaline derivatives. *Chem. Biol. Drug Des.*, **2011**, 78, 988-998.
- Parrino, B., Carbone, A., Span, V., Montalbano, A., Giallombardo, D., Barraja, P., Attanzio, A., Tesoriere, L., Sissi, C., Palumbo, M., Cirrincione, G., Diana, P. Aza-isoindolo and isoindolo-azaquinoxaline derivatives with antiproliferative activity. *Eur. J. Med. Chem.*, **2015**, 94, 367-377.
- Podsiadly, R., Podemska, K., Szymczak, A. M. Novel visible photoinitiators systems for free-radical/cationic hybrid photopolymerization. *Dyes Pigm.*, **2011**, 91, 422-426.
- Raju, G. N., Sravani, Y., Naga Swathi Sri, K., Revathi, B., Ramarao, N. Quinoxaline derivatives: potent antimicrobial agents. *World J. Pharm. Pharm. Sci.*, **2015**, 4(5), 2019-2030.
- Ramli, Y., Moussaif, A., Karrouchi, K., Essassi, E. Pharmacological profile of quinoxalinone. *J. Chem.*, **2014**, 1-22.
- Reddy, V. M., O'Sullivan, J. F., Gangadharam, R. J. Antimycobacterial activities of riminophenazines. *J. Antimicrob. Chemother.*, **1999**, 43, 615-623.

- Spek, A. L. Single-crystal structure validation with the program PLATON. *J. Appl. Cryst.*, **2003**, 36, 7-13.
- Sharma, A., Suhas, R., Gowda, D. C. Ureas/thioureas of benzo[d]isothiazole analog conjugated glutamic acid: synthesis and biological evaluation. *Arch. Pharm. Chem. Life Sci.*, **2013**, 346, 359–366.
- Shantharam, C. S., Suyoga Vardhan, D. M., Suhas, R., Channe Gowda, D. Design and synthesis of amino acids-conjugated heterocycle derived ureas/thioureas as potent inhibitors of protein glycation. *Russ. J. Bioorg. Chem.*, **2014**, 40(4), 443-454.
- Sridevi, C., Balaji, K., Naidu, A. Synthesis and pharmacological evaluation of some phenylpyrazolo indoquinoxaline derivatives. *E-J. Chem.*, **2011**, 8(2), 924-930.
- Suhas, R., Chandrashekar, S., Channe Gowda, D. A new family of highly potent inhibitors of microbes: synthesis and conjugation of elastin based peptides to piperazine derivative. *Int. J. Pept. Res. Ther.*, **2012**, 18, 89-98.
- Suhas, R., Chandrashekar, S., Channe Gowda, D. Synthesis of elastin based peptides conjugated to benzisoxazole as a new class of potent antimicrobials - A novel approach to enhance biocompatibility. *Eur. J. Med. Chem.*, **2011**, 46, 704-711.
- Vázquez, R. Z., Ivanova, S., Moreno, M., Hernandez-Alvarez, M. I., Giralt, E., Chanal, A. B., Zorzano, A., Albericio, F., Puche, J. T. A new quinoxaline-containing peptide induces apoptosis in cancer cells by autophagy modulation. *Chem. Sci.*, **2015**, 6, 4537–4549.
- Vicente, E., Villar, R., Silanes, S. P., Aldana, I., Goldman, R. C., Monge, A. Quinoxaline 1,4-di-*N*-oxide and the potential for treating tuberculosis. *Infect. Disord. Drug Targets*, **2011**, 11, 196-204.
- Zhang, M., Dai, Z. C., Qian, S. S., Liu, J. Y., Xiao, Y., Lu, A. M., Zhu, H. L., Wang, J. X., Ye, Y. H. Design, synthesis, antifungal, and antioxidant activities of (*E*)-6-((2-phenylhydrazono)methyl)quinoxaline derivatives. *J. Agric. Food Chem.*, **2014**, 62, 9637–9643.

Chapter 5. Biological evaluation and docking study of synthesized amino acid tethered quinoxalines

* The compounds referred to in the chapter are referred to elsewhere in the thesis with an **A** preceding the number of the compound. For example **6a-n** is referred to as **A6a-n** elsewhere in the thesis.

Abstract

A total of 14 amino acid-tethered-quinoxalines (**A6a-A6n**) were evaluated for their antimicrobial, anti-oxidant and anti-diabetic activity. Preliminary structure-activity relationship studies showed that compounds with an alanine (**A6a**), threonine (**A6m**) and serine (**A6n**) residues possessed a broader spectrum of antimicrobial activity than the other quinoxalines tested. Compound **A6g** with a benzyl group appeared to have strain specific activity against *Escherichia coli* and *Pseudomonas aeruginosa* (MBC 0.08 mM and 0.17 mM), compared to the standard ciprofloxacin (0.002 mM). Compounds **A6a**, **A6d** and **A6f** showed the most potent anti-diabetic activity, with the **A6d** derivative (leucine residue) showing the most potent activity against both α -Glucosidase (IC₅₀ 0.01 mM) and α -amylase (IC₅₀ 1.41 mM) enzymes respectively compared to the standard acarbose (IC₅₀ 0.088 and 0.104 mM). Five of the molecules (**A6a**, **A6d**, **A6e**, **A6h** and **A6j**) showed antioxidant activity, with two of the molecules (**A6h** and **A6d**) showing good antioxidant activity (IC₅₀ 0.15 mM) compared to that of ascorbic acid (IC₅₀ 0.10 mM). Furthermore, *in silico* molecular docking simulations were conducted to support the anti-bacterial and anti-diabetic activity profiles of the synthesized compounds using the bacterial topoisomerase II (PDB code: 2XCT) and α -glucosidase proteins.

Keywords: Quinoxaline, amino acids, antimicrobial, antioxidant, anti-diabetic, docking

5.1 Introduction

Quinoxaline is a heterocyclic core structure used as a back-bone for the synthesis of bioactive compounds. It is formed by two aromatic rings, benzene and pyrazine. This core structure is rare in nature but is easy to synthesize chemically. By varying the functional groups and moieties on the quinoxaline scaffold, a wide variety of compounds were synthesized, many of which had good biological activity (Ajani et al., 2014; Ramli et al., 2014; Ameen et al., 2015; Padvi et al., 2015).

Various quinoxaline derivatives have shown antibacterial, antifungal, antiviral, anti-HIV, anti-tuberculosis, antimalarial, leishmanicidal, antitumor, antioxidant, anti-inflammatory, analgesic, antidepressant, antidiabetic, enzyme inhibitory, kinase inhibitory, receptor antagonist, multi-drug resistant antagonist, antithrombotic, antiamebic, anticonvulsant, antiepileptic and Gonadotropin releasing hormone antagonistic activities (Lawrence et al., 2001; Waring et al., 2002; Burguete et al., 2011; Noolvi et al., 2011; Kakodkar et al., 2011; Puratchikody et al., 2011; Habib et al., 2012; Kulkarni et al., 2012; Kotra et al., 2013; Soliman et al., 2013; Ajani et al., 2014; Ramli et al., 2014; Srinivas et al., 2014a, 2014b; Vieira et al., 2014; Ameen et al., 2015; Ismail et al., 2015; Wei et al., 2015; Padvi et al., 2015; Anand et al., 2015; Raju et al., 2015). Their wide range of bioactivity makes them a versatile scaffold for pharmaceuticals.

Amino acids are the building blocks of peptides and proteins as well as other naturally occurring substances such as alkaloids, antibiotics and heterocyclic peptides (Hughes et al., 2007; Nolan et al., 2009; Fester et al., 2010; Albers et al., 2013). Being a natural ligand, they are water soluble and less toxic than other synthetic ligands used in drug design. Simple α -amino acids were used to form conjugated piperazinyl benzoisothiazole complexes with anti-ulcer activity (Sharma et al.,

2013a, 2013b) and conjugated benzisoxazole derivatives with potent antimicrobial activity (Suhas et al., 2011), showing that these amino acids have the ability to form bioactive molecules when coupled with heterocyclic rings. Cinnamic acid analogues combined with amino acids showed promising anti-diabetic activity (Prakash et al., 2014).

The amino acids themselves, such as 4-hydroxyisoleucine and 3-guanidinopropionic acid and its semi-synthetic derivatives, polypeptides such as polypeptide-k and proteins such as ADMc1 from the seed extract of *Momordica charantia* has shown good anti-diabetic properties (Larsen et al., 2001; Ahmad et al., 2012; Patel et al., 2012; Chhabra and Dixit, 2013; Sridevi et al., 2014; Shukla and Rangari, 2015). Peptides have also been used in the design of antimicrobials (Friedrich et al., 2000; Laverty et al., 2011; Mojsoska et al., 2015; Kalita et al., 2015). The beta-defensin-3 peptide has shown a broad spectrum of antimicrobial activity (Dhople et al., 2006). Amino acids are also found in thiostrepton-derived thiopeptide antibiotics (Baringo et al., 2014; Wang et al., 2015). Copper and cobalt amino acid complexes have shown the ability to be developed into antibiotics (Stanila et al., 2011) and amino acids conjugated to thiazole and oxazole moieties showed good to moderate antimicrobial activity (Stanchev et al., 1999; Prakasha et al., 2011). A report on the synthesis of quinoxalines with β -amino acid derivatives has shown good antibacterial and antifungal activity (Mickeviciene et al., 2015).

Due to the vast range of bioactivity of quinoxalines reported we have synthesized quinoxaline amino acid conjugates (**A6a-A6n**) with the aim of testing them for antimicrobial and antidiabetic activities (Thesis chapter 4). We herein report the antimicrobial, antidiabetic and antioxidant activities of some amino acid-tethered-quinoxalines.

5.2 Experimental

5.2.1 Test compounds

The amino acid-tethered-quinoxalines (**A6a-A6n**) were previously synthesized in our laboratory (Thesis chapter 4). These molecules contain a 1,2,3,4-tetrahydroquinoxaline heterocyclic skeleton with an ester group at position 6 and various amino acids at position 2. These amino acids contain aliphatic and aromatic groups and are either polar or non-polar in nature (**Table 5-1**).

5.2.2 *In vitro* antimicrobial studies

The microbial cultures were grown overnight at 37 °C in nutrient broth (UKZN Biolab, South Africa), adjusted to 0.5 McFarland standard using distilled water and lawn inoculated onto Mueller-Hinton agar (MHA) plates. A volume of 10 µL of each sample (29.84 – 45.44 mM, 1 mL DMSO) was inoculated onto antibiotic assay discs (6 mm diameter) and placed on the MHA plates which were incubated overnight at 37°C for 24 hours. After the incubation period, zones of inhibition were measured in mm. Compounds showing an inhibition zone of > 9 mm were selected to determine their MBC values using the broth dilution assay with ampicillin and ciprofloxacin as the controls following the method in Andrews (2001). Compounds **A6a-b**, **A6d-h**, **A6j**, and **A6m-n** were selected to determine their MBC values by the broth dilution method.

In the MBC method, the microbial cultures were prepared as described previously for the disc diffusion method and adjusted to a 0.5 McFarland standard. The test compounds were dissolved in DMSO (10 mg/mL) and subject to a 50% serial dilution in 1 mL eppendorf tubes with Mueller-Hinton Broth (MHB), inoculated with bacterial cultures (20 µL) and then incubated at 37°C for 18 h. The total volume in each eppendorf was 200 µL. A volume of 10 µL of each dilution was spotted on MHA plates and incubated at 37°C for 18 h to determine the MBC (in mM). Ampicillin,

ciprofloxacin and tioconazole served as the standard drugs for the antibacterial and antifungal studies respectively. All experiments were performed in duplicate.

5.2.3 *In vitro* antioxidant studies

DPPH radical scavenging activity

The total free radical scavenging activity of the synthesized amino acid-tethered quinoxaline compounds (**A6a-A6n**) was determined and compared to that of ascorbic acid using a slightly modified method described by Tuba and Gulcin et al., 2008. A 0.3 mM solution of DPPH was prepared in methanol and 500 μL of this solution added to 50 μL of the compounds (dissolved in DMSO) at different concentrations (50-200 $\mu\text{g mL}^{-1}$). These solutions were mixed and incubated in the dark for 30 min at room temperature. Absorbance was then measured at 517 nm against a blank sample lacking scavenger.

5.2.4 Anti-diabetic activity

In vitro α -Glucosidase inhibitory activity

The α -Glucosidase inhibitory activity of the synthesized amino acid-tethered quinoxaline compounds (**A6a-n**) was determined according to the method described by Ademiluyi *et al.* (2013), with slight modifications. Briefly, 50 μL of each compound or acarbose dissolved in DMSO at different concentrations (50-200 $\mu\text{g mL}^{-1}$), was incubated with 100 μL of 1.0 U mL^{-1} α -glucosidase solution in 100 mM phosphate buffer (pH 6.8) at 37 °C for 15 min. Thereafter, 50 μL of pNPG solution (5 mM) in 100 mmol L^{-1} phosphate buffer (pH 6.8) was added and the mixture was further incubated at 37 °C for 20 min. The absorbance of the released *p*-nitrophenol was measured at 405 nm and the inhibitory activity expressed as a percentage of the control sample without inhibitors.

In vitro α -Amylase inhibitory activity

The α -Amylase inhibitory activity of the compounds **A6a-n**, was determined according to the method described by Shai *et al.* 2010, with slight modifications. A volume of 50 μ L of each compound dissolved in DMSO or acarbose at different concentrations (50-200 μ g mL⁻¹) was incubated with 100 μ L of porcine pancreatic amylase (2 U mL⁻¹) in 100 mM phosphate buffer (pH 6.8) at 37 °C for 20 min. 50 μ L of 1% starch dissolved in 100 mM phosphate buffer (pH 6.8) was then added to the reaction mixture and incubated at 37 °C for 1 h. 100 μ L of 3,5-dinitrosalicylic acid (DNS) colour reagent was then added and boiled for 10 min. The absorbance of the resulting mixture was measured at 540 nm and the inhibitory activity was expressed as percentage of a control sample without inhibitors. All assays were carried out in triplicate.

5.2.5 Docking methodology

Initial structures of the representative compounds (RCs) (**A6d**, **A6f**, **A6g** and **A6n**) in protein data bank (pdb) format were drawn in the Discovery Studio software (DS). Different isomers of the compounds were generated at the physiological pH (7.0) using the “Prepare Ligands” algorithm, and further geometrically minimized using the “minimize ligands” module. The CHARMM force field was considered to develop the partial atomic charges of each atom. The X-ray structure of topoisomerase II DNA-gyrase (pdb id: 2xct, resolution 3.5Å) was downloaded from the protein data bank (PDB) database (www.rcsb.org). The bound ligands and water molecules were removed from the protein while the manganese ion (Mn⁺²) present in the active site was retained (Bax et al., 2010). The “Prepare Protein” module in DS was used to add missing atoms/loops and protonates amino acid residues according the physiological conditions. Since, the X-ray structure of α -glucosidase is not known, homology modelling method was used to generate it's 3D structure

using the crystal structure of *S. cerevisiae* from isomaltase (pdb id: 3AJ7) as a template, using MODELER algorithm (Eswar et al., 2006) in Discovery Studio (DS). Prior to docking, a binding sphere covering the active site residues of proteins was developed. CDOCKER (Wu et al., 2003), a grid-based program, was used to dock RCs in the active site of the protein where a conformational profile of the ligands was explored by the molecular dynamics sampling method. The most favourable pose of each RC was chosen based on the CDOCKER energy (CDE), where the most negative CDE indicates the strongest interaction with the receptor.

5.3 Results and Discussion

5.3.1 Chemical structures

The chemical structures of the compounds used in the structure activity relationship (SAR), have a 1,2,3,4-tetrahydroquinoxaline base core moiety which is formed by the fusion of the phenyl group and amino acids (**Figure 5-1**). Compounds **A6a-n** contain precursors of different amino acids, two secondary amine groups and a methyl ester at position 6. These functional groups are believed to play an important role in antimicrobial and antioxidant activities (Ghorab et al., 2004; Shivakumara et al., 2009; Kumar et al., 2011; Abedini et al., 2013; Goszczyn'ska et al., 2015). Compounds **A6b**, **A6g**, **A6h** and **A6i** contain aromatic R groups and **A6a**, **A6c-f** and **A6j-6n**, either polar or non-polar aliphatic side chain R groups. The R groups in **A6a-n** are tabulated in **Table 5-1**.

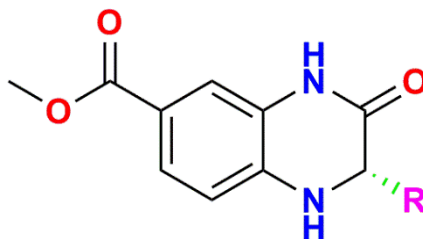


Figure 5-1 The core structure of amino acid tethered quinoxalines

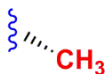
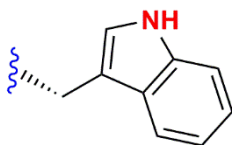
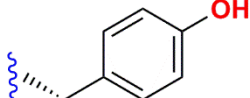
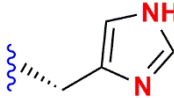
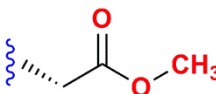
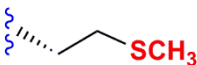
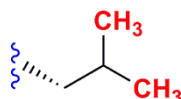

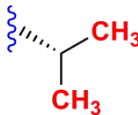
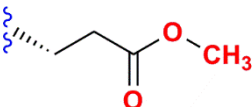
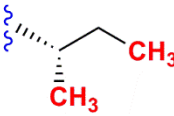
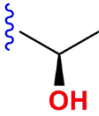
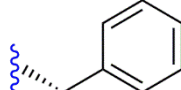
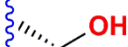
5.3.2 Antimicrobial activity

The compounds were evaluated for their *in vitro* antimicrobial activity against two Gram +ve strains *S. aureus* (ATCC 25923) and methicillin resistant *S. aureus* (MRSA) (ATCC BAA-1683) and three Gram -ve strains *E. coli* (ATCC 25922), *K. pneumonia* (ATCC 31488) and *P. aeruginosa* (ATCC 27853) as well as one fungal strain, *C. albicans* (ATCC 10231). The disc diffusion assay was used to screen all the synthesized compounds and to select compounds to determine their MBC values. Compounds with a zone of inhibition between 8-35 mm were selected (**Table 5-2**).

Compounds **A6a**, **A6m** and **A6n** with alanine, threonine and serine side chains showed a broad spectrum of antimicrobial activity with MBCs of between 0.31 to 1.42 mM for both *Staphylococcus* species and MBCs of 0.25 to 5.68 mM against the Gram -ve strains and 0.63 to 2.84 for *C. albicans*. The activity of **A6m** and **A6n** could possibly be due to the hydroxy groups in the side chain. The fact that **A6a** is more active than **A6d-f** may be due to the branched chains hindering interaction between the molecule and the active sites of the enzymes in the bacteria.

Compound **A6b** with a tyrosine side chain showed strain specific activity to *S. aureus*, *MRSA* and *E. coli* with IC₅₀ values of 0.38, 1.00 and 0.38 mM, better than the standard ampicillin. The other compounds with aromatic side chains, **A6g** (phenylalanine side chain) and **A6h** (tryptophan residue) also showed strain specific activity, **A6g** being active against *E. coli* and *P. aeruginosa* with IC₅₀ values of 0.08 and 0.17 mM respectively and **A6h** being active in all strains except *MRSA* with the best activity being against *K. pneumoniae* (0.18 mM) and *E. coli* (0.35 mM).

Table 5-1 Side chains of compounds **A6a-n**

Compound	R	Compound	R
A6a		A6h	
A6b		A6i	
A6c		A6j	
A6d		A6k**	
A6e		A6l	
A6f		A6m	
A6g		A6n	

**Proline and quinoxaline conjugated together

Table 5-2 Minimum Bactericidal Concentration (MBC in mM) of compounds **A6a-n**

No.	Gram +ve		Gram -ve			Fungi
	<i>S. aureus</i>	<i>MRSA</i>	<i>E. coli</i>	<i>P. aeruginosa</i>	<i>K. pneumoniae</i>	<i>C. albicans</i>
A6a	1.42	0.71	5.68	5.68	4.26	2.84
A6b	0.38	1.00	0.38	-	4.01	1.00
A6c	-	-	-	-	-	-
A6d	2.89	2.89	0.27	0.72	-	5.78
A6e	-	1.89	2.52	0.24	5.04	-
A6f	0.60	-	0.34	-	0.15	0.15
A6g	-	-	0.08	0.17	-	-
A6h	0.70	-	0.35	1.87	0.18	1.87
A6i	-	-	-	-	-	-
A6j	-	-	0.21	1.12	0.42	-
A6k	-	-	-	-	-	-
A6l	-	-	-	-	-	-
A6m	0.47	0.31	1.25	0.39	0.31	0.63
A6n	0.41	0.37	0.66	0.25	0.25	0.99
ampicilin	0.06	1.79	0.89	3.58	0.89	0.89
ciprofloxacin	0.002	0.007	0.002	0.002	0.004	0.002
tioconazole	-	-	-	-	-	25.79
DMSO	-	-	-	-	-	-

Highlighted values indicate the best results

Amongst the compounds with branched alkyl side chains (**A6d-f**), **A6d** with a leucine side chain showed good activity with IC₅₀ values of 0.27 and 0.72 mM against *E. coli* and *P. aeruginosa*, **A6e** was active against *P. aeruginosa* at 0.24 mM and **A6f** was active against four of the test strains, including the fungal strain, with IC₅₀ values of 0.60 and 0.34 mM against *S. aureus* and *E. coli* and 0.15 mM each against both *Klebsiella pneumonia* and *C. albicans*. Compound **A6j** a methionine side chain was active against *E. coli*, *P. aeruginosa* and *K. pneumonia* with IC₅₀ values of 0.21,

1.12 and 0.42 mM respectively. The compounds with the best antifungal activity against *C. albicans* was **A6f** and **A6m** with IC₅₀ values of 0.15 and 0.63 mM respectively.

Compounds **A6c**, **A6i**, **A6k** and **A6l** with an esterified aspartic acid side chain, a histidine side chain, proline side chain and esterified glutamic acid side chain all showed no activity against all of the test strains.

5.3.3 Antioxidant Activity

Antioxidant properties of the synthesized compounds were tested by the DPPH radical scavenging activity, which determines the effectiveness of the compounds in scavenging free radicals. These results are presented in **Table 5-3**. The antioxidant activity was dependent on the side chain attached at C-2. Compounds **A6a**, **A6d-e**, **A6h** and **A6j** showed good scavenging activity, with IC₅₀ values of 0.20 mM or less in comparison to ascorbic acid (IC₅₀ of 0.10 mM). Compounds **A6d** and **A6h** showed the best activity with IC₅₀ values of 0.15 mM each. Of the active compounds, three of these, **A6a**, **A6d** and **A6e** contained aliphatic side chains with one or more methyl groups. The aliphatic side chain of **A6j** also contained an aliphatic side chain, but with a thiomethyl group. The other active residue (in **A6h**) contained an indole moiety.

Table 5-3 Antioxidant activity of the synthesized compounds **A6a-n** (mM)

Sample No.	DPPH (IC ₅₀ (mM))	Sample No.	DPPH (IC ₅₀ (mM))
A6a	0.20±0.02^{bc}	A6h	0.15±0.01^{bc}
A6b	0.32±0.02 ^{ef}	A6i	0.40±0.01 ^{fg}
A6c	0.30±0.02 ^{de}	A6j	0.18±0.01^{bc}
A6d	0.15±0.01^b	A6k	0.50±0.01 ^g
A6e	0.19±0.02^{bc}	A6l	0.30±0.02 ^e
A6f	0.25±0.03 ^{cd}	A6m	0.24±0.07 ^{bc}
A6g	0.38±0.04 ^{fg}	A6n	0.36±0.01 ^e
Ascorbic acid		0.10±0.02 ^a	

Data are presented as mean ± SD values of triplicate determinations.

^{a-d} Different letters stand for significantly different values from each other within a column (Tukey's-HSD multiple range *post hoc* test, $p < 0.05$); the same letters stand for non-significant difference. Highlighted values indicate the best results.

5.3.4 Anti-diabetic activity

In order to investigate the *in vitro* anti-diabetic activity of the synthesized amino acid tethered quinoxalines, two enzymes, α -glucosidase and α -amylase were used. The results are summarized in **Table 5-4**. In comparison to acarbose (IC₅₀ of 0.88 mM), **A6a**, **A6d** and **A6f** showed better α -glucosidase inhibitory activity with IC₅₀ values of 0.056, 0.012 and 0.042 mM respectively. These compounds contained amino acid residues with aliphatic side chains with at least one or two methyl groups. The test compounds were however not as active against the α -amylase enzyme with IC₅₀ values of 14 fold or greater than the standard acarbose.

Table 5-4 *In vitro* α -Glucosidase and α -amylase activity of **A6a-n** (IC₅₀ in mM)

No	α -Glucosidase	α -amylase	No	α -Glucosidase	α -amylase
A6a	0.056±0.002^{ab}	3.564±0.192 ^a	A6h	0.114±0.030 ^{abc}	5.714±2.795 ^a
A6b	0.332±0.019 ^{de}	8.558±0.598 ^a	A6i	0.415±0.004 ^c	8.959±2.70 ^a
A6c	0.231±0.024 ^c	33.054±0.101 ^{ab}	A6j	0.159±0.076 ^{bc}	5.165±0.216 ^a
A6d	0.012±0.0^a	1.414±0.241 ^a	A6k	0.482±0.021 ^e	8.026±0.126 ^a
A6e	0.168±0.016 ^{bc}	11.417±0.407 ^a	A6l	0.203±0.043 ^c	102.295±0.81 ^b
A6f	0.042±0.021^{ab}	8.729±2.252 ^a	A6m	0.190±0.056 ^c	2.206±0.038 ^a
A6g	0.353±0.031 ^{de}	2.839±0.824 ^a	A6n	0.297±0.008 ^{cd}	4.644±0.599 ^a
Ac*	0.088±0.005 ^c	0.104 ±0.028 ^a	Ac*	0.088±0.005 ^c	0.104 ±0.028 ^a

Data are presented as mean \pm SD values of triplicate determinations.

^{a-d} Different letters stand for significantly different values from each other within a column (Tukey's-HSD multiple range *post hoc* test, $p < 0.05$); the same letters stand for non-significant difference.

Ac* = acarbose standard. Highlighted values indicate the best results.

5.3.5 Molecular docking

The inhibition of bacterial type II topoisomerases (topoisomerase IV and DNA-gyrase) is one of the mechanisms associated with anti-bacterial action of several drugs including ciprofloxacin, enoxacin, and lomefloxacin (Mitscher et al., 2005). In order to examine the binding modes of the synthesized molecules with topoisomerase and DNA-gyrase, compounds **A6g** and **A6n** (chosen as representative compounds (RCs)), were flexibly docked into the binding cavity of bacterial topoisomerase II DNA-gyrase (PDB id: 2XCT) using the CDOCKER module in discovery studio (DS) (Wu et al., 2003). The docking efficiency of the docking protocol was first assessed by re-docking ciprofloxacin (co-crystallized ligand) into the active site of the bacterial protein. Overlay of the sampled conformation of ciprofloxacin and its X-ray structure (**Figure 5-2**) showed the root mean square deviation (RMSD, all atoms) to be $<1\text{\AA}$. This demonstrated the accuracy and good predictive efficiency of the docking protocol.

The scoring function, -CDOCKER energy (CDE) that includes the receptor interaction energy and internal ligand strain energy was computed to assess the binding affinity of ligands with the receptor. A more negative CDE indicates stronger interaction for the receptor. The CDE of **A6g** was found to be $-20.1 \text{ kcal mol}^{-1}$ and **A6n** $-18.5 \text{ kcal mol}^{-1}$, which was not as strong as the standard ciprofloxacin which had a CDE of $-28.6 \text{ kcal mol}^{-1}$. **Figure 5-3** and **Figure 5-4** contain the complexes of **A6g**, **A6n** and ciprofloxacin with the bacterial protein, which were visualized (using DS) to get a deeper understanding of their binding modes and interacting forces.

Generally, hydrogen bonding was found to be essential in locking the conformation of the compounds in the binding site of the protein. Compound **A6g**, for instance, formed two concurrent hydrogen bonds (conventional) with Asp437 (proton acceptor) through its piperazinyl nitrogen (proton donor) and another single hydrogen bond with the same amino acid (proton donor) through its ester carbonyl (proton acceptor) moiety in addition to three non-conventional hydrogen bonds with Glu435 and Gly436 (**Figure 5-3**). Compound **A6n** also displayed prominent hydrogen bonding (**Figure 5-4**) with Ser1084, Arg458, Glu477 and Lys460 amino acids. Typically, the conformation of **A6g** was more folded in comparison to **A6n**, and supported its greater interaction with the binding cavity of the bacterial protein, as evidenced by its lower CDE ($-20.1 \text{ kcal mol}^{-1}$). Both compounds, however, missed interaction with Mg^{2+} . Ciprofloxacin (**Figure 5-4**), on the other hand, exhibited two co-ordinate bonds (2.6 and 2.8 \AA) with the Mg^{2+} by its two oxygen atoms, in addition to its engagement with Glu477, Lys460 and Arg458 amino acid residues of the protein through hydrogen bonding. Enhanced antibacterial activity of ciprofloxacin, compared to **A6g** and **A6n**, could be attributed to this additional interaction with the Mg^{2+} metal which led to its tighter binding with the bacterial protein.

Since, the synthesized compounds exhibited good potency against α -glucosidase, it was thought worthwhile to support their activity profiles by illuminating their binding characteristics into the active site of the protein. However, the 3D structure for α -glucosidase obtained from *S. cerevisiae* used in our study was not available in the protein database. Literature survey, nonetheless, indicated the utilization of its homology models in several publications (Khan et al., 2014; Lee et al., 2014; Huang et al., 2015). Since, these modelled structures are not available publicly, we built the 3D structure of α -glucosidase by homology modelling method using the Discovery Studio program.

The amino acid sequence for *S. cerevisiae* α -glucosidase (access code P53341) was downloaded from UniProt protein data bank (<http://www.uniprot.org/>). Different protein templates were subsequently identified using BLAST, a program which searches against a query sequence database constructed from proteins deposited in PDB repository. The crystal structure of *S. cerevisiae* from isomaltase (pdb id: 3AJ7) was found to be the best match based on its high sequence identity (71.4%) and sequence similarity (86.9%) with the query sequence, and selected as a template for homology modelling. 3D structure was generated using MODELER algorithm (Eswar et al., 2006) in DS considering default parameters, and verified using Verify Protein (Profiles-3D) module. Finally, the generated model was energetically minimized up to 0.1 RMS gradient in DS.

Two most active compounds, **A6d** ($IC_{50} = 0.012 \pm 0.0$ mM) and **A6f** (0.042 ± 0.021 mM) (**Table 5-4**) were subsequently docked into the active site of modelled structure of the α -glucosidase. The computed scoring function (CDE) suggested the favorable binding of both compounds for the

protein with the most active compound (**A6d**) showing comparatively the stronger interaction (CDE = -38.0 kcal mol⁻¹) in comparison to **A6f** (BE = -29.1 kcal mol⁻¹). Compound **A6d** established a conventional hydrogen bond (2.74Å) with His 280 through its NH (piperazine moiety), and three non-conventional hydrogen bonds with Glu 277 and His 240 residues of α -glucosidase (**Figure 5-5**). Additionally, hydrophobic (alkyl and π -alkyl types) interactions between **A6d** and the active site residues (Phe 178, His 240 and Arg 315) of protein were also observed. Compound **A6f**, on the other hand, displayed predominantly hydrophobic interactions with the active site residues e.g., Arg 442, Arg315, Phe 158 and Phe 303, in addition to a non-conventional hydrogen bond with Asp 411 residues (**Figure 5-5**). The presence of strong hydrogen bonding network in **A6d** probably accounts for its stronger binding affinity (lower CDE) for the protein and supports its higher anti-diabetic action observed under experimental conditions.

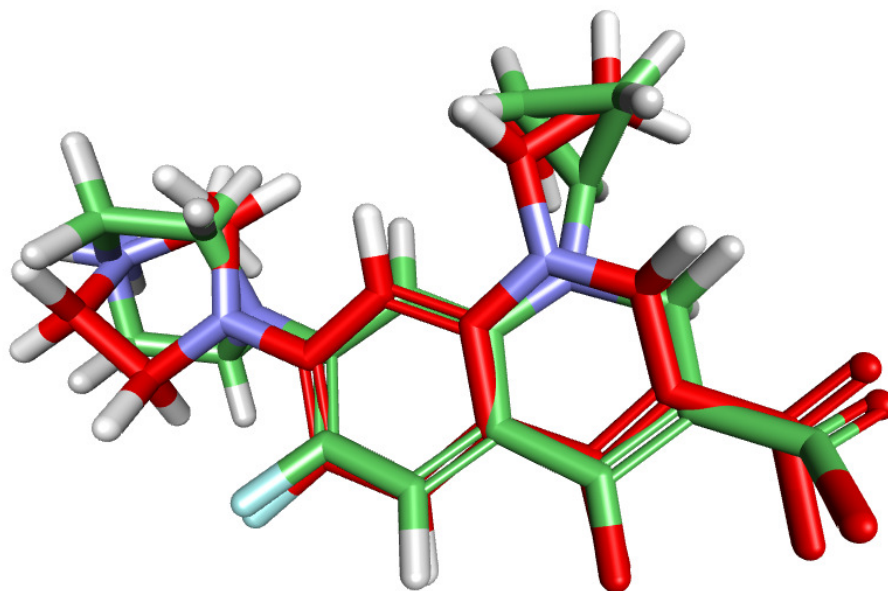


Figure 5-2 Superimposition of the conformation (from docking) of ciprofloxacin (in red sticks) on its original X-ray structure (in green sticks)

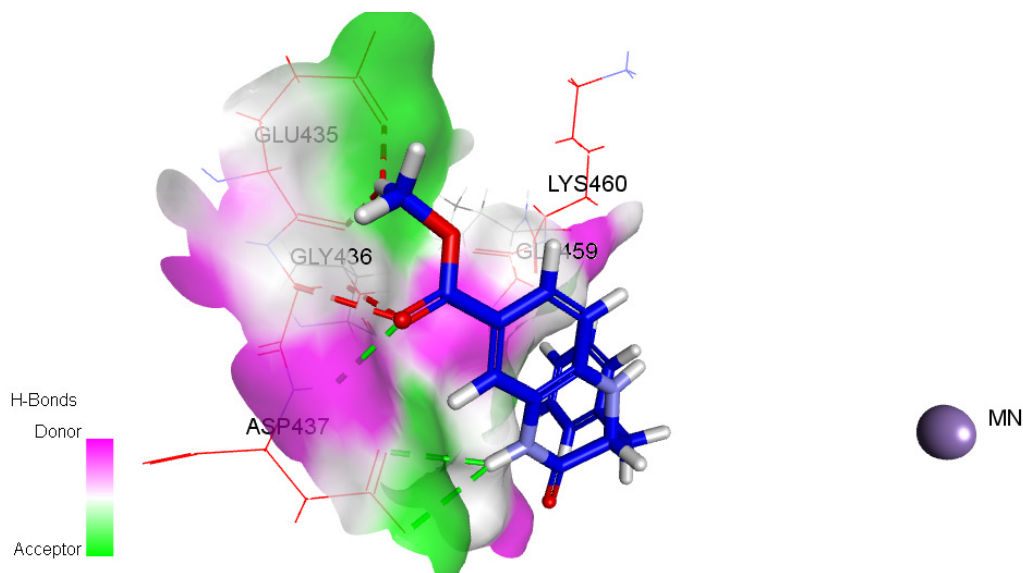


Figure 5-3 Docked conformation (in blue sticks) of **A6g** in the binding cavity of the bacterial protein (shown as red lines). Green dotted lines represent conventional H-bonds whereas red dotted lines depict non-conventional H-bonds

5.4 Conclusion

Compounds **A6a**, **A6m** and **A6n** showed broad spectrum antibacterial activity with several other compounds also showing very good strain specific activity to at least one of the bacterial strains tested against. Five of the synthesized compounds **A6a**, **A6d-e**, **A6h** and **A6j** demonstrated antioxidant activity with IC_{50} values of 0.20 mM or less (good in comparison to ascorbic acid with an IC_{50} of 0.10 mM). Compounds **A6a**, **A6d** and **A6f** showed better α -glucosidase inhibitory activity (IC_{50} values of 0.056, 0.012 and 0.042 mM respectively) in comparison to acarbose (IC_{50} of 0.88 mM). Docking simulations of **A6g** and **A6n** with the bacterial topoisomerase II enzyme indicated the significance of Mg^{2+} interaction in the stability of complexes. The inability to interact with Mg^{2+} decreased the stability of the RCs, **A6g** ($BE = -20.1 \text{ kcal mol}^{-1}$) and **A6n** ($BE = -18.5 \text{ kcal mol}^{-1}$) relative the standard ciprofloxacin ($BE = -28.6 \text{ kcal mol}^{-1}$), and probably accounts for their lower anti-bacterial activity. The docking of two most active anti-diabetic compounds (**A6d**,

A6f) in the binding site of modelled *S. cerevisiae* α -glucosidase revealed the predominance of hydrophobic and hydrogen bonding interactions in their host-guest relationship. Of all the synthesized compounds, **A6a** was active in all three assays (antibacterial, anti-oxidant and anti-diabetic) and may be a good pharmaceutical lead compound.

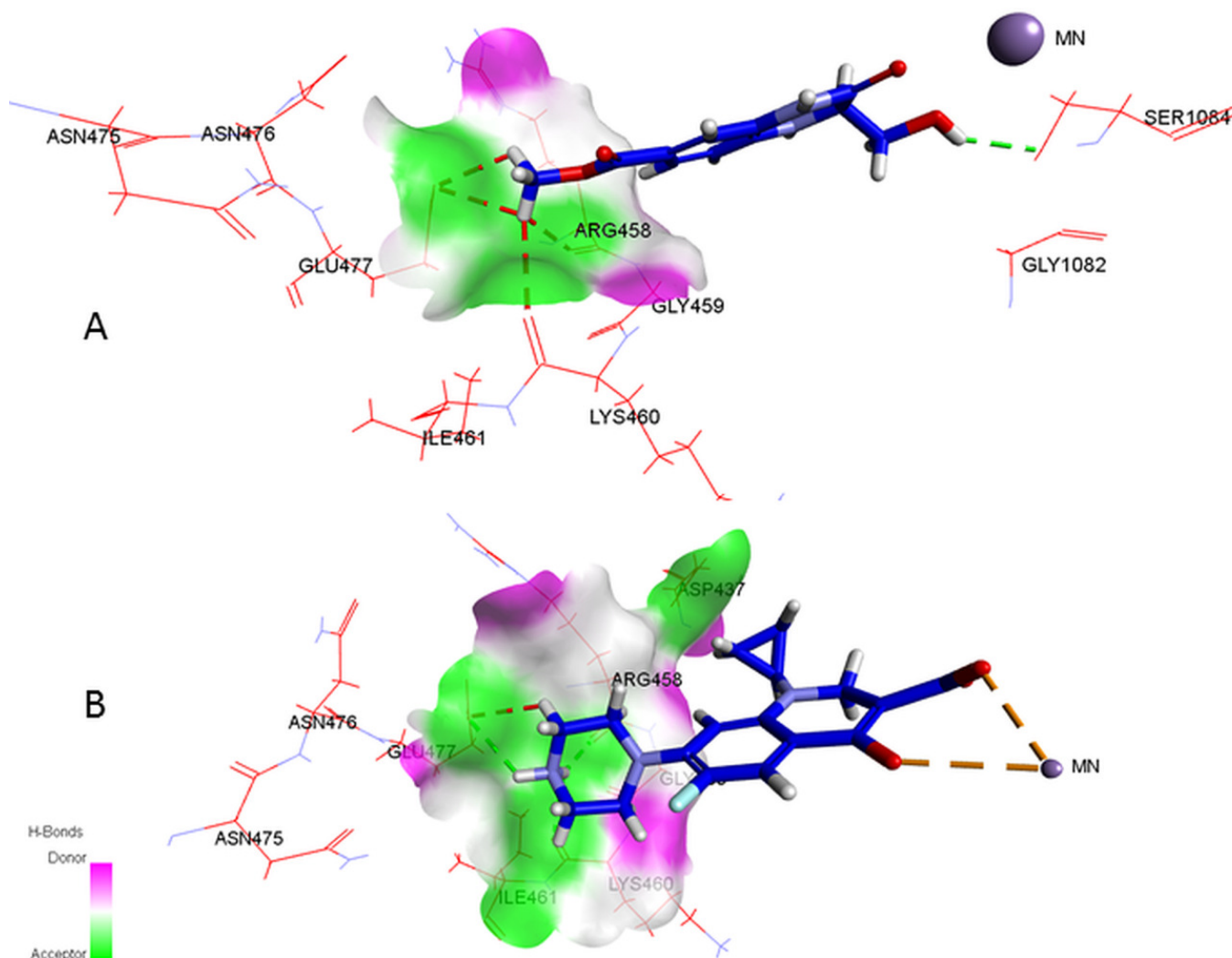


Figure 5-4 Docked conformation (in blue sticks) of **A6n** (A) and ciprofloxacin (B) in the binding cavity of the bacterial protein (shown as red lines). A green dotted line represents conventional H-bonds, red dotted lines non-conventional H-bonds and golden dotted lines represent the co-ordinate bonds

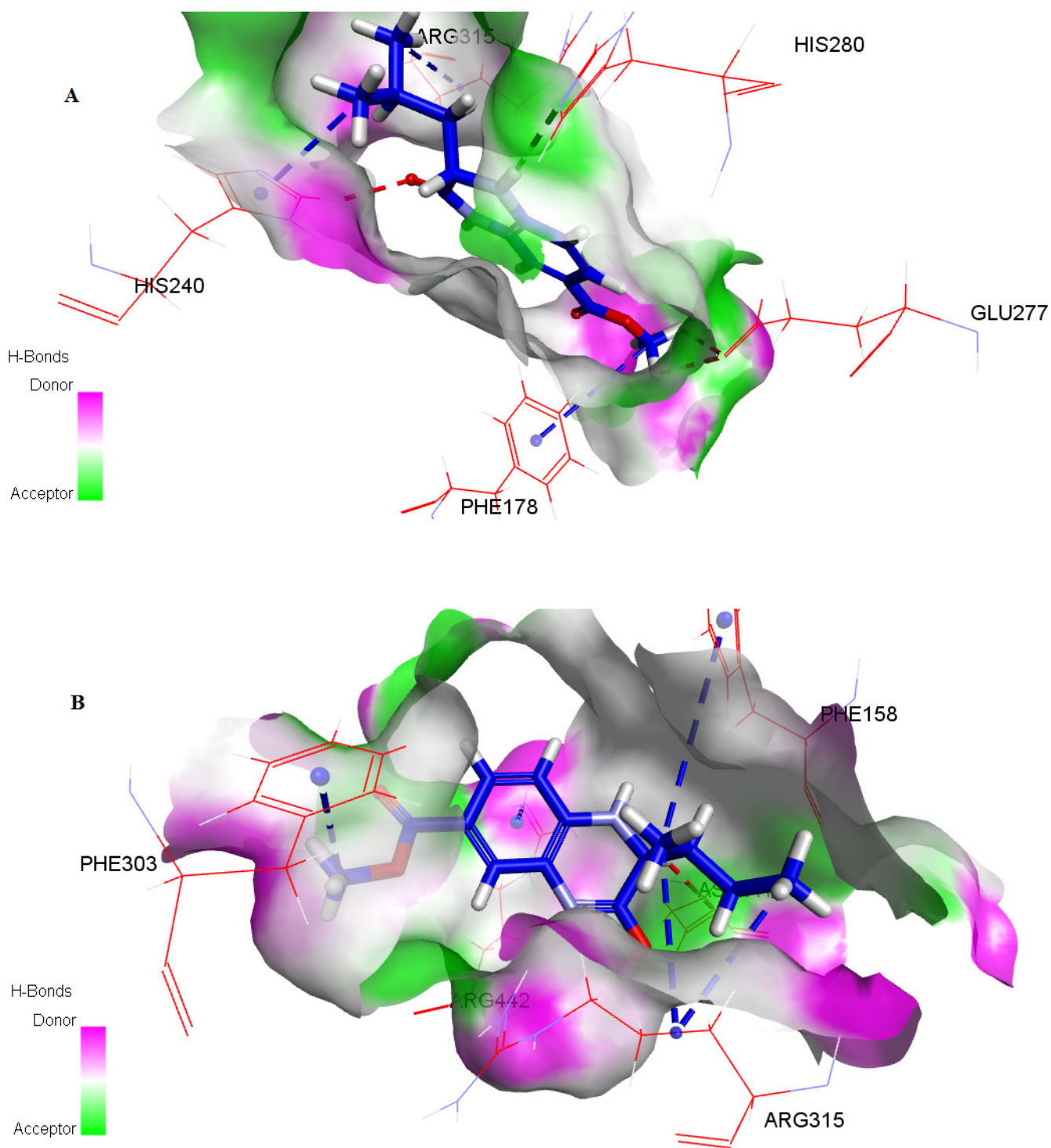


Figure 5-5 Docked conformation (in blue sticks) of **A6d** (A) and **A6f** (B) in the binding cavity of the α -glucosidase (red lines). Conventional H-bonds are shown as green dotted lines, non-conventional H-bonds (red dotted lines) and hydrophobic forces (blue dotted lines)

Acknowledgements

The authors gratefully acknowledge the Centre for High Performance Computing (CHPC), an initiative supported by the Department of Science and Technology of South Africa for Discovery Studio facility. This research was supported by grants from the National Research Foundation (NRF), South Africa and was supported by the South African Research Chairs Initiative of the Department of Science and Technology.

5.5 References

- Abedini, A., Roumy, V., Mahieux, S., Biabiany, M., Standaert-Vitse, A., Rivière, C., Sahpaz, S., Bailleul, F., Neut, C., Hennebelle, T. Rosmarinic acid and its methyl ester as antimicrobial components of the hydromethanolic extract of *hyptis atrorubens* poit. (Lamiaceae). *Evid. Based Complement. Alternat. Med.*, **2013**, 1-11.
- Ademiluyi, A. O., Oboh, G. Soybean phenolic-rich extracts inhibit key-enzymes linked to type 2 diabetes (α -amylase and α -glucosidase) and hypertension (angiotensin I converting enzyme) *in vitro*. *Exp. Toxicol. Pathol.*, **2013**, 65, 305- 309.
- Ahmad, Z., Zamhuri, K. F., Yaacob, A., Siong, C. H., Selvarajah, M., Ismail, A., Hakim, M. N. *In vitro* anti-diabetic activities and chemical analysis of polypeptide-k and oil isolated from seeds of *momordica charantia* (Bitter Gourd). *Molecules*, **2012**, 17, 9631-9640.
- Andrews, J. M. Determination of minimum inhibitory concentrations. *J. Antimicrob. Chemother.*, **2001**, 48(S1), 5-16.
- Ajani, O. O. Present status of quinoxaline motifs: Excellent pathfinders in therapeutic medicine. *Eur. J. Med. Chem.*, **2014**, 85, 688-715.
- Albers, M. F., Hedberg, C. Amino acid building blocks for fmoc solid-phase synthesis of peptides phosphocholinated at serine, threonine, and tyrosine. *J. Org. Chem.*, **2013**, 78, 2715-2719.
- Ameen, A., Hashe, A. Synthesis, reactions and biological activity of quinoxaline derivatives. *Am. J. Org. Chem.*, **2015**, 5(1), 14-56.
- Anand, N., Upadhyaya, K., Tripathi, R. Drug development pipeline for the treatment of tuberculosis: Needs, challenges, success and opportunities for the future. *Chem. Biol. Interface*, **2015**, 5(2), 84-127.
- Baringo, X. J., Albericio, F., Alvarez, M. Thiopeptide antibiotics: retrospective and recent advances. *Mar. Drugs.*, **2014**, 12, 317-351.

- Bax, B. D., Chan, P. F., Eggleston, D. S., Fosberry, A., Gentry, D. R., Gorrec, F., Giordano, I., Hann, M. M., Hennessy, A., Hibbs, M., Huang, J., Jones, E., Jones, J., Brown, K. K., Lewis, C. J., May, E. W., Saunders, M. R., Singh, O., Spitzfaden, C. E., Shen, C., Shillings, A., Theobald, A. J., Wohlkonig, A., Pearson, N. D., Gwynn, M. N. Type IIA topoisomerase inhibition by a new class of antibacterial agents. *Nature*, **2010**, 466, 935-943.
- Burguete, A., Pontiki, E., Litina, D. H., Ancizu, S., Villar, R., Solano, B., Moreno, E., Torres, E., Pe´rez, S., Aldana, I., Monge, A. Synthesis and biological evaluation of new quinoxaline derivatives as antioxidant and anti-inflammatory agents. *Chem. Biol. Drug Des.*, **2011**, 77, 255-267.
- Chhabra, G., Dixit, A. Structure modeling and antidiabetic activity of a seed protein of *Momordica charantia* in non-obese diabetic (NOD) mice. *Bioinformation*, **2013**, 9(15), 766-770.
- Dhople, V., Krukemeyer, A., Ramamoorthy, A. The human beta-defensin-3, an antibacterial peptide with multiple biological functions. *Biochim. Biophys. Acta*, **2006**, 1758, 1499-1512.
- Eswar, N., Webb, B., Marti-Renom, M. A., Madhusudhan, M.S., Eramian, D., Shen, M. Y., Pieper, U., Sali, A. “Comparative protein structure modelling using modeller”, *Curr. Protoc. Bioinformatics*, **2006**, Chapter 5, Unit 5-6.
- Fester, K. Plant alkaloids. **2010**. DOI:10.1002/9780470015902.a0001914.pub2.
- Friedrich, C. L., Moyles, D., Beveridge, T. J., Hancock, R. W. Antibacterial action of structurally diverse cationic peptides on Gram-positive bacteria. *Antimicrob. Agents Chemother.*, **2000**, 44(8), 2086-2092.
- Ghorab, M. M., Ismail, Z. H., Abdel-Gawad, S. M., Aziem, A. A. Antimicrobial activity of amino acid, imidazole, and sulfonamide derivatives of pyrazolo[3,4-*d*]pyrimidine. *Heteroat. Chem.*, **2004**, 15, 57-62.
- Goszczynska, A., Kwiecien, H., Fijałkowski, K. Synthesis and antibacterial activity of schiff bases and amines derived from alkyl 2-(2-formyl-4-nitrophenoxy)alkanoates. *Med. Chem. Res.*, **2015**, 24, 3561-3577.
- Habib, S. A., Ibrahim, I. T., Abd-Eldaye, M. A., El-Sheshtawey, M. M., Waly, H. M. *N*-Butylpyridoquinoxaline 1,4-dioxide (NBPQD) as a new potent for tumor imaging and therapy. *Nat. Sci.*, **2012**, 4, 1074-1084.
- Huang, T. M., Wu, P., Cheng, A. M., Qin, J., Zhang, K., Zhao, S. Q. A hydrophilic conjugate approach toward the design and synthesis of ursolic acid derivatives as potential antidiabetic agent, *RSC Adv.*, **2015**, 5, 44234-44246.
- Hughes, R. A., Moody, C. J. From amino acids to heteroaromatics-thiopeptide antibiotics, nature’s heterocyclic peptides. *Angew. Chem. Int. Ed.*, **2007**, 46, 7930 -7954.
- Ismail, T. M., Ghamry, M. A., Abu-El-Wafa, S. M., Sallam, D. F. Synthesis, characterization, 3D modeling, biological activities of some metal complexes of novel sulpha drug schiff base ligand and its nano Cu complex. *Mod. Chem.*, **2015**, 3(2), 18-30.

- Kakodkar, N. C., Peddinti, R., Kletzel, M., Tian, Y., Guerrero, L. J., Undevia, S. D., Geary, D., Chlenski, A., Yang, Q., Salwen, H. R., Cohn, S. L. The quinoxaline anti-tumor agent (R+)XK469 inhibits neuroblastoma tumor growth. *Pediatr. Blood Cancer*, **2011**, 56, 164-167.
- Kalita, D. J. Antimicrobial Peptides: The next generation therapeutic agents. *Int. J. Curr. Microbiol. App. Sci.*, **2015**, 4(6), 731-736.
- Kotra, V., Pradeep, K., Vasanthi, R. Synthesis, characterization and pharmacological evaluation of some novel quinoxaline derived chalcones. *Pharma Chem.*, **2013**, 5(4), 301-307.
- Khan, K. M., Rahim, F., Wadood, A., Kosar, N., Taha, M., Lalani, S., Khan, A., Fakhri, M. I., Junaid, M., Rehman, W., Khan, M., Perveen, S., Sajid, M., Choudhary, M. I. Synthesis and molecular docking studies of potent α -glucosidase inhibitors based on biscoumarin skeleton, *Eur. J. Med. Chem.*, **2014**, 81, 245-252.
- Kulkarni, N. V., Revankar, V. K., Kirasur, B. N., Hugar, M. H. Transition metal complexes of thiosemicarbazones with quinoxaline hub: an emphasis on antidiabetic property. *Med. Chem. Res.*, **2012**, 21, 663-671.
- Kumar, S., Bawa, S., Kaushik, D., Panda, B. P. Synthesis and *in-vitro* antimicrobial activity of secondary and tertiary amines containing 2-chloro-6-methylquinoline moiety. *Arch. Pharm. Chem. Life Sci.*, **2011**, 344, 474-480.
- Larsen, S. D., Connell, M. A., Cudahy, M. M., Evans, B. R., May, P. D., Meglasson, M. D., O'Sullivan, T. J., Schostarez, H. J., Sih, J. C., Stevens, F. C., Tanis, S. P., Tegley, C. M., Tucker, J. A., Vaillancourt, V. A., Vidmar, T. J., Watt, W., Yu, J. H. Synthesis and biological activity of analogues of the antidiabetic/antiobesity agent 3-guanidinopropionic acid: Discovery of a novel aminoguanidinoacetic acid antidiabetic agent. *J. Med. Chem.*, **2001**, 44, 1217-1230.
- Laverty, G., Gorman, S. P., Gilmore, B. F. The potential of antimicrobial peptides as biocides. *Int. J. Mol. Sci.*, **2011**, 12, 6566-6596.
- Lawrence, D. S., Copper, J. E., Smith, C. D. Structure-activity studies of substituted quinoxalinones as multiple-drug-resistance antagonists. *J. Med. Chem.*, **2001**, 44, 594-601.
- Lee, Y., Kim, S., Kim, J. Y., Arooj, M., Kim, S. Binding mode analyses and pharmacophore model development for stilbene derivatives as a novel and competitive class of α -glucosidase inhibitors. *PLoS ONE*, **2014**, 9(1), e85827. doi:10.1371/journal.pone.0085827.
- Mickevičienė, K., Baranauskaitė, R., Kantminiene, K., Stasevych, M., Porokhnyavets, O. K., Novikov, V. Synthesis and antimicrobial activity of *N*-substituted- β -amino acid derivatives containing 2-hydroxyphenyl, benzo[*b*]phenoxazine and quinoxaline moieties. *Molecules*, **2015**, 20, 3170-3189.
- Mitscher, L. A. Bacterial topoisomerase inhibitors: Quinolone and pyridone antibacterial Agents. *Chem. Rev.*, **2005**, 105, 559-592.
- Mojoska, B., Jenssen, H. Peptides and peptidomimetics for antimicrobial drug design. *Pharmaceuticals*, **2015**, 8, 366-415.

- Nolan, E. M., Walsh, C. T. How nature morphs peptide scaffolds into antibiotics. *ChemBioChem*, **2009**, 10(1), 34-53.
- Noolvi, M. N., Patel, H. M., Bhardwaj, V. Chauhan, A. Synthesis and *in vitro* antitumor activity of substituted quinoxaline and quinoxaline derivatives: Search for anticancer agent. *Eur. J. Med. Chem.*, **2011**, 46, 2327-2346.
- Padvi, P., Mahale, G., Pawar, D., Falak, C., Kendre, A. Synthesis and biological activity of quinoxaline derivatives. *World J. Pharm. Res.*, **2015**, 4(7), 1892-1900.
- Prakasha, K. C., Raghavendra, G. M., Harisha, R., and Gowda, D. C. Design, synthesis and antimicrobial screening of amino acids conjugated 2-amino-4-arylthiazole derivatives. *Int. J. Pharm. Pharm. Sci.*, **2011**, 3(3), 120-125.
- Prakash, S., Maji, D., Samanta, S., Sinha, R. K. Design, synthesis and antidiabetic, cardiomyopathy studies of cinnamic acid-amino acid hybrid analogs. *Med. Chem.*, **2014**, 4(2), 345-350.
- Patel, D. K., Prasad, S. K., Kumar, R., Hemalatha, S. An overview on antidiabetic medicinal plants having insulin mimetic property. *Asian Pac. J. Trop. Biomed.*, **2012**, 2(4), 320-330.
- Puratchikody, A., Natarajan, R., Jayapal, M., Doble, M. Synthesis, *in vitro* antitubercular activity and 3D-QSAR of novel quinoxaline derivatives. *Chem. Biol. Drug Des.*, **2011**, 78, 988-998.
- Raju, G. N., Sai, K. B., Myneni, R. T., Navya, N., Ysaswini, R. S., Nadendla, R. R. Synthesis, characterization and antimicrobial evaluation of novel 2,3-diphenylquinoxaline-1,4-di-*N*-oxide derivatives. *World J. Pharm. Res.*, **2015**, 4(5), 2625-2633.
- Ramli, Y., Moussaif, A., Karrouchi, K., Essassi, E. Pharmacological profile of quinoxalinone. *J. Chem.*, **2014**, 1-21.
- Shai, L. J., Masoko, P., Mokgotho, M. P., Magano, S. R., Mogale, A. M., Boaduo, N., Eloff, J. N. Yeast alpha glucosidase inhibitory and antioxidant activities of six medicinal plants collected in Phalaborwa, South Africa. *S. Afr. J. Bot.*, **2010**, 76, 465-470.
- Shivakumar, A. K. N., Prakasha, K. C., Gowda, D. C. Synthesis and antimicrobial activity of amino acids conjugated diphenylmethylpiperazine derivatives. *E-J. Chem.*, **2009**, 6(S1), S473-S479.
- Sharma, A., Suhas, R., Gowda, D. C. Urea's/thioureas of benzo[*d*]isothiazole analog conjugated glutamic acid: synthesis and biological evaluation. *Arch. Pharm. Chem. Life Sci.*, **2013**, 346, 359-366.
- Sharma, A., Suhas, R., Chandana, K. V., Banu, S. H., Gowda, D. C. Tert-Butyl 1,5-bis(4-(benzo[*d*]isothiazol-3-yl)piperazin-1-yl)-1,5-dioxopentan-2-ylcarbamate urea/thiourea derivatives as potent H⁺/K⁺-ATPase inhibitors. *Bioorg. Med. Chem. Lett.*, **2013**, 23, 4096-4098.
- Shukla, P., Rangari, V. Enhancement of anti-diabetic activity of 4-hydroxyisoleucine in combination with natural bioavailability enhancers. *Int. J. Pharm. Pharm. Sci.*, **2015**, 17(4), 302-306.
- Soliman, D. H. Synthesis, characterization, anti-bacterial and anti-fungal activities of new quinoxaline 1,4-di-*N*-oxide derivatives. *Int. J. Org. Chem.*, **2013**, 3, 65-72.

- Srinivas, K., Himabindu, V., Reddy, G. M., Balram, B. Synthesis and antibacterial activity of novel quinoxaline-6-carboxamide derivatives. *Int. J. Pharm. Sci. Health Care*, **2014**, 4(4), 48-58.
- Srinivas, K., Reddy, T. R., Himabindu, V., Reddy, G. M., Mohan, N. J. Synthesis and antibacterial activity of novel quinoxaline-5-carboxamide derivatives. *J. Applicable Chem.*, **2014**, 3(4), 1432-1439.
- Sridevi, P., Bhagavan, R. M., Harikumar, V. V., Rangarao, P. Synthesis of derivatives of 4-hydroxy isoleucine from fenugreek and evaluation of their antidiabetic activity. *Int. J. Phytopharm.*, **2014**, 4(1), 6-10.
- Stanila, A., Braicu, C., Stanila, S., Pop, R. M. Antibacterial activity of copper and cobalt amino acid complexes. *Notulae Botanicae Horti Agrobotanici.*, **2011**, 39(2), 124-129.
- Stanchev, M., Tabakova, S., Videnov, G., Golovinsky, E., Jung, G. Synthesis and antimicrobial activity *in vitro* of new amino acids and peptides containing thiazole and oxazole moieties. *Arch. Pharm.*, **1999**, 332(9), 297-304.
- Suhas, R., Chandrashekar, S., Gowda, D. C. Synthesis of elastin based peptides conjugated to benzisoxazole as a new class of potent antimicrobials-A novel approach to enhance biocompatibility. *Eur. J. Med. Chem.*, **2011**, 46, 704-711.
- Tuba, A. K., Gulcin, I. Antioxidant and radical scavenging properties of curcumin. *Chem. Biol. Interact.*, **2008**, 174, 27-37.
- Vieira, M., Pinheiro, C., Fernandes, R., Noronha, J. P., Prudencio, C. Antimicrobial activity of quinoxaline 1,4-dioxide with 2- and 3-substituted derivatives. *Microbiol. Res.*, **2014**, 169, 287-293.
- Waring, M. J., Hadda, T. B., Kotchevar, A. T., Ramdani, A., Touzani, R., Elkadiri, S., Hakkou, A., Bouakka, M., and Ellis, T. 2,3-Bifunctionalized quinoxalines: Synthesis, DNA interactions and evaluation of anticancer, anti-tuberculosis and antifungal activity. *Molecules*, **2002**, 7, 641-656.
- Wang, S., Zheng, Q., Wang, J., Zhao, Z., Li, Q., Yu, Y., Wang, R., Liu, W. Target-oriented design and biosynthesis of thiostrepton-derived thiopeptide antibiotics with improved pharmaceutical properties. *Org. Chem. Frontiers*, **2015**, 2, 106-109.
- Wei, Q., Liu, H., Zhou, H., Zhang, D., Zhang, Z., Zhou, Q. Anticancer activity of a thymidine quinoxaline conjugate is modulated by cytosolic thymidine pathways. *BMC Cancer*, **2015**, 15(159), 1-11.
- Wu, G., Robertson, D. H., Brooks, C. L., Vieth, M. Detailed analysis of grid-based molecular docking: A case study of CDOCKER- a CHARMM-based MD docking algorithm. *J. Comput. Chem.*, **2003**, 24, 1549-1562.

Chapter 6. Synthesis, *in vitro* antimicrobial, antioxidant and antidiabetic activities of amino acid linked thiazolidine-quinoxaline derivatives

* The compounds referred to in the chapter are referred to elsewhere in the thesis with an **B** preceding the number of the compound. For example **5a-c** and **6a-l** is referred to as **B5a-c** and **B6a-l** elsewhere in the thesis.

Abstract

A novel protocol for the rapid assembly of a hybrid framework based on amino acid, thiazolidine and quinoxaline scaffolds has been demonstrated by microwave irradiation. The amino acid quinoxalines **B5a-B5c** were prepared in three steps from 2,4-dinitrofluorobenzene and the amino acids, valine, methionine and tyrosine and subsequently reacted with four different aldehydes and thioglycolic acid to produce thiazolidine-quinoxaline-amino acid hybrids **B6a-B6l**. All synthesized compounds were evaluated for their *in vitro* antimicrobial, antioxidant and antidiabetic activities. Compounds **B6f**, **B6j** and **B6k** showed broad spectrum antimicrobial activity against Gram +ve and Gram -ve bacteria, whilst **B6h**, **B6k** and **B6l** showed the best antioxidant activity in the same order of magnitude to that of ascorbic acid. Four of the compounds, **B5c**, **B6d**, **B6g** and **B6k** showed activity against α -glucosidase and α -amylase similar to acarbose. Those compounds showing antibacterial activity possessed 4-fluorophenyl and 4-methoxyphenyl groups along with methionine and tyrosine residues while the compounds showing antioxidant, α -glucosidase and α -amylase activity contained 4-nitrophenyl and 4-methoxyphenyl groups on the thiazolidine moiety with mainly methionine and tyrosine amino acid residues. The α -glucosidase and α -amylase inhibitory compound **B5c** did not have a thiazolidine moiety and **B6d** was the only active compound with a valine amino acid moiety. Compound **B6k** with a tyrosine amino acid residue and a 4-methoxyphenylthiazolidine moiety on the quinoxaline scaffold showed good bioactivity in all three assays.

Keywords: Microwave irradiation, thermal, antimicrobial, antioxidant, antidiabetic, α -glucosidase, α -amylase.

6.1 Introduction

Thiazolidinones consists of a heterocyclic 5-membered ring containing a thioether and amide group. This moiety is found in many highly active natural products (Riego et al., 2005; Davyt et al., 2010; Sahoo et al., 2015; Zhang et al., 2015). Thiazolidine derivatives have been studied extensively and found to have diverse chemical reactivities (Teresa et al., 2006; Bayuelo et al., 2012; Fernanda et al., 2013; Lobana et al., 2015) and a broad-spectrum of biological activities, such as anti-microbial, antidiabetic, anti-obesity, anti-inflammatory, antioxidant, anti-proliferative, antitumor, anti-HIV, anticancer and anti-tubercular (Siddiqui et al., 2009; Malik et al., 2011; Vinay et al., 2011; Singh et al., 2011; Singh et al., 2011; Geronikaki et al., 2013).

Quinoxaline is commonly called 1,4-diazanaphthalene or benzopyrazine. Quinoxaline and its derivatives are mostly of synthetic origin (Baumann et al., 2013; Srivastava et al., 2014; Padvi et al., 2015). They have been described as a part of a bicyclic desipeptide antibiotic having activity against Gram +ve bacteria and certain tumours by inhibiting RNA synthesis (Waring et al., 1979; Eike et al., 2011; Noorulla et al., 2011; Noolvi et al., 2011; Kotra et al., 2013; Mishra et al., 2013; Al-Marhabi et al., 2015). The quinoxaline moiety can be found in a number of antibiotics such as echinomycin, levomycin and actinomycin (Katagiri et al., 1975; Patidar et al., 2011; Pai et al., 2011; Dhanaraj et al., 2015).

Simple α -amino acids have been known to be converted into complex arrays of heteroaromatic rings with interesting and potent biological activities (Suhas et al., 2011; Sharma et al., 2013; Hashash et al., 2013; Sharma et al., 2015). Amino acid coupled to other heterocyclic scaffolds (benzo-phenoxazine, indole), or amides of amino acids and metal complexes increased the

bioactivity of the molecular scaffolds themselves (Yang et al., 1998; Aiyelabola et al., 2012; Saxena et al., 2014; Mickevičienė et al., 2015). Thus far, there have been two reports on the synthesis of quinoxalines using amino acids (Holley et al., 1952; Tung et al., 2004). Amino acids attached to quinoxaline derivatives which have shown antimicrobial, and glutamate receptor activity have also been described (Faham et al., 2002; Demmer et al., 2015; Mickevičienė et al., 2015). In addition, there have been reports of thiazolidine containing quinoxalines, which showed good antibacterial and antitubercular activity (Pawar et al., 2007, 2008; Puratchikody et al., 2011).

We herein report an efficient microwave-assisted synthesis of amino acid linked thiazolidine-quinoxaline compounds and tested them in antimicrobial, antioxidant and antidiabetic assays.

6.2 Experimental

6.2.1 Materials and methods

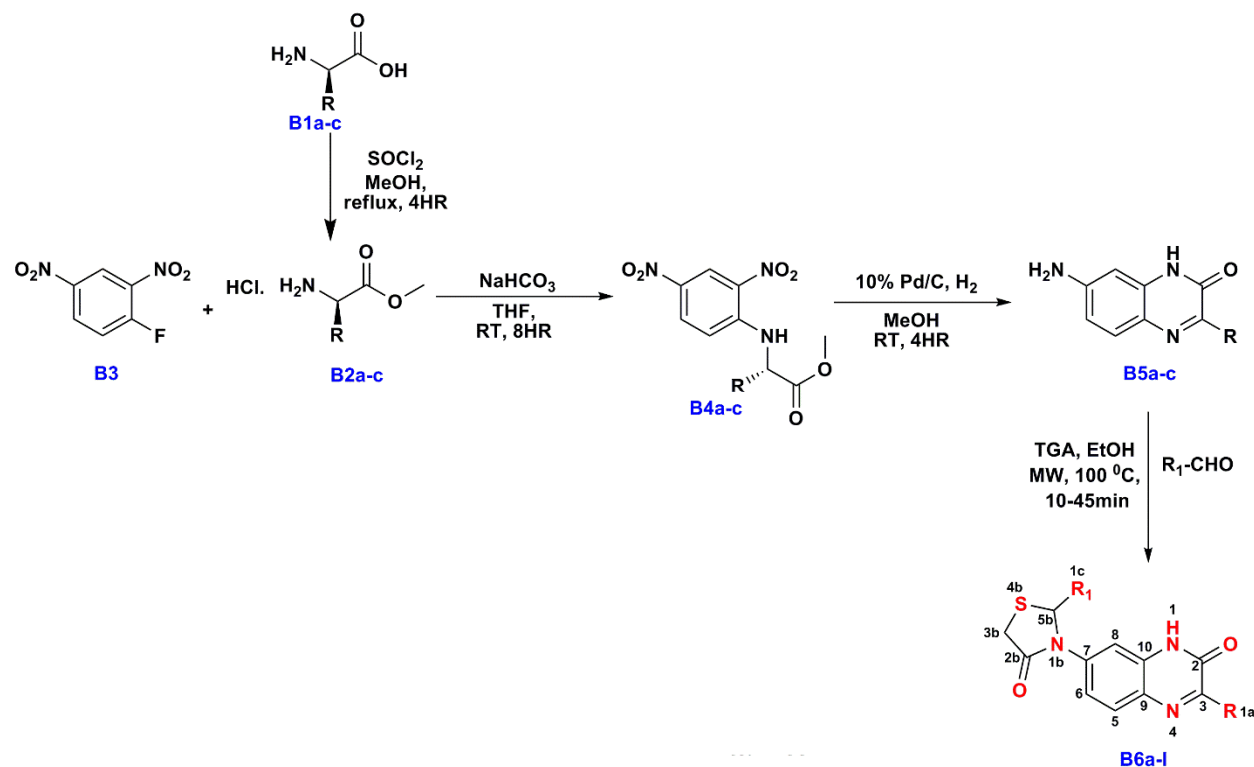
All chemicals were supplied by Sigma-Aldrich *via* Capital Lab, South Africa. All organic solvents were redistilled and dried according to standard procedures. Silica gel 60 F₂₅₄ plates (Merck) were used for thin layer chromatography. Products were purified by column chromatography using silica gel (60-120 mesh) with ethyl acetate : hexane as the eluent. Melting points were recorded using a Stuart Scientific SMP3 apparatus. UV spectra were obtained on a Varian Cary UV-VIS spectrophotometer using MeOH as a solvent. IR spectra were recorded on a Perkin Elmer 100 FT-IR spectrophotometer with universal attenuated total reflectance sampling accessory. Microwave reactions were performed using a CEM Discover, Explorer-12 Hybrid microwave instrument. ¹H, ¹³C NMR and all 2D NMR spectra were recorded on a Bruker Avance instrument operating at 400 MHz. Chemical shifts were reported as δ values (ppm) relative to an internal standard of

tetramethylsilane (TMS) or to the solvent line of DMSO-*d*₆ ($\delta_{\text{H}} = 2.50$, $\delta_{\text{C}} = 39.52$). High-resolution mass data were obtained using a Bruker micro TOF-Q II ESI instrument operating at ambient temperature.

General procedure for the preparation of amino acid methyl ester hydrochloride (B2)

Methanol (20 mL) was added to different amino acids (**B1a-c**) (0.1 mol) followed by gradual addition of thionyl chloride (0.3 mol) at room temperature. The resulting solution was stirred at 70 °C for 4h and the reaction mixture concentrated on a rotary evaporator producing the respective amino acid ester hydrochlorides in yields of > 90 %.

The general scheme for the reaction sequence is shown in **Scheme 6-1** below.



Scheme 6-1 Synthesis of amino acid linked thiazolidine-quinoxaline compounds

General procedure for the preparation of compounds (**B4a-c**)

1-Fluoro-2,4-dinitrobenzene **B3** (0.50 g, 2.34 mmol), amino acid ester (3.51 mmol) and NaHCO₃ (0.005 g, 4.68 mmol) were mixed in THF (10 mL). The reaction mixture was stirred overnight at room temperature. After completion of the reaction (monitored by TLC), the reaction mixture was washed with water (2 × 10 mL), followed by 10% Na₂CO₃ solution (10 mL). The organic layer was separated from the aqueous layer by adding a small amount of ethyl acetate to distinguish the THF and aqueous layers. The organic layer was then dried over anhydrous Na₂SO₄ and concentrated under reduced pressure to afford **B4a-c**, which was subsequently purified by column chromatography (hexane/ethyl acetate) to afford the desired product in good yields (80-90%).

General procedure for the preparation of compounds (**B5a-c**)

The 2,4-dinitrophenyl amino acid compounds **B4a-c** (1 mmol) was added to methanol (10 mL), to which 10% Pd/C (50 mg) was added. The reaction mixture was stirred for 4h at room temperature under H₂ atmosphere. The reaction mixture was then filtered through Celite 545 to remove the catalyst. The filtrate was evaporated under reduced pressure and the obtained solid was purified by column chromatography (hexane/ethyl acetate) to afford the desired product in good yield (80-85%).

General procedure for the preparation of amino acid linked thiazolidine-quinoxaline derivatives (**B6a-l**)

A mixture of 3-substituted-7-amino quinoxalin-2(1*H*)-one (**B5a-c**) (1.0 mmol), the appropriate substituted benzaldehyde (1.5 mmol) and thioglycolic acid (5.0 mmol) was placed in a 10 mL reaction vial containing absolute ethanol (3 mL) and a stirring bar. The vial was sealed tightly

with a Teflon septum, placed into the microwave cavity and irradiated at 100 °C using 100 W as the maximum power for 10-45 min. Upon completion, the reaction mixture was rapidly cooled by gas jet cooling to ambient temperature, the contents dissolved in ethyl acetate and washed with 5% aqueous citric acid (2 × 5 mL), water and aqueous sodium hydrogen carbonate (2 × 5 mL). The organic layer was then separated and dried over sodium sulphate, evaporated under reduced pressure and the solid obtained purified by column chromatography (hexane/ethyl acetate) to afford the desired product in good yield (80-90%).

(B5a) 7-Amino-3-isopropylquinoxalin-2(1H)-one, dark brown solid; mp 238-240 °C; UV λ_{max} (MeOH) nm (log ϵ) 222 (3.40), 282 (2.40), 364 (3.02); IR ν_{max} 3460 (NH₂), 3331 (NH), 1650, 1622 (C=O) cm⁻¹; ¹H NMR (400 MHz, DMSO) δ_{H} 11.87 (s, 1H, H-1), 7.33 (d, J = 8.0 Hz, 1H, H-5), 6.51 (dd, J = 8.0, 2.2 Hz, 1H, H-6), 6.32 (d, J = 2.2 Hz, 1H, H-8), 5.80 (s, 2H, H-11), 3.28-3.39 (m, 1H, H-1a), 1.15 (d, J = 6.8 Hz, 6H, H-2a/H-3a); ¹³C NMR (400 MHz, DMSO) δ_{C} 157.4 (C, C-3), 154.9 (C, C-2), 150.3 (C, C-7), 133.6 (C, C-9), 129.1 (CH, C-5), 124.0 (C, C-10), 111.5 (CH, C-6), 95.9 (CH, C-8), 29.3 (CH, C-1a), 20.3 (2CH₃, C-2a/3a); HRMS (m/z): calc. for C₁₁H₁₃N₃ONa (M + Na)⁺: 226.0956, found: 226.0956.

(B5b) 7-amino-3-(2-(methylthio)ethyl)quinoxalin-2(1H)-one, brown solid; mp 178-180 °C; UV λ_{max} (MeOH) nm (log ϵ) 230 (3.14), 283 (2.97), 390 (3.02); IR ν_{max} 3337 (NH), 2809 (C-H), 1671, 1637 (C=O), 1521 cm⁻¹; ¹H NMR (400 MHz, DMSO) δ_{H} 12.01 (s, 1H, H-1), 7.34 (d, J = 8.5 Hz, 1H, H-5), 6.53 (d, J = 8.5 Hz, 1H, H-6), 6.33 (bs, 1H, H-8), 5.89 (s, 2H, H-11), 3.14-3.20 (m, 2H, H-2a), 2.97-3.05 (m, 2H, H-1a), 2.58 (s, 3H, H-4a); ¹³C NMR (400 MHz, DMSO) δ_{C} 155.2 (C, C-3), 150.7 (C, C-2), 150.7 (C, C-7), 133.9 (C, C-10), 129.0 (CH, C-5), 124.0 (C, C-9), 111.7 (CH,

C-6), 95.9 (CH, C-8), 49.9 (CH₂, C-2a), 38.0 (CH₃, C-4a), 25.2 (CH₂, C-1a); HRMS (*m/z*): calc. for C₁₁H₁₂N₃OS (M + H)⁺: 234.0701, found: 234.0708.

(B5c) 3-(4-hydroxybenzyl)-7-aminoquinoxalin-2(1*H*)-one, light yellow solid; mp 164-166 °C; UV λ_{max} (MeOH) nm (log ε) 224 (3.51), 249 (3.0), 279 (2.78), 371 (3.15); IR ν_{max} 3461 (NH₂), 3332 (NH), 1651, 1622 (C=O) cm⁻¹; ¹H NMR (400 MHz, DMSO) δ_H 11.91 (s, 1H, H-1), 9.17 (s, 1H, H-8a), 7.33 (d, *J* = 8.6 Hz, 1H, H-5), 7.08 (d, *J* = 8.2 Hz, 2H, H-3a/7a), 6.65 (d, *J* = 8.2 Hz, 2H, H-4a/6a), 6.51 (dd, *J* = 8.6, 1.6 Hz, 1H, H-6), 6.31 (d, *J* = 1.6 Hz, 1H, H-8), 5.84 (s, 2H, H-11), 3.85 (s, 2H, H-1a); ¹³C NMR (400 MHz, DMSO) δ_C 155.7 (C, C-3), 155.3 (C, C-5a), 152.6 (C, C-2), 150.6 (C, C-7), 133.9 (C, C-9), 129.8 (2CH, C-3a/7a), 129.1 (CH, C-5), 128.6 (C, C-10), 124.2 (C, C-2a), 115.0 (2CH, C-4a/6a), 111.6 (CH, C-6), 95.9 (CH, C-8), 37.6 (CH₂, C-1a); HRMS (*m/z*): calc. for C₁₅H₁₃N₃O₂Na (M + Na)⁺: 290.0905, found: 290.0910.

(B6a) 3-isopropyl-7-(4-oxo-2-phenylthiazolidin-3-yl)quinoxalin-2(1*H*)-one, white solid; mp 280-282 °C; UV λ_{max} (MeOH) nm (log ε) 231 (3.13), 287 (2.59), 341 (2.81); IR ν_{max} 3151 (NH), 1683 (C=O), 1652, 1616 cm⁻¹; ¹H NMR (400 MHz, DMSO) δ_H 12.27 (s, 1H, H-1), 7.60 (d, *J* = 8.8 Hz, 1H, H-5), 7.38 (dd, *J* = 7.7, Hz, 2H, H-2c/6c), 7.31 (d, *J* = 2.2 Hz, 1H, H-8), 7.26 (dd, *J* = 7.7, 7.7 Hz, 2H, H-3c/5c), 7.22 (dd, *J* = 7.7, 2.2 Hz, 1H, H-4c), 7.20 (dd, *J* = 8.8, 2.2 Hz, 1H, H-6), 6.58 (s, 1H, H-5b), 4.06 (d, *J* = 15.9 Hz, 1H, H-3bi), 3.92 (d, *J* = 15.9 Hz, 1H, H-3bii), 3.39 (sep, *J* = 6.9 Hz, 1H, H-1a), 1.16 (d, *J* = 6.9 Hz, 3H, H-2a), 1.15 (d, *J* = 6.9 Hz, 3H, H-3a); ¹³C NMR (400 MHz, DMSO) δ_C 170.8 (C, C-2b), 165.5 (C, C-3), 154.1 (C, C-2), 139.7 (C, C-1c), 138.1 (C, C-7), 131.7 (C, C-9*), 129.4 (C, C-10*), 128.7 (2CH, C-3c/5c), 128.6 (CH, C-4c), 128.3 (CH, C-5), 126.9 (2CH, C-2c/6c), 119.3 (CH, C-8), 111.3 (CH, C-6), 63.3 (CH, C-5b), 32.8 (CH₂, C-3b),

29.8 (CH, C-1a), 19.99 (CH₃, C-2a), 19.97 (CH₃, C-3a); HRMS (*m/z*): calc. for C₂₀H₁₉N₃O₂SNa (M + Na)⁺: 388.1096, found: 388.1096. *indicates that assignments are interchangeable.

(B6b) 7-(2-(4-fluorophenyl)-4-oxothiazolidin-3-yl)-3-isopropylquinoxalin-2(1*H*)-one, white solid; mp 252-254 °C; UV λ_{max} (MeOH) nm (log ε) 230 (3.29), 287 (2.72), 340 (2.95); IR ν_{max} 3178 (NH), 1657 (C=O), 1615, 1510 cm⁻¹; ¹H NMR (400 MHz, DMSO) δ_H 12.27 (s, 1H, H-1), 7.61 (d, *J* = 8.7 Hz, 1H, H-5), 7.45 (dd, *J* = 8.7, 5.4, Hz, 2H, H-2c/6c), 7.27 (d, *J* = 2.2 Hz, 1H, H-8), 7.19 (dd, *J* = 8.7, 2.2 Hz, 1H, H-6), 7.12 (t, *J* = 8.8 Hz, 2H, H-3c/5c), 6.59 (s, 1H, H-5b), 4.06 (d, *J* = 15.8 Hz, 1H, H-3bi), 3.92 (d, *J* = 15.8 Hz, 1H, H-3bii), 3.42 (septet, *J* = 6.8 Hz, 1H, H-1a), 1.16 (d, *J* = 6.8 Hz, 3H, H-2a), 1.15 (d, *J* = 6.8 Hz, 3H, H-3a); ¹³C NMR (400 MHz, DMSO) δ_C 170.7 (C, C-2b), 165.6 (C, C-3), 161.9 (d, *J*_{C-F} = 243.9 Hz, C, C-4c), 154.1 (C, C-2), 137.9 (C, C-7), 135.9 (d, *J* = 2.8 Hz, C, C-1c), 131.7 (C, C-9*), 129.5 (C, C-10*), 129.3 (d, *J* = 8.6 Hz, 2CH, C-2c/6c), 128.4 (CH, C-5), 119.4 (CH, C-6), 115.6 (d, *J* = 21.7 Hz, 2CH, C-3c/5c), 111.5 (CH, C-8), 62.6 (CH, C-5b), 32.8 (CH₂, C-3b), 29.8 (CH, C-1a), 19.99 (CH₃, C-2a*), 19.96 (CH₃, C-3a*); HRMS (*m/z*): calc. for C₂₀H₁₈N₃O₂SFNa (M + Na)⁺: 406.1001, found: 406.0999. *indicates that assignments are interchangeable.

(B6c) 3-isopropyl-7-(2-(4-methoxyphenyl)-4-oxothiazolidin-3-yl)quinoxalin-2(1*H*)-one, brown solid; mp 268-270 °C; UV λ_{max} (MeOH) nm (log ε) 230 (3.67), 284 (3.03), 341 (3.22); IR ν_{max} 3144 (NH), 1682 (C=O), 1657, 1609 cm⁻¹; ¹H NMR (400 MHz, DMSO) δ_H 12.26 (s, 1H, H-1), 7.59 (d, *J* = 8.6 Hz, 1H, H-5), 7.31 (d, *J* = 8.8 Hz, 2H, H-2c/6c), 7.26 (d, *J* = 2.2 Hz, 1H, H-8), 7.18 (dd, *J* = 8.6, 2.2 Hz, 1H, H-6), 6.82 (d, *J* = 8.8 Hz, 2H, H-3c/5c), 6.52 (s, 1H, H-5b), 4.03 (d, *J* = 15.7 Hz, 1H, H-3bi), 3.91 (d, *J* = 15.7 Hz, 1H, H-3bii), 3.67 (s, 3H, H-8c), 3.38 (septet, *J* = 6.8

Hz, 1H, H-1a), 1.16 (d, $J = 6.8$ Hz, 3H, H-2a), 1.15 (d, $J = 6.8$ Hz, 3H, H-3a); ^{13}C NMR (400 MHz, DMSO) δ_{C} 171.1 (C, C-2b), 165.9 (C, C-3), 159.5 (C, C-4c), 154.3 (C, C-2), 138.4 (C, C-7), 131.8 (C, C-1c), 131.2 (C, C-9*), 129.7 (C, C-10*), 129.1 (2CH, C-2c/6c), 128.5 (CH, C-5), 120.2 (CH, C-6), 114.3 (2CH, C-3c/5c), 111.9 (CH, C-8), 63.5 (CH, C-5b), 55.3 (CH₃, C-8c), 33.2 (CH₂, C-3b), 30.1 (CH, C-1a), 20.2 (2CH₃, C-2a/3a); HRMS (m/z): calc. for C₂₁H₂₁N₃O₃SNa (M + Na)⁺: 418.1201, found: 418.1213. *indicates that assignments are interchangeable.

(B6d) 3-isopropyl-7-(2-(4-nitrophenyl)-4-oxothiazolidin-3-yl)quinoxalin-2(1H)-one, light yellow solid; mp 274-276 °C; UV λ_{max} (MeOH) nm (log ϵ) 229 (3.48), 341 (3.12); IR ν_{max} 3088 (NH), 1694, 1664 (C=O), 1624 cm⁻¹; ^1H NMR (400 MHz, DMSO) δ_{H} 12.28 (s, 1H, H-1), 8.15 (d, $J = 8.7$ Hz, 2H, H-3c/5c), 7.70 (d, $J = 8.7$ Hz, 2H, H-2c/6c), 7.62 (d, $J = 8.8$ Hz, 1H, H-5), 7.32 (d, $J = 2.2$ Hz, 1H, H-8), 7.24 (dd, $J = 8.8, 2.2$ Hz, 1H, H-6), 6.75 (s, 1H, H-5b), 4.13 (d, $J = 15.8$ Hz, 1H, H-3bi), 3.96 (d, $J = 15.8$ Hz, 1H, H-3bii), 3.39 (septet, $J = 6.8$ Hz, 1H, H-1a), 1.16 (d, $J = 6.8$ Hz, 3H, H-2a), 1.15 (d, $J = 6.8$ Hz, 3H, H-3a); ^{13}C NMR (400 MHz, DMSO) δ_{C} 170.7 (C, C-2b), 165.7 (C, C-3), 154.0 (C, C-2), 147.5 (C, C-4c), 147.4 (C, C-1c), 137.8 (C, C-7), 131.8 (C, C-9*), 129.5 (C, C-10*), 128.5 (CH, C-5), 128.1 (2CH, C-2c/6c), 124.1 (2CH, C-3c/5c), 118.9 (CH, C-6), 110.9 (CH, C-8), 62.1 (CH, C-5b), 32.7 (CH₂, C-3b), 29.8 (CH, C-1a), 19.98 (CH₃, C-2a), 19.95 (CH₃, C-3a); HRMS (m/z): calc. for C₂₀H₁₇N₄O₄S (M - H)⁻: 409.0971, found: 409.0966. *indicates that assignments are interchangeable.

(B6e) 3-(2-(methylthio)ethyl)-7-(4-oxo-2-phenylthiazolidin-3-yl)quinoxalin-2(1H)-one, brown solid; mp 258-260 °C; UV λ_{max} (MeOH) nm (log ϵ) 230 (3.34), 294 (2.74), 344 (2.98); IR ν_{max} 3173 (NH), 1678 (C=O), 1654, 1618 cm⁻¹; ^1H NMR (400 MHz, DMSO) δ_{H} 12.32 (s, 1H, H-

1), 7.61 (d, $J = 8.7$ Hz, 1H, H-5), 7.38 (d, 1H, $J = 7.3$ Hz, H-2c/6c), 7.33 (d, 1H, $J = 2.2$ Hz, H-8), 7.29 (t, $J = 7.3$ Hz, 2H, H-3c/5c), 7.23 (t, $J = 7.3$ Hz, 2H, H-4c), 7.21 (dd, $J = 8.7, 2.2$ Hz, H-6), 6.58 (s, 1H, H-5b), 4.06 (d, $J = 15.9$ Hz, 1H, H-3bi), 3.92 (d, $J = 15.9$ Hz, 1H, H-3bii), 3.01 (t, $J = 7.7$ Hz, 2H, H-2a), 2.82 (t, $J = 7.7$ Hz, 2H, H-1a), 2.07 (s, 3H, H-4a); ^{13}C NMR (400 MHz, DMSO) δ_{C} 170.8 (C, C-2b), 160.1 (C, C-3), 154.5 (C, C-2), 139.7 (C, C-1c), 138.3 (C, C-7), 131.9 (C, C-9*), 129.4 (C, C-10*), 128.7 (2C, C, C-3c/5c), 128.6 (CH, C-5), 128.3 (CH, C-4c), 126.9 (CH, C-2c/6c), 119.3 (CH, C-6), 111.3 (CH, C-8), 63.3 (CH, C-5b), 32.8 (CH₂, C-3b), 32.6 (CH₂, C-2a), 29.9 (CH₂, C-1a), 14.6 (CH₃, C-4a); HRMS (m/z): calc. for C₂₀H₁₈N₃O₂S₂ (M - H)⁺: 396.0840, found: 396.0856. *indicates that assignments are interchangeable.

(B6f) 7-(2-(4-fluorophenyl)-4-oxothiazolidin-3-yl)-3-(2-(methylthio)ethyl)quinoxalin-2(1H)-one, dark brown solid; mp 264-266 °C; UV λ_{max} (MeOH) nm (log ϵ) 231 (3.27), 293 (2.68), 343 (2.92); IR ν_{max} 3173 (NH), 1679 (C=O), 1655, 1618, 1604, 1508 cm⁻¹; ^1H NMR (400 MHz, DMSO) δ_{H} 12.33 (s, 1H, H-1), 7.62 (d, $J = 8.7$ Hz, 1H, H-5), 7.46 (dd, $J = 8.8, 5.4$ Hz, 2H, H-2c/6c), 7.28 (d, $J = 2.0$ Hz, 1H, H-8), 7.20 (dd, $J = 8.7, 2.0$ Hz, 1H, H-6), 7.12 (dd, $J = 8.8, 8.8$ Hz, 2H, H-3c/5c), 6.59 (s, 1H, H-5b), 4.07 (d, $J = 15.7$ Hz, 1H, H-3bi), 3.93 (d, $J = 15.7$ Hz, 1H, H-3bii), 3.01 (t, $J = 7.0$ Hz, 2H, H-2a), 2.83 (t, $J = 7.6$ Hz, 2H, H-1a), 2.07 (s, 3H, H-4a); ^{13}C NMR (400 MHz, DMSO) δ_{C} 170.7 (C, C-2b), 161.9 (d, $J = 243.7$ Hz, C, C-4c), 160.2 (C, C-3), 154.5 (C, C-2), 138.2 (C, C-7), 135.9 (d, $J = 2.9$ Hz, C, C-1c), 131.9 (C, C-9*), 129.5 (C, C-10*), 129.3 (d, $J = 8.4$ Hz, 2CH, C-2c/6c), 128.3 (CH, C-5), 119.5 (CH, C-6), 115.7 (d, $J = 21.2$ Hz, 2CH, C-3c/5c), 111.5 (CH, C-8), 62.6 (CH, C-5b), 32.8 (CH₂, C-3b), 32.6 (CH₂, C-2a), 29.9 (CH₂, C-1a), 14.6 (CH₃, C-4a); HRMS (m/z): calc. for C₂₀H₁₈FN₃O₂S₂Na (M + Na)⁺: 438.0722, found: 438.0722. *indicates that assignments are interchangeable.

(B6g) 7-(2-(4-methoxyphenyl)-4-oxothiazolidin-3-yl)-3-(2-(methylthio)ethyl)quinoxalin-2(1H)-one, yellow solid; mp 258-260 °C; UV λ_{max} (MeOH) nm (log ϵ) 230 (3.09), 279 (2.95), 389 (3.06); IR ν_{max} 3321 (NH), 1685 (C=O), 1616, 1525 cm^{-1} ; ^1H NMR (400 MHz, DMSO) δ_{H} 12.36 (s, 1H, H-1), 7.61 (d, J = 8.7 Hz, 1H, H-5), 7.32 (d, J = 8.6 Hz, 2H, H-2c/6c), 7.28 (d, J = 2.1, 1H, H-8), 7.21 (dd, J = 8.7, 2.1 Hz, 1H, H-6), 6.83 (d, J = 8.6 Hz, 2H, H-3c/5c), 6.53 (s, 1H, H-5b), 4.03 (d, J = 15.9 Hz, 1H, H-3bi), 3.91 (d, J = 15.9 Hz, 1H, H-3bii), 3.67 (s, 3H, H-8c), 3.16-3.10 (m, 2H, H-2a), 3.06-2.96 (m, 2H, H-1a), 2.57 (s, 3H, H-4a); ^{13}C NMR (400 MHz, DMSO) δ_{C} 170.6 (C, C-2b), 159.4 (C, C-4c), 159.2 (C, C-3), 154.4 (C, C-2), 138.4 (C, C-1c), 138.4 (C, C-7), 131.9 (C, C-9*), 131.1 (C, C-10*), 128.7 (2CH, C-2c/6c), 128.2 (CH, C-5), 119.6 (CH, C-6), 113.9 (2CH, C-3c/5c), 111.6 (CH, C-8), 63.1 (CH, C-5b), 55.0 (CH₃, C-8c), 49.3 (CH₂, C-3b), 37.9 (CH₃, C-4a), 32.9 (CH₂, C-2a), 25.5 (CH₂, C-1a); HRMS (m/z): calc. for C₂₁H₂₂N₃O₃S₂ (M-H)⁺: 428.1103, found: 428.1084. *indicates that assignments are interchangeable.

(B6h) 3-(2-(methylthio)ethyl)-7-(2-(4-nitrophenyl)-4-oxothiazolidin-3-yl)quinoxalin-2(1H)-one, reddish brown solid; mp 240-242 °C; UV λ_{max} (MeOH) nm (log ϵ) 233 (2.92), 344 (2.60); IR ν_{max} 3175 (NH), 1681 (C=O), 1655, 1619, 1515 cm^{-1} ; ^1H NMR (400 MHz, DMSO) δ_{H} 12.34 (s, 1H, H-1), 8.16 (d, J = 8.7 Hz, 2H, H-3c/5c), 7.70 (d, J = 8.7 Hz, 2H, H-2c/6c), 7.63 (d, J = 8.8 Hz, 1H, H-5), 7.34 (d, J = 2.2 Hz, 1H, H-8), 7.25 (dd, J = 8.8, 2.2 Hz, 1H, H-6), 6.76 (s, 1H, H-5b), 4.13 (d, J = 15.9 Hz, 1H, H-3bi), 3.96 (d, J = 15.9 Hz, 1H, H-3bii), 3.01 (t, J = 7.6 Hz, 2H, H-2a), 2.82 (t, J = 7.6 Hz, 2H, H-1a), 2.06 (s, 3H, H-4a); ^{13}C NMR (400 MHz, DMSO) δ_{C} 170.8 (C, C-2b), 160.3 (C, C-3), 154.5 (C, C-2), 147.5 (C, C-4c), 147.4 (C, C-1c), 137.9 (C, C-7), 132.0 (C, C-9*), 129.5 (C, C-10*), 128.5 (CH, C-5), 128.1 (2CH, C-2c/6c), 124.1 (2CH, C-3c/5c), 119.0 (CH,

C-6), 111.0 (CH, C-8), 62.1 (CH, C-5b), 32.7 (CH₂, C-3b), 32.6 (CH₂, C-2a), 29.9 (CH₂, C-1a), 14.6 (CH₃, C-4a); HRMS (*m/z*): calc. for C₂₀H₁₇N₄O₄S₂ (M + H)⁺: 441.0691, found: 441.0696.

*indicates that assignments are interchangeable.

(B6i) 3-(4-hydroxybenzyl)-7-(4-oxo-2-phenylthiazolidin-3-yl)quinoxalin-2(1H)-one, yellow solid; mp 134-136 °C; UV λ_{max} (MeOH) nm (log ε) 228 (3.39), 346 (3.01); IR ν_{max} 3177 (NH), 1656 (C=O), 1614, 1510 cm⁻¹; ¹H NMR (400 MHz, DMSO) δ_H 12.31 (s, 1H, H-1), 9.19 (s, 1H, H-8a), 7.60 (d, *J* = 8.5 Hz, 1H, H-5), 7.38 (d, 2H, *J* = 7.0 Hz, H-2c/6c), 7.32 (s, 1H, H-8), 7.28 (dd, 2H, *J* = 7.0, 7.0, H-3c/5c), 7.19-7.23 (m, 2H, H-4c, H-6), 7.07 (d, *J* = 7.6 Hz, 2H, H-3a/7a), 6.64 (d, *J* = 7.6 Hz, 2H, H-4a/6a), 6.57 (s, 1H, H-5b), 4.06 (d, *J* = 15.8 Hz, 1H, H-3bi), 3.93 (bs, 2H, H-1a), 3.91 (d, *J* = 15.8 Hz, 1H, H-3bii); ¹³C NMR (400 MHz, DMSO) δ_C 170.8 (C, C-2b), 160.6 (C, C-3), 155.9 (C, C-2), 154.4 (C, C-5a), 139.7 (C, C-1c), 138.3 (C, C-7), 132.0 (C, C-9*), 130.0 (2C, CH, C-3a/7a), 129.5 (C, C-10*), 128.8 (2C, CH, C-2c/6c), 128.6 (CH, C-5), 128.3 (CH, C-4c), 127.2 (C, C-2a), 126.9 (2C, CH, C-3c/5c), 119.3 (CH, C-6), 115.1 (2CH, C-4a/6a), 111.2 (CH, C-8), 63.3 (CH, C-5b), 38.0 (CH₂, C-1a), 32.8 (CH₂, C-3b); HRMS (*m/z*): calc. for C₂₄H₁₈N₃O₃S (M + H)⁺: 428.1069, found: 428.1073. *indicates that assignments are interchangeable.

(B6j) 3-(4-hydroxybenzyl)-7-(2-(4-fluorophenyl)-4-oxothiazolidin-3-yl)quinoxalin-2(1H)-one, yellow solid; mp 268-270 °C; UV λ_{max} (MeOH) nm (log ε) 230 (3.03), 286 (2.52), 345 (2.75); IR ν_{max} 3384 (OH), 3125 (NH), 1678 (C=O), 1615, 1509 cm⁻¹; ¹H NMR (400 MHz, DMSO) δ_H 12.31 (s, 1H, H-1), 9.18 (s, 1H, H-8a), 7.61 (d, *J* = 8.7 Hz, 1H, H-5), 7.44 (dd, *J* = 8.6, 5.4 Hz, 2H, H-2c/6c), 7.27 (d, *J* = 2.2 Hz, 1H, H-8), 7.19 (dd, *J* = 8.7, 2.2 Hz, 1H, H-6), 7.11 (dd, *J* = 8.6, 8.6

Hz, 2H, H-3c/5c), 7.08 (d, $J = 8.5$ Hz, 2H, H-3a/7a), 6.64 (d, $J = 8.5$ Hz, 2H, H-4a/6a), 6.58 (s, 1H, H-5b), 4.07 (d, $J = 15.7$ Hz, 1H, H-3bi), 3.93 (bs, 2H, H-1a), 3.92 (d, $J = 15.7$ Hz, 1H, H-3bii); ^{13}C NMR (400 MHz, DMSO) δ_{C} 170.7 (C, C-2b), 161.9 (d, $J = 238.8$ Hz, C, C-4c), 160.6 (C, C-3), 155.9 (C, C-5a), 154.4 (C, C-2), 138.2 (C, C-7), 135.9 (d, $J = 2.8$ Hz, C, C-1c), 132.0 (C, C-10*), 130.0 (2C, CH, C-3a/7a), 129.5 (C, C-9*), 129.2 (2C, CH, d, $J = 8.4$ Hz, C-2c/6c), 128.4 (CH, C-5), 127.2 (C, C-2a), 119.4 (CH, C-6), 115.6 (2C, CH, d, $J = 21.7$ Hz, C-3c/5c), 115.1 (2C, CH, C-4a/6a), 111.4 (CH, C-8), 62.6 (CH, C-5b), 38.0 (CH₂, C-1a), 32.8 (CH₂, C-3b); HRMS (m/z): calc. for C₂₄H₁₈FN₃O₃SNa (M + Na)⁺: 470.0951, found: 470.0947. *indicates that assignments are interchangeable.

(B6k) 3-(4-hydroxybenzyl)-7-(2-(4-methoxyphenyl)-4-oxothiazolidin-3-yl)quinoxalin-2(1H)-one, yellow solid; mp 194-196 °C; UV λ_{max} (MeOH) nm (log ϵ) 232 (2.91), 348 (2.56); IR ν_{max} 3200 (NH), 1659 (C=O), 1609, 1510 cm⁻¹; ^1H NMR (400 MHz, DMSO) δ_{H} 12.32 (s, 1H, H-1), 9.21 (d, $J = 3.5$ Hz, 1H, H-8a), 7.60 (d, $J = 8.3$ Hz, 1H, H-5), 7.30 (d, $J = 8.4$ Hz, 2H, H-3a/7a), 7.27 (bs, 1H, H-8), 7.17 (d, $J = 8.3$ Hz, 1H, H-6), 7.06 (d, $J = 8.3$ Hz, 2H, H-2c/6c), 6.81 (d, $J = 8.4$ Hz, 2H, H-4a/6a), 6.63 (d, $J = 8.3$ Hz, 2H, H-3c/5c), 6.52 (s, 1H, H-5b), 4.02 (d, $J = 15.8$ Hz, 1H, H-3bi), 3.93 (d, $J = 8.3$ Hz, 2H, H-1a), 3.92 (d, $J = 15.8$ Hz, 1H, H-3bii), 3.67 (s, 3H, H-8c); ^{13}C NMR (400 MHz, DMSO) δ_{C} 170.7 (C, C-2b), 160.6 (C, C-3), 159.3 (C, C-4c), 155.9 (C, C-5a), 154.4 (C, C-2), 138.4 (C, C-7), 131.9 (C, C-9*), 131.1 (C, C-10*), 130.0 (2C, CH, C-2c/6c), 129.5 (C, C-1c), 128.5 (2C, CH, C-3a/7a), 128.3 (CH, C-5), 127.3 (C, C-2a), 119.7 (CH, C-6), 115.1 (2C, CH, C-3c/5c), 114.1 (2C, CH, C-4a/6a), 111.5 (CH, C-8), 63.1 (CH, C-5b), 55.1 (CH₃, C-8c), 38.1 (CH₂, C-1a), 32.9 (CH₂, C-3b); HRMS (m/z): calc. for C₂₅H₂₀N₃O₄S (M + H)⁺: 458.1175, found: 458.1187. *indicates that assignments are interchangeable.

(B6l) 3-(4-hydroxybenzyl)-7-(2-(4-nitrophenyl)-4-oxothiazolidin-3-yl)quinoxalin-2(1H)-one, yellow solid; mp 260-262 °C; UV λ_{max} (MeOH) nm (log ϵ) 233 (2.58), 344 (2.37); IR ν_{max} 3185 (NH), 1660 (C=O) cm^{-1} ; ^1H NMR (400 MHz, DMSO) δ_{H} 12.33 (s, 1H, H-1), 9.18 (s, 1H, H-8a), 8.14 (d, J = 8.1 Hz, 2H, H-3c/5c), 7.68 (d, J = 8.1 Hz, 2H, H-2c/6c), 7.62 (d, J = 8.4 Hz, 1H, H-5), 7.32 (bs, 1H, H-8), 7.23 (d, J = 8.4 Hz, 1H, H-6), 7.05 (d, J = 7.7 Hz, 2H, H-3a/7a), 6.74 (s, 1H, H-5b), 6.63 (d, J = 7.7 Hz, 2H, H-4a/6a), 4.12 (d, J = 15.8 Hz, 1H, H-3bi), 3.94 (d, J = 15.8 Hz, 1H, H-3bii), 3.92 (bs, 2H, H-1a); ^{13}C NMR (400 MHz, DMSO) δ_{C} 170.8 (C, C-2b), 160.8 (C, C-3), 155.9 (C, C-2), 154.4 (C, C-5a), 147.5 (C, C-4c), 147.3 (C, C-1c), 137.9 (C, C-7), 132.1 (C, C-9*), 129.9 (2C, CH, C-3a/7a), 129.6 (C, C-10*), 128.6 (CH, C-5), 128.0 (2C, CH, C-2c/6c), 127.2 (C, C-2a), 124.1 (2C, CH, C-3c/5c), 118.9 (CH, C-6), 115.1 (2C, CH, C-4a/6a), 110.9 (CH, C-8), 62.1 (CH, C-5b), 38.0 (CH₂, C-1a), 32.6 (CH₂, C-3b); HRMS (m/z): calc. for C₂₄H₁₇N₄O₅S (M + H)⁺: 473.0920, found: 473.0935. *indicates that assignments are interchangeable.

6.2.2 *In vitro* antimicrobial studies

The microbial cultures were grown overnight at 37 °C in nutrient broth (UKZN Biolab, South Africa), adjusted to 0.5 McFarland standard using distilled water and lawn inoculated onto Mueller-Hinton agar (MHA) plates. A volume of 10 μL of each sample (21.08 - 49.20 μM , 1 mL DMSO) was inoculated onto antibiotic assay discs (6 mm diameter) and placed on the MHA plates which were incubated overnight at 37 °C for 24 hours. After the incubation period, zones of inhibition were measured in mm. Compounds showing an inhibition zone of > 9 mm were selected to determine their MBC values using the broth dilution assay with ampicillin and ciprofloxacin as

the controls following the method in Andrews (2001). Compounds **B5a-c**, **B6a-c**, **B6f-h**, **B6j** and **B6k** were chosen for the broth dilution method to determine their MBCs.

For the broth dilution method, the microbial cultures (adjusted to 0.5 McFarland) were prepared as described previously for the disc diffusion method. The test compounds were dissolved in DMSO (10 mg mL^{-1}) and subject to a 50% serial dilution in 1 mL Eppendorf tubes with Mueller-Hinton Broth (MHB), inoculated with bacterial cultures ($20 \text{ }\mu\text{L}$) and then incubated at 37°C for 18 h. The total volume in each Eppendorf was $200 \text{ }\mu\text{L}$. A volume of $10 \text{ }\mu\text{L}$ of each dilution was spotted on MHA plates and incubated at 37°C for 18 h to determine the MBC (μM). Ampicillin, ciprofloxacin and tioconazole served as the standard drugs for the antimicrobial and antifungal studies respectively. All experiments were performed in duplicate.

6.2.3 DPPH radical scavenging activity (*in vitro* antioxidant activity)

The total free radical scavenging activity of the tested compounds was determined and compared to that of ascorbic acid using a slightly modified method described by Tuba and Gulcin (2008). A 0.3 mM solution of DPPH was prepared in methanol and $500 \text{ }\mu\text{L}$ added to $50 \text{ }\mu\text{L}$ of the compounds (dissolved in DMSO) at different concentrations ($50\text{--}200 \text{ }\mu\text{g mL}^{-1}$). These solutions were mixed and incubated in the dark for 30 min at room temperature. Absorbance was then measured at 517 nm against a blank sample lacking scavenger.

6.2.4 Antidiabetic activity

In vitro α -glucosidase inhibitory activity

The α -glucosidase inhibitory activity was determined according to the method described by Ademiluyi *et al.* (2013) with slight modifications. Briefly, 50 μ L of each compound or acarbose dissolved in DMSO at different concentrations (50-200 μ g mL⁻¹), was incubated with 100 μ L of 1.0 U mL⁻¹ α -glucosidase solution in 100 mM phosphate buffer (pH 6.8) at 37 °C for 15 min. Thereafter, 50 μ L of pNPG solution (5 mM) in 100 mM phosphate buffer (pH 6.8) was added and the mixture incubated at 37 °C for 20 min. The absorbance of the released *p*-nitrophenol was measured at 405 nm and the inhibitory activity expressed as a percentage of the control sample without inhibitors.

In vitro α -amylase inhibitory activity

The α -amylase inhibitory activity was determined according to the method described by Shai *et al.* (2010) with slight modifications. A volume of 50 μ L of each compound dissolved in DMSO or acarbose at different concentrations (50-200 μ g mL⁻¹) was incubated with 100 μ L of porcine pancreatic amylase (2 U mL⁻¹) in 100 mM phosphate buffer (pH 6.8) at 37 °C for 20 min. 50 μ L of 1 % starch dissolved in 100 mM phosphate buffer (pH 6.8) was then added to the reaction mixture and incubated at 37 °C for 1 h. 100 μ L of DNS colour reagent was then added and boiled for 10 min. The absorbance of the resulting mixture was measured at 540 nm and the inhibitory activity expressed as a percentage of the control sample without inhibitors. All assays were carried out in triplicate.

6.3 Results and discussion

Our synthetic design incorporates two fundamental methodologies; microwave irradiation and conventional synthesis. This project was aimed at synthesizing hybrid molecules of quinoxaline, amino acid and thiazolidine core structures. Variation was introduced in the molecules at the thiazolidine ring by varying the aromatic aldehydes used to form the thiazolidine moiety and in the amino acid side chains at position 3 on the quinoxaline ring by using different amino acids. The phenyl ring on the thiazolidine moiety was either unsubstituted or substituted at the *para* position with an electron donating methoxy group or electron withdrawing groups (F and NO₂). We used three different amino acids, valine (aliphatic), methionine (sulfur based) and tyrosine (aromatic).

6.3.1 Chemistry

The quinoxaline-thiazolidine-amino acid hybrids were synthesized in a four-step reaction. This reaction series first involved esterification of the amino acids **B1a-c** with thionyl chloride and methanol and then an aromatic nucleophilic substitution of the fluorine on 1-fluoro-2,4-dinitrobenzene **B3** with the various amino acid esters **B2a-c** under mildly basic conditions forming the amino acid ester 2,4-dinitrobenzene intermediates **B4a-c**. Reduction of the nitro groups and formation of the quinoxalines were carried out in a single step with Pd/C in the presence of H₂ and methanol. Under microwave irradiation, the thiazolidine ring was formed with the primary amino group in the quinoxaline intermediates with thioglycolic acid and the four different aldehydes forming the target molecules as racemic mixtures **B6a-l** (Scheme 6-1).

Formation of the Schiff base with aldehydes and further cyclisation to thiazolidines with thioglycolic acid was carried out in a single step under microwave conditions. An attempt to form the product by the conventional method, first forming the Schiff base with aldehydes and subsequent cyclisation with thioglycolic acid did not work. However, the microwave reaction was carried out within 10-45 minutes depending on the different substituents used (**Table 6-1**).

6.3.2 Structural elucidation

The synthesized products were characterized using NMR and MS analysis. Using **B6j** as a representative sample, ^1H and ^{13}C NMR resonances were unambiguously assigned as indicated below. The quinoxaline core structure contained four proton resonances at δ_{H} 12.31 for the H-1 amino group. The aromatic protons H-5, H-6 and H-8 appeared at δ_{H} 7.61 (d, $J = 8.7$ Hz), δ_{H} 7.19 (dd, $J = 8.7, 2.2$ Hz) and δ_{H} 7.27 (d, $J = 2.2$ Hz) respectively. The NH-1 resonance was distinguished from the OH-8a resonance at δ_{H} 9.18 since it showed a NOESY correlation to H-8. The resonances at δ_{C} 138.2, 132.0 and 129.5 all showed correlations to H-5 and were assigned to carbon resonances on the same ring. The most deshielded resonance (δ_{C} 138.2) was assigned to C-7 and the resonance at δ_{C} 129.5 was assigned to C-9 due to a HMBC correlation with H-6. The remaining resonance at δ_{C} 132.0 was assigned to C-10.

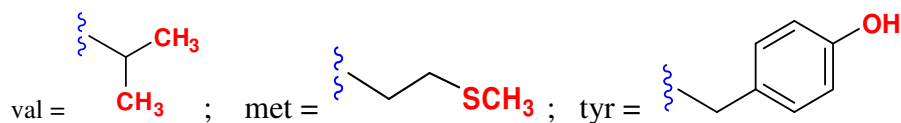
There were five deshielded carbon resonances between δ_{C} 154.4 and 170.7. The resonances at δ_{C} 154.4 and 160.6 both showed HMBC correlations to H-1a at δ_{H} 3.93 and were assigned to C-2 and C-3 respectively, the latter assigned due to an HMBC correlation to H-5. The resonance at δ_{C} 170.7 showed HMBC correlations to H-3bi, H-3bii and H-5b and was assigned to C-2b. The H-

3bi and H-3bii resonances appeared as a pair of doublets with geminal coupling of 15.7 Hz and H-5b occurred as a singlet. C-5a was assigned to δ_c 155.9 due to an HMBC correlation with H-4a/6a and H-3a/7a. The remaining carbon resonance of the five between δ_c 154.4 and 170.7 was a doublet carbon resonance with $J = 238.8$ Hz and was assigned to the carbon bearing the fluorine atom (C-4c).

Table 6-1 Yields and duration of microwave synthesis for the amino acid linked quinoxaline-thiazolidinones

Entry	R*	R ₁	Yield d (%)	Time (min)
B5a	val	-	-	-
B5b	met	-	-	-
B5c	tyr	-	-	-
B6a	val	Ph	90	10
B6b	val	4-F Ph	85	10
B6c	val	4-OMe Ph	82	30
B6d	val	4-NO ₂ Ph	80	45
B6e	met	Ph	90	10
B6f	met	4-F Ph	86	10
B6g	met	4-OMe Ph	83	30
B6h	met	4-NO ₂ Ph	80	45
B6i	tyr	Ph	87	10
B6j	tyr	4-F Ph	90	10
B6k	tyr	4-OMe Ph	82	30
B6l	tyr	4-NO ₂ Ph	85	45

NR: no reaction; * amino acid side chain;



The aromatic protons of the benzyl group H-3a/7a and H-4a/6a each occurred as doublets at δ_H 7.08 and δ_H 6.64 respectively with coupling constants of 8.5 Hz. The singlet C-2a and C-5a resonances occurred at δ_C 127.2 and δ_C 155.9 respectively. The H-3c/5c and H-2c/6c proton resonances each occurred as doublet doublets with coupling constants of $J_{H-3c/H-5c,F} = J_{H-3c/H-5c,H-2c/6c} = 8.6$ Hz, $J_{H-2c/6c,H-3c/5c} = 8.6$ Hz and $J_{H-2c/6c,F} = 5.4$ Hz, typical for a *para* fluorinated aromatic moiety (Gopaul et al., 2016).

Selected HMBC correlations used in the structural elucidation of **B6j** are provided in **Figure 6-1**.

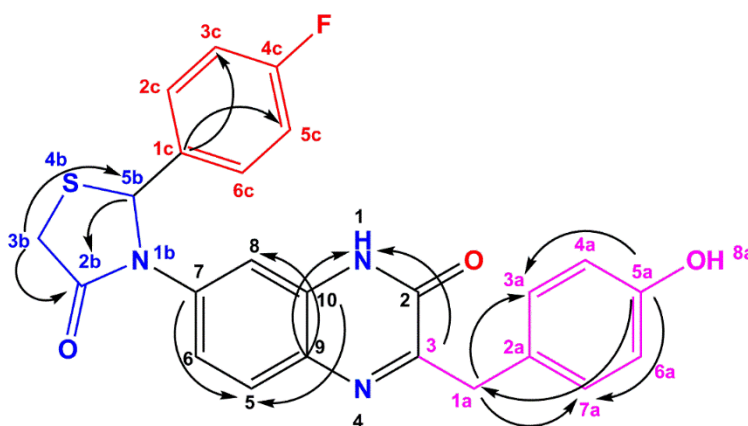


Figure 6-1 Selected HMBC correlations of compound **B6j** (H→C)

6.3.3 Antimicrobial activity

The tested compounds were evaluated for their antifungal activity against *Candida albicans* (ATCC 10231) with tioconazole as the reference drug and antibacterial activity against two Gram +ve strains, *S. aureus* (ATCC 25923) and methicillin resistant *S. aureus* (MRSA)(ATCC BAA-1683) and three Gram -ve strains (*Escherichia coli* (ATCC 25922), *K. pneumonia* (ATCC 31488) and *Pseudomonas aeruginosa* (ATCC 27853)) using ciprofloxacin and ampicillin as standards.

The disc diffusion assay was used as an initial screen to select potentially active compounds. Compounds showing a zone of inhibition >8 mm were chosen to determine their MBC values. Compounds **B5a-c**, **B6a-c**, **B6f-h**, **B6j** and **B6k** all satisfied this criterion and their MBC values were further explored.

Table 6-2 Antimicrobial activity of the synthesized compounds, MBCs in μM

Compound	Gram +ve bacteria		Gram -ve bacteria			Fungi
	<i>S. aureus</i>	MRSA	<i>E. coli</i>	<i>P. aeruginosa</i>	<i>K. pneumoniae</i>	<i>C. albicans</i>
B5a	-	-	-	-	658.6	164.7
B5b	249.0	498.0	-	-	-	62.3
B5c	73.1	-	-	-	-	438.5
B6a	-	-	851.2	-	-	-
B6b	101.4	38.0	202.9	405.7	811.4	50.7
B6c	49.2	393.4	-	196.7	786.9	-
B6f	23.4	93.7	46.8	70.3	11.7	35.1
B6g	90.9	34.1	181.9	136.4	363.8	545.6
B6h	-	-	-	-	706.2	353.1
B6j	43.5	87.0	32.6	21.7	87.0	65.2
B6k	15.9	63.8	21.2	680.1	-	85.0
Ampicillin	55.9	894.4	447.2	1788.7	447.2	447.2
Ciprofloxacin	1.8	7.4	1.8	1.8	3.7	1.8
Tioconazole	-	-	-	-	-	100.8

- denotes that the compounds were inactive at the highest concentration tested. The shaded values indicate activity < 100 μM . Highlighted values indicate the best results.

Compounds **B6b**, **B6f- B6g** and **B6j** showed broad-spectrum antimicrobial activity, being active against all bacterial strains tested against (**Table 6-2**). Of these active compounds, **B6b**, **B6f** and **B6j** contained a 4-fluorobenzaldehyde moiety on the thiazolidinone ring and were active regardless of the amino acid residue present at C-3 on the core structure. When a 4-methoxybenzaldehyde moiety was present at the same position, only **B6g** containing a methionine residue showed broad spectrum activity. Compounds **B6f** and **B6j** with methionine and tyrosine

residues were particularly active having MBC values < 100 μM against all the strains tested against. It is worth noting that **B6b** and **B6g** were active at concentrations < 40 μM against MRSA. The best activity was seen with **B6f**, being active against *K. pneumonia* at three times that of ciprofloxacin. In general, the activity of the synthesized compounds was better than that of ampicillin, but 10 fold or greater than that of ciprofloxacin.

Compounds **B6b**, **B6f** and **B6j** discussed above also showed good antifungal activity, being active at < 100 μM against *C. albicans* better than the control, tioconazole, active at 100.8 μM against *C. albicans*. The other quinoxaline-thiazolidine hybrid showing activity at < 100 μM against *C. albicans* was **B6k** with a 4-methoxybenzaldehyde moiety on the thiazolidine ring and a tyrosine unit at C-3. The quinoxaline core structure with a methionine residue at C-3 (**B5b**) also showed good antifungal activity, being active at 62.3 μM .

The antibacterial and antifungal activity of the synthesized hybrid compounds showed better activity than compounds with either quinoxaline or thiazolidine in its core structure (Ali et al., 2015; Anh et al., 2015; Issa et al., 2015; Krishna et al., 2015; Liu et al., 2011).

Antioxidant activity

The free radical scavenging activity of all synthesized amino acid linked thiazolidine-quinoxaline compounds **B5a-5c** and **B6a- B6l** was carried out in presence of the stable free radical (1,1-diphenyl-2-picrylhydrazyl) DPPH using ascorbic acid (AA), as a positive control. Although a number of methods are available for the determination of the antioxidant activity, the DPPH

method is very common, rapid and has been shown to be one of the most appropriate (Bondet et al., 1997).

There was no real trend in the structure of the compounds and their antioxidant activity. Two of the four compounds with a tyrosine residue and *para* methoxybenzaldehyde (**B6k**) or *para* nitrobenzaldehyde moiety (**B6l**) on the thiazolidine ring and a third compound with a methionine residue and a *para* nitrobenzaldehyde moiety (**B6h**) on the thiazolidine ring showed very good results with IC₅₀ values of 19.60, 10.53 and 28.95 μ M respectively compared to the standard, ascorbic acid at 16.86 μ M (**Table 6-3**).

Table 6-3 Antioxidant activity of the synthesized compounds, IC₅₀ (μ M)

Compound	DPPH (IC ₅₀ (μ M))	Compound	DPPH (IC ₅₀ (μ M))
B5a	469.68 \pm 304.64 ^{abc}	B6f	155.74 \pm 3.99 ^{ab}
B5b	756.87 \pm 9.95 ^{bc}	B6g	1307.26 \pm 594.08 ^d
B5c	131.10 \pm 27.23 ^{ab}	B6h	28.95 \pm 6.28 ^a
B6a	220.84 \pm 2.60 ^{abc}	B6i	550.05 \pm 14.72 ^{cd}
B6b	320.09 \pm 4.11 ^{abc}	B6j	239.16 \pm 9.44 ^{abc}
B6c	163.64 \pm 23.18 ^{ab}	B6k	19.60 \pm 3.23 ^a
B6d	162.19 \pm 23.69 ^{ab}	B6l	10.53 \pm 1.20 ^a
B6e	47.82 \pm 4.34 ^{ab}	-	-
Ascorbic acid	16.86 \pm 9.26 ^a		

Data are presented as mean \pm SD values of triplicate determinations.

^{a-d} Different letters stand for significantly different values from each other within a column (Tukey's-HSD multiple range *post hoc* test, $p < 0.05$); the same letters stand for non-significant difference. The shaded cells indicate IC₅₀ values of $< 30 \mu$ M. Highlighted values indicate the best results.

6.3.4 Antidiabetic activity (α -glucosidase and α -amylase activity)

Among the synthesized compounds, **B5c**, **B6d**, **B6g** and **B6k** showed *in vitro* enzymatic inhibitory activity (**Table 4**). Compounds **B6d** and **B6k** showed significant α -glucosidase activity with IC₅₀ values of 301.15 and 276.27 μ M respectively. Compound **B6d** contains a *para*

nitrobenzaldehyde group on the thiazolidinone moiety and a valine amino acid side chain at C-3 and **B6k** contains a *para* methoxybenzaldehyde moiety on the thiazolidinone portion with a tyrosine side chain at C-3.

The quinoxaline core structure with a tyrosine moiety at C-3 and a primary amine at C-7 (**B5c**) and **B6g** with a methionine residue at C-3 and a *para* methoxybenzaldehyde moiety on the thiazolidinone ring showed moderate α -glucosidase activity compared to acarbose, the reference drug, active in the same assay with a IC_{50} value of 135.34 μ M against α -glucosidase.

Compounds **B6d** and **B6k** whose structures are discussed above showed significant *in vitro* α -amylase inhibitory activity with IC_{50} values of 356.32 and 301.59 μ M respectively, approximately twice that of acarbose (IC_{50} 149.11 μ M) (**Table 6-4**).

Table 6-4 α - Glucosidase and α -amylase inhibition of the synthesized compounds, IC_{50} (μ M)

Compounds	α -Glucosidase	α -Amylase
	IC_{50} (μ M)	
B5c	411.67 \pm 0.21 ^b	-
B6d	301.15 \pm 0.86 ^{bc}	356.32 \pm 3.32 ^a
B6g	428.72 \pm 1.64 ^d	-
B6k	276.27\pm2.90^c	301.59\pm2.27^a
Acarbose	135.34 \pm 0.09 ^a	149.11 \pm 4.28 ^a

Data are presented as mean \pm SD values of triplicate determinations.

^{a-d} Different letters stand for significantly different values from each other within a column (Tukey's-HSD multiple range *post hoc* test, $p < 0.05$); the same letters stand for non-significant difference.

6.4 Conclusion

This is the first report of a new synthetic procedure to synthesize a new class of amino acid linked thiazolidine-quinoxaline hybrid molecules. These molecules were synthesized by developing an

efficient, cost effective and short reaction *via* microwave methods. Compounds **B6f** and **B6j** were the most potent antimicrobials, **B6k** and **B6l** the most potent antioxidants and **B6d** and **B6k** were significant antidiabetic agents. Compound **B6k** showing good results in all three assays could be a good starting point for the design of lead compounds for the pharmaceutical industry.

6.5 References

- Ademiluyi, A. O., Oboh, G. Soybean phenolic-rich extracts inhibit key-enzymes linked to type 2 diabetes (α -amylase and α -glucosidase) and hypertension (angiotensin I converting enzyme) *in vitro*. *Exp. Toxicol. Pathol.*, **2013**, 65, 305-309.
- Aiyelabola, T. O., Ojo, T. A., Adebajo, A. C., Ogunlusi, G. O., Oyetunji, O., Akinkunmi, E. O., Adeoye, A. O. Synthesis, characterization and antimicrobial activities of some metal(II) amino acids' complexes. *Adv. Biol. Chem.*, **2012**, 2, 268-273.
- Ali, A., Hashem, A. Synthesis, reactions and biological activity of quinoxaline derivatives. *Am. J. Org. Chem.*, **2015**, 5(1), 14-56.
- Al-Marhabi, A. R., Abbas, H. S., Ammar, Y. A. Synthesis, characterization and biological evaluation of some quinoxaline derivatives: A promising and potent new class of antitumor and antimicrobial agents. *Molecules*, **2015**, 20, 19805-19822.
- Andrews, J. M. Determination of minium inhibitory concentration. *J. Antimicrob. Chemother.*, **2001**, 48(S1), 5-16.
- Anh, H. L. T., Cuc, N. T., Tai, B. H., Yen, P. H., Nhiem, N. X., Thao, D. T., Nam, N. H., Minh, C. V., Kiem, P. V., Kim, Y. H. *Molecules*, **2015**, 20, 1151-1160.
- Baumann, M., Baxendale, I. R. An overview of the synthetic routes to the best selling drugs containing 6-membered heterocycles. *Beilstein J. Org. Chem.*, **2013**, 9, 2265-2319.
- Bayuelo, A. M., Baldiris, R., Torres, J., Torres, J. E., Reyes, R. V. Theoretical study of the chemical reactivity and molecular quantum similarity in a series of derivatives of 2-adamantylthiazolidine-4-one using density functional theory and the topo-geometrical superposition approach. *Int. J. Quantum Chem.*, **2012**, 112, 2681-2687.
- Bondet, V., Brand-Williams, W., Berset, C. Kinetics and mechanisms of antioxidant activity using the DPPH free radical method. *LWT – Food Sci. Technol.*, **1997**, 30, 609-615.
- Davyt, D., Serra, G. Thiazole and oxazole alkaloids: Isolation and synthesis. *Mar. Drugs.*, **2010**, 8, 2755-2780.

- Demmer, C. S., Møller, C., Brown, P. M. G. E., Han, L., Pickering, D. S., Nielsen, B., Bowie, D., Frydenvang, K., Kastrup, J. S., Bunch, L. Binding mode of an α -amino acid-linked quinoxaline-2,3-dione analogue at glutamate receptor subtype GluK1. *ACS Chem. Neurosci.*, **2015**, 6, 845–854.
- Dhanaraj, C. J., Johnson, J. Metal complexes of quinoxaline derivatives: review (part-II). *Res. J. Chem. Sci.*, **2015**, 5(4), 64-84.
- Estela, R., Heranandez, D., Albericio, F., Alvarez, M. Directly linked polyazoles: Important moieties in natural products. *Synthesis*, **2005**, 12, 1907-1922.
- Faham, A. E., El-Massry, A. M., Amer, A., Gohar, Y. M. A versatile synthesis route to chiral quinoxaline derivatives from amino acids precursors. *Lett. Pept. Sci.*, **2002**, 9, 49-54.
- Fernanda, M. R. L., Clara, S. B. G., Teresa, M. V. D. P. M. Reactivity of sarcosine and 1,3-thiazolidine-4-carboxylic acid towards salicylaldehyde-derived alkynes and allenes. *Tetrahedron*, **2013**, 69, 10081-10090.
- Geronikaki, A. A., Pitta, E. P., Liaras, K. S. Thiazoles and thiazolidinones as antioxidants. *Curr. Med. Chem.*, **2013**, 20(36), 4460-4480.
- Gopaul, K., Koorbanally, N. A. Synthesis and structure elucidation of a series of chloroquinoline-2-chalcones by the Doebner–Miller reaction. *Magn. Reson. Chem.*, **2016**, 54(8), 677-683.
- Hashash, M. A., Rizk, S. A. Synthesis of novel antibacterial and antifungal α -amino acids and heterocyclic compounds. *Eur. Chem. Bull.*, **2013**, 2(9), 637-641.
- Holley, R. W., Holley, A. D. A new stepwise degradation of peptides. *J. Am. Chem. Soc.*, **1952**, 74(21), 5445-5448.
- Issa, D. A. E., Habib, N. S., Wahab, A. E. A. Design, synthesis and biological evaluation of novel 1,2,4-triazolo and 1,2,4-triazino[4,3- α]quinoxalines as potential anticancer and antimicrobial agents. *Med. Chem. Commun.*, **2015**, 6, 202-211.
- Katagiri, K., Yoshida, T., Sato, K. Quinoxaline antibiotics, in *Antibiotics III. Mechanism of action of antimicrobial and antitumour agents*, Corcoran, J. W., Hahn, F. E., Snell, J. F., Arora, K. L. (Eds), **1975**, Vol. 3, p. 234-251.
- Kotra, V., Pradeep, K., Vasanthi, R. Synthesis, characterization and pharmacological evaluation of some novel quinoxaline derived chalcones. *Pharma Chem.*, **2013**, 5(4), 301-307.
- Krishna, S. M., Padmalatha, Y., Ravindranath, L. K. Thiazolidinone as a core unit biological evaluation agent. *Int. J. Med. Pharm. Res.*, **2015**, 3(2), 999-1003.
- Liu, Y., Jing, F., Xu, Y., Xie, Y., Shi, F., Fang, H., Li, M., Xu, W. Design, synthesis and biological activity of thiazolidine-4-carboxylic acid derivatives as novel influenza neuraminidase inhibitors. *Bioorg. Med. Chem.*, **2011**, 19(7), 2342-2348.
- Lobana, T. S., Rani, A., Jassal, A. K., Jasinski, J. P. Reactivity of thiazolidine-2-thione towards CuI/CuII: Synthesis and structures of [3-(2-thiazolin-2-yl)thiazolidine-2-thione]copper(I) bromide and [bis(2,2-bipyridine)nitratocopper(II)] nitrate. *J. Chem. Sci.*, **2015**, 127(1), 149-153.

- Malik, S., Upadhyaya, P. K., Miglani, S. Thiazolidinediones: A plethora of biological load. *Int. J. PharmTech Res.*, **2011**, 3(1), 62-75.
- Mickevičienė, K., Baranauskaitė, R., Kantminienė, K., Stasevych, M., Porokhnyavets, O. K., Novikov, V. Synthesis and antimicrobial activity of *N*-substituted- β -amino acid derivatives containing 2-hydroxyphenyl, benzo[β]phenoxazine and quinoxaline moieties. *Molecules*, **2015**, 20, 3170-3189.
- Mishra, A., Nagwanshi, T. K., Sahu, R. L., Verma, L. K., Yadav, R. A review on quinoxaline - pharmacophore and derivatives with diverse biological properties. *World J. Pharm. Pharm. Sci.*, **2013**, 2(6), 6486-6506.
- Noolvi, M. N., Patel, H. M., Bhardwaj, V., Chauhan, A. Synthesis and *in vitro* antitumor activity of substituted quinazoline and quinoxaline derivatives: Search for anticancer agent. *Eur. J. Med. Chem.*, **2011**, 46, 2327-2346.
- Noorulla, S., Sreenivasulu, N. Antibacterial activity of novel substituted quinoxaline heterocycles with isoniazide. *Int. J. Res. Pharm. Biomed. Sci.*, **2011**, 2(3), 1100-1106.
- Padvi, P. A., Mahale, G. H., Pawar, D. E., Falak, C. S., Kendre, A. V. Synthesis and biological activity of quinoxaline derivatives. *World J. Pharm. Res.*, **2015**, 4(7), 1892-1900.
- Pai, N. R., Vishwasrao, S. G. A novel synthesis of quinoxaline- 6-carbaldehyde and its evaluation as potential antimicrobial agent. *Pharma Chem.*, **2011**, 3(6), 591-598.
- Patidar, A. K., Jeyakandan, M., Mobiya, A. K., Selvam, G. Exploring potential of quinoxaline moiety. *Int. J. PharmTech Res.*, **2011**, 3(1), 386-392.
- Pawar, P. Y., Bhise, S. B. Synthesis and antibacterial activity of some new quinoxalinedione derivatives. *Int. J. Chem. Sci.*, **2007**, 5(2), 700-710.
- Pawar, P. Y., Bhise, S. B. Synthesis of 6,7-bis[2-(substituted phenyl)-4-oxo-thiazolidin-3-yl]quinoxaline-2,3-(1*H*,4*H*)-diones as antitubercular agents. *J. Pharm. Res.*, **2008**, 7(4), 226-228.
- Puratchikody, A., Natarajan, R., Jayapal, M., Doble, M. Synthesis, *in vitro* antitubercular activity and 3D-QSAR of novel quinoxaline derivatives. *Chem. Biol. Drug Des.*, **2011**, 78, 988-998.
- Sachs, E. F., Nadler, A., Diederichsen, U. Triostin, a derived hybrid for simultaneous DNA binding and metal coordination. *Amino Acids*, **2011**, 41, 449-456.
- Sahoo, J., Mekap, S. K., Kumar, P. S. Synthesis, spectral characterization of some new 3-heteroaryl azo 4-hydroxy coumarin derivatives and their antimicrobial evaluation. *J. Taibah Univ. Sci.*, **2015**, 9, 187-195.
- Saxena, C. M., Saxena, A., Shukla, N. K. Synthesis and biological activities of some new amides of amino acid. *Am. Int. J. Res. Formal Appl. Nat. Sci.*, **2014**, 7(1), 88-90.
- Shai, L. J., Masoko, P., Mokgotho, M. P., Magano, S. R., Mogale, A. M., Boaduo, N., Eloff, J. N. Yeast α -glucosidase inhibitory and antioxidant activities of six medicinal plants collected in Phalaborwa, South Africa. *S. Afr. J. Bot.*, **2010**, 76, 465-470.

- Sharma, A., Suhas, R., Gowda, D. C. Ureas/Thioureas of benzo[d]isothiazole analog conjugated glutamic acid: Synthesis and biological evaluation. *Arch. Pharm. Chem. Life Sci.*, **2013**, 346, 359-366.
- Sharma, M. C. An insight into antimicrobial activity substituted benzimidazole derivatives through QSAR studies. *Drug Des.*, **2015**, 4(2), 1-7.
- Siddiqui, N., Arshad, M. F., Ahsan, W., Alam, M. S. Thiazoles: A valuable insight into the recent advances and biological activities. *Int. J. Pharm. Sci. Drug Res.*, **2009**, 1(3), 136-143.
- Singh, A. K., Mishra, G., Jyoti, K. Review on biological activities of 1,3,4-thiadiazole derivatives. *J. Appl. Pharm. Sci.*, **2011**, 1(5), 44-49.
- Singh, T. P., Sharma, P. K., Kaur, P. K., Mondal, S. C., Gupta, A. Pharmacological evaluation of thiazolidinone derivatives: A prespective review. *Pharma Chem.*, **2011**, 3(1), 194-206.
- Srivastava, S., Banerjee, J., Srestha, N. Quinoxaline as a potent heterocyclic moiety. *Int. Organization Sci. Res. J. Pharm.*, **2014**, 4(12), 17-27.
- Suhas, R., Chandrashekar, S., Gowda, D. C. Synthesis of elastin based peptides conjugated to benzisoxazole as a new class of potent antimicrobials - A novel approach to enhance biocompatibility. *Eur. J. Med. Chem.*, **2011**, 46, 704-711.
- Teresa, M. V. D. P. M. Exploiting azafulvenium methides chemistry. *ARKIVOC*, **2006**, 7, 89-104.
- Tuba, A. K., Gulcin, I. Antioxidant and radical scavenging properties of curcumin. *Chem. Biol. Interact.*, **2008**, 174, 27-37.
- Tung, C. L., Sun, C. M. Liquid phase synthesis of chiral quinoxalinones by microwave irradiation. *Tetrahedron Lett.*, **2004**, 45, 1159-1162.
- Vinay, V., Lakshika, K. A review on antimicrobial activity of 4-thiazolidinone derivatives. *Int. J. Res. Pharm Sci.*, **2011**, 1(1), 17-27.
- Waring, M. J. Echinomycin, triostion, and related antibiotics. *Antibiotics*, **1979**, 5(2), 173-194.
- Yang, L., Berk, S. C., Rohrer, S. P., Mosley, R. T., Guo, L., Underwood, D. J., Arison, B. H., Birzin, E. T., Hayes, E. C., Mitra, S. W., Parmar, R. M., Cheng, K., Wu, T. J., Butler, B. S., Foor, F., Pasternak, A., Pan, Y., Silva, M., Reidinger, R. M., Smith, R. G., Chapman, K., Schaeffer, J. M., Patchett, A. A. Synthesis and biological activities of potent peptidomimetics selective for somatostatin receptor subtype 2. *Proc. Natl. Acad. Sci.*, **1998**, 95, 10836-10841.
- Zhang, Y., Islam, M. D. A., McAlpine, S. R. Synthesis of the natural product marthiapeptide A. *Org. Lett.*, **2015**, 17, 5149-5151.

Chapter 7. Expedient synthesis, antimicrobial, antioxidant activities and docking study of 2-substituted methyl 1-(4-fluorophenyl)-1*H*-benzimidazole-5-carboxylates

* The compounds referred to in the chapter are referred to elsewhere in the thesis with an **C** preceding the number of the compound. For example **5a-v** is referred to as **C5a-v** elsewhere in the thesis.

Abstract

A library of 2-substituted fluorinated benzimidazoles (**C5a-C5v**) was synthesized by an easy, efficient, rapid and inexpensive route for the synthesis of benzimidazoles using microwave conditions. The synthesized compounds were tested for their antimicrobial and antioxidant behaviour. The benzimidazoles **C5p** and **C5r** showed strong antimicrobial (MBCs: 14-555 and 25-446 μM respectively) and antioxidant activities (IC_{50} : 386.55 and 306.71 μM respectively) compared to the standards used for comparison. Docking studies of **C5h** and **C5r** (one inactive and one active compound) into the active site of topoisomerase II DNA-gyrase were used to explain the crucial interaction with the Mn^{2+} ion in the active site of the enzyme for anti-bacterial activity.

Keywords: Benzimidazole, microwave, thermal, antimicrobial, antioxidant, docking.

7.1 Introduction

The development of new, robust, efficient and environmentally friendly chemical processes for the synthesis of *bis*-heterocyclic compounds is needed in the pharmaceutical and chemical industries (Dua et al., 2011; Jain et al., 2013). Greener and more sustainable chemical syntheses focus on minimal or no use of solvents or the use of water as a solvent, reduction of waste, use of ambient conditions, shortening of reaction times, and developing easy methods of product separation and purification.

Nitrogen containing compounds are important chemical compounds due to their numerous applications. The benzimidazole moiety has gained importance in recent years having anticancer, antiviral, antibacterial, antioxidant, antifungal, anthelmintic, antiparasitic, antimycobacterial, antidiabetic, antihypertensive, analgesic, antipsychotic, anticoagulant, cardiovascular, and anti-inflammatory properties (Vazquez et al., 2001; Tomic et al., 2004; Biron et al., 2006; Kuş et al., 2009; Narasimhan et al., 2010; Vyas et al., 2010; Kalyankar et al., 2012; Barot et al., 2013; Gurvinder et al., 2013; Jain et al., 2013; Yoon et al., 2014; Keri et al., 2015; Singla et al., 2015).

Benzimidazoles are generally synthesized by coupling reactions between *o*-phenylenediamines with carboxylic acids, carboxylic acid chlorides or aldehydes and in some cases esters and amides (Panda et al., 2012; Khanna et al., 2012; Prajapati et al., 2015; Saberi et al., 2015; Saleh et al., 2015; Rithe et al., 2015; Kattimani et al., 2015; Keri et al., 2015; Carvalho et al., 2015; Azizian et al., 2016). They are also synthesized from *o*-phenylenediamines and reagents other than acid derivatives or aldehydes (Khanna et al., 2012). When two moles of *o*-phenylenediamines are reacted with dicarboxylic acid derivatives, symmetric *bis*benzimidazoles are formed (Khanna et

al., 2012). These symmetric bisbenzimidazoles are also formed with *o*-phenylenediamines and hexachloro-2-propanone (Rezende et al., 2001) or with symmetric diacids or dialdehydes (Khanna et al., 2012). Symmetric bisbenzimidazoles are also synthesized with [1,1'-biphenyl]-3,3',4,4'-tetraamines and a number of different reagents (Khanna et al., 2012).

There have been numerous reports of benzimidazoles being synthesized using classical organic chemistry in the presence of Lewis acid catalysts containing Sn, Ti, Zr, Bi, In, Co, Ce, B, Zn and Hf (Zhang et al., 2007), Ir (Tateyama et al., 2016), La (Kamal et al., 2014), acetic acid (Jain et al., 2013) and *p*-toluenesulfonic acid (Xiangming et al., 2007; Funel et al., 2014), basic catalysts such as NaOH (Rajasekhar et al., 2010), KOH (Al-Mohammed et al., 2013), or inorganic salts for example NaHSO₃ (Jain et al., 2013) and Na₂S₂O₅ (Yoon et al., 2015). Although benzimidazoles are synthesized widely with the use of a catalyst, several of these catalysts are quite costly such as (TiCl₄, Ir, HfCl₄, Bi(NO₃)₅ and ZrCl₄) (Zhang et al., 2007). Although several synthetic procedures to the benzimidazoles use non-environmentally friendly solvents such as DMF (Yoon et al., 2015), CHCl₃ (Gupta Atyam et al., 2010) and toluene (Funel et al., 2014), other reported procedures have made use of greener solvents such as methanol and water (Borhade et al., 2012; Chen et al., 2012; Rao et al., 2014).

The grinding method (Banerjee et al., 2014), ultrasound (Patil et al., 2014) and visible light promoted (Park et al., 2014) were all used to synthesize benzimidazoles without the use of a catalyst. In recent years there has been much interest in microwave syntheses (Das et al., 2012; Gawande M et al., 2014; Jacob et al., 2012). Using microwave synthesis, benzimidazoles were synthesized without the use of catalysts and organic solvents (Abdullah et al., 2012; Eren et al.,

2014;). Its advantages are therefore that it is a green technique, cheaper, carried out in shorter times and uses less energy than conventional synthesis. Benzimidazoles were also synthesized under microwave conditions using NaHSO_3 as a catalyst (López et al., 2009).

In our study, we have synthesized fluorinated benzimidazole derivatives from the *o*-phenylenediamine (methyl 3-amino-4-(4-fluorophenylamino)benzoate) and various substituted aldehydes using three methods, conventional organic synthesis with a sodium metabisulphite catalyst and ethanol as solvent, the grinding method with iodine as a catalyst and under microwave conditions with no catalyst or solvent, and compared the yields and reaction times of these methods. We synthesized a total of twenty-two 2-substituted fluorinated benzimidazoles (**C5a-C5v**) and tested them for their antimicrobial and antioxidant activity.

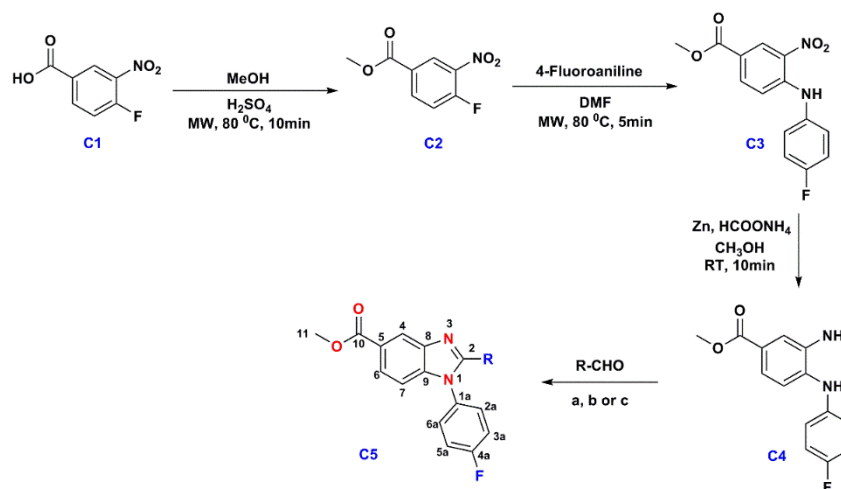
7.2 Experimental

7.2.1 General experimental procedures

All chemicals were supplied by Sigma-Aldrich *via* Capital Lab, South Africa. Organic solvents were redistilled and dried according to standard procedures. Silica gel 60 F₂₅₄ plates (Merck) were used for thin layer chromatography. Crude compounds were purified by column chromatography using silica gel (60-120 mesh) and a mobile phase of varying ratios of EtOAc : Hexane. Melting points were recorded using a Stuart Scientific SMP3 apparatus. UV spectra were obtained on a Varian Cary UV-VIS spectrometer in MeOH. IR spectra were recorded on a Perkin Elmer 100 FT-IR spectrometer with universal attenuated total reflectance sampling accessory.

Microwave assisted reaction: All reactions which involved microwave irradiation were performed using a CEM Discover, Explorer-12 Hybrid microwave. ^1H , ^{13}C and all 2D NMR spectra were recorded on a Bruker Avance instrument operating at 400 MHz. Chemical shifts are reported in δ values (ppm) relative to an internal standard of tetramethylsilane (TMS) and referenced to the solvent line of CDCl_3 (7.24 ppm for ^1H ; 77.0 ppm for ^{13}C), CD_3OD (3.31 ppm for ^1H ; 49.0 ppm for ^{13}C) or $\text{DMSO}-d_6$ (2.5 ppm for ^1H ; 39.5 ppm for ^{13}C). High-resolution mass data were obtained using a Bruker micro TOF-Q II ESI instrument operating at ambient temperature. The purity of the compounds were determined by analytical HPLC on a Shimadzu-20A5 fitted with a C8 (150mm x $5\mu\text{m}$ x 4.6) column using a mobile phase (A) of 0.1M KH_2PO_4 buffer and (B) methanol, with a linear gradient of 0 to 70% over a period of 60 minutes at a flow rate of 1 mL min^{-1} .

The general scheme for the reaction is shown below in **Scheme 7-1**.



Scheme 7-1 Synthesis of fluorinated benzimidazoles **C5a-v**; **a** MW $110\text{ }^\circ\text{C}$, 3-8 min; **b** grinding, I_2 (10 mol%), 5-45 min; **c** $\text{Na}_2\text{S}_2\text{O}_5$ (20 mol%), EtOH, reflux, 8-18 h

General procedure for the preparation of methyl 4-fluoro-3-nitrobenzoate (**C2**)

4-Fluoro-3-nitrobenzoic acid (0.5 g, 2.7 mmol) was dissolved in methanol (5 mL) and conc. H₂SO₄ (0.5 mL) at room temperature. The reaction mixture was heated with stirring in a 10 mL microwave process vial for 10 min at 80 °C. After completion of the reaction (as evident from TLC), the solvent was evaporated under reduced pressure, the reaction mixture basified by sodium bicarbonate and the aqueous layer extracted into ethyl acetate (3 × 5 mL). The organic layer was dried over anhydrous Na₂SO₄ and concentrated under reduced pressure to yield **C2** as a cream-colored powder (95%). ¹H NMR (CDCl₃, 400 MHz) δ 8.73 (1H, dd, *J* = 7.2, 2.2 Hz, H-2), 8.31 (1H, m, H-6), 7.38 (1H, dd, *J* = 10.2, 8.8 Hz, H-5), 3.95 (3H, s, H-8); ¹³C NMR (CDCl₃, 100 MHz) δ 164.1 (C-7), 158.1 (d, *J*_{CF} = 270.0 Hz, C-4), 137.3 (C-3), 136.5 (d, *J* = 9.7 Hz, C-6), 127.8 (C-2), 127.2 (d, *J* = 4.2 Hz, C-1), 118.8 (d, *J* = 21.2 Hz, C-5), 52.9 (C-8); ¹⁹F NMR (CDCl₃, 376.5 MHz) δ -110.55.

General procedure for the preparation of methyl 4-(4-fluorophenylamino)-3-nitrobenzoate (**C3**)

Methyl-4-fluoro-3-nitrobenzoate **C2** (0.5 g, 2.34 mmol) and 4-fluorophenyl aniline (0.36 mL, 2.34 mmol) were mixed in DMF (2 mL). The reaction mixture was subject to microwave irradiation with stirring in a 10 mL microwave process vial for 5 min at 80 °C. After completion of the reaction (monitored by TLC), the reaction mixture was washed with water (2 × 10 mL) followed by 10% Na₂CO₃ (10 mL). The organic layer was dried over anhydrous Na₂SO₄ and concentrated under reduced pressure to afford **C3** as a crude product. The solid was purified by column chromatography (30% ethyl acetate in hexane) to afford the desired product as a vermilion (reddish) solid in good yields (90%). ¹H NMR (CDCl₃, 400 MHz) δ 9.67 (1H, s, NH-10), 8.90

(1H, d, J = 2.0 Hz, H-2), 7.95 (1H, dd, J = 9.0, 2.0 Hz, H-6), 7.29 (2H, dd, J = 8.8, 4.7 Hz, H-2a/6a), 7.18 (2H, t, J = 8.8 Hz, H-3a/5a), 7.03 (1H, d, J = 9.0 Hz, H-5), 3.89 (3H, s, H-8); ^{13}C NMR (CDCl_3 , 100 MHz) δ 165.3 (C-7), 161.2 (d, J_{CF} = 245.8 Hz, C-4a), 146.4 (C-4), 136.0 (C-2), 133.5 (d, J = 3.3 Hz, C-1a), 132.1 (C-3), 129.24 (C-6), 127.5 (d, J = 8.5 Hz, 2C, C-2a/6a), 119.2 (C-1), 116.9 (d, J = 22.7 Hz, 2C, C-3a/5a), 115.3 (C-5), 52.2 (C-8); ^{19}F NMR (CDCl_3 , 376.5 MHz) δ -114.14.

General procedure for the preparation of methyl 3-amino-4-(4-fluorophenylamino) benzoate (C4)

Methyl 4-(4-fluorophenylamino)-3-nitrobenzoate **C3** (0.5 g, 1 mmol), Zn (0.06 g, 0.5 mmol) and ammonium formate (0.54 g, 5 mmol) were added to methanol (5 mL). The reaction mixture was stirred at room temperature for 10 min. Upon completion of the reaction (monitored by TLC), it was filtered through Celite 545 to remove the zinc. The filtrate was evaporated under reduced pressure and the solid purified by column chromatography (30% ethyl acetate in hexane) to afford the desired product as a brown solid in good yield (92%). ^1H NMR (CDCl_3 , 400 MHz) δ 7.50 (1H, d, J = 1.7 Hz, H-2), 7.47 (1H, dd, J = 8.2, 1.7 Hz, H-6), 7.03 (1H, d, J = 8.2 Hz, H-5), 6.99 (d, J = 8.3 Hz, 2H, H-2a/6a), 6.95 (2H, dd, J = 9.0, 8.3 Hz, H-3a/5a), 5.55 (s, 1H, NH-10), 3.85 (3H, s, H-8), 3.16 (2H, s, NH-9); ^{13}C NMR (CDCl_3 , 100 MHz) δ 167.0 (C-7), 158.3 (d, J_{CF} = 239.4 Hz, C-4a), 138.3 (C-1a), 137.1 (C-4), 136.0 (C-3), 123.6 (C-1), 122.6 (C-6), 120.6 (d, J = 7.7 Hz, 2C, C-2a/6a), 118.4 (C-2), 116.7 (C-5), 116.1 (d, J = 22.5 Hz, 2C, C-3a/5a), 51.8 (C-8); ^{19}F NMR (CDCl_3 , 376.5 MHz) δ -121.46.

General procedure for the preparation of fluorinated benzimidazole (C5a- C5v)

Microwave method

The mixture of methyl 3-amino-4-(4-fluorophenylamino) benzoate **C4** (1 mmol) and various aldehydes (1 mmol) were heated in a 5 mL microwave process vial for 5-10 min at 110 °C to obtain compounds (**C5a-C5v**). After completion of the reaction (monitored by TLC), the reaction mixture was washed with water (2 × 5 mL) followed by brine solution (10 mL). The aqueous layer was extracted into ethyl acetate (3 × 5 mL). The organic layer was dried over anhydrous Na₂SO₄, concentrated under reduced pressure and the obtained solid purified by column chromatography (30-50% ethyl acetate in hexane) to afford the desired product in good yield (85-96%).

Grinding (Mechanochemical) method

A mixture of methyl 3-amino-4-(4-fluorophenylamino) benzoate **C4** (1 mmol), various aldehydes (1 mmol), and iodine (10 mol %) were ground together using a mortar and pestle at room temperature between 5-45 min (**Table 1**). After completion of the reaction (confirmed by TLC), the mixture was treated with aqueous Na₂S₂O₃. The aqueous layer was extracted with ethyl acetate (3 × 5 mL), and the organic layer dried over anhydrous Na₂SO₄ and concentrated under reduced pressure. The solid obtained was purified by column chromatography (hexane/ethyl acetate) to afford the desired product (**C5a-C5v**) in moderate to good yields (10-56%).

Conventional method

3-Amino-4-(4-fluorophenylamino) benzoate **C4** (1 mmol), various aldehydes (1 mmol) and Na₂S₂O₅ (20 mol%) was refluxed in ethanol (20 mL) between 8-18h. After completion of the reaction (as evident from TLC), the solvent was evaporated under reduced pressure and the crude

mass washed with water (2×10 mL). The aqueous layer was extracted with ethyl acetate (3×25 mL), and the organic layer dried over anhydrous Na_2SO_4 and concentrated under reduced pressure to afford **C5a-C5v** as crude products. The solid obtained was purified by column chromatography (hexane/ethyl acetate) to afford the desired product in good yields (60-90%).

(C5a) methyl 1-(4-fluorophenyl)-2-phenyl-1*H*-benzo[*d*]imidazole-5-carboxylate, white solid (90% yield); Purity 99%; mp 160-162 °C; UV λ_{max} (MeOH) nm (log ϵ) 247 (2.63), 302 (2.19); IR ν_{max} 3069 (CH), 1713 (C=O), 1357 (C-F), 1185 (C-O) cm^{-1} ; ^1H NMR (CDCl_3 , 400 MHz) δ 8.58 (1H, bs, H-4), 7.98 (1H, d, $J = 8.6$ Hz, H-6), 7.54 (2H, d, $J = 7.4$ Hz, H-2b/6b), 7.38 (1H, m, H-4b), 7.32 (2H, m, H-2a/6a), 7.29 (2H, m, H-3b/5b), 7.23 (1H, m, H-7), 7.20 (2H, m, H-3a/5a), 3.94 (3H, s, H-11); ^{13}C NMR (CDCl_3 , 100 MHz) δ 167.4 (C-10), 162.4 (d, $J_{\text{CF}} = 248.6$ Hz, C-4a), 154.0 (C-2), 142.2 (C-8), 140.2 (C-9), 132.2 (d, $J = 3.3$ Hz, C-1a), 130.0 (C-4b), 129.2 (C-6b), 129.1 (d, $J = 8.7$ Hz, 2C, C-2a/6a), 129.07 (C-2b), 129.0 (C-1b), 128.5 (2C, C-3b/5b), 125.4 (C-5), 125.1 (C-6), 122.2 (C-4), 117.1 (d, $J = 22.7$ Hz, 2C, C-3a/5a), 109.3 (C-7), 52.1 (C-11); ^{19}F NMR (CDCl_3 , 376.5 MHz) δ -108.08; HRMS (m/z): 347.1198 M^+ (calculated for $\text{C}_{21}\text{H}_{16}\text{FN}_2\text{O}_2$: 347.1196).

(C5b) methyl 1,2-bis(4-fluorophenyl)-1*H*-benzo[*d*]imidazole-5-carboxylate, yellow solid (90% yield); Purity 98%; mp 130-132 °C; UV λ_{max} (MeOH) nm (log ϵ) 247 (2.7), 301 (2.4); IR ν_{max} 3071 (CH), 1711 (C=O), 1379 (C-F), 1157 (C-O) cm^{-1} ; ^1H NMR (CDCl_3 , 400 MHz) δ 8.56 (1H, bs, H-4), 7.99 (1H, dd, $J = 8.6, 1.4$ Hz, H-6), 7.54 (2H, dd, $J = 8.8, 5.2$ Hz, H-2b/6b), 7.29 (2H, dd, $J = 8.9, 4.8$ Hz, H-2a/6a), 7.23 (2H, m, H-3a/5a), 7.19 (1H, d, $J = 8.6$ Hz, H-7), 7.02 (2H, t, $J = 8.8$ Hz, H-3b/5b), 3.95 (3H, s, H-11); ^{13}C NMR (CDCl_3 , 100 MHz) δ 167.3 (C-10), 163.7 (d,

$J_{\text{CF}} = 250.4$ Hz, C-4b), 162.5 (d, $J_{\text{CF}} = 249.2$ Hz, C-4a), 153.0 (C-2), 142.1 (C-8), 140.2 (C-9), 132.2 (d, $J = 3.2$ Hz, C-1a), 131.5 (d, $J = 8.6$ Hz, 2C, C-2b/6b), 129.2 (d, $J = 8.7$ Hz, 2C, C-2a/6a), 125.6 (C-5), 125.2 (C-6), 122.1 (C-4), 117.3 (d, $J = 23.0$ Hz, 2C, C-3a/5a), 115.8 (d, $J = 21.8$ Hz, C-3b/5b), 110.0 (C-7), 52.2 (C-11); ^{19}F NMR (CDCl_3 , 376.5 MHz) δ -110.71, -109.46; HRMS (m/z): 365.1111 M^+ (calculated for $\text{C}_{21}\text{H}_{15}\text{F}_2\text{N}_2\text{O}_2$: 365.1102). * C-1b could not be detected.

(C5c) methyl 2-(4-chlorophenyl)-1-(4-fluorophenyl)-1H-benzo[d]imidazole-5-carboxylate, yellow solid (86% yield); Purity 96%; mp 185-187 °C; UV λ_{max} (MeOH) nm (log ϵ) 251 (3.23), 304 (2.85); IR ν_{max} 3059 (CH), 1708 (C=O), 1357 (C-F), 1181 (C-O), 729 (C-Cl) cm^{-1} ; ^1H NMR (CDCl_3 , 400 MHz) δ 8.58 (1H, bs, H-4), 8.01 (1H, d, $J = 8.5$ Hz, H-6), 7.51 (2H, d, $J = 8.4$ Hz, H-2b/6b), 7.31 (4H, d, $J = 8.5$ Hz, H-2a/6a, H-3b/5b), 7.25 (2H, d, $J = 6.44$ Hz, H-3a/5a), 7.20 (1H, d, $J = 8.8$ Hz, H-7), 3.95 (3H, s, H-11); ^{13}C NMR (CDCl_3 , 100 MHz) δ 167.3 (C-10), 162.5 (d, $J_{\text{CF}} = 249.2$ Hz, C-4a), 152.8 (C-2), 142.0 (C-8), 140.1 (C-9), 136.5 (C-4b), 132.1 (d, $J = 3.0$ Hz, C-1a), 130.7 (2C, C-2b/6b), 129.1 (d, $J = 8.7$ Hz, 2C, C-2a/6a), 128.9 (C-3b), 127.4 (C-1b), 125.7 (C-5), 125.3 (C-6), 122.2 (C-4), 117.3 (d, $J = 22.8$ Hz, 2C, C-3a/5a), 110.1 (C-7), 52.2 (C-11); ^{19}F NMR (CDCl_3 , 376.5 MHz) δ -110.35; HRMS (m/z): 381.0818 M^+ (calculated for $\text{C}_{21}\text{H}_{15}\text{ClFN}_2\text{O}_2$: 381.0806).

(C5d) methyl 2-(4-bromophenyl)-1-(4-fluorophenyl)-1H-benzo[d]imidazole-5-carboxylate, cream coloured solid (82% yield); Purity 97%; mp 203-205 °C; UV λ_{max} (MeOH) nm (log ϵ) 253 (3.28), 305 (2.92); IR ν_{max} 3072 (CH), 1707 (C=O), 1357 (C-F), 1153 (C-O), 523 (C-Br) cm^{-1} ; ^1H NMR (CDCl_3 , 400 MHz) δ 8.57 (1H, s, H-4), 8.00 (1H, dd, $J = 8.6, 1.4$ Hz, H-6), 7.47 (2H, d, $J = 8.6$ Hz, H-3b/5b), 7.42 (2H, d, $J = 8.6$ Hz, H-2b/6b), 7.29 (2H, dd, $J = 9.0, 4.8$ Hz, H-2a/6a), 7.23

(2H, t, $J = 10.8$ Hz, H-3a/5a), 7.19 (1H, d, $J = 8.6$ Hz, H-7), 3.95 (3H, s, H-11); ^{13}C NMR (CDCl_3 , 100 MHz) δ 167.3 (C-10), 162.6 (d, $J_{\text{CF}} = 249.2$ Hz, C-4a), 152.8 (C-2), 142.1 (C-8), 140.2 (C-9), 132.2 (d, $J = 3.3$ Hz, C-1a), 131.9 (2C, C-3b/5b), 130.9 (2C, C-2b/6b), 129.1 (d, $J = 8.7$ Hz, 2C, C-2a/6a), 127.9 (C-5), 125.7 (C-1b), 125.4 (C-6), 124.9 (C-4b), 122.2 (C-4), 117.4 (d, $J = 22.8$ Hz, 2C, C-3a/5a), 110.1 (C-7), 52.2 (C-11); ^{19}F NMR (CDCl_3 , 376.5 MHz) δ -110.53; HRMS (m/z): 425.0310 M^+ (calculated for $\text{C}_{21}\text{H}_{15}\text{BrFN}_2\text{O}_2$: 425.0301).

(C5e) methyl 1-(4-fluorophenyl)-2-(4-(trifluoromethyl)phenyl)-1H-benzo[d]imidazole-5-carboxylate, white solid (84% yield); Purity 98%; mp 171-173 °C; UV λ_{max} (MeOH) nm (log ϵ) 250 (2.83), 304 (2.5); IR ν_{max} 3081 (CH), 1712 (C=O), 1358 (C-F), 1196 (C-O) cm^{-1} ; ^1H NMR (CDCl_3 , 400 MHz) δ 8.59 (1H, bs, H-4), 8.01 (1H, dd, $J = 8.6, 1.4$ Hz, H-6), 7.68 (2H, d, $J = 8.3$ Hz, H-3b/5b), 7.58 (2H, d, $J = 8.3$ Hz, H-2b/6b), 7.30 (2H, dd, $J = 8.9, 4.8$ Hz, H-2a/6a), 7.24 (2H, t, $J = 10.5$ Hz, H-3a/5a), 7.21 (1H, d, $J = 8.6$ Hz, H-7), 3.95 (3H, s, H-11); ^{13}C NMR (CDCl_3 , 100 MHz) δ 167.2 (C-10), 162.6 (d, $J_{\text{CF}} = 249.4$ Hz, C-4a), 152.3 (C-2), 142.3 (C-8), 140.3 (C-9), 132.6 (C-1b), 132.1 (d, $J = 3.16$ Hz, C-1a), 131.8 (q, $J_{\text{CF}} = 260.0$ Hz, C-7b), 129.7 (2C, C-3b/5b), 129.1 (d, $J = 8.7$ Hz, 2C, C-2a/6a), 125.8 (C-5), 125.6 (C-6), 125.5 (q, $J = 3.9$ Hz, 2C, C-2b/6b), 122.5 (C-4), 117.5 (d, $J = 22.8$ Hz, 2C, C-3a/5a), 110.2 (C-7), 52.2 (C-11); ^{19}F NMR (CDCl_3 , 376.5 MHz) δ - 62.98; HRMS (m/z): 415.1078 M^+ (calculated for $\text{C}_{22}\text{H}_{15}\text{F}_4\text{N}_2\text{O}_2$: 415.1070).

(C5f) methyl 1-(4-fluorophenyl)-2-(4-nitrophenyl)-1H-benzo[d]imidazole-5-carboxylate, yellow solid (70% yield); Purity 98%; mp 214-216 °C; UV λ_{max} (MeOH) nm (log ϵ) 229 (2.84), 320 (2.47); IR ν_{max} 3078 (CH), 1714 (C=O), 1510 (N-O), 1380 (C-F), 1204 (C-O) cm^{-1} ; ^1H NMR (CDCl_3 , 400 MHz) δ 8.60 (1H, bs, H-4), 8.18 (2H, d, $J = 8.1$ Hz, H-3b/5b), 8.04 (1H, d, $J = 8.4$

Hz, H-6), 7.76 (2H, d, $J = 8.1$ Hz, H-2b/6b), 7.32 (2H, m, H-2a/6a), 7.27 (2H, m, H-3a/5a), 7.23 (1H, d, $J = 8.4$ Hz, H-7), 3.96 (3H, s, H-11); ^{13}C NMR (CDCl_3 , 100 MHz) δ 167.1 (C-10), 162.9 (d, $J_{\text{CF}} = 250.2$ Hz, C-4a), 151.2 (C-4b), 148.4 (C-2), 142.0 (C-8), 140.3 (C-9), 134.9 (C-1b), 131.8 (d, $J = 3.1$ Hz, C-1a), 130.3 (2C, C-2b/6b), 129.2 (d, $J = 8.7$ Hz, 2C, C-2a/6a), 126.2 (C-5), 126.1 (C-6), 123.7 (2C, C-3b/5b), 122.6 (C-4), 117.7 (d, $J = 22.8$ Hz, 2C, C-3a/5a), 110.4 (C-7), 52.3 (C-11); ^{19}F NMR (CDCl_3 , 376.5 MHz) δ -109.63; HRMS (m/z): 392.1055 M^+ (calculated for $\text{C}_{21}\text{H}_{15}\text{FN}_3\text{O}_4$: 392.1047).

(C5g) methyl 1-(4-fluorophenyl)-2-p-tolyl-1H-benzo[d]imidazole-5-carboxylate, white solid (80% yield); Purity 96%; mp 156-158 °C; UV λ_{max} (MeOH) nm (log ϵ) 214 (3.21), 250 (3.36), 304 (2.93); IR ν_{max} 3074 (CH), 1711 (C=O), 1381 (C-F), 1185 (C-O) cm^{-1} ; ^1H NMR (CDCl_3 , 400 MHz) δ 8.57 (1H, bs, H-4), 7.98 (1H, dd, $J = 8.5, 1.3$ Hz, H-6), 7.43 (2H, d, $J = 8.1$ Hz, H-2b/6b), 7.29 (2H, dd, $J = 8.7, 4.8$ Hz, H-2a/6a), 7.21 (2H, t, $J = 8.7$ Hz, H-3a/5a), 7.18 (1H, d, $J = 8.5$ Hz, H-7), 7.13 (2H, d, $J = 8.1$ Hz, H-3b/5b), 3.94 (3H, s, H-11), 2.34 (3H, s, H-7b); ^{13}C NMR (CDCl_3 , 100 MHz) δ 167.3 (C-10), 162.5 (d, $J_{\text{CF}} = 248.7$ Hz, C-4a), 154.0 (C-2), 140.6 (C-8), 140.1 (2C, C-4/4b), 132.4 (d, $J = 3.6$ Hz, C-1a), 129.4 (2C, C-3b/5b), 129.3 (2C, C-2b/6b), 129.2 (d, $J = 8.7$ Hz, 2C, C-2a/6a), 125.7 (C-1b), 125.5 (C-5), 125.1 (C-6), 121.8 (C-4), 117.2 (d, $J = 22.8$ Hz, 2C, C-3a/5a), 110.0 (C-7), 52.2 (C-11), 21.4 (C-7b); ^{19}F NMR (CDCl_3 , 376.5 MHz) δ -111.18; HRMS (m/z): 361.1354 M^+ (calculated for $\text{C}_{22}\text{H}_{18}\text{FN}_2\text{O}_2$: 361.1352).

(C5h) methyl 1-(4-fluorophenyl)-2-(4-methoxyphenyl)-1H-benzo[d]imidazole-5-carboxylate, white solid (78% yield); Purity 98%; mp 138-140 °C; UV λ_{max} (MeOH) nm (log ϵ) 225 (2.9), 258 (3.0), 307 (2.75); IR ν_{max} 3080 (CH), 1710 (C=O), 1385 (C-F), 1180 (C-O) cm^{-1} ; ^1H NMR (CDCl_3 ,

400 MHz) δ 8.54 (1H, d, J = 1.5 Hz, H-4), 7.96 (1H, dd, J = 8.5, 1.5 Hz, H-6), 7.48 (2H, d, J = 8.9 Hz, H-2b/6b), 7.29 (2H, dd, J = 8.7, 4.8 Hz, H-2a/6a), 7.21 (2H, t, J = 8.7 Hz, H-3a/5a), 7.16 (1H, d, J = 8.5 Hz, H-7), 6.83 (2H, d, J = 8.9 Hz, H-3b/5b), 3.94 (3H, s, H-11), 3.79 (3H, s, H-7b); ^{13}C NMR (CDCl_3 , 100 MHz) δ 167.6 (C-10), 162.5 (d, J_{CF} = 248.6 Hz, C-4a), 161.0 (C-4b), 154.0 (C-2), 142.3 (C-8), 140.3 (C-9), 132.6 (d, J = 3.3 Hz, C-1a), 131.0 (2C, C-2b/6b), 129.2 (d, J = 8.7 Hz, 2C, C-2a/6a), 125.3 (C-5), 124.8 (C-6), 121.8 (C-4), 121.3 (C-1b), 117.2 (d, J = 22.7 Hz, 2C, C-3a/5a), 114.1 (2C, C-3b/5b), 109.9 (C-7), 55.3 (C-7b), 52.1 (C-11); ^{19}F NMR (CDCl_3 , 376.5 MHz) δ -111.23; HRMS (m/z): 377.1310 M^+ (calculated for $\text{C}_{22}\text{H}_{18}\text{FN}_2\text{O}_3$: 377.1301).

(C5i) methyl 2-(4-aminophenyl)-1-(4-fluorophenyl)-1*H*-benzo[*d*]imidazole-5-carboxylate, orange solid (75% yield); Purity 97%; mp 225-227 °C; UV λ_{max} (MeOH) nm (log ϵ) 233 (3.51), 327 (3.41); IR ν_{max} 3473 (NH), 3077 (CH), 1710 (C=O), 1382 (C-F), 1197 (C-O) cm^{-1} ; ^1H NMR ($\text{DMSO-}d_6$, 400 MHz) δ 8.26 (1H, d, J = 1.3 Hz, H-4), 7.83 (1H, dd, J = 8.5, 1.3 Hz, H-6), 7.52 (2H, dd, J = 8.7, 5.0 Hz, H-2a/6a), 7.44 (2H, t, J = 8.7 Hz, H-3a/5a), 7.21 (2H, d, J = 8.6 Hz, H-2b/6b), 7.17 (1H, d, J = 8.5 Hz, H-7), 6.49 (2H, d, J = 8.6 Hz, H-3b/5b), 5.61 (2H, s, H-7b), 3.88 (3H, s, H-11); ^{13}C NMR ($\text{DMSO-}d_6$, 100 MHz) δ 166.7 (C-10), 161.8 (d, J_{CF} = 244.9 Hz, C-4a), 155.1 (C-2), 150.6 (C-4b), 142.4 (C-8), 140.5 (C-9), 132.9 (d, J = 3.0 Hz, C-1a), 130.4 (2C, C-2b/6b), 129.9 (d, J = 8.9 Hz, 2C, C-2a/6a), 123.9 (C-5), 123.6 (C-6), 120.0 (C-4), 117.0 (d, J = 22.9 Hz, 2C, C-3a/5a), 115.4 (C-1b), 113.1 (2C, C-3b/5b), 110.0 (C-7), 52.0 (C-11); ^{19}F NMR ($\text{DMSO-}d_6$, 376.5 MHz) δ -112.32; HRMS (m/z): 362.1307 M^+ (calculated for $\text{C}_{21}\text{H}_{17}\text{FN}_3\text{O}_2$: 362.1305).

(C5j) methyl 1-(4-fluorophenyl)-2-(4-hydroxyphenyl)-1*H*-benzo[*d*]imidazole-5-carboxylate, white solid (80% yield); Purity 96%; mp 252-254 °C; UV λ_{max} (MeOH) nm (log ϵ) 226 (2.88), 259 (2.92), 308 (2.74); IR ν_{max} 3058 (CH), 1710 (C=O), 1384 (C-F), 1196 (C-O) cm^{-1} ; ^1H NMR (MeOH- d_4 , 400 MHz) δ 8.41 (1H, d, J = 1.4 Hz, H-4), 7.97 (1H, dd, J = 8.6, 1.4 Hz, H-6), 7.42 (2H, dd, J = 8.7, 4.9 Hz, H-2a/6a), 7.38 (2H, d, J = 8.7 Hz, H-2b/6b), 7.33 (2H, t, J = 8.7 Hz, H-3a/5a), 7.27 (1H, d, J = 8.6 Hz, H-7), 6.76 (2H, d, J = 8.7 Hz, H-3b/5b), 3.94 (3H, s, H-11); ^{13}C NMR (MeOH- d_4 , 100 MHz) δ 168.8 (C-10), 164.1 (d, J_{CF} = 246.7 Hz, C-4a), 161.1 (C-4b), 156.6 (C-2), 143.0 (C-8), 141.5 (C-9), 133.8 (d, J = 3.4 Hz, C-1a), 132.4 (2C, C-2b/6b), 130.9 (d, J = 9.0 Hz, 2C, C-2a/6a), 126.5 (C-5), 125.9 (C-6), 121.7 (C-4), 120.8 (C-1b), 118.1 (d, J = 23.2 Hz, 2C, C-3a/5a), 116.5 (2C, C-3b/5b), 111.5 (C-7), 52.7 (C-11); ^{19}F NMR (MeOH- d_4 , 376.5 MHz) δ -113.54; HRMS (m/z): 385.0970 $\text{M}^+ \text{Na}^+$ (calculated for $\text{C}_{21}\text{H}_{15}\text{FN}_2\text{O}_3 \text{Na}$: 385.0964).

(C5k) methyl 2-(4-(dimethylamino)phenyl)-1-(4-fluorophenyl)-1*H*-benzo[*d*]imidazole-5-carboxylate, brown solid (90% yield); Purity 87%; mp 184-186 °C; UV λ_{max} (MeOH) nm (log ϵ) 205 (3.18), 235 (3.30), 337 (3.23); IR ν_{max} 3049 (CH), 1707 (C=O), 1363 (C-F), 1196 (C-O) cm^{-1} ; ^1H NMR (CDCl_3 , 400 MHz) δ 8.54 (1H, bs, H-4), 7.94 (1H, dd, J = 8.5, 1.4 Hz, H-6), 7.45 (2H, d, J = 8.9 Hz, H-2b/6b), 7.34 (2H, dd, J = 8.8, 4.8 Hz, H-2a/6a), 7.24 (2H, t, J = 8.8 Hz, H-3a/5a), 7.13 (1H, d, J = 8.5 Hz, H-7), 6.59 (2H, d, J = 8.9 Hz, H-3b/5b), 3.95 (3H, s, H-11), 2.98 (6H, s, H-7b/8b); ^{13}C NMR (CDCl_3 , 100 MHz) δ 167.5 (C-10), 162.3 (d, J_{CF} = 248.0 Hz, C-4a), 154.8 (C-4b), 151.1 (C-2), 142.4 (C-8), 140.4 (C-9), 133.1 (d, J = 3.2 Hz, C-1a), 130.5 (2C, C-2b/6b), 129.3 (d, J = 8.7 Hz, 2C, C-2a/6a), 124.9 (C-1b), 124.3 (C-6), 121.3 (C-4), 117.0 (d, J = 22.8 Hz, 2C, C-3a/5a), 115.7 (C-5), 111.4 (C-3b/5b), 109.4 (C-7), 52.0 (C-11), 40.0 (2C, C-7b/8b); ^{19}F NMR

(CDCl₃, 376.5 MHz) δ -111.47; HRMS (m/z): 390.1620 M⁺ (calculated for C₂₃H₂₁FN₃O₂: 390.1618).

(C5l) methyl 1-(4-fluorophenyl)-2-(4-(methylthio)phenyl)-1*H*-benzo[*d*]imidazole-5-carboxylate, yellow solid (90% yield); Purity 90%; mp 182-184 °C; UV λ_{max} (MeOH) nm (log ϵ) 207 (3.16), 238 (3.21), 277 (2.96), 316 (3.14); IR ν_{max} 3059 (CH), 1697 (C=O), 1377 (C-F), 1155 (C-O) cm⁻¹; ¹H NMR (CDCl₃, 400 MHz) δ 8.55 (1H, d, J = 1.4 Hz, H-4), 7.97 (1H, dd, J = 8.5, 1.4 Hz, H-6), 7.46 (2H, d, J = 8.5 Hz, H-2b/6b), 7.30 (2H, dd, J = 7.2, 4.8 Hz, H-2a/6a), 7.22 (2H, t, J = 7.2 Hz, H-3a/5a), 7.19 (1H, d, J = 7.3 Hz, H-7), 7.14 (2H, d, J = 8.5 Hz, H-3b/5b), 3.94 (3H, s, H-11), 2.46 (3H, s, H-7b); ¹³C NMR (CDCl₃, 100 MHz) δ 167.3 (C-10), 162.5 (d, J_{CF} = 249.1 Hz, C-4a), 153.5 (C-2), 142.2 (2C, C-9/4b), 140.1 (C-9), 132.3 (d, J = 3.2 Hz, C-1a), 129.6 (2C, C-2b/6b), 129.2 (d, J = 8.7 Hz, 2C, C-2a/6a), 125.6 (C-1b), 125.5 (2C, C-3b/5b), 125.2 (C-6), 124.8 (C-5), 121.8 (C-4), 117.3 (d, J = 22.8 Hz, 2C, C-3a/5a), 109.9 (C-7), 52.2 (C-11), 14.9 (C-7b); ¹⁹F NMR (CDCl₃, 376.5 MHz) δ -110.83; HRMS (m/z): 415.0885 M⁺ + Na⁺ (calculated for C₂₂H₁₇FN₂O₂SNa: 415.0892).

(C5m) methyl 1-(4-fluorophenyl)-2-(naphthalen-2-yl)-1*H*-benzo[*d*]imidazole-5-carboxylate, marigold solid (85% yield); Purity 99%; mp 169-171 °C; UV λ_{max} (MeOH) nm (log ϵ) 210 (3.33), 252 (3.62), 311 (3.10); IR ν_{max} 3064 (CH), 1701 (C=O), 1362 (C-F), 1156 (C-O) cm⁻¹; ¹H NMR (CDCl₃, 400 MHz) δ 8.61 (1H, bs, H-4), 8.09 (1H, s, H-2b), 8.01 (1H, dd, J = 8.6, 1.2 Hz, H-6), 7.80 (1H, d, J = 8.2 Hz, H-9b), 7.75 (2H, t, J = 8.8 Hz, H-4b/7b), 7.58 (1H, dd, J = 8.2, 1.6 Hz, H-10b), 7.51 (1H, t, J = 7.0 Hz, H-5b*), 7.47 (1H, t, J = 7.0 Hz, H-6b*), 7.33 (2H, dd, J = 8.2, 4.7 Hz, H-2a/6a), 7.22 (1H, d, J = 8.6 Hz, H-7), 7.20 (2H, t, J = 8.2 Hz, H-3a/5a), 3.96 (3H, s, H-11);

^{13}C NMR (CDCl_3 , 100 MHz) δ 167.4 (C-10), 162.5 (d, $J_{\text{CF}} = 248.8$ Hz, C-4a), 154.0 (C-2), 142.4 (C-8), 140.3 (C-9), 133.7 (C-3b), 132.8 (C-1b), 132.6 (d, $J = 3.2$ Hz, C-1a), 130.0 (C-2b), 129.2 (d, $J = 8.7$ Hz, 2C, C-2a/6a), 128.7 (C-7b), 128.2 (C-4b), 127.5 (C-9b[#]), 127.7 (C-6b[#]), 126.7 (C-5b), 126.4 (C-5), 125.8 (C-10b), 125.5 (C-8b), 125.2 (C-6), 122.2 (C-4), 117.2 (d, $J = 22.8$ Hz, 2C, C-3a/5a), 110.0 (C-7), 52.2 (C-11); ^{19}F NMR (CDCl_3 , 376.5 MHz) δ -110.01; HRMS (m/z): 397.1349 M^+ (calculated for $\text{C}_{25}\text{H}_{18}\text{FN}_2\text{O}_2$: 397.1352). * and [#] assignments may be interchanged.

(C5n) (*E*)-methyl 1-(4-fluorophenyl)-2-styryl-1*H*-benzo[*d*]imidazole-5-carboxylate, white solid (87% yield); Purity 97%; mp 210-212 °C; UV λ_{max} (MeOH) nm (log ϵ) 227 (3.21), 268 (3.04), 332 (3.06); IR ν_{max} 3078 (CH), 1704 (C=O), 1635 (C=C), 1392 (C-F), 1154 (C-O) cm^{-1} ; ^1H NMR (CDCl_3 , 400 MHz) δ 8.52 (1H, bs, H-4), 8.05 (1H, d, $J = 16.0$ Hz, H-1b), 7.95 (1H, dd, $J = 8.5$, 1.0 Hz, H-6), 7.46 (2H, m, H-4b/8b), 7.43 (2H, m, H-2a/6a), 7.31-7.35 (5H, m, H-5b, H-6b, H-7b, H-3a/5a), 7.13 (1H, d, $J = 8.5$ Hz, H-7), 6.74 (1H, d, $J = 16.0$ Hz, H-2b), 3.94 (3H, s, H-11); ^{13}C NMR (CDCl_3 , 100 MHz) δ 167.4 (C-10), 162.8 (d, $J_{\text{CF}} = 249.1$ Hz, C-4a), 152.5 (C-2), 142.3 (C-8), 139.6 (C-9), 138.9 (C-1b), 135.5 (C-3b), 130.9 (d, $J = 3.1$ Hz, C-1a), 129.5 (2C, C-5b/7b), 129.4 (2C, d, $J = 8.8$ Hz, C-2a/6a), 128.8 (C-6b), 127.4 (2C, C-4b/8b), 125.6 (C-5), 124.9 (C-6), 121.5 (C-4), 117.3 (d, $J = 23.9$ Hz, 2C, C-3a/5a), 112.8 (C-2b), 109.6 (C-7), 52.2 (C-11); ^{19}F NMR (CDCl_3 , 376.5 MHz) δ -110.43; HRMS (m/z): 373.1355 M^+ (calculated for $\text{C}_{23}\text{H}_{18}\text{FN}_2\text{O}_2$: 373.1352).

(C5o) methyl 2-(6-chloroquinolin-2-yl)-1-(4-fluorophenyl)-1*H*-benzo[*d*]imidazole-5-carboxylate, marigold solid (85% yield); Purity 98%; mp 228-230 °C; UV λ_{max} (MeOH) nm (log ϵ) 257 (3.43), 321 (2.94), 336 (2.98); IR ν_{max} 3068 (CH), 1702 (C=O), 1386 (C-F), 1190 (C-O),

750 (C-Cl) cm^{-1} ; ^1H NMR (CDCl_3 , 400 MHz) δ 8.64 (1H, bs, H-4), 8.47 (1H, d, J = 8.6 Hz, H-9b), 8.21 (1H, d, J = 8.6 Hz, H-10b), 8.03 (1H, dd, J = 8.6, 1.3 Hz, H-6), 7.72 (1H, d, J = 9.2 Hz, H-4b), 7.46 (2H, m, H-5b/7b), 7.38 (2H, dd, J = 9.2, 4.8 Hz, H-2a/6a), 7.24 (2H, t, J = 9.2 Hz, H-3a/5a), 7.19 (1H, d, J = 8.6 Hz, H-7), 3.96 (3H, s, H-11); ^{13}C NMR (CDCl_3 , 100 MHz) δ 167.3 (C-10), 162.5 (d, J_{CF} = 247.3 Hz, C-4a), 151.2 (C-2), 149.2 (C-1b), 147.3 (C-8b), 141.9 (C-8), 141.2 (C-9), 136.5 (C-10b), 135.8 (C-6b), 133.7 (d, J = 3.1 Hz, C-1a), 129.6 (d, J = 8.7 Hz, 2C, C-2a/6a), 128.8 (C-7b*), 128.6 (C-5b*), 128.5 (C-4b), 126.2 (C-3b), 126.0 (C-6), 125.8 (C-5), 122.7 (C-4), 121.6 (C-9b), 116.3 (d, J = 22.8 Hz, 2C, C-3a/5a), 110.7 (C-5), 52.2 (C-11); ^{19}F NMR (CDCl_3 , 376.5 MHz) δ -112.10; HRMS (m/z): 432.0931 M^+ (calculated for $\text{C}_{24}\text{H}_{16}\text{ClFN}_3\text{O}_2$: 432.0915).
 *assignments may be interchanged.

(C5p) methyl 1-(4-fluorophenyl)-2-(2-hydroxy-4,6-dimethoxyphenyl)-1H-benzo[d]imidazole-5-carboxylate, white solid (65% yield); Purity 99%; mp 68-70 $^{\circ}\text{C}$; UV λ_{max} (MeOH) nm (log ϵ) 229 (2.86), 267 (2.33), 297 (3.93); IR ν_{max} 3398 (O-H), 3074 (CH), 1712 (C=O), 1359 (C-F), 1153 (C-O) cm^{-1} ; ^1H NMR (CDCl_3 , 400 MHz) δ 8.51 (1H, bs, H-4), 8.00 (1H, dd, J = 8.5, 1.0 Hz, H-6), 7.31 (1H, d, J = 8.5 Hz, H-7), 7.26 (2H, dd, J = 8.6, 4.9 Hz, H-2a/6a), 7.16 (2H, t, J = 8.6 Hz, H-3a/5a), 6.32 (1H, d, J = 1.9 Hz, H-3b), 5.77 (1H, d, J = 1.9 Hz, H-5b), 3.94 (3H, s, H-11), 3.77 (3H, s, H-8b), 3.15 (3H, s, H-9b); ^{13}C NMR (CDCl_3 , 100 MHz) δ 167.2 (C-10), 163.1 (C-4b), 162.2 (d, J_{CF} = 247.1 Hz, C-4a), 160.1 (C-2b), 157.6 (C-6b), 151.8 (C-2), 140.4 (C-8), 138.5 (C-9), 133.8 (d, J = 2.8 Hz, C-1a), 126.9 (d, J = 8.5 Hz, 2C, C-2a/6a), 125.5 (C-5), 125.0 (C-6), 120.7 (C-4), 116.3 (d, J = 22.8 Hz, 2C, C-3a/5a), 110.0 (C-7), 96.2 (C-1b), 94.0 (C-3b), 90.8 (C-5b), 55.4 (C-8b), 54.3 (C-9b), 52.2 (C-11); ^{19}F NMR (CDCl_3 , 376.5 MHz) δ -112.41; HRMS (m/z): 445.1168 $\text{M}^+ \text{Na}^+$ (calculated for $\text{C}_{23}\text{H}_{19}\text{FN}_2\text{O}_5 \text{Na}$: 445.1176).

(C5q) methyl 2-(3,4-dihydroxyphenyl)-1-(4-fluorophenyl)-1H-benzo[d]imidazole-5-carboxylate, cream solid (65% yield); Purity 97%; mp 230-232 °C; UV λ_{max} (MeOH) nm (log ϵ) 226 (3.17), 264 (2.91), 313 (2.85); IR ν_{max} 3501 (O-H), 3062 (CH), 1712 (C=O), 1377 (C-F), 1177 (C-O) cm^{-1} ; ^1H NMR (MeOH- d_4 , 400 MHz) δ 8.40 (1H, d, J = 1.5 Hz, H-4), 7.97 (1H, dd, J = 8.5, 1.5 Hz, H-6), 7.42 (2H, dd, J = 8.7, 4.9 Hz, H-2a/6a), 7.33 (2H, t, J = 8.7 Hz, H-3a/5a), 7.26 (1H, d, J = 8.5 Hz, H-7), 7.01 (1H, d, J = 2.1 Hz, H-2b), 6.86 (1H, dd, J = 8.2, 2.2 Hz, H-6b), 6.7 (1H, d, J = 8.2 Hz, H-5b), 3.95 (3H, s, H-11); ^{13}C NMR (MeOH- d_4 , 100 MHz) δ 168.8 (C-10), 164.1 (d, J_{CF} = 246.8 Hz, C-4a), 156.9 (C-2), 149.2 (C-3b), 146.6 (C-4b), 143.0 (C-8), 141.5 (C-9), 133.8 (d, J = 2.8 Hz, C-1a), 130.9 (d, J = 8.9 Hz, 2C, C-2a/6a), 126.5 (C-5), 125.9 (C-6), 123.1 (C-6b), 121.6 (C-4), 121.2 (C-1b), 118.1 (2C, d, J = 23.2 Hz, C-3a/5a), 117.7 (C-2b), 116.3 (C-5b), 111.5 (C-7), 52.7 (C-11); ^{19}F NMR (MeOH- d_4 , 376.5 MHz) δ -113.67; HRMS (m/z): 379.1094 M^+ (calculated for $\text{C}_{21}\text{H}_{16}\text{FN}_2\text{O}_4$: 379.1110).

(C5r) methyl 1-(4-fluorophenyl)-2-(2,3,4-trihydroxyphenyl)-1H-benzo[d]imidazole-5-carboxylate, green solid (85% yield); Purity 99%; mp 214-216 °C; UV λ_{max} (MeOH) nm (log ϵ) 230 (3.27), 322 (3.0); IR ν_{max} 3483 (O-H), 3069 (CH), 1709 (C=O), 1345 (C-F), 1152 (C-O) cm^{-1} ; ^1H NMR (MeOH- d_4 , 400 MHz) δ 8.34 (1H, d, J = 1.4 Hz, H-4), 7.92 (1H, dd, J = 8.5, 1.4 Hz, H-6), 7.46 (2H, dd, J = 8.7, 4.9 Hz, H-2a/6a), 7.36 (2H, t, J = 8.7 Hz, H-3a/5a), 7.12 (1H, d, J = 8.5 Hz, H-7), 6.35 (1H, d, J = 8.9 Hz, H-6b), 6.15 (1H, d, J = 8.9 Hz, H-5b), 3.93 (3H, s, H-11); ^{13}C NMR (MeOH- d_4 , 100 MHz) δ 168.9 (C-10), 164.4 (d, J_{CF} = 247.2 Hz, C-4a), 155.2 (C-2), 149.5 (C-4b), 149.4 (C-2b), 141.5 (C-8), 141.0 (C-9), 134.6 (C-3b), 134.2 (d, J = 3.3 Hz, C-1a), 131.1 (d, J = 8.9 Hz, 2C, C-2a/6a), 126.5 (C-5), 125.8 (C-6), 121.0 (C-4), 120.4 (C-6b), 118.3 (d, J = 23.3 Hz, 2C, C-3a/5a), 111.0 (C-7), 107.8 (C-5b), 106.5 (C-1b), 52.7 (C-11); ^{19}F NMR (MeOH-

d_4 , 376.5 MHz) δ -113.12; HRMS (m/z): 417.0874 $M^+ + Na^+$ (calculated for $C_{21}H_{15}FN_2O_5Na$: 417.0863).

(C5s) methyl 1-(4-fluorophenyl)-2-(thiophen-2-yl)-1H-benzo[d]imidazole-5-carboxylate, white solid (74% yield); Purity 90%; mp 156-158 °C; UV λ_{max} (MeOH) nm (log ϵ) 219 (3.26), 254 (3.28), 322 (3.18); IR ν_{max} 3073 (CH), 1711 (C=O), 1386 (C-F), 1192 (C-O) cm^{-1} ; 1H NMR ($CDCl_3$, 400 MHz) δ 8.53 (1H, bs, H-4), 7.95 (1H, dd, J = 8.5, 1.0 Hz, H-6), 7.41 (2H, dd, J = 8.2, 4.8 Hz, H-2a/6a), 7.39 (1H, d, J = 4.4 Hz, H-3b), 7.30 (2H, t, J = 8.2 Hz, H-3a/5a), 7.03 (1H, d, J = 8.5 Hz, H-7), 7.02 (1H, bs, H-5b), 6.95 (1H, t, J = 4.4 Hz, H-4b), 3.93 (3H, s, H-11); ^{13}C NMR ($CDCl_3$, 100 MHz) δ 167.3 (C-10), 163.2 (d, J_{CF} = 249.6 Hz, C-4a), 149.0 (C-2), 142.2 (C-8), 142.1 (C-1b), 140.6 (C-9), 131.7 (d, J = 3.4 Hz, C-1a), 130.2 (d, J = 8.8 Hz, 2C, C-2a/6a), 129.4 (C-3b), 129.2 (C-5b), 127.7 (C-4b), 125.5 (C-5), 125.1 (C-6), 121.7 (C-4), 117.5 (d, J = 22.8 Hz, 2C, C-3a/5a), 109.7 (C-7), 52.1 (C-11); ^{19}F NMR ($CDCl_3$, 376.5 MHz) δ -109.62; HRMS (m/z): 353.0761 M^+ (calculated for $C_{19}H_{14}FN_2O_2S$: 353.0760).

(C5t) methyl 1-(4-fluorophenyl)-2-(furan-2-yl)-1H-benzo[d]imidazole-5-carboxylate, dark brown solid (76% yield); Purity 98%; mp 139-141 °C; UV λ_{max} (MeOH) nm (log ϵ) 258 (3.15), 313 (3.11), 326 (3.01); IR ν_{max} 3069 (CH), 1711 (C=O), 1359 (C-F), 1195 (C-O) cm^{-1} ; 1H NMR ($CDCl_3$, 400 MHz) δ 8.53 (1H, d, J = 1.4 Hz, H-4), 7.96 (1H, dd, J = 8.5, 1.4 Hz, H-6), 7.48 (1H, bs, H-3b), 7.40 (2H, dd, J = 8.5, 4.7 Hz, H-2a/6a), 7.29 (2H, td, J = 8.5 Hz, H-3a/5a), 7.06 (1H, d, J = 8.5 Hz, H-7), 6.39-6.40 (2H, m, H-4b/5b), 3.93 (3H, s, H-11); ^{13}C NMR ($CDCl_3$, 100 MHz) δ 167.3 (C-10), 163.0 (d, J_{CF} = 249.2 Hz, C-4a), 145.7 (C-2), 144.9 (C-3b), 143.6 (C-8), 140.0 (C-9), 131.7 (d, J = 3.2 Hz, C-1a), 129.8 (d, J = 8.8 Hz, 2C, C-2a/6a), 125.7 (C-5), 125.4 (C-6), 122.0

(C-4), 117.2 (d, $J = 22.8$ Hz, 2C, C-3a/5a), 113.6 (C-5b), 111.8 (C-4b), 109.8 (C-7), 52.1 (C-11); ^{19}F NMR (CDCl_3 , 376.5 MHz) δ -110.00; HRMS (m/z): 337.0994 M^+ (calculated for $\text{C}_{19}\text{H}_{14}\text{FN}_2\text{O}_3$: 337.0988).

(C5u) methyl 1-(4-fluorophenyl)-2-propyl-1H-benzo[d]imidazole-5-carboxylate, cream solid (70% yield); Purity 100%; mp 102-104 °C; UV λ_{max} (MeOH) nm (log ϵ) 227 (3.16), 267 (2.40); IR ν_{max} 3083 (CH), 1715 (C=O), 1360 (C-F), 1166 (C-O) cm^{-1} ; ^1H NMR (CDCl_3 , 400 MHz) δ 8.49 (1H, d, $J = 1.4$ Hz, H-4), 7.94 (1H, dd, $J = 8.5, 1.4$ Hz, H-6), 7.34 (2H, dd, $J = 8.2, 5.2$ Hz, H-2a/6a), 7.29 (2H, t, $J = 8.2$ Hz, H-3a/5a), 7.05 (1H, d, $J = 8.5$ Hz, H-7), 3.92 (3H, s, H-11), 2.76 (2H, t, $J = 7.5$ Hz, H-1b), 1.76-1.86 (2H, sextet, H-2b), 0.94 (3H, t, $J = 7.5$ Hz, H-3b); ^{13}C NMR (CDCl_3 , 100 MHz) δ 167.4 (C-10), 162.8 (d, $J_{\text{CF}} = 249.3$ Hz, C-4a), 156.9 (C-2), 141.7 (C-8), 139.5 (C-9), 131.2 (d, $J = 2.8$ Hz, C-1a), 129.2 (d, $J = 8.8$ Hz, 2C, C-2a/6a), 125.1 (C-5), 124.8 (C-6), 121.2 (C-4), 117.3 (d, $J = 22.8$ Hz, 2C, C-3a/5a), 109.6 (C-7), 52.1 (C-11), 29.4 (C-1b), 21.1 (C-2b), 13.9 (C-3b); ^{19}F NMR (CDCl_3 , 376.5 MHz) δ -110.53; HRMS (m/z): 335.1161 M^+ + Na^+ (calculated for $\text{C}_{18}\text{H}_{17}\text{FN}_2\text{O}_2\text{Na}$: 335.1172).

(C5v) methyl 1-(4-fluorophenyl)-2-hexyl-1H-benzo[d]imidazole-5-carboxylate, brown solid (70% yield); Purity 61%; mp 66-68 °C; UV λ_{max} (MeOH) nm (log ϵ) 227 (3.53), 264 (2.81); IR ν_{max} 3075 (CH), 1708 (C=O), 1399 (C-F), 1156 (C-O) cm^{-1} ; ^1H NMR (CDCl_3 , 400 MHz) δ 8.48 (1H, bs, H-4), 7.94 (1H, dd, $J = 8.5, 1.2$ Hz, H-6), 7.36 (2H, dd, $J = 8.6, 5.0$ Hz, H-2a/6a), 7.30 (2H, t, $J = 8.6$ Hz, H-3a/5a), 7.06 (1H, d, $J = 8.5$ Hz, H-7), 3.94 (3H, s, H-11), 2.76 (2H, t, $J = 7.5$ Hz, H-1b), 1.77 (2H, quintet, $J = 7.5$ Hz, H-2b), 1.25-1.35 (2H, m, H-3b), 1.23-1.26 (2H, m, H-5b), 0.88-0.90 (2H, m, H-4b), 0.84 (3H, t, $J = 6.8$ Hz, H-6b); ^{13}C NMR (CDCl_3 , 100 MHz) δ 167.6

(C-10), 162.9 (d, $J_{\text{CF}} = 249.0$ Hz, C-4a), 157.2 (C-2), 141.7 (C-8), 139.6 (C-9), 131.5 (d, $J = 3.1$ Hz, C-1a), 129.2 (d, $J = 8.8$ Hz, 2C, C-2a/6a), 124.8 (C-5), 124.5 (C-6), 121.3 (C-4), 117.2 (d, $J = 22.8$ Hz, 2C, C-3a/5a), 109.4 (C-7), 52.0 (C-11), 31.3 (C-4b), 28.9 (C-3b), 27.6 (C-1b), 27.6 (C-2b), 22.4 (C-5b), 13.9 (C-6b); ^{19}F NMR (CDCl_3 , 376.5 MHz) δ -110.80; HRMS (m/z): 355.1816 M^+ (calculated for $\text{C}_{21}\text{H}_{24}\text{FN}_2\text{O}_2$: 355.1822).

^1bs -broad singlet.

7.2.2 Single Crystal X-ray Diffraction Analysis

Crystals suitable for X-ray diffraction were obtained by slow evaporation in a combination of ethyl acetate and n-hexane at room temperature. A cube-shaped single crystal was selected and glued onto the tip of a glass fiber and mounted in a stream of cold nitrogen at 173 K and centered in the X-ray beam using a video camera. The crystal evaluation and data collection were performed on a Bruker Smart APEX II diffractometer with Mo $\text{K}\alpha$ radiation ($\lambda = 0.71073$ Å). The diffractometer to crystal distance was set at 4.00 cm. The initial cell matrix was obtained from three series of scans at different starting angles. Each series consisted of 12 frames collected at intervals of 0.5° in a 6° range with the exposure time of 10s per frame. The reflections were successfully indexed by an automated indexing routine built in the APEX II program suite. The final cell constants were calculated from a set of 4762 strong reflections from the actual data collection. Data collection method involved ω scans of width 0.5° . Data reduction was carried out using the program System Administrator's Integrated Network Tool+. The structure was solved by direct methods using SHELXS and refined. Non-H atoms were first refined isotropically and then by anisotropic refinement with full-matrix least-squares calculations based on F^2 using SHELXS. All H atoms were positioned geometrically and allowed to ride on their respective parent atoms. All

H atoms were refined isotropically. The absorption correction was based on fitting a function to the empirical transmission surface as sampled by multiple equivalent measurements. The final least-squares refinement of 265 parameters against 4762 data resulted in residuals R (based on F^2 for $I \geq 2\sigma$) and wR (based on F^2 for all data) of 0.0465 and 0.1048, respectively. The final difference Fourier map was featureless. The programs Olex-2 and Ortep-3 were used within the WinGX software package to prepare artwork representation (Spek et al., 2003; Farrugia et al., 2012). Crystallographic data (excluding structure factors) for the structure in this paper has been deposited with the Cambridge Crystallographic Data Centre, CCDC, 12 Union Road, Cambridge CB21EZ, UK. Copies of the data can be obtained free of charge on quoting the depository number CCDC 1454700 (Fax: +44-1223-336-033; E-Mail: deposit@ccdc.cam.ac.uk, <http://www.ccdc.cam.ac.uk>).

7.2.3 *In vitro* antimicrobial studies

The microbial cultures were grown overnight at 37 °C in nutrient broth (UKZN Biolab, South Africa), adjusted to 0.5 McFarland standard using distilled water and lawn inoculated onto Mueller-Hinton agar (MHA) plates. A volume of 10 μ L of each sample (23.20 - 32.04 μ M in 1 mL DMSO) was inoculated onto antibiotic assay discs (6 mm diameter) and placed on the MHA plates which were incubated overnight at 37°C for 24 hours. After the incubation period, zones of inhibition were measured in mm. Compounds showing an inhibition zone of > 9 mm were selected to determine their MBC values using the broth dilution assay with ampicillin and ciprofloxacin as the controls following the method in Andrews (2001). Compounds **C5b**, **C5e**, **C5h**, **C5k-l**, and **C5o-t** were chosen for the broth dilution method to determine their MBCs.

For the broth dilution method the microbial cultures (adjusted to 0.5 McFarland) were prepared as described previously for the disc diffusion method. The test compounds were dissolved in DMSO (10 mg mL^{-1}) and subject to a 50% serial dilution in 1 mL Eppendorf tubes with Mueller-Hinton Broth (MHB), inoculated with bacterial cultures ($20 \text{ }\mu\text{L}$) and then incubated at $37 \text{ }^{\circ}\text{C}$ for 18 h. The total volume in each Eppendorf was $200 \text{ }\mu\text{L}$. A volume of $10 \text{ }\mu\text{L}$ of each dilution was spotted on MHA plates and incubated at $37 \text{ }^{\circ}\text{C}$ for 18 h to determine the MBC (μM). Ampicillin, ciprofloxacin and tioconazole served as the standard drugs for the antimicrobial and antifungal studies respectively. All experiments were performed in duplicate.

7.2.4 *In vitro* antioxidant studies

The scavenging activity (antioxidant capacity) of the synthesized fluorinated benzimidazole compounds (**C5a-v**) on the stable radical, DPPH was evaluated according to a method by Murthy (Murthy et al., 2012) with some modifications. A volume of $150 \text{ }\mu\text{L}$ of methanolic solution of the test compounds at different concentrations ($1000, 500, 200, 50, 20$ and $10 \text{ }\mu\text{g mL}^{-1}$) was mixed with $2850 \text{ }\mu\text{L}$ of the methanolic solution of DPPH (0.1 mM). An equal amount of MeOH and DPPH without sample served as a control. After 30 min of reaction at room temperature in the dark, the absorbance was measured at 517 nm against methanol as a blank using a UV spectrophotometer as mentioned above. The percentage free radical scavenging activity was calculated according to the following equation:

$$\% \text{ Scavenging activity} = [(A_{\text{control}} - A_{\text{sample}}) / A_{\text{blank}}] \times 100$$

Where ' A_{control} ' is the absorbance of the control reaction (containing all reagents except the test compound) and ' A_{sample} ' is the absorbance of the reagents with a particular test compound.

7.2.5 Docking methodology

The “Prepare Protein” module was used to protonate the amino acid residues of the X-ray structure of topoisomerase II DNA-gyrase (PDB ID: 2XCT, resolution 3.35Å). The native ligand and water molecules were removed from the protein, while the manganese ion (Mn^{+2}) present in the active site was retained. Different isomers of the representative compounds (RCs) (**C5h** and **C5r**) were generated at physiological pH using the “Prepare Ligands” module and subsequently minimized. The partial atomic charges on each atom were developed using the CHARMM force field. A binding sphere of diameter 7.6 Å was developed around the active site residues. The automated docking was performed using the CDocker algorithm (Wu et al., 2003) by generating new conformations of the ligands using the molecular dynamics method. The best pose of each RC was chosen based on the scoring function (-CDOCKER energy), and subjected further to the binding energy calculations.

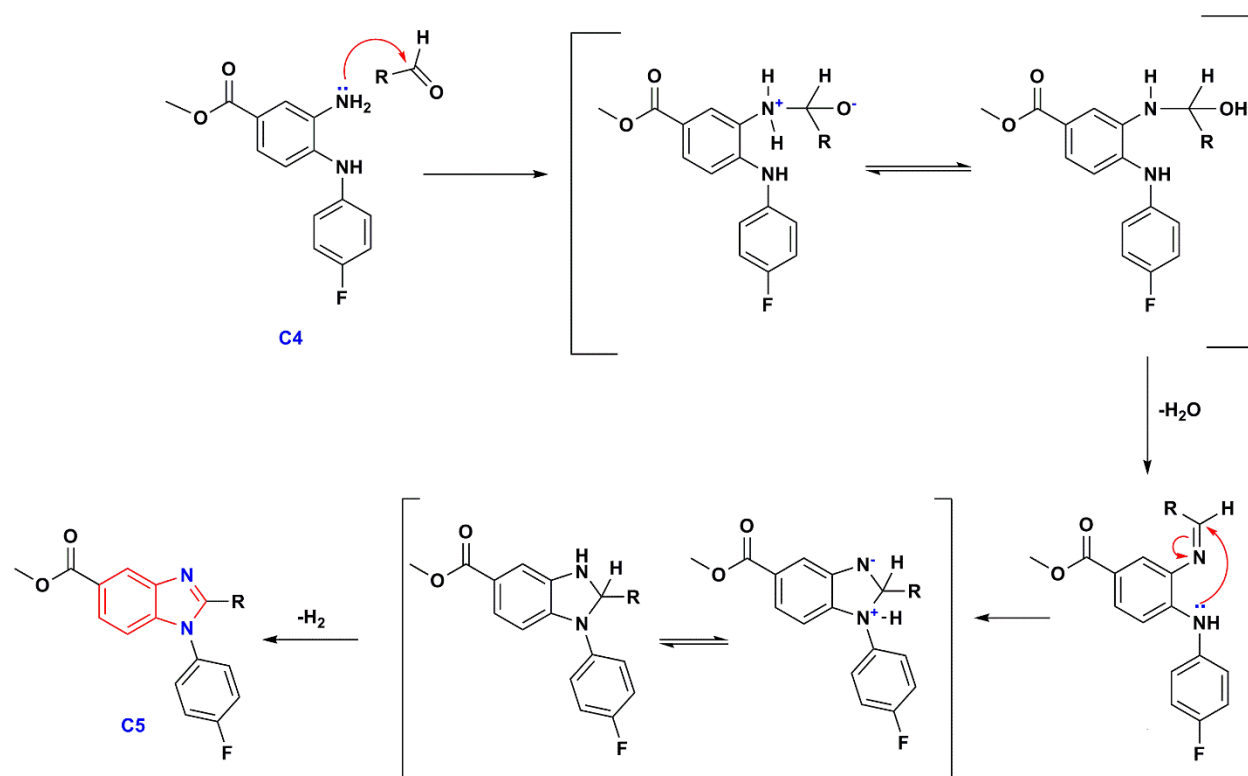
7.3 Results and Discussion

7.3.1 Chemistry

Three fundamental methodologies were used in this study: microwave, conventional and mechanochemical synthesis. A series of 22 benzimidazole molecules (**C5a-v**) were synthesized employing these synthetic methods with different substituents at C-2 on the benzimidazole skeleton. The different substituents were all aldehyde derived and are indicated in **Table 7-1**. These contained *para* halogenated phenyl groups, phenyl groups with *para* substituted electron donating and withdrawing groups as well as other heterocyclic ring moieties such as quinoline, furan, naphthalene and thiophene and the alkyl chains butane and heptane. In addition to the different substituents present on the aromatic ring attached to C-2, an ester moiety was present at C-5 and a *p*-fluoro benzyl moiety at N-1 (**Scheme 7-1**).

The synthesis started with the esterification of 4-fluoro-3-nitrobenzoic acid (**C1**), since the subsequent nucleophilic step is easier to perform with esters rather than acids due to the acidic nature of benzoic acids. The conversion to the ester (**C2**) occurred in 95% yield. The fluoro substituent on the ester was then substituted with 4-fluoroaniline producing **C3** in a 90% yield. Prior to the aldehyde being added, the nitro group of the methyl benzoate (**C3**) was reduced (92% yield) with zinc and ammonium formate forming the *o*-diamino phenyl precursor (**C4**) to the benzimidazoles (**Scheme 7-1**).

In the last step of the synthesis, different aldehydes were added to the precursor **C4** using three methods: (i) without the use of solvents or catalysts in a microwave at 110 °C, (ii) grinding equimolar amounts of **C4** and the aldehydes in the presence iodine as a catalyst at room temperature and (iii) refluxing the amino benzoate (**C4**) and various aldehydes with ethanol in the presence of Na₂S₂O₅ to produce 22 benzimidazoles (**C5a-v**). The probable mechanism of the final step is imine formation of the aldehyde with the primary amino group followed by nucleophilic attack by the secondary amine to the imine carbon. Proton transfer from one nitrogen to the other followed by loss of H₂ resulted in the formation of the benzimidazoles **C5a- C5v** (**Scheme 7-2**). Their structures were confirmed by NMR spectroscopy (1D and 2D NMR) and single crystal X-ray diffraction.



Scheme 7-2 The proposed mechanism for the final step of the benzimidazole synthesis

Three different methods (microwave, mechanochemical and conventional reflux) were employed to synthesize the benzimidazoles (**C5a-v**) to investigate the best possible method for the final step of the synthesis. Using microwave synthesis, the reaction was carried out without the use of solvents and a catalyst and performed at 110 °C for 3-8 minutes with overall yields of between 85-96% (**Table 7-1**). In the grinding method, the reaction was carried out at room temperature in the presence of iodine. This process lasted for between 10-40 minutes. The yields obtained for this reaction was 10-56%. The conventional reflux method containing ethanol as a solvent and Na₂S₂O₅ as the catalyst produced yields of 60-90%. The time taken for the reaction to occur was the longest in the conventional reflux method (8-18 h) followed by the grinding method (10-45 min) and then the microwave method (3-8 min). The yields of the microwave reaction were by far the best (85-97%) followed by the reflux method (60-90%) and lastly the grinding method (10-

56%). In the grinding method starting material was still detected after the reactants were ground together in a mortar and pestle, accounting for the low yields of the reaction. In terms of economy, the microwave method was the best, using only the starting materials. A solvent and catalyst was not needed to produce the products in high yields.

7.3.2 Structural elucidation

Using **C5i** (methyl 2-(4-aminophenyl)-1-(4-fluorophenyl)-1*H*-benzo[*d*]imidazole-5-carboxylate) as a representative fluorinated benzimidazole, H-7, H-6 and H-4 on the benzimidazole core skeleton occurs at δ_{H} 7.17 (d, $J = 8.5$ Hz), δ_{H} 7.83 (dd, $J = 8.5, 1.5$ Hz) and δ_{H} 8.26 (d, $J = 1.3$ Hz) respectively. The ester methyl resonance (H-11) occurred as a singlet at δ_{H} 3.89. The ester carbonyl resonance (C-10) was identified from the HMBC correlation to H-11 and appeared at δ_{C} 166.7. The two aromatic $\underline{\text{C}}$ -N singlet resonances C-8 and C-9 were assigned to δ_{C} 142.4 and δ_{C} 140.5. The C-8 resonance was distinguished from C-9 due to an HMBC correlation with H-6. The C-5 resonance to which the ester group was attached was assigned to δ_{C} 123.9. This resonance showed an HMBC correlation to H-7. The C-2 carbon on the imidazole core skeleton was present at δ_{C} 155.1.

The aromatic protons of phenyl group H2a/6a appeared as a dd at δ_{H} 7.52 Hz with $J = 9.8, 5.0$ Hz), coupling to both F and H3a/5a, which resonated at δ_{H} 7.44 Hz, appearing as a triplet due to the same J values (8.6 Hz) for both coupling to the F and to H-2a/6a. The C-4a fluorinated carbon resonance occurred as a doublet at δ 161.8 ($J = 244.9$ Hz). These assignments were supported by HMBC correlations between C-4a and H-2a/6a as well as H-3a/5a and C-1a which occurred at δ

132.9 (d, $J = 3.0$ Hz). C-2a/6a appeared as a doublet at δ 129.9 ($J = 8.9$ Hz) and C-3a/5a appeared as a doublet at δ 117.0 ($J = 22.9$ Hz).

Table 7-1 Comparison of the yields and duration of the final step in the benzimidazole synthesis using three methods

No.	R	Microwave		Grinding		Conventional	
		Time (min)	Yield ^a (%)	Time (min)	Yield ^{a,b} (%)	Time (h)	Yield ^a (%)
C5a	Ph	3	96	10	55	10	90
C5b	4-F Ph	3	93	10	53	8	85
C5c	4-Cl Ph	3	89	10	50	10	75
C5d	4-Br Ph	3	85	10	48	10	74
C5e	4-CF ₃ Ph	5	90	10	45	8	70
C5f	4-NO ₂ Ph	8	85	45	20	18	60
C5g	4-CH ₃ Ph	6	88	20	30	12	72
C5h	4-OCH ₃ Ph	6	90	25	25	16	60
C5i	4-NH ₂ Ph	5	85	20	10	18	65
C5j	4-OH Ph	5	90	10	20	16	70
C5k	4-N(CH ₃) ₂ Ph	5	90	20	35	12	87
C5l	4-S(CH ₃) Ph	4	90	20	40	16	85
C5m	2-Naphthyl	5	95	20	56	12	80
C5n	α -(E)-prop-1-en-1-yl Ph	5	97	25	50	12	75
C5o	2-(6-Chloroquinoliny)	6	92	25	50	12	73
C5p	2-OH-4,6-(OCH ₃) ₂ Ph	5	90	30	30	16	60
C5q	3,4-(OH) ₂ Ph	4	85	35	20	16	60
C5r	2,3,4-(OH) ₃ Ph	8	85	40	20	16	76
C5s	2-Thiophenyl	3	95	30	50	15	75
C5t	2-Furanyl	3	95	30	50	15	75
C5u	<i>n</i> -Butyl	6	90	25	30	18	70
C5v	<i>n</i> -Heptyl	6	90	25	30	18	70

^aIsolated yield after column chromatography, ^bStarting material was not consumed totally and yield was after purification; Some amount starting materials and imine were also isolated.

For the phenyl group (B) attached to C-2, the aromatic proton resonance of H2b/6b appeared as a doublet at δ_H 7.21 ($J = 8.6$ Hz) and H3b/5b appeared at δ_H 6.49 (d, $J = 8.6$ Hz). An HMBC correlation between the corresponding C-3b/5b carbon resonance at δ 113.1 and the proton resonance at δ_H 5.61 confirmed the assignment of C-3b/5b and allowed the NH₂ proton resonance

to be assigned to δ_{H} 5.61. The assignment of H-2b/6b was confirmed by a HMBC correlation with C-2. Selected HMBC correlations used in the structural elucidation of **C5i** are provided in **Figure 7-1**.

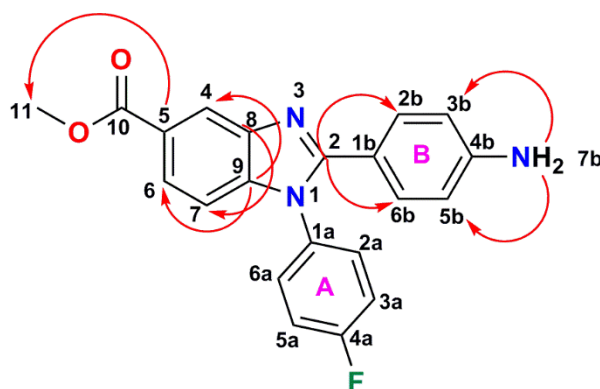


Figure 7-1 Selected HMBC correlations of compound **C5i** (H \rightarrow C)

7.3.3 Antimicrobial activity

The synthesized compounds were tested for their antibacterial and antifungal activity *in vitro* against the Gram +ve bacterial strains: *Staphylococcus aureus* (ATCC 25923) and methicillin resistant *S. aureus* (MRSA) (ATCC BAA-1683) and Gram -ve strains (*Escherichia coli* (ATCC 25922), *Klebsiella pneumonia* (ATCC 31488) and *Pseudomonas aeruginosa* (ATCC 27853)) using ciprofloxacin and ampicillin as the standards. For the antifungal assay *C. albicans* (ATCC 10231) was tested against with tioconazole as the reference drug. A disc diffusion assay was used as an initial screening test to select potentially active compounds. The results were expressed as the mean zone of inhibition in mm using a concentration of 10 mg mL⁻¹ of the test samples. The test samples that showed a zone of inhibition between 8-35 mm was selected for further tests using the Minimum Bactericidal Concentration (MBC) assay. The samples chosen were **C5b**, **C5e**, **C5h**, **C5k-l** and **C5o-t**.

Compounds **C5r** and **C5p** showed broad spectrum activity against all strains of bacteria with the exception of MRSA (**Table 7-2**). Their MBC values ranged between 14.45-115.65 μM (**C5p**) and 25.55-74.32 μM (**C5r**). The activity of both these compounds were 10 fold or greater, higher than that of ampicillin in the same assay. Compound **C5r** was 2b,3b,4b-trisubstituted with hydroxyl groups at each of the positions on the aromatic B ring and **C5p** was 2b,4b,6b-trisubstituted with a hydroxy group at the 2b-position and methoxy groups at the 4b and 6b positions. Consequently, these were the only two trioxxygenated molecules from the 22 compounds that was synthesized. It is likely that this oxygenation has something to do with its broad spectrum activity. However, the test compounds were not as active as ciprofloxacin whose MBC was at least one order of magnitude better than the test compounds, including **C5r** and **C5p**.

The other compound worth mentioning is **C5e** with a trifluoromethane moiety at the *para* position of the aromatic B ring. This compound was active against MRSA with an MBC of 70.73 μM and against *K. pneumonia* (24.32 μM) and *C. albicans* (94.33 μM). With regard to antifungal activity, only **C5e** showed comparable activity to Tioconazole (MBC of 100.84 μM) against *C. albicans*.

7.3.4 Antioxidant activity

For antioxidant activity, the DPPH radical scavenging activity assay was used. The DPPH radical scavenging assay measures the ability to scavenge free radicals *in situ* (Murthy et al., 2012). The trioxxygenated compounds **C5r** (306.71 μM , IC_{50}) and **C5p** (386.55 μM , IC_{50}) with hydroxy and methoxy groups showed antioxidant activity comparable to ascorbic acid (264.50 μM , IC_{50}) (**Table 7-3**). Two other compounds, **C5q** (1129.01 μM , IC_{50}) with dihydroxy moieties and **C5j** with a monohydroxy group (1326.93 μM , IC_{50}) was five times worse than ascorbic acid. All the other

compounds were greater than five times worse than ascorbic acid. Thus, the only compounds that could be considered as having antioxidant potential were **C5r** and **C5p**. Other methods to test for antioxidant activity was not carried out as this was only a preliminary antioxidant test for these compounds.

Table 7-2 Antimicrobial activity of the synthesized compounds, MBCs in μM

Compound	Gram-positive bacteria		Gram-negative bacteria			Fungus
	<i>S. aureus</i>	<i>MRSA</i>	<i>E. coli</i>	<i>P. aeruginosa</i>	<i>K. pneumoniae</i>	
						<i>C.albicans</i>
C5b	268.19	536.42	321.83	536.42	107.28	214.56
C5e	141.49	70.73	282.98	565.98	24.32	94.33
C5h	2492.54	1661.69	103.85	623.12	830.85	1246.27
C5k	803.02	401.51	200.76	250.93	301.11	803.02
C5l	398.18	1992.48	149.43	199.24	149.43	398.18
C5o	1087.38	906.13	407.76	362.46	724.92	362.46
C5p	115.65	555.21	92.53	115.65	14.45	369.85
C5q	206.61	439.06	232.45	-	-	3305.99
C5r	74.32	446.03	49.56	37.15	25.55	421.24
C5s	-	-	1109.50	-	-	443.81
C5t	-	-	348.66	-	-	1859.62
Ampicilin	55.89	894.36	447.18	1788.73	447.18	447.18
Ciprofloxacin	1.84	7.36	1.84	1.84	3.68	1.84
Tioconazole	-	-	-	-	-	100.84

Highlighted values indicate the best activity

Table 7-3 Antioxidant activity of the synthesized compounds from the DPPH assay, IC₅₀ in μM

Compound	IC ₅₀ (μM)	Compound	IC ₅₀ (μM)
C5j	1326.93	C5q	1129.01
C5p	386.55	C5r	306.71
Ascorbic Acid (AA)	264.50		

Highlighted values indicate the best activity

7.3.5 Docking discussion

Several drugs including ciprofloxacin and lomefloxacin exhibit their antibacterial action by inhibition of bacterial type II topoisomerases (topoisomerase IV and DNA-gyrase) (Mitscher et al., 2005). In order to support the antibacterial results and to gain some insight into the binding characteristics of the compounds with bacterial proteins, two representative compounds (RCs), **C5r** (most potent) and **C5h** (least potent) were docked into the empty active site of the topoisomerase II DNA-gyrase enzyme. 3D-coordinates of the enzyme co-crystallized with its inhibitor ciprofloxacin (pdb id: 2XCT (Bax B et al., 2010)) were downloaded from the RCSB protein data bank. A binding sphere covering the active site was generated and docking of the RCs was performed using the CDOCKER module (Wu G et al., 2003) implemented in the Discovery Studio *ver* 4.0 (Accelrys) along with ciprofloxacin.

The binding affinity of the docked compounds was assessed by computing their binding energies (BEs) [$E_{\text{complex}} - (E_{\text{protein}} + E_{\text{ligand}})$]. The more negative the BE, the stronger the interaction with the enzyme. Compound **C5r** exhibited stronger interaction ($\text{BE} = -124.2 \text{ kcal mol}^{-1}$) with the enzyme in comparison to **C5h** ($\text{BE} = -24.3 \text{ kcal mol}^{-1}$). This consequently supports the experimental results as **C5r** showed the highest MBC in the experimental assay performed. The BE of **C5r** showed a

difference of approximately 30 kcal mol⁻¹ compared to the computed BE of ciprofloxacin (-156 kcal mol⁻¹).

The best docked pose of **C5r** and **C5h** in the active site of topoisomerase II DNA-gyrase (**Figure 7-2**) showed that both the RCs interacted with similar amino acid residues (Arg458, Lys460 and Glu477). This was also observed for ciprofloxacin (**Figure 7-3**). Compound **C5r** (**Figure 7-2**), which was the most active antibacterial agent formed a classical hydrogen bond with Ser 1084 (1.98 Å) and four non-classical hydrogen bonds with Arg458 (2.61 Å), Lys460 (2.45 Å) and Glu477 (2.71 Å, 2.76 Å). The least active compound (**C5h**) displayed three hydrogen bonds with Glu477 (2.61 Å) and Lys460 (3.03 Å, 3.05 Å) in addition to hydrophobic interactions with Arg458 (**Figure 7-2**). The fewer and relatively longer hydrogen bond distances in **C5h** could have led to its weaker binding with the enzyme and in turn lower activity. Ciprofloxacin (the native ligand) fitted nicely into the active site of the enzyme through five hydrogen bonds with Glu477 (2.78 Å, 2.80 Å), Lys460 (2.34 Å, 2.40 Å) and Arg458 (2.14 Å) amino residues and formed another two co-ordinate bonds with Mn²⁺ (**Figure 7-3**).

Overall, the present docking result revealed that the interaction with the Mn²⁺ in the active site is crucial for the antibacterial activity. Both compounds failed to show any interaction with Mn²⁺, which may be responsible for them not being as active as ciprofloxacin.

7.3.6 Crystal structure

The crystal structure of the parent compound, methyl 2-(4-(dimethylamino)phenyl)-1-(4-fluorophenyl)-1*H*-benzo[*d*]imidazole-5-carboxylate (**C5k**) was obtained and the refinement data

are contained in the supplementary file (**Table 7-S1***). **C5k** crystallized in the monoclinic P 21/c space group with two molecules in the asymmetric unit. The ester group and *N*-dimethyl group point away from each other and all groups are in the plane except the 4-fluoro phenyl group, which is perpendicular to the benzimidazole moiety on N-1. Weak hydrogen bond interactions (C-H...O, C-H...F and C-H...N) were observed in the crystal structure (**Table 7-4**). Further selected bond length were described in the supplementary file (**Table 7-S2***). An ortep diagram of **C5k** is given in **Figure 7-4**.

* Present in the supplementary material

Table 7-4 Hydrogen bond interactions for **C5k**

D-H...A	d(D-H)	d(H...A)	d(D...A)	<(DHA)
C(5b)-H(5b)...O(2)#1	0.95	2.49	3.4101(14)	162.3
C(8b)-H(8bi)...O(2)#1	0.98	2.63	3.3278(15)	128.3
C(7)-H(7)...F(1)#2	0.95	2.59	3.1002(13)	113.6
C(2a)-H(2a)...N(3)#3	0.95	2.46	3.2737(14)	143.3
C(6a)-H(6a)...N(3)#4	0.95	2.52	3.4611(14)	171.9

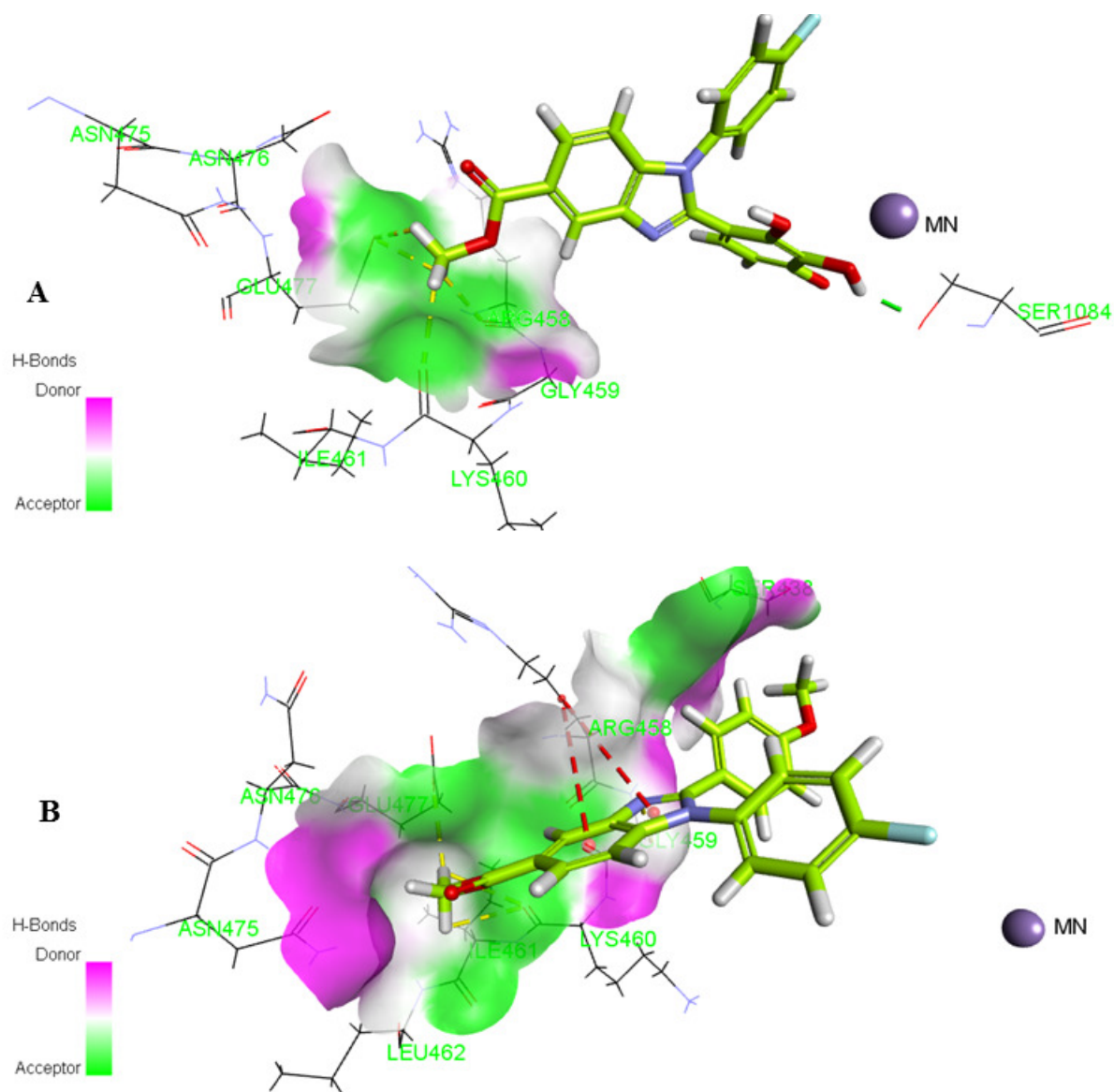


Figure 7-2 The orientation of **C5r** (A) and **C5h** (B) in the active site of topoisomerase II DNA-gyrase. Ligands are shown as sticks (lemon color) and amino acids of the protein as lines. Green dotted lines represent classical H-bonds, yellow dotted lines, non-classical H-bonds and red dotted lines hydrophobic interactions

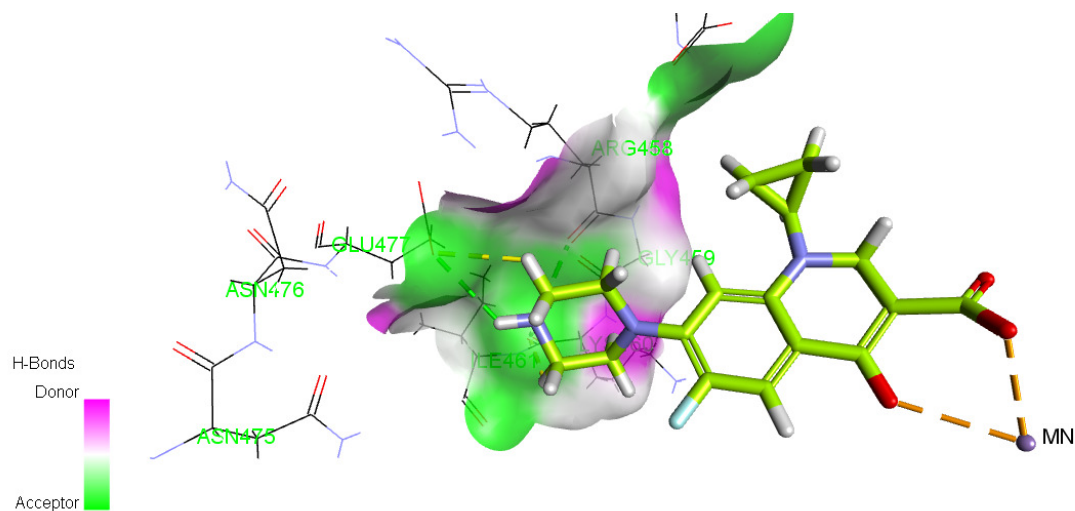


Figure 7-3 The orientation of ciprofloxacin in the active site of topoisomerase II DNA-gyrase. Ligand is shown in sticks (lemon) and amino acids of protein are depicted in the lines format. classical H-bonds (green), non-classical H-bonds (yellow) and co-ordinate bonds (gold)

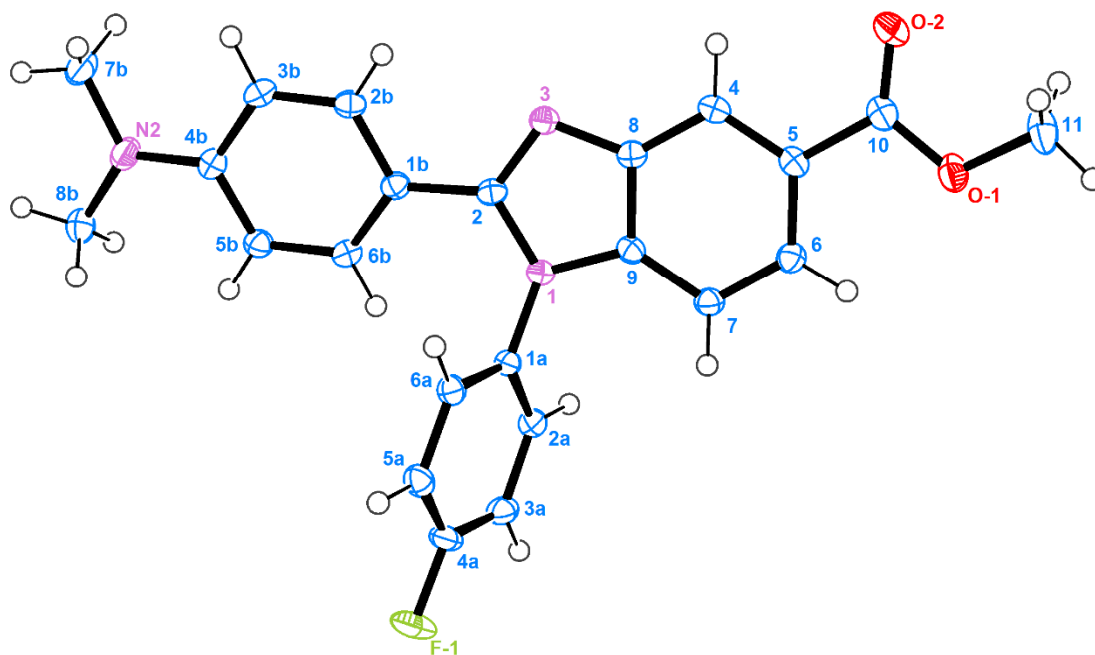


Figure 7-4 Ortep diagram for C5k

7.4 Conclusion

We have developed an efficient, cost effective and faster route for 2-substituted fluorinated benzimidazoles *via* a solvent and catalyst free microwave method. The synthesized compounds were screened for their antibacterial and antioxidant activities. Of the twenty-two compounds tested, eleven compounds showed good antimicrobial activity and two showed good antioxidant activity. Compounds **C5p** and **C5r** showed better activity than ampicillin against the microbial strains used in the assays. These two compounds could be good leads for antimicrobial agents.

Acknowledgements

The authors gratefully acknowledges the Centre for High Performance Computing (CHPC), an initiative supported by the Department of Science and Technology of South Africa for Discovery Studio facility.

7.5 References

- Abdullah, J. M., Sulaiman, M. M., Mohammed, S. J. Microwave-assisted one-pot synthesis of 2-aryl (1*H*) benzimidazoles without catalyst. *J. Edu. Sci.*, **2012**, 25(1), 58-63.
- Al-Mohammed, N. N., Alias, Y., Abdullah, Z., Shakir, R. M., Taha, E. M., Hamid, A. A. Synthesis and antibacterial evaluation of some novel imidazole and benzimidazole sulfonamides. *Molecules*, **2013**, 18, 11978-11995.
- Andrews, J. M. Determination of minimum inhibitory concentrations. *J. Antimicrob. Chemother.*, **2001**, 48(S1), 5-16.
- Azizian, J., Torabi, P., Noei, J. Synthesis of benzimidazoles and benzoxazoles using TiCl_3OTf in ethanol at room temperature. *Tetrahedron Lett.*, **2016**, 57(2), 185-188.
- Banerjee, M., Chatterjee, A., Kumar, V., Bhutia, Z. T., Khandare, D. G., Majik, M. S., Roy, B. G. A simple and efficient mechanochemical route for the synthesis of 2-aryl benzothiazoles and substituted benzimidazoles. *RSC Adv.*, **2014**, 4, 39606–39611.
- Bax, B. D., Chan, P. F., Eggleston, D. S., Fosberry, A., Gentry, D. R., Gorrec, F., Giordano, I., Hann, M. M., Hennessy, A., Hibbs, M., Huang, J., Jones, E., Jones, J., Brown, K. K., Lewis, C. J., May, E. W., Saunders, M. R., Singh, O., Spitzfaden, C. E., Shen, C., Shillings, A., Theobald, A. J., Wohlkonig, A., Pearson, N. D., and Gwynn, M. N. Type IIA topoisomerase inhibition by a new class of antibacterial agents. *Nature*, **2010**, 466, 935-943.

- Barot, K. P., Nikolova, S., Ivanov, I., Ghate, M. D. Novel research strategies of benzimidazole derivatives: A Review. *Mini-Rev. Med. Chem.*, **2013**, 13(10), 1-27.
- Biron, K. K. Antiviral drugs for cytomegalovirus diseases. *Antiviral Res.*, **2006**, 71, 154-163.
- Borhade, A. V., Tope, D. R., and Patil, D. R. An efficient synthesis of benzimidazole by cyclization-oxidation processes using Fe/MgO as a heterogeneous recyclable catalyst. *J. Chem. Pharm. Res.*, **2012**, 4(5), 2501-2506.
- Carvalho, L. C. R., Ribeiro, D., Seixas, R. S. G. R., Silva, A. M. S., Nave, M., Martins, A. C., Erhardt, S., Fernandes, E., Cabrita, E. J., Marques, M. M. B. Synthesis and evaluation of new benzimidazole based COX inhibitors: a naproxen-like interaction detected by STD-NMR. *RSC Adv.*, **2015**, 5, 49098–49109.
- Chen, C., Chen, C., Li, B., Tao, J., Peng, J. Aqueous synthesis of 1*H*-2-substituted benzimidazoles *via* transition-metal-free intramolecular amination of aryl iodides. *Molecules*, **2012**, 17, 12506-12520.
- Das, R., Mehta, D., Bhardawaj, H. An Overview on microwave mediated synthesis. *Int. J. Res. Dev. Pharm. Life Sci.*, **2012**, 1(2), 32-39.
- Dua, R., Shrivastava, S., Sonwane, S. K., Srivastava, S. K. Pharmacological significance of synthetic heterocycles scaffold: A Review. *Adv. Biol. Res.*, **2011**, 5 (3), 120-144.
- Eren, B., Bekdemir, Y. Simple, mild, and highly efficient synthesis of 2-substituted benzimidazoles and bis-benzimidazoles. *Quim. Nova*, **2014**, 37(4), 643-647.
- Farrugia, L. J. WinGX and ORTEP for Windows: an update. *J. Appl. Cryst.*, **2012**, 45, 849–854.
- Funel, J. A., Brodbeck, S., Guggisberg, Y., Litjens, R., Seidel, T., Struijk, M., Abele, S. Diastereospecific enolate addition and atom-efficient benzimidazole synthesis for the production of L/T calcium channel blocker ACT-280778. *Org. Process Res. Dev.*, **2014**, 18, 1674-1685.
- Gawande, M. B., Shelke, S. N., Zboril, R., Varma, R. S. Microwave-assisted chemistry: synthetic applications for rapid assembly of nanomaterials and organics. *Acc. Chem. Res.*, **2014**, 47, 1338–1348.
- Gupta Atyam, V. S. S. S., Sarva Raidu, C., Nannapaneni, D. T., Reddy, M. I. Synthesis, characterization, and biological evaluation of benzimidazole derivatives as potential anxiolytics. *J. Young Pharm.*, **2010**, 2(3), 273-279.
- Gurvinder, S., Maninderjit, K., Mohan, C. Benzimidazoles: The latest information on biological activities. *Int. Res. J. Pharm.*, **2013**, 4(1), 82-87.
- Jacob, J. Microwave assisted reactions in organic chemistry: A review of recent advances. *Int. J. Chem.*, **2012**, 4(6), 29-43.
- Jain, S., Rathish, I. G., Sankaran, R. A review on current industrial trends for synthesis of medicinal compounds. *Int. J. Pharm. Pharm. Sci.*, **2013**, 5 (4), 33-45.
- Jain, Z. J., Kankate, R. S., Chaudhari, B. N., Kakad, R. D. Action of benzimidazolo-piperazinyl derivatives on dopamine receptors. *Med. Chem. Res.*, **2013**, 22, 520–530.
- Kalyankar, T. M., Pekamwar, S. S., Wadher, S. J., Tiprale, P. S., Shinde, G. H. Review on benzimidazole derivative. *Int. J. Chem. Pharm. Sci.*, **2012**, 3(4), 1-10.

- Kamal, A., Narasimha Rao, M. P., Swapna, P., Srinivasulu, V., Bagul, C., Shaik, A. B., Mullagiri, K., Kovvuri, J., Reddy, V. S., Vidyasagar, K., Nagesh, N. Synthesis of β -carboline-benzimidazole conjugates using lanthanum nitrate as a catalyst and their biological evaluation. *Org. Biomol. Chem.*, **2014**, 12, 2370-2387.
- Kattimani, P. P., Kamble, R. R., Meti, G. Y. Expedient synthesis of benzimidazoles using amides. *RSC Adv.*, **2015**, 5, 29447–29455.
- Keri, R. S., Hiremathad, A., Budagumpi, S., Nagaraja, B. M. Comprehensive review in current developments of benzimidazole-based medicinal chemistry. *Chem. Biol. Drug Des.*, **2015**, 86, 19-65.
- Khanna, L., Panda, S. S., Khanna, P. Synthetic routes to symmetric bisbenzimidazoles: A Review. *Mini-Rev. Org. Chem.*, **2012**, 9(4), 381-396.
- Kus, C., Ayhan-Kılıçgil, G., Tunçbilek, M., Altanlar, N., Çoban, T., Can-Eke, B., Iscan, M. Synthesis, antimicrobial and antioxidant activities of some benzimidazole derivatives. *Lett. Drug Des. Discovery*, **2009**, 6(5), 1-6.
- López, S. E., Restrepo, J., Pérez, B., Ortiz, S., Salazar, J. One pot microwave promoted synthesis of 2-aryl-1H-benzimidazoles using sodium hydrogen sulfite. *Bull. Korean Chem. Soc.*, **2009**, 30(7), 1628-1630.
- Mitscher, L. A. Bacterial topoisomerase inhibitors: Quinolone and pyridone antibacterial agents. *Chem. Rev.*, **2005**, 105, 559-592.
- Murthy, P. S., Manjunatha, M. R., Sulochannama, G., Naidu, M. M. Extraction, characterization and bioactivity of coffee anthocyanins. *Eur. J. Biol. Sci.*, **2012**, 4(1), 13-19.
- Narasimhan, B., Sharma, D., Kumar, P. Benzimidazole: A medicinally important heterocyclic moiety. *Med. Chem. Res.*, **2010**, 21(3), 269-283.
- Park, S., Jung, J., Cho, E. J. Visible-light-promoted synthesis of benzimidazoles. *Eur. J. Org. Chem.*, **2014**, 4148-4154.
- Panda, S. S., Malik, R., Jain, S. C. Synthetic approaches to 2-arylbenzimidazoles: A Review. *Curr. Org. Chem.*, **2012**, 16(16), 1905-1919.
- Patil, A. A., Kamble, S. B., Rashinkar, G. S., Salunkhe, R. S. Ultrasound promoted synthesis of 1,2-disubstituted benzimidazoles using aqueous hydrotropic solution. *Chem. Sci. Rev. Lett.*, **2014**, 3(10), 214-220.
- Prajapati, S. K., Nagarsenkar, A., Guggilapu, S. D., Babu, B. N. B(C₆F₅)₃ as versatile catalyst: an efficient and mild protocol for the one-pot synthesis of functionalized piperidines and 2-substituted benzimidazole derivatives. *Tetrahedron Lett.*, **2015**, 56, 6795–6799.
- Rajasekhar, K. K., Ananth, V. S., Nithiyananthan, T. S., Hareesh, G., Kumar, P. N., Reddy, R. S. P. Comparative study of conventional and microwave induced synthesis of selected heterocyclic molecules. *Int. J. ChemTech Res.*, **2010**, 2(1), 592-597.
- Rao, S. S., Reddy, C. V. R., Dubey, P. K. An Ultrasound mediated green synthesis of benzimidazolylthio unsaturated nitriles using water as a green solvent. *Org. Chem. Int.*, **2014**, Article ID 403803, 5 pages. <http://dx.doi.org/10.1155/2014/403803>.
- Rezende, M. C., Dall'Oglio, E. L., Zucco, C. An alternative preparation of bisbenzimidazoles. *Synth. Commun.*, **2001**, 31(4), 607-613.

- Rithe, S. R., Jagtap, R. S., Ubarhande, S. S. One pot synthesis of substituted benzimidazole derivatives and their characterization. *J. Chem.*, **2015**, 8(2), 213-217.
- Saberi, A. Efficient synthesis of benzimidazoles using zeolite, alumina and silica gel under microwave irradiation. *Iranian J. Sci. Technol.*, **2015**, 39(A1), 7-10.
- Saleh, V., Khazaei, A., Abizadeh, H., Saednia, S. Synthesis, characterization, and application of poly(*N,N'*-dibromo-*N*-ethylnaphthyl-2,7-disulfonamide) as an efficient reagent for the synthesis of 2-arylbenzimidazole and 2-aryl-1-arylmethyl-1*H*-1,3-benzimidazole derivatives. *Org. Chem. Int.*, **2015**, Article ID 635630, 9 pages. <http://dx.doi.org/10.1155/2015/635630>.
- Singla, M., Ranjan, R., Mahiya, K., Mohapatra, S. C., Ahmad, S. Nitric oxide inhibition, antioxidant, and antitumour activities of novel copper(II) bis-benzimidazole diamide nanocoordination complexes. *New. J. Chem.*, **2015**, 39, 4316-4327.
- Spek, A. L. Single-crystal structure validation with the program PLATON. *J. Appl. Cryst.*, **2003**, 36, 7-13.
- Tateyama, K., Wada, K., Miura, H., Hosokawa, S., Abe, R., Inoue, M. Dehydrogenative synthesis of benzimidazoles under mild conditions with supported iridium catalysts. *Catal. Sci. Technol.*, **2016**, 6, 1677-1684.
- Tomic, M., Kundakovic, M., Butorovic, B., Jana, B., Andric, D., Rogli, G., Ignjatovic, D., Rajacic, S. K. Pharmacological evaluation of selected arylpiperazines with atypical antipsychotic potential. *Bioorg. Med. Chem. Lett.*, **2004**, 14, 4263-4266.
- VaÂzquez, G. N., Cedillo, R., Campos, A. H., YeÂpez, L., HernaÂndez-Luis, A., Valdez, J., Morales, R. I., CorteÂs, R., HernaÂndez, M., Castillo, R. Synthesis and antiparasitic activity of 2-(trifluoromethyl)-benzimidazole derivatives. *Bioorg. Med. Chem. Lett.*, **2001**, 11, 187-190.
- Vyas, K. V., Ghate, M. Substituted benzimidazole derivatives as angiotensin II-AT1 receptor antagonist: A Review. *Mini-Rev. Med. Chem.*, **2010**, 10(14), 1366-1384.
- Wu, G., Robertson, D. H., Brooks, C. L., Vieth, M. Detailed analysis of grid-based molecular docking: A case study of CDOCKER-A CHARMM-based MD docking algorithm. *J. Comput. Chem.*, **2003**, 24(13), 549-62.
- Xiangming, H., Huiqiang, M., Yulu, W. *p*-TsOH catalyzed synthesis of 2-arylsubstituted benzimidazoles. *ARKIVOC*, **2007**, 13, 150-154.
- Yoon, Y. K., Ali, M. A., Wei, A. C., Choon, T. S., Osman, H., Parang, K., Shirazi, A. N. Synthesis and evaluation of novel benzimidazole derivatives as sirtuin inhibitors with antitumor activities. *Bioorg. Med. Chem.*, **2014**, 22, 703-710.
- Yoon, Y. K., Ali, M. A., Wei, A. C., Choon, T. S., Ismail, R. Synthesis and evaluation of antimycobacterial activity of new benzimidazole aminoesters. *Eur. J. Med. Chem.*, **2015**, 93, 614-624.
- Zhang, Z. H., Yin, L., Wang, Y. M. An expeditious synthesis of benzimidazole derivatives catalyzed by Lewis acids. *Catal. Commun.*, **2007**, 8, 1126-1131.

Chapter 8. Conclusion

Seventeen derivatives of chiral amino acid tethered quinoxalines (**A6a-A6n** and **B5a-c**), 12 derivatives of quinoxaline-amino acid-thiazolidines (**B6a-l**) and 22 derivatives of benzimidazole (**C5a-v**) were successfully synthesized with yields in excess of 75%. Each of the synthesized compounds were fully characterised using NMR and mass spectrometry along with crystal structures of selected compounds. The synthesis of quinoxaline-amino acid-thiazolidines and benzimidazoles under microwave conditions is a quick and efficient way of synthesizing these molecules. In addition, the benzimidazole synthesis under microwave is a solvent free reaction, which can be considered a green method for the synthesis of these compounds. Thermal studies supported by DFT and MD calculations on **A6d** indicated that H-2 was capable of hydrogen bonding interactions.

Of the three classes that were synthesized, the best antimicrobial activity was seen by several compounds in the quinoxaline-amino acid-thiazolidine class. Compounds **B6b-c**, **B6f-g** and **B6j-k** all showed good broad spectrum activity with several MBC values <100 μ M against the strains tested against. **B6f** and **B6j** were the best overall antimicrobial agents with a broad spectrum of activity, being active at <100 μ M against all of the strains tested against. In addition, **B6k** was active at <100 μ M against both *S. aureus* and MRSA with MBC values of 15.9 and 63.8 μ M respectively. Both **B6f** and **B6j** have a 4-fluorophenyl moiety on the thiazolidine group, but a methionine and tyrosine amino acid residue respectively. **B6b** also has a 4-fluorophenyl group as **B6f** and **B6j**, however it has a valine residue instead, indicating that the amino acid interaction is also essential for activity since **B6b** is not as active as **B6f** and **B6j**. The thiazolidine group is essential for activity, since the quinoxalines with only amino acids coupled to it (**A6a-n** and **B5a-**

c) did not show as good antimicrobial activity as the thiazolidine hybrids. In general the benzimidazoles were not as active as the quinoxaline-amino acid-thiazolidine hybrids with only two compounds (**C5p** and **C5r**) showing strain specific activity to *Klebsiella pneumoniae* with MBC values of 14.45 and 25.55 μM respectively. Thus, the quinoxaline-amino acid-thiazolidine core structure with a 4-fluorophenyl moiety on the thiazolidine ring is a good lead for antimicrobial activity. Further work can be explored where different amino acids can be coupled to this core structure to identify the amino acid that shows the best activity. The results can be compared to the core structure with valine, methionine and tyrosine, which was carried out in this work.

In general, the quinoxaline-amino acids were more active than the quinoxaline-amino acid-thiazolidine derivatives in that all of the synthesized compounds of the series **A6a-n** were active in both the α -glucosidase and α -amylase assays. Specifically, **A6a**, **A6d** and **A6f** have better activity than acarbose (IC_{50} of 88 μM) in the α -glucoside enzyme inhibition assay with IC_{50} values of 56, 12 and 42 μM respectively. Combining a thiazolidine group to this core structure decreased activity as only three compounds were now active in these antidiabetic assays with high IC_{50} values of between 276 to 428 μM .

Two quinoxaline-amino acid-thiazolidine hybrids, **B6k** and **B6l** showed IC_{50} values of 19.60 and 10.53 μM respectively in the antioxidant assay carried out, comparable to ascorbic acid (IC_{50} 16.86 μM). These compounds and their scaffolds, containing a tyrosine residue could be a lead for other antioxidant compounds, which have the potential to be anticancer agents. Future work will involve making a series of quinoxaline-tyrosine-thiazolidine hybrids with a variety of substituted phenyl rings on the thiazolidine group and testing them for their antioxidant and anticancer activity.

Adding a thiazolidine moiety on the quinoxaline-amino acid scaffold only increased the antimicrobial activities of the compounds and not the antidiabetic activity. Future work will involve reacting the amino group on the quinoxaline-amino acid scaffold and generate other classes of hybrid molecules or other derivatives at this position, for example carboxamides, Schiff bases and β -lactams to determine whether or not they have a positive effect in increasing the antimicrobial and antidiabetic activity of the compounds.